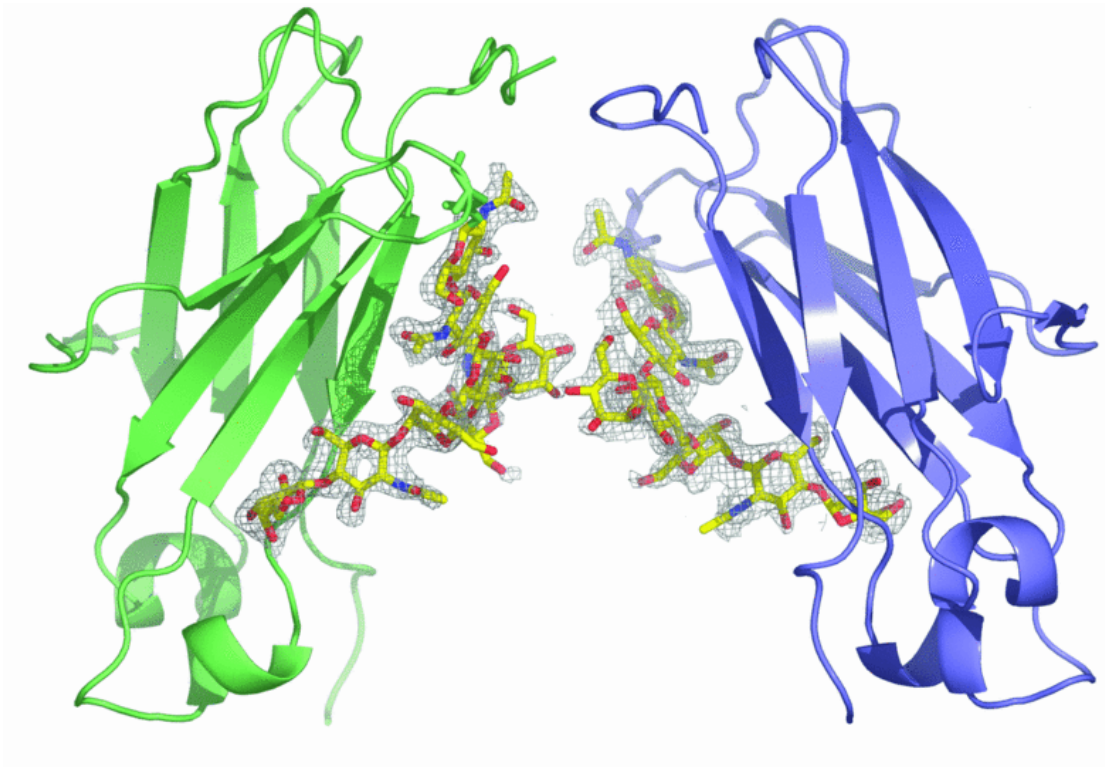


# ***N*-glycosylation of serum proteins in mouse models of chronic liver disease and in human conditions with liver disease**



**Bram Blomme**

Thesis submitted in fulfillment of the requirements for the degree of  
Doctor in Biomedical Sciences



FACULTEIT GENEESKUNDE EN  
GEZONDHEIDSWETENSCHAPPEN

**Ghent University Hospital**

**Department of Gastroenterology and Hepatology**

***N*-glycosylation of serum proteins in mouse models of  
chronic liver disease and in human conditions with  
liver disease**

**Bram Blomme**

Promotor: Prof. Dr. Hans Van Vlierberghe

Thesis submitted as fulfillment for the requirements  
for the degree of  
**“Doctor in the Biomedical Sciences”**

**Academic year 2010-2011**

Thesis submitted as fulfillment to the requirements for the degree of “doctor in the Biomedical Sciences”

Academic year 2010-2011

Promotor:

Prof. Dr. Hans Van Vlierberghe  
*Ghent University, Belgium*

Chairman of the Examination Committee:

Prof. Dr. Apr. Johan Van de Voorde  
*Ghent University, Belgium*

Members of the Examination Committee:

Prof. Dr. Jean Claude Michalski  
*Université des Sciences et Technologies de Lille, France*

Dr. Sven Francque  
*Antwerp University, Belgium*

Prof. Dr. Peter Stärkel  
*Université catholique de Louvain, Belgium*

Prof. Dr. Jean-Marc Kaufman  
*Ghent University, Belgium*

Prof. Dr. Romain Lefebvre  
*Ghent University, Belgium*

Prof. Dr. Johannes Ruige  
*Ghent University, Belgium*

Prof. Dr. Harald Peeters  
*Ghent University, Belgium*

Cover image: The carbohydrate structure of rabbit IgG-Fc (*Biochemical journal* 2009; volume 417, 77-83)

# TABLE OF CONTENT

---

List of abbreviations	6
Summary	12
Samenvatting	14
<b>Chapter 1 General Introduction</b>	<b>16</b>
<b>1.1 Chronic liver disease</b>	<b>17</b>
1.1.1 General introduction	17
1.1.1.1 The liver: structural and functional	17
1.1.1.2 Bilirubin metabolism	19
1.1.1.3 Liver fibrosis	21
1.1.2 Alcoholic liver disease	24
1.1.3 Viral liver disease	26
1.1.3.1 General aspects	26
1.1.3.2 Host mechanisms	27
1.1.3.3 Mechanisms of fibrosis in hepatitis C	28
1.1.4 Cholestatic liver disease	30
1.1.5 Non-alcoholic fatty liver disease	31
1.1.6 Hepatocellular carcinoma	35
1.1.7 References	39
<b>1.2 Protein <i>N</i>-glycosylation and Glycomics</b>	<b>48</b>
1.2.1 General introduction and biosynthesis	48
1.2.2 Glycomic techniques	53
1.2.2.1 Glycomics and mass spectrometry	53
1.2.2.2 Glycomics and high performance liquid chromatography	55
1.2.2.3 Glycomics and capillary electrophoresis	57
1.2.2.4 Glycomics and lectin-based microarrays	58
1.2.2.5 Glycomics and nuclear magnetic resonance	59
1.2.3 <i>N</i> -glycosylation in disease	61
1.2.3.1 The role of <i>N</i> -glycosylation in receptor responses	61

1.2.3.2	Congenital disorders of glycosylation	62
1.2.3.3	Glyco-biomarkers of cancer and chronic inflammation	63
1.2.4	References	64
<b>1.3</b>	<b>Non-invasive alternatives for liver biopsy</b>	<b>71</b>
1.3.1	Liver biopsy: limitations and complications	71
1.3.2	Imaging techniques	71
1.3.2.1	Imaging of fibrosis/cirrhosis	72
1.3.2.2	Imaging of hepatocellular carcinoma	73
1.3.3	Serum markers	74
1.3.3.1	Serum markers for fibrosis/cirrhosis	74
1.3.3.2	Serum markers for hepatocellular carcinoma	76
1.3.4	References	77
<b>1.4</b>	<b>Alteration of protein glycosylation in liver diseases</b>	<b>82</b>
Blomme B, Van Steenkiste C, Callewaert N, Van Vlierberghe H		
J Hepatol 2009 Mar;50(3):592-603		
<b>Chapter 2</b>	<b>Aims and outline of the thesis</b>	<b>95</b>
<b>Chapter 3</b>	<b>Results</b>	<b>98</b>
<b>3.1</b>	<b>Impact of elevation of total bilirubin level and etiology of the liver disease on serum N-glycosylation patterns in mice and humans</b>	<b>99</b>
Blomme B, Van Steenkiste C, Vanhuysse J, Colle I, Callewaert N, Van Vlierberghe H		
Am J Physiol Gastrointest Liver Physiol 2010 May;298(5):G615-24		
<b>3.2</b>	<b>Alterations of serum protein N-glycosylation in two models of chronic liver disease are hepatocyte and not B cell driven</b>	<b>110</b>
Blomme B, Van Steenkiste C, Grassi P, Dell A, Callewaert N, Van Vlierberghe H		
Accepted for publication in Am J Physiol Gastrointest Liver Physiol		
<b>3.3</b>	<b>Serum N-glycosylation patterns in diethylnitrosamine-induced hepatocellular carcinoma mice and their evolution after inhibition of the Placental Growth Factor</b>	<b>134</b>

Blomme B, Heindryckx F, Stassen JM, Geerts A, Colle I, Van Vlierberghe H

Submitted to Mol Carcinog

**3.4 *N*-glycosylation based biomarker distinguishing NASH from steatosis independently of fibrosis in patients with non-alcoholic steatohepatitis 151**

Blomme B, Francque S, Trépo E, Libbrecht L, Vanderschaeghe D, Verrijken A, Pattyn P, Van Nieuwenhove Y, Van De Putte D, Geerts A, Colle I, Delanghe J, Moreno C, Van Gaal L, Callewaert N, Van Vlierberghe H.

Submitted to Liver Int, in revision

**3.5 Serum protein *N*-glycosylation patterns in pediatric NAFLD 170**

Blomme B, T. Tshiamala I, Fitzgerald E, De Bruyne R, Callewaert N, Van Vlierberghe H.

Additional study

**3.6 The Unfolded Protein Response in plasma cells of patients with non-alcoholic fatty liver disease 181**

Blomme B, Olievier K, Laukens D, Van Vlierberghe H.

Pilot study

**Chapter 4 General Discussion – Algemene Discussie 192**

Curriculum vitae 204

Dankwoord 207

## LIST OF ABBREVIATIONS

---

1D-PAGE: one-dimensional polyacrylamide gel electrophoresis

2-AA: 2-aminobenzoic acid

2-AB: 2-aminobenzamide

AAL: *Aleuria auantia*

AAT:  $\alpha$ 1-antitrypsin

ADH: aldehyde dehydrogenase

AFP:  $\alpha$ -fetoprotein

AGP:  $\alpha$ 1-acid glycoprotein

ALD: alcohol liver disease

ALDH: alcohol dehydrogenase

ALT: alanine aminotransferase

AMA: anti-mitochondrial antibodies

AMPK: AMP kinase

Ang-2: angiopoietin-2

ANTS: 8-aminonaphthalene-1,3,6-trisulfonate

ANOVA: analysis of variance

AP (or ALP): alkaline phosphatase

APC: adenomatous polyposis coli

Apo E: apolipoprotein E

APTS: 8-aminopyrene-1,3,6-trisulfonic acid

APRI: aminotransferase to platelet ratio

ASH: alcoholic steatohepatitis

Asn: asparagine

AST: aspartate aminotransferase

ATF: activating transcription factor

AUC: area under the curve

bFGF: basic fibroblast growth factor

BMI: body mass index

BSEP: bile salt export pump

bZIP: basic-region leucine zipper

Cav1: caveolin1

CBDL: common bile duct ligation

CCl<sub>4</sub>: carbon tetrachloride

CD: cluster of differentiation

CD14: monocyte differentiation antigen

CDC: complement dependent cytotoxicity

CDG: congenital disorder of glycosylation

cDNA: complementary DNA

CDT: carbohydrate deficient transferrin  
CE: capillary electrophoresis  
CEUS: contrast enhanced ultrasound  
CFG: Consortium for functional glycomics  
CHOP: CCAAT/enhancer binding protein homologous protein  
CK-18: cytokeratin 18  
CMAR: cellular adhesion regulating molecule  
Con A: *Concanavalin A*  
CRP: C-reactive protein  
CT: computed tomography  
CTGF: connective tissue growth factor  
CYP2E1: cytochrome P450 2E1  
DAB: 3,3-diaminobenzidine  
DDIT3: DNA-damage inducible transcript 3  
DEN: diethylnitrosamine  
Dol: dolichol  
DSA-FACE: DNA sequencer-assisted fluorophore-assisted capillary electrophoresis  
DTT: dithiothreitol  
EC: endothelial cells  
ECM: extracellular matrix  
EDTA: ethylenediaminetetraacetic acid  
EGFR: epidermal growth factor receptor  
EIA: enzyme immunoassay  
eIF2A: eukaryotic initiation factor 2A  
eIF2AK3: eukaryotic initiation factor 2A kinase 3  
ELISA: enzyme linked immunosorbant assay  
EM: electromagnetic  
EMT: epithelial-to-mesenchymal transition  
EPC: endothelial progenitor cell  
E-PHA: *Phaseolus vulgaris*: erythroagglutinating  
ER: endoplasmic reticulum  
ERK: extracellular signal-regulated kinase  
E-selectin: endothelial-selectin  
ESI: electrospray ionization  
ET-1: endothelin-1  
Ets-1: E26 transformation-specific sequence  
FFA: free fatty acid  
FI: fucosylation index  
FIC-1: familial intrahepatic cholestasis 1  
FSA: free sialic acid



FXR: farnesoid X receptor  
GADD34: growth arrest and DNA damage inducible protein  
Gal: galactose  
GalNAc: *N*-acetylgalactosamine  
GAPDH: glyceraldehydes-3 phosphate dehydrogenase  
GalT: galactosyltransferase  
GDP: guanosine diphosphate  
GGT: gamma-glutamyl transferase  
Glc: Glucose  
GlcNAc: *N*-acetylglucosamine  
GnT: *N*-acetylglucosaminyltransferase  
GM1: monosialotetrahexosylganglioside  
GPC3: Glypican 3  
Grp: glucose regulated protein  
HAV: hepatitis A virus  
Hb: hemoglobin  
HBeAg: hepatitis B “e” antigen  
HBV: hepatitis B virus  
HBsAg: hepatitis B surface antigen  
HBX: HBV X-protein  
HCC: hepatocellular carcinoma  
HCV: hepatitis C virus  
HDL: high density lipoprotein  
HDV: hepatitis D virus  
HEV: hepatitis E virus  
HIF-1: hypoxia-inducible factor-1  
HIV: human immunodeficiency virus  
HOMA-index: homeostatic model assessment index  
Hp: haptoglobin  
HPAEC: high performance anion-exchange chromatography  
HPLC: high performance liquid chromatography  
HRP: horse radish peroxidase  
HSC: hepatic stellate cell  
HSPA5: heat shock 70 kDa protein 5  
ICAM-1: intercellular adhesion molecule 1  
ICR: ion cyclotron resonance  
IFN- $\gamma$ : interferon-gamma  
Ig: immunoglobulin  
IGF: insulin-like growth factor  
IL: interleukin

iNOS: inducible NO synthase  
INR: international normalized ratio  
IP: intraperitoneal  
IR: insulin resistance  
IRE-1: inositol requiring enzyme-1  
JNK: Jun N-terminal kinase  
JCGGDB: Japan consortium for glycobiology and glycotecchnology databases  
LAL: lysosomal acid lipase  
LAD-II: leukocyte adhesion deficiency type II  
LCA: *Lens culinaris agglutinin*  
LDS: lithium dodecyl sulphate  
L-PHA: *Phaseolus vulgaris, leuco-agglutinating*  
LPS: lipopolysaccharide  
MALDI: matrix-assisted laser desorption/ionization  
Man: mannose  
MAPK: mitogen-activated protein kinase  
MCP-1: monocyte chemoattractant protein 1  
MELD: Model for End-stage Liver Disease  
MMP: matrix metalloproteinase  
Mn-SOD: Mn-superoxide dismutase  
MRI: magnetic resonance imaging  
MTTP: microsomal triglyceride transport protein  
MS: massspectrometry  
Mw: molecular weight  
NA2: bigalacto biantennary  
NA2F: bigalacto  $\alpha$ 1,6-fucosylated biantennary  
NA2FB: bigalacto  $\alpha$ 1,6-fucosylated bisecting biantennary  
NA3: triantennary  
NA3Fb: branching  $\alpha$ 1,3-fucosylated triantennary  
NA3Fc: core  $\alpha$ 1,6-fucosylated triantennary  
NA3Fbc: branching  $\alpha$ 1,3-fucosylated core  $\alpha$ 1,6-fucosylated triantennary  
NA4: tetra-antennary  
NA4Fb: branching  $\alpha$ 1,3-fucosylated tetra-antennary  
NADPH: nicotinamide adenine dinucleotide phosphate  
NAFLD: non-alcoholic fatty liver disease  
NAS: NAFLD activity score  
NASH: non-alcoholic steatohepatitis  
NF- $\kappa$ B: nuclear factor-kappaB  
NGA2F: agalacto  $\alpha$ 1,6-fucosylated biantennary  
NGA2FB: agalacto  $\alpha$ 1,6-fucosylated bisecting biantennary

NG1A2F: single agalacto  $\alpha$ 1,6-fucosylated biantennary  
NK: natural killer  
NMR: nuclear magnetic resonance  
NO: nitric oxide  
NP: normal phase  
NS: nonstructural  
OST: oligosaccharyltransferase  
PA: 2-aminopyridine  
PAD: pulsed amperometric detection  
PBC: primary biliary cirrhosis  
PBS: phosphate buffered saline  
PCHE: pseudocholinesterase  
PD-1: programmed death-1  
PDC-E2: dihydrolipoamide acetyltransferase component of pyruvate dehydrogenase complex  
PDGF: platelet-derived growth factor  
PERK: double-stranded RNA-activated protein kinase like ER kinase  
PET: positron emission tomography  
PFIC1: progressive familial intrahepatic cholestasis, type 1  
PHT: portal hypertension  
PKC: protein kinase C  
PLC: primary liver cancer  
PIGF: placental growth factor  
PMI: phosphomannose isomerase  
PNA: *Arachis hypogaea*  
PNGase F: peptide N-glycanase F  
PPAR- $\alpha$ : peroxisome proliferation activated receptor-alpha  
PPVL: partial portal vein ligation  
PSC: primary sclerosing cholangitis  
PVDF: polyvinylidene fluoride  
PVP: portal venous pressure  
PUFA: poly-unsaturated fatty acids  
qRT-PCR: quantitative real time polymerase chain reaction  
RA: rheumatoid arthritis  
RAGE: receptor for advanced glycation products  
RES: reticulo-endothelial system  
RIA: radioimmunoassay  
RIG-I: retinoic acid inducible gene-I  
RIPA: radioimmuno precipitation assay  
ROI: region of interest  
ROS: reactive oxygen species

RP: reverse phase  
S1P: sphingosine-1-phosphate  
S2P: sphingosine-2-phosphate  
SAA: serum amyloid A  
SC: subcutaneous  
SCCA: squamous cell carcinoma antigen  
SDHA: succinate dehydrogenase complex, subunit A  
SDS-PAGE: sodium dodecyl sulphate polyacrylamide gel electrophoresis  
Ser: Serine  
SFA: saturated fatty acids  
SLe<sup>x</sup>: sialyl Lewis x  
ST6Gall:  $\beta$ -galactoside  $\alpha$ 2,6 sialyltransferase  
Tbiln: total bilirubin  
TBS: Tris buffered saline  
TBST: Tris buffered saline Tween  
TCR: T cell receptor  
TF: transferrin  
TG: triglycerides  
TGF- $\beta$ 1: transforming growth factor-beta 1  
Thr: threonine  
TIMP-1: tissue inhibitor of matrix metalloproteinase 1  
TLR: Toll-like receptor  
TNF $\alpha$ : tumor necrosis alpha  
TOF: time of flight  
Tris: tris(hydroxymethyl)aminomethane  
TSA: total sialic acid  
UCA: ultrasound contrast reagents  
UDP: uridine diphosphate  
UGS: undergalactosylation  
UPR: unfolded protein response  
VE-cadherin: vascular endothelial-cadherin  
VEGF: vascular endothelial growth factor  
VLDL: very low density lipoprotein  
WB: western blot  
WHR: waist-to-hip-ratio  
WT: wild type  
XBP-1(s): X-box binding protein 1 (spliced)  
 $\alpha$ 1-6FT: alpha 1,6 fucosyltransferase  
 $\beta$ 3GnT2: beta-1,3-*N*-acetylglucosaminyltransferase  
 $\beta$ -NAG: beta-*N*-acetylglucosaminidase

---

## SUMMARY

---

A liver biopsy is the current 'golden' standard to determine etiology, severity and progression of chronic liver disease. However, this has diagnostic limitations because only a small fraction of the liver is removed (1/50 000 of total mass) and due to its invasive nature, it is difficult to use as a follow-up tool. Moreover, a liver biopsy is associated with several complications of which internal hemorrhages are most frequent. In recent years, numerous non-invasive alternatives were developed, but none could completely avoid liver biopsies in the diagnosis of chronic liver disease. The general goal of this thesis was a continuation of the research into the *N*-glycosylation of serum proteins as biomarker for liver diseases. Previously, it was shown that by quantifying serum *N*-glycans, a distinction could be made between cirrhotic and non-cirrhotic patients with high specificity (>95%) and sensitivity (60%-80%).

The latter study was predominantly performed in hepatitis C patients. Therefore, other important etiologies were investigated to determine if the same features applied. There are three important *N*-glycosylation alterations present in fibrotic and cirrhotic liver disease. An undergalactosylation on immunoglobulins and an increase of bisecting *N*-acetylglucosamine modified glycans and decrease of multi-antennary glycans on liver-produced proteins (with the exception of multi-antennary glycans carrying the sialyl Lewis x antigen). None of these features were significantly different between the different etiologies of chronic liver disease. Nevertheless, important sub-significant differences were apparent. Alcoholic patients showed the highest score for the GlycoCirrhoTest and patients with non-alcoholic steatohepatitis (NASH) presented the quantitatively most important undergalactosylation. Liver patients with an elevated serum bilirubin concentration had a significantly increased fucosylation-index. This is the summation of all  $\alpha$ -1,6 fucosylated glycans and we were able to extrapolate this finding to a mouse model for secondary biliary cirrhosis, the 'common bile duct ligation' (CBDL) model. A second mouse model was induced by chronically injecting mice with CCl<sub>4</sub>. This mouse model did not show an increased fucosylation-index, but had a significant increase of all multi-antennary glycans. Importantly, these alterations already occurred early in the fibrotic development (F1-F2). In mice induced with a partial portal vein ligation, fewer *N*-glycan alterations were observed and these were inconsistent in both time points studied in contrast to the fibrotic models. Therefore, it can be concluded that portal hypertension does not contribute to *N*-glycan alteration in chronic liver disease.

There are two sources of *N*-glycosylated serum protein: the liver and B cells. The liver produces the vast majority, but B cells are responsible for the production of a quantitatively important group in humans, the immunoglobulins. It was previously shown that *N*-glycosylation alterations on immunoglobulins are the dominating factor in the alterations that occur in total serum of human liver patients. However, in a study with B cell deficient mice, we could determine that the *N*-glycan alterations on immunoglobulin G has no impact on the total serum alterations in two fibrotic mouse models (CBDL and CCl<sub>4</sub>). An important observation was that the B cell deficient state had a different effect on the fibrotic development in these mouse models. A significant decrease of fibrosis could be determined in the B cell deficient CCl<sub>4</sub> mouse in comparison to the wild type CCl<sub>4</sub> mouse, whereas a significant increase of fibrosis was observed in the B cell deficient CBDL mouse in comparison to its wild type counterpart.

In continuation of the *N*-glycosylation alterations that were observed in fibrotic mouse models, an investigation was performed into the changes that occurred in a mouse model for

hepatocellular carcinoma (HCC). This mouse model was induced by chronic injections with diethylnitrosamine (DEN). In analogy with the fibrotic models, maximum altered phenotype on the *N*-glycosylation level was reached at an early stage when the first neoplastic nodules started to appear (20w DEN). Most mice showed exophytically growing, well vascularized tumors after 30 weeks of DEN-treatment. Subsequently, the latter mice were treated with anti-PlGF, a monoclonal antibody directed against the placental growth factor. The majority of the significantly altered peaks evolved back in the direction in which they were observed in control mice. There was a prominent decrease of all multi-antennary glycans after anti-PlGF treatment. On the histological level, anti-PlGF treatment resulted in a significant decrease of tumor burden and a significantly increased survival of HCC-mice was observed. Ets-1 is a transcription factor that is necessary for the transcription of genes of which the corresponding enzymes are responsible for the production of multi-antennary glycans and it also plays an important role in various stages of neo-angiogenesis. Importantly, we observed a significant decrease of the number of Ets-1 positive cells in anti-PlGF treated mice.

In the second part of this thesis, we developed a biomarker based on the *N*-glycosylation of serum proteins that could distinguish patients with simple steatosis from NASH patients. The glycomarker was developed in a population of gastric bypass patients of which none had a significant amount of fibrosis. Fibrosis is a confounding factor in the development of a biomarker that is specific for NASH, because it is attended with its own glycomic alterations. The glycomarker was determined by the undergalactosylation of IgG and showed a good correlation with the amount of lobular inflammation. In an univariate analysis, six of the thirteen investigated markers were significant, but our glycomarker displayed the lowest *P*-value when these were evaluated in a multivariate analysis. The glycomarker was subsequently validated in a large, independent population of 224 patients. The glycomarker again had a good correlation with the amount of lobular inflammation and was not significantly different across the fibrotic stages. The current best serological marker for NASH is the apoptosis-related CK-18 marker. In the validation cohort, we were able to show that CK-18 is strongly associated with the fibrotic stage in NASH patients.

A similar glyco-analysis was performed in pediatric NAFLD patients and the results corresponded very well with the adult NAFLD population. A mechanism explaining this undergalactosylation on immunoglobulins has not been determined. Several lines of evidence indicate that endoplasmic reticulum (ER) stress could play an important role in this. ER stress happens as misfolded proteins accumulate in the ER and an 'unfolded protein response' (UPR) is initiated. In a small pilot study, we showed that obese patients with liver inflammation have an increased expression of ER stress genes in their plasma cells in comparison to obese patients without liver inflammation.

## SAMENVATTING

---

De huidige 'gouden' standaard om etiologie, ernst en progressie van chronisch leverlijden te bepalen is een lever biopsie. Deze heeft echter diagnostische limitaties omdat maar een klein gedeelte van de lever wordt afgenomen (1/50 000). Door zijn invasief karakter kan het ook moeilijk als follow-tool gebruikt worden. Een lever biopsie gaat gepaard met verschillende complicaties. Inwendige bloedingen zijn het vaakst voorkomend, maar ook pneumothorax of het aanprikken van de galwegen kan occasioneel voorkomen. In de loop der jaren zijn er verschillende niet-invasieve alternatieven ontwikkeld, maar geen enkele was in staat om een lever biopsie volledig te vermijden. Het overkoepelende doel van deze thesis was een voortzetting van het onderzoek naar *N*-glycosyatie van serum eiwitten als biomarker voor leverlijden. Er werd eerder al aangetoond dat een onderscheid kan gemaakt worden tussen cirrotische en niet-cirrotische patiënten met zeer hoge specificiteit (>95%) en sensitiviteit (60-80%) door een kwantificatie van serum *N*-glycanen.

Aangezien deze studie grotendeels in hepatitis C patiënten werd uitgevoerd, werd eerst bij andere belangrijke leveretiologieën onderzocht of we dezelfde glycomische veranderingen konden vaststellen. Er zijn drie belangrijke *N*-glycosylatie veranderingen die optreden bij fibrotisch en cirrotisch leverlijden: een ondergalactosylatie op immunoglobulines en een toename van bisecting *N*-acetylglucosamine gemodificeerde glycanen en afname van multi-antennaire glycanen op lever-geproduceerde eiwitten (met uitzondering van multi-antennaire glycanen die het sialyl Lewis x antigeen bevatten). Geen enkele van deze veranderingen was significant verschillend bij de verschillende etiologieën van leverlijden. Er konden echter belangrijke sub-significante verschillen waargenomen worden. Alcoholische patiënten vertoonden de hoogste score voor de GlycoCirrhoTest en bij patiënten met niet-alcoholisch steatohepatitis (NASH) kon de kwantitatief belangrijkste ondergalactosylatie vastgesteld worden. Leverpatiënten met een verhoogde serum bilirubine concentratie hadden een significant toegenomen fucosylatie-index. Dit is de som van alle  $\alpha$ -1,6 gefucosyleerde glycanen en dit kon geëxtrapoleerd worden naar een muis model voor een secundaire biliaire cirrose, het 'common bile duct ligation' (CBDL) model. Een tweede muismodel werd geïnduceerd door muizen chronisch te behandelen met  $\text{CCl}_4$ . Dit muismodel vertoonde geen verhoogde fucosylatie-index, maar had een significante toename van alle multi-antennaire glycanen. Opvallend was dat deze veranderingen zich al vroeg in het proces van fibrotische ontwikkeling manifesteerden (F1-F2). In muizen die geïnduceerd werden met een partial portal vein ligation, werden minder *N*-glycaan veranderingen vastgesteld en deze veranderingen waren niet consistent in de onderzochte tijdstippen in tegenstelling tot de fibrotische modellen. Hierdoor kan geconcludeerd worden dat portale hypertensie niet bijdraagt tot *N*-glycaan veranderingen bij chronisch leverlijden.

Er zijn 2 bronnen van *N*-glycosyleerde serum eiwitten: de lever en B cellen. De lever produceert de overgrote meerderheid, maar B cellen zijn verantwoordelijk voor de productie van een kwantitatief belangrijke groep bij de mens: de immunoglobulines. Bij leverpatiënten werd eerder aangetoond dat de *N*-glycosylatie veranderingen op immunoglobulines de meest bepalende factor zijn in de veranderingen die optreden in totaal serum. In een studie met B cel deficiënte muizen kon echter vastgesteld worden dat de *N*-glycosylatie veranderingen op immunoglobuline G geen belangrijke invloed heeft op de totaal serum veranderingen in twee fibrotische muismodellen (CBDL en  $\text{CCl}_4$ ). Een belangrijke observatie was dat de B cel deficiënte status een verschillende uitwerking had op de fibrose

ontwikkeling in de twee muismodellen. In de B cel deficiënte CCl<sub>4</sub> muis kon een significante afname van de hoeveelheid fibrose vastgesteld worden in vergelijking met de wild type CCl<sub>4</sub> muis, terwijl er een significante toename van fibrose werd geobserveerd in de B cel deficiënte CBDL muis in vergelijking tot de wild type CBDL muis.

In aanvulling op de *N*-glycosylatie veranderingen die geobserveerd werden bij fibrotische muismodellen, werd ook onderzoek gedaan naar de veranderingen die optreden bij een muismodel voor hepatocellulaire carcinoma (HCC). Dit muismodel werd geïnduceerd door chronische injecties met diethylnitrosamine (DEN). In overeenstemming met de fibrotische modellen werd het maximale fenotype op *N*-glycosylatie niveau reeds bereikt in een vroeg stadium van carcinogenese. De meesten muizen vertoonden exofytisch groeiende, gevasculeerde tumoren wanneer ze 30 weken werden geïnjecteerd met DEN. Vervolgens werden de muizen behandeld met anti-PIGF, een monoclonaal antilichaam gericht tegen de placentale groei factor. De meerderheid van de significant gewijzigde pieken evolueerden terug in de richting waarin ze geobserveerd werden in controlemuizen. Opvallend was de significante afname van alle multi-antennaire glycanen na anti-PIGF behandeling. Op histologisch vlak zorgde de anti-PIGF behandeling voor een afname van het aantal en de grootte van de tumoren en werd er een significant toegenomen overleving van de HCC-muizen vastgesteld. Ets-1 is een transcriptiefactor die noodzakelijk is voor de transcriptie van genen waarvan de corresponderende enzymen verantwoordelijk zijn voor de productie van multi-antennaire glycanen, maar Ets-1 speelt ook een belangrijke rol in verschillende stadia van neo-angiogenese. We observeerden een significante afname van het aantal Ets-1 positieve cellen in anti-PIGF behandelde muizen.

In een tweede luik van deze thesis werd een biomerker ontwikkeld op basis van de *N*-glycosylatie van serum eiwitten die een onderscheid kon maken tussen patiënten met steatose en NASH patiënten. De glycomerker werd ontwikkeld in een populatie van gastric bypass patiënten waarvan geen enkele patiënt een significante hoeveelheid fibrose vertoonde. Fibrose is een confounding factor in de ontwikkeling van een biomerker die specifiek is voor NASH, omdat het zijn eigen glycomische veranderingen vertoont. De glycomerker werd bepaald door de ondergalactosylatie van IgG en vertoonde een goede correlatie met de hoeveelheid lobulaire inflammatie. In een univariate analyse waren zes van de dertien onderzochte merkers significant, maar onze glycomerker vertoonde de laagste *P*-waarde wanneer deze geëvalueerd werden in een multivariate analyse. De glycomerker werd vervolgens gevalideerd in een grote, onafhankelijke NAFLD populatie van 224 patiënten. Wederom werd een goede correlatie gevonden met de hoeveelheid lobulaire inflammatie en de glycomerker was niet significant verschillend in de verschillende fibrose stadia. De beste serologische merker voor NASH is de apoptose-gerelateerde CK-18 merker. In de validatie-populatie konden we aantonen dat CK-18 sterk geassocieerd is met het fibrose stadium in NASH patiënten.

Een gelijkaardige glyco-analyse werd uitgevoerd bij pediatrie NAFLD patiënten. De resultaten goed overeenstemden met de volwassen NAFLD populatie. Het mechanisme die deze ondergalactosylatie op immunoglobulines verklaart, is nog niet opgehelderd. Er zijn sterke aanwijzingen dat endoplasmatisch reticulum (ER) stress hierin een belangrijk rol speelt. ER stress is het gevolg van een accumulatie van misopgevouwen eiwitten in het ER en doet een 'unfolded protein response' (UPR) ontstaan. In een kleine piloot studie konden we aantonen dat obese patiënten met lever inflammatie een sterk toegenomen UPR hebben in hun plasma cellen in vergelijking met obese patiënten zonder lever inflammatie.



# **Chapter 1: General Introduction**

---

## 1.1

## Chronic liver disease

---

### 1.1.1 General introduction

#### 1.1.1.1 The liver: structural and functional

The liver is the largest gland of the human body weighing approximately one and a half kilo. It is secured by the thoracic cage and it is situated in the right upper quadrant of the abdominal cavity inferior to the diaphragm which separates it from the pleura, lungs, pericardium and heart.

The liver lobule which measures 1-2 mm in diameter, forms the structural unit of the liver. It is composed of cords of liver cells (hepatocytes) radiating from a central vein. The boundary of each lobule is formed by a portal tract made up of connective tissue containing a branch of the hepatic artery, portal vein and bile duct. Between the cords of hepatocytes are vascular spaces, called sinusoids, that are lined by endothelial cells and Kupffer cells. The latter cells are phagocytic macrophages capable of ingesting bacteria or other foreign material from the blood that flows through the sinusoids. Primary bile canaliculi are located between the hepatocytes (Figure 1.1). Two third of the liver is composed of parenchymal hepatocytes, whereas one third consists of non-parenchymal cells: macrophages (Kupffer cells, endothelial cells, bile duct epithelial cells, natural killer (NK) cells and retinoid-storing hepatic stellate cells (HSCs) [1, 2].

Alternatively, a hepatic acinus is the functional unit of the liver [3, 4]. The acinus is more difficult to visualize than the lobule, but represents a unit that is of more relevance to hepatic function because it is oriented around the afferent vascular system. It is smaller than a portal lobule and can be defined as a diamond-shaped mass of liver parenchyma surrounding a portal tract. The acinus is divided into three zones. The periportal zone I is nearest to entering vascular supply and receives the most oxygenated blood. In contrast, the centrilobular zone III has the poorest oxygenation and is more sensitive to ischemic injury. Functionally, zone I hepatocytes are specialized for oxidative liver functions such as gluconeogenesis,  $\beta$ -oxidation of fatty acids and cholesterol synthesis, whereas zone III cells are more important for glycolysis, lipogenesis and cytochrome P-450 based detoxification. The functions of the liver are not limited to these, it is the most versatile organ of the human body capable of performing over 500 functions. The most important functions are summarized in Table 1.1.

**Table 1.1 Overview of the most important functions of the liver**

<b>Synthesis</b>	<b>Breakdown</b>	<b>Other functions</b>
<ul style="list-style-type: none"> <li>• Amino acid synthesis</li> </ul>	<ul style="list-style-type: none"> <li>• Insulin and other hormones</li> </ul>	<ul style="list-style-type: none"> <li>• Storage:</li> </ul>
<ul style="list-style-type: none"> <li>• Carbohydrate metabolism:               <ul style="list-style-type: none"> <li>-gluconeogenesis</li> <li>-glucogenolysis</li> <li>-glycogenesis</li> </ul> </li> </ul>	<ul style="list-style-type: none"> <li>• Hemoglobin, creating metabolites added to bile (bilirubin and biliverdin)</li> <li>• Toxic substances and medicinal products. Mostly conjugated.</li> </ul>	<ul style="list-style-type: none"> <li>-Glucose (in the form of glycogen)</li> <li>-vitamin A (1-2 years' supply)</li> <li>-vitamin D (1-4 months' supply)</li> </ul>
<ul style="list-style-type: none"> <li>• Protein metabolism: synthesis</li> </ul>	<ul style="list-style-type: none"> <li>• Protein metabolism: degradation</li> </ul>	<ul style="list-style-type: none"> <li>-vitamin B12 (1-3 years' supply)</li> </ul>
<ul style="list-style-type: none"> <li>• Lipid metabolism               <ul style="list-style-type: none"> <li>-cholesterol synthesis</li> <li>-lipogenesis: production of triglycerides</li> </ul> </li> </ul>	<ul style="list-style-type: none"> <li>• Conversion of ammonia to urea.</li> </ul>	<ul style="list-style-type: none"> <li>-iron and copper</li> </ul>
<ul style="list-style-type: none"> <li>• Coagulation factors I (fibrinogen), II (prothrombin), V, VII, IX, X and XI, protein C, protein S and antithrombin</li> </ul>		<ul style="list-style-type: none"> <li>• Immunological effects:               <p>The reticulo-endothelial system contains many immunological active cells</p> </li> </ul>
<ul style="list-style-type: none"> <li>• Production of bile for emulsifying fats</li> </ul>		<ul style="list-style-type: none"> <li>• Production albumin: osmolarity</li> </ul>
<ul style="list-style-type: none"> <li>• Insulin-like growth factor, important for growth in children and anabolic effects in adults</li> </ul>		<ul style="list-style-type: none"> <li>• Production of angiotensin: blood pressure control</li> </ul>
<ul style="list-style-type: none"> <li>• Thrombopoietin: production of platelets by bone marrow</li> </ul>		

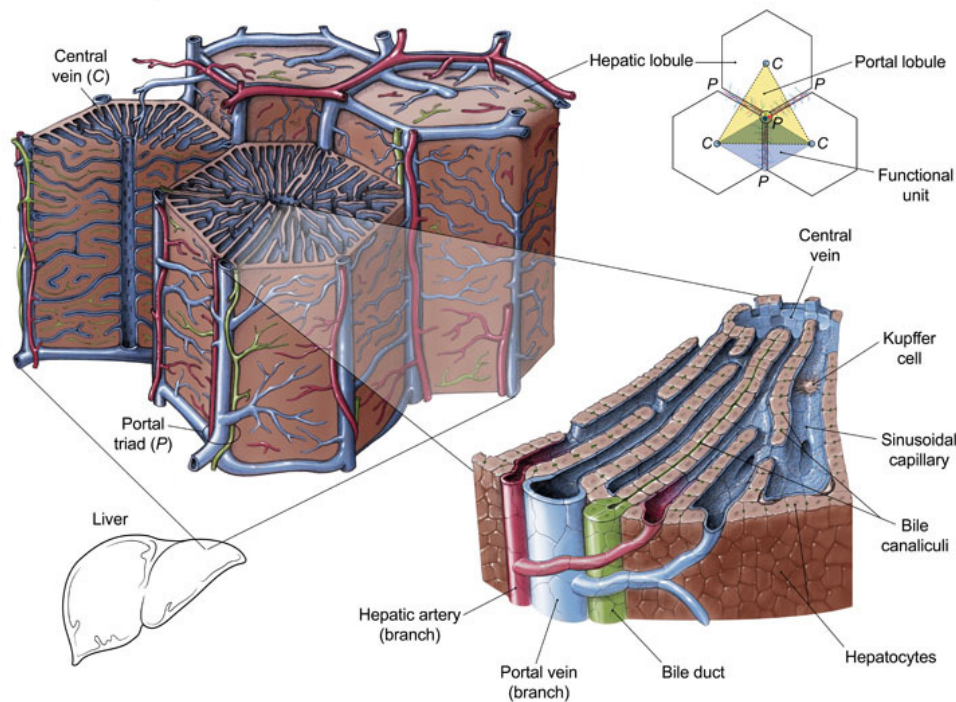


**Figure 1.1 Structural and functional unit of the liver.** Adapted from Liver Lobule Anatomy © UT Southwestern Medical Center.

### 1.1.1.2

#### Bilirubin metabolism

A specific function of the liver that necessitates special attention in the context of this thesis is the metabolism of bilirubin. This metabolism is determined by the reticulo-endothelial system (RES) (Figure 1.2) [5]. Eighty percent of bilirubin is formed from haeme each day. Haeme is a prosthetic group that consists of an iron atom contained in the center of a large heterocyclic organic ring called a porphyrin. The remaining twenty percent comes from red blood cell precursors destroyed in the bone marrow (ineffective erythropoiesis) and from other haeme proteins such as myoglobin, cytochrome, catalase and peroxidase. Iron is removed from the ring and the porphyrin ring is opened to form bilirubin. Bilirubin is soluble in lipid solvents, but almost insoluble in water. These characteristics enable it to cross cell membrane readily, but special mechanisms are needed to make it water-soluble for carriage in plasma by protein-binding mainly to albumin forming indirect or unconjugated bilirubin. In this form, it does not readily enter most tissues, nor it is filtered at the glomerulus.

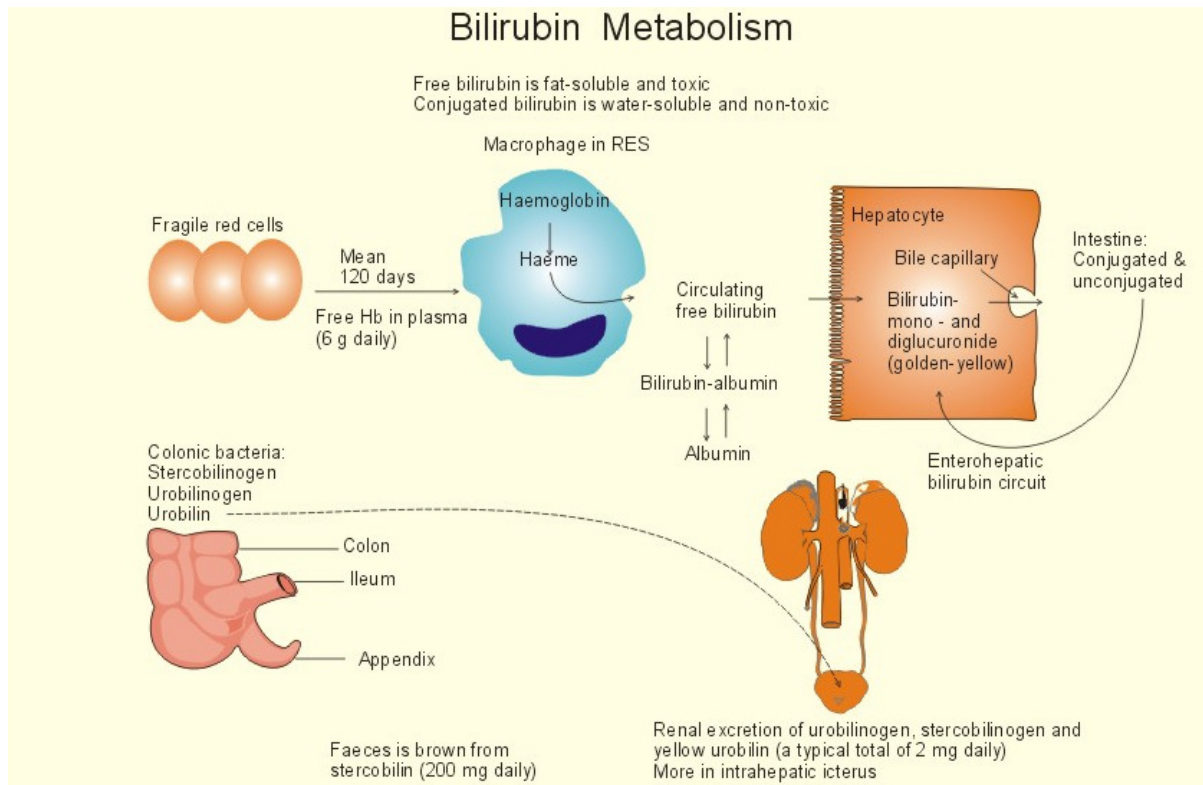


**Figure 1.2 Normal bilirubin metabolism.** The free bilirubin is fat-soluble and toxic. The conjugated bilirubin is water-soluble bilirubin-glucuronide and non-toxic. RES, reticulo-endothelial system; Hb, hemoglobin. Adapted from <http://www.1cro.com/medicalphysiology/chapter23/kap%2023.htm#1.%20Bile>

The second phase of the bilirubin metabolism is the hepatic uptake. The bilirubin-albumin complex appears to be associated by receptors on the plasma membrane of the hepatocytes. Bilirubin is taken up by a specific carrier (facilitated diffusion), leaving albumin in the plasma. Bilirubin is conjugated within the hepatocyte by the enzyme bilirubin-UDP-glucuronyl transferase with the formation of bilirubin-diglucuronide (direct bilirubin) making it water-soluble. Finally, bilirubin is secreted into bile against a high concentration gradient through a carrier mediated energy dependent process (active secretion).

Bile is a complex fluid containing water, electrolytes and a battery of organic molecules including bile acids, cholesterol, phospholipids and bilirubin that flows through the biliary tract into the small intestine. The bile acids present in bile are critical for digestion and absorption of fats and fat-soluble vitamins in the small intestine [6]. Bilirubin diglucuronide is degraded by bacterial action, mainly in the colon, being deconjugated and then converted into a mixture of compounds collectively termed urobilinogen (stercobilinogen). This is water-soluble and mostly excreted in the feces, but a small percentage (20%) is reabsorbed and then mostly re-excreted by the liver. After excretion, urobilinogen (colorless) is oxidized to urobilin (stercobilin) which gives stool its brown color. Some of the reabsorbed urobilinogen passes through the liver and into the systemic circulation and is then excreted in the urine (urobilin) giving it its yellow color [7-9].

The pathological accumulation of bilirubin (hyperbilirubinemia) is called jaundice which causes yellowish discoloration of the skin and sclera [10-11]. Jaundice can be classified into three forms. First, pre-hepatic jaundice occurs when the production rate of bilirubin is increased, exceeding the excretory capacity of the liver. Overproduction of bilirubin occurs in all forms of hemolytic anemia and, less commonly, in conditions where erythropoiesis is ineffective (e.g. pernicious anemia). Hematomas can also cause pre-hepatic jaundice and this results in an increase of unconjugated bilirubin in plasma. In this case, bilirubin is not excreted in urine, but urinary urobilinogen is increased.

A second form is hepatocellular jaundice. Hepatocellular damage due to viral hepatitis or toxins may interfere with the uptake of bilirubin, or with its conjugation or with secretion of conjugated bilirubin in bile. Therefore, both indirect and direct hyperbilirubinemia may occur in hepatocellular jaundice. Bilirubin and excess urobilinogen are found in urine. Finally, obstructive (cholestatic) jaundice is due to impaction of gallstones in the common bile duct or carcinoma of the head of pancreas or of the biliary tree. This jaundice is due to conjugated (direct) bilirubin and bilirubin is detected in urine.

#### 1.1.1.3 Liver fibrosis

Fibrosis represents the consequence of a sustained wound healing response to chronic liver injury from a variety of causes including viral, autoimmune, drug induced, cholestatic and metabolic diseases [12]. Cirrhosis can be defined as the end stage consequence of the hepatic parenchyma resulting in nodule formation and altered hepatic function. Up to 40% of patients with cirrhosis are asymptomatic and may remain so for more than a decade, but progressive deterioration is inevitable once complications develop including ascites, variceal hemorrhage or encephalopathy [13].

Hepatic stellate cells have been identified as the key cell type in the liver that is responsible for liver fibrosis [1,14]. Following chronic injury, these quiescent cells are 'activated' into their myofibroblastic counterparts. They are the source of an array of mediators, matrix molecules, proteases and their inhibitors that orchestrate the wound healing response in the liver. Myofibroblasts are proliferative, fibrogenic and contractile cells that lose their characteristic retinoid (vitamin A) droplets. Stellate cells activation is a complex but tightly programmed response that can be divided in three phases: initiation, perpetuation and resolution (Figure 1.3).

Initiation encompasses rapid changes in gene expression and phenotype that render the cells responsive to cytokines and other local stimuli. Cellular responses following initiation have been termed perpetuation, which encompasses those cellular events that amplify the activated phenotype through enhanced growth factor expression and responsiveness. This component of activation results from autocrine and paracrine stimulation, as well as accelerated extracellular matrix (ECM) remodeling. Finally, resolution of stellate cells activation represents an essential step towards reversibility of fibrosis [12].

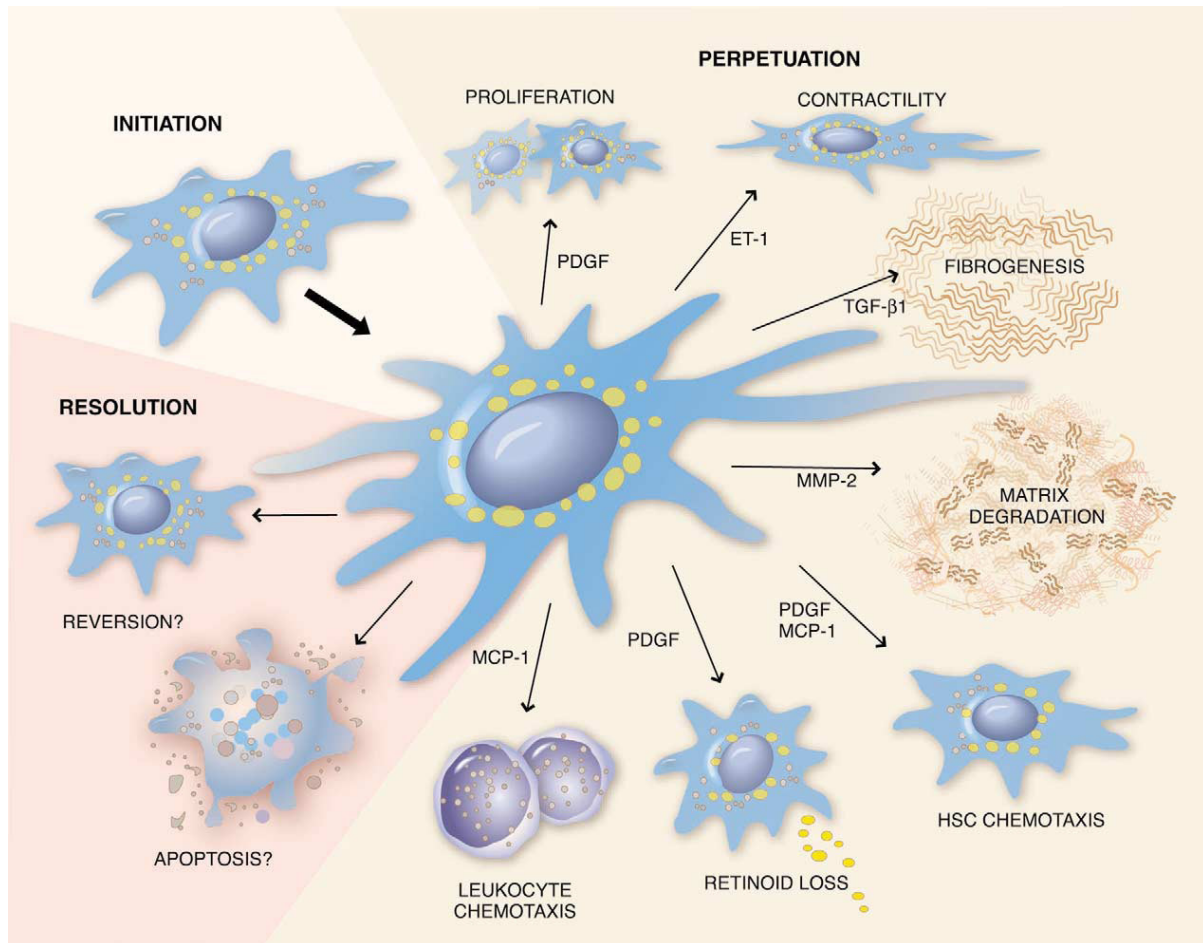


**Figure 1.3 Pathways of stellate cell activation and resolution during liver injury.** PDGF, Platelet-derived Growth Factor; ET-1, Endothelin-1; TGF- $\beta$ 1, Transforming Growth Factor-beta1; MMP-2, Matrix Metalloproteinase 2; MCP-1, Monocyte Chemoattractant Protein 1. Adapted from [12].

The earliest changes in stellate cells reflect paracrine stimulation by all neighboring cell types, including sinusoidal endothelium, Kupffer cells, hepatocytes, platelets and leukocytes.

- Sinusoidal endothelium: injury to sinusoidal endothelial cells stimulate production of a splice variant of cellular fibronectin, which has an activating effect on stellate cells. endothelial cells are also likely to participate in HSC activation via conversion of TGF- $\beta$ 1 from the latent to active, profibrogenic form [1].
- Kupffer cells: the promotion of fibrogenesis by Kupffer cells is associated with the release of a range of pro-fibrogenic cytokines (e.g. IL-1 $\beta$ , TGF- $\beta$ 1, TNF $\alpha$ ) and reactive oxygen species (ROS) as part of their inflammatory response to liver damage. Another means by which Kupffer cells can influence stellate cells is through secretion of matrix metalloproteinase 9 (MMP-9). MMP-9 can activate latent TGF- $\beta$ 1 which in turn can stimulate stellate cell collagen synthesis. Kupffer cells also produce eicosanoids including prostaglandins and thromboxanes. Eicosanoids modulate stellate cell

contractility, with thromboxanes typically promoting contraction and prostaglandins mediating relaxation [15].

- Hepatocytes: hepatocytes are, next to Kupffer cells, a potent source of ROS. Moreover, HSC phagocytose apoptotic hepatocytes and up-regulate TGF- $\beta$ 1 and also collagen-I mRNA [16]. Finally, activation of MMP-2 from HSCs requires interactions with hepatocytes [17].
- Platelets: these are the first cells recruited to the site of injury, playing an essential role in wound healing, as they limit blood loss by forming aggregates at the end of damaged blood vessels and act as a platform for the formation of fibrin to fibrinogen. Furthermore, their alpha-granules are rich in growth factors such as platelet-derived growth factor (PDGF), transforming growth factor  $\beta$ 1 (TGF- $\beta$ 1) and vascular endothelial growth factor (VEGF), which released upon activation are potent stimulators of fibroblast and other mesenchymal cells relevant for tissue healing [18].
- Leukocytes: in addition to Kupffer cells, many other leukocytes play an important role in HSC activation. Mast cells, derived from circulating basophils, are a source of pro-fibrogenic cytokines, including TGF- $\beta$ 1, PDGF and basic fibroblast growth factor (bFGF) [19]. Recent studies also indicate that the cells of the adaptive immune system also play an important role in fibrogenesis. In a carbon tetrachloride-induced mouse model of liver fibrosis, T-cell deficient mice develop severe liver fibrosis; however, in B-cell deficient mice, hepatic fibrosis was attenuated [20]. Finally, the anti-fibrotic effect of NK cells has been demonstrated to be mediated by their capability to specifically kill early-activated but not quiescent HSCs [21, 22].

Once activated by neighboring cell types the HSC is sensitive to and releases a broad range of cytokines that contributes to fibrogenesis:

- Platelet derived Growth Factor (PDGF): PDGF is the most potent mitogen for HSCs with effects in growth stimulation, chemotaxis and intracellular signaling [23]. NADPH oxidase is expressed in HSCs and produce ROS via activation of NADPH oxidase in response to PDGF. ROS further induce HSC proliferation through the phosphorylation of p38 MAPK [24]. In addition, retinoid loss following activation of HSCs is PDGF-dependent [25].
- Endothelin-1 (ET-1): a number of vasoactive molecules can trigger contractile response in HSCs with ET-1 being the most potent constrictor. Activated HSCs gain contractile function, which contributes to the intrahepatic hemodynamic changes in cirrhosis [26]. Activated stellate cells express  $\alpha$ -smooth muscle actin, a marker of non-muscle cell contractility.
- Transforming Growth factor beta1 (TGF- $\beta$ 1): in stellate cells TGF- $\beta$ 1 up-regulates the expression of collagens I, II and IV, fibronectin and laminin and accelerates transformation of quiescent stellate cells to myofibroblasts. In fibroblasts it reduces collagenase and stromelysin gene expression and up-regulates the expression of protease inhibitors such as tissue inhibitor of matrix metalloproteinase 1 (TIMP-1) and plasminogen activator inhibitor, which may protect the matrix from degradation [27].



- Matrix metalloproteinase-2 (MMP-2): because MMP-2 can degrade type IV collagen, these cells appear to be capable of localized pericellular degradation of normal liver matrix (which contains collagen IV), while also having a more global effect on inhibiting degradation of the fibrillar collagens found in fibrotic liver. The disruption of the interaction of HSCs with normal liver matrix could be an important aspect of promoting further progression of liver fibrosis [28].
- Monocyte chemoattractant protein 1 (MCP-1): MCP-1 plays a role in the recruitment and maintenance of the inflammatory infiltrate during liver injury [29]. It has been recently shown that hepatitis C patients (HCV) that are genetically predisposed to greater amounts of MCP-1 seem to be more prone to hepatic inflammation and fibrogenesis [30].

### 1.1.2 Alcoholic liver disease

Alcohol liver disease (ALD) is damage to the liver and its function due to alcohol abuse and usually occurs after years of excessive drinking. Changes in the liver include fatty liver, inflammation and cirrhosis [31, 32]. Moreover, chronic alcohol abuse is an established risk factor for the development of hepatocellular carcinoma (HCC) in patients with liver cirrhosis [33, 34]. Evidence suggests that daily ethanol consumption exceeding 40-80g/d for men and 20-40g/d for women for 10-12 years may lead to ALD.

The susceptibility of individuals to the toxic effects of alcohol consumption may involve complex interactions between genes and the environment. To date, genes encoding the principal alcohol-metabolizing enzymes, alcohol dehydrogenase (ADH) and aldehyde dehydrogenase (ALDH), are the only genes that have been firmly linked to vulnerability to alcoholism and possible risk for ALD [35, 36]. In addition, reports indicate that polymorphisms in these genes observed among Asians, African Americans and Caucasians are important biological factors contributing to differences in cell and tissue damage, intolerance to alcohol or both [36].

Ethanol produces a wide spectrum of hepatic injuries. The most characteristic being interference in lipid metabolism. Hepatic lipid homeostasis is maintained by balanced lipid synthesis, catabolism ( $\beta$ -oxidation) and secretion. Alcohol metabolism changes the redox state of the liver, which leads to alterations in hepatic lipid, carbohydrate, protein, lactate and uric acid metabolism. Ethanol is metabolized predominantly in the liver via two well-characterized pathways [37-39]. The first involves ADH, an  $\text{NAD}^+$ -dependent enzyme located in the hepatic cytosol, which catalyzes the conversion of ethanol to acetaldehyde, a potent toxicant that accounts for the most toxic effects of ethanol. Acetaldehyde produced from ethanol is further converted to the non-toxic acetate by a mitochondrial ALDH [40]. Both steps are coupled with the reduction of  $\text{NAD}^+$  to NADH. The increased NADH/ $\text{NAD}^+$  ratio affects the metabolism of carbohydrates and lipids in cytoplasm and mitochondria. This leads to impaired gluconeogenesis and diminished substrate flow through the citric acid cycle, with acetyl-CoA diverted to fatty acid synthesis. The NADH-induced inhibition of mitochondrial fatty acid  $\beta$ -oxidation, combined with increased fatty acid synthesis, contributes to the pathogenesis of fatty liver, the initial stage of ALD. Besides ADH, another enzyme that affects ethanol action is CYP2E1, a microsomal enzyme that metabolizes vitamin A, acetaminophen and protease inhibitors. CYP2E1 activity is induced 2-10 fold after

chronic ethanol exposure and has been implicated as the source of oxidative stress [41] (Figure 1.4).

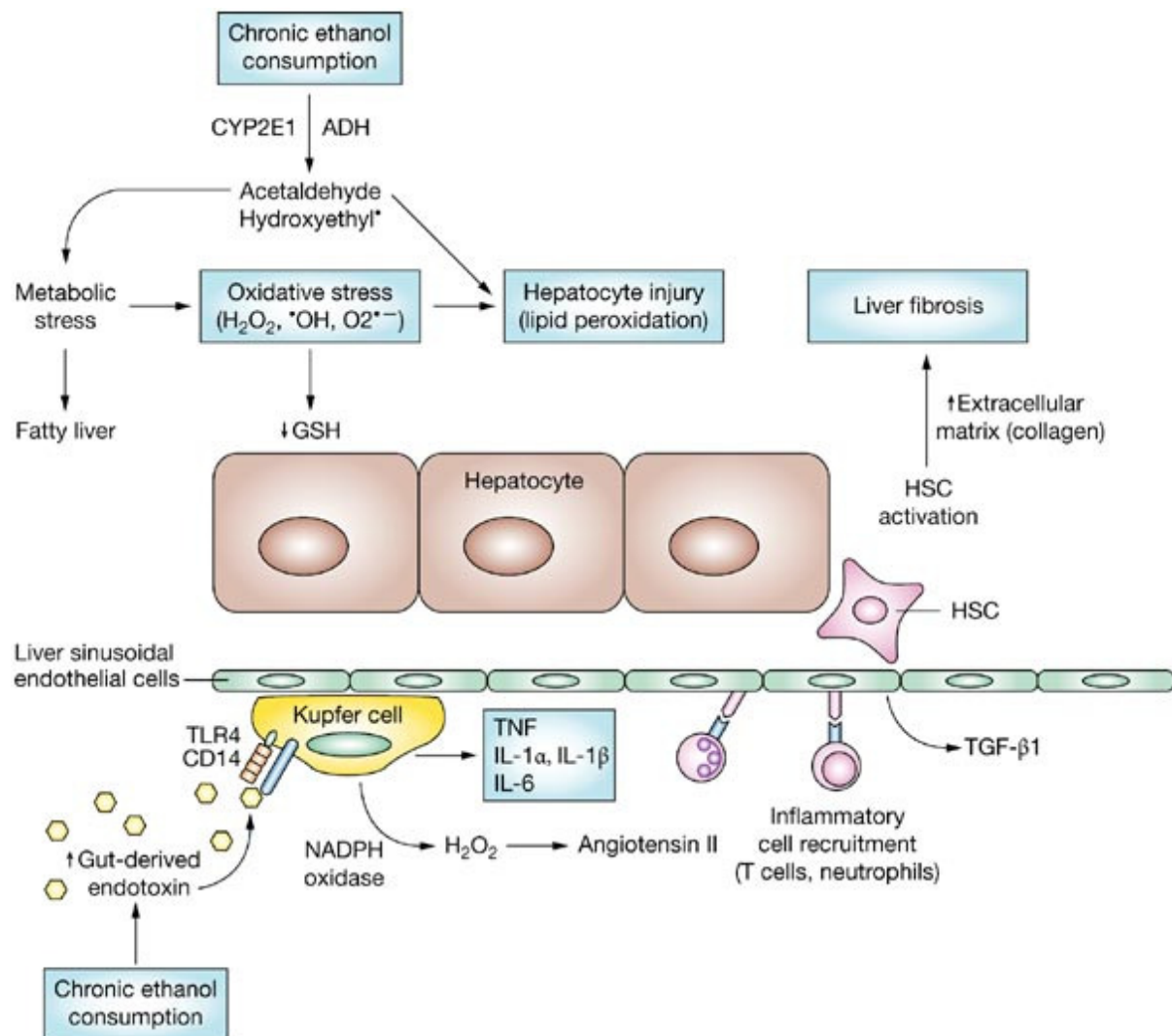


**Figure 1.4 The current view of the pathogenesis of alcohol-induced liver inflammation and the role of the innate immune system.** ADH, alcohol dehydrogenase; ASH: alcoholic steatohepatitis; CD14, monocyte differentiation antigen; CYP2E1, cytochrome P450 2E1; HSC, hepatic stellate cells; IL, interleukin; ROS: reactive oxygen species; TLR, Toll-like receptor; TGF, transforming growth factor, TNF, tumor necrosis factor. Adapted from [158]

Alternatively, chronic ethanol-mediated microbial proliferation enhance the passage or release of endotoxins into the intestinal lumen, which are later transported to liver. However, when excess amount of endotoxin are not cleared efficiently by the liver and accumulate in blood circulation, Kupffer cells, are activated, leading to the release of various pro-inflammatory cytokines, chemokines, and other factors. Activated kupffer cells express phagocytic NADPH oxidase, which generates large amounts of ROS (including  $H_2O_2$ ). It has been shown that these NADPH oxidase-derived ROS play a major role in angiotensin-II induced activation of HSCs [42].

The histological features of alcohol-induced hepatic injury vary, depending on the extent and stage of injury. These may include steatosis, lobular inflammation, periportal fibrosis, Mallory bodies, nuclear vacuolation, bile ductal proliferation and fibrosis or cirrhosis [43]. However, these may co-exist in the same biopsy, and are not individually exclusive to ALD.

### 1.1.3 Viral liver disease

#### 1.1.3.1 General aspects

Chronic viral hepatitis is a major global health problem. In particular hepatitis B and C have high prevalences, especially in developmental countries. Of the approximately 2 billion people who have been infected worldwide with the hepatitis B virus (HBV), more than 350 million are chronic carriers [44]. HBV infection accounts for 0.6 to 1.2 millions death each year [45, 46]. In addition, the hepatitis C virus (HCV) is the cause that approximately 130-170 million people are chronically infected [47]. An overview of all hepatic viruses is given in Table 1.2 and a short description of each is given in the following paragraphs (information World Health Organization, [www.who.int](http://www.who.int)). In addition to the hepatitis viruses, other viruses that also can cause hepatitis include herpes simplex, cytomegalovirus, Epstein-Barr virus or Yellow fever [48].

**Table 1.2 Hepatitis viruses**

	<b>Hepatitis A</b>	<b>Hepatitis B</b>	<b>Hepatitis C</b>	<b>Hepatitis D</b>	<b>Hepatitis E</b>
Transmission	Enteric	Parental	Parental	Parental	Enteric
Classification	Picornavirus	Hepadnavirus	Hepacivirus	Deltavirus	Hepevirus
Genome	+ssRNA	+dsDNA	+ssRNA	-ssRNA	+ssRNA
Antigens		HBsAg, HBeAg	Core antigen	Delta antigen	
Incubation period	15-45 days	45-160 days	15-150 days	30-60 days	15-60 days
Chronicity	No	Yes (uncommon)	Yes (common)	Yes – with hepatitis B	No

Hepatitis A virus (HAV) is a self-limited disease which results in fulminant hepatitis and death only in a small proportion of patients. However, it is a significant cause of morbidity and socio-economic losses in many parts of the world. Transmission of HAV is typically by the faecal-oral route. Infections occur early in life in areas where sanitation is poor and living conditions are crowded. The course of hepatitis A may be extremely variable. Patients with inapparent or subclinical hepatitis have neither symptoms nor jaundice. Children generally belong to this group. These asymptomatic cases can only be recognized by detecting biochemical or serologic alterations in the blood. The severity of the disease increases with age at time of infection.

Hepatitis B is a potentially life-threatening liver infection. It is a major global health problem and the most serious type of viral hepatitis. It can cause chronic liver disease and puts people at high risk of death from cirrhosis of the liver and liver cancer. A vaccine against hepatitis B has been available since 1982. Hepatitis B vaccine is 95% effective in preventing HBV infection and its chronic consequences, and is the first vaccine against a major human cancer. HBV can also cause a chronic liver infection that can later develop into cirrhosis of the liver or liver cancer. Hepatitis B virus is transmitted between people by contact with blood or other body fluids (i.e. semen and vaginal fluid) of an infected person. Modes of transmission are the same for the human immunodeficiency virus (HIV), but HBV is 50 to 100 times more infectious. Unlike HIV, HBV can survive outside the body for at least 7 days. During that time, the virus can still cause infection if it enters the body of a person who is not infected or vaccinated.

Hepatitis C is spread primarily by direct contact with human blood and mainly transmitted parenterally and vertically (from mother to child). The major causes of HCV infection worldwide are use of unscreened blood transfusions and re-use of needles and syringes that have not been adequately sterilized. At present, no vaccine against HCV is available. Chronic hepatitis C can be successfully treated with combination therapy including pegylated forms of interferon plus ribavirin

The hepatitis D virus (HDV) cannot replicate and infect someone unless the person is already infected with the HBV. HDV requires the outer coating of the HBV, called the surface antigen, in order to reproduce itself in a human host. The virus currently infects 15 million children worldwide and is most common among injecting drug users and in countries bordering the Mediterranean Sea. HDV infection symptoms are similar to those of hepatitis B.

The hepatitis E virus (HEV) is transmitted via the faecal-oral route. Hepatitis E is a waterborne disease, and contaminated water or food supplies have been implicated in major outbreaks. The risk factors for HEV infection are related to poor sanitation in large areas of the world, and HEV shedding in faeces. In general, hepatitis E is a self-limiting viral infection followed by recovery.

#### 1.1.3.2 Host mechanisms

Host mechanisms in viral hepatitis depend on the function of the innate immune system [49]. Pathogens such as hepatitis viruses are recognized by 'pattern recognition receptors' which bind double-stranded RNA [50, 51]. The most important receptors during virus infection are the Toll-like receptors (TLR) 3, 7, 8 and 9 as well as the RNA-helicase RIG-I [52]. The clinical course of hepatitis viral infection depends on the function of CD8 T cells [53, 54]. Those cells limit the spread of the virus and protect against persistent virus infection. If however, the viral infection has become persistent, the activation of CD8 T cells contribute to tissue injury [55, 56].

The priming and function of CD8 T cells critically depend on the activity of dendritic cells [57]. Expression of Programmed Death 1 (PD-1) correlated with exhaustion of T cell function

during chronic HCV infection, indicating that dysregulation of the receptor contributes to T-cell dysfunction during persistent HCV infection. In addition, polymorphisms in the IL-10 gene have similarly been shown to influence the outcome of HCV infection, whereby enhanced IL-10 activity fosters the development of the persistence of the virus [58, 59]. In absence of IL-10, the expansion of CD8 T cells is enhanced [60, 61]. Accordingly, blockade of IL-10 was followed by improved virus control [62]. CD8 T cells express perforins and interferon-gamma (IFN- $\gamma$ ). IFN- $\gamma$  exerts a direct antiviral action [63], whereas the role of perforins in human hepatitis remains elusive at present.

The clinical course of an infection is not only a function of the immune system. Liver injury triggers the production of nitric oxide (NO) [64, 65]. In some cell types, NO triggers apoptosis and is therefore likely to be involved in virus control [65-67]. During inflammation, NO is in large part produced by inducible NO synthase (iNOS) [64, 65]. Finally, NO influences the microcirculation, which in turn might affect the control of the virus [68-70].

### 1.1.3.3 Mechanisms of fibrosis in hepatitis C

The immune activation and modulation outlined in previous section is a key mechanism in the pathogenic process that leads to tissue injury, scarring and ultimately cirrhosis. TLRs will induce pro-inflammatory cytokines such as interleukins and TNF $\alpha$  and cytotoxic CD8 T cells will cause tissue damage through perforins, Fas/FasL and TNF pathways in the context of inefficient viral clearance [71].

Despite the key role of the immune system, a great deal of work has now demonstrated that HCV can directly mediate apoptosis, stellate activation and liver damage. It is well known that engulfment of apoptotic bodies by phagocytes, including stellate cells, is profibrogenic [72]. Levels of caspases are consistently up-regulated in HCV-patients and correlate with both inflammatory and fibrotic liver injury [73, 74]. Apoptosis up-regulates collagen and TGF- $\beta$ 1 genes in stellate cells and a key mechanism behind HCV-induced apoptosis occurs by way of external Fas/FasL mediated pathways [75, 76].

HCV can also directly stimulate fibrogenesis by ways of interactions between infected hepatocytes, viral proteins and HSCs. Battaller and colleagues [77] showed *in vitro* that core and NS3 viral proteins were able to increase intracellular calcium concentrations and ROS production. As a consequence, infection of HSCs with HCV proteins (NS3-NS5) led to a marked increase in pro-inflammatory chemokines and adhesion molecules (IL-8, MCP-1 and ICAM-1) (Figure 1.5A). These molecules participate in the recruitment and activation of lymphocytes [78]. Additionally, HCV-infected hepatocytes demonstrated a threefold increase in TGF- $\beta$ 1 mRNA and a sixfold increase in TGF- $\beta$ 1 protein levels compared to non-infected controls [79] (Figure 1.5B). In the activated HSCs, there was a shift to a more fibrogenic state with increases in connective tissue growth factor (CTGF), procollagen  $\alpha$ 1 and TIMP-1. There is also an increase in MMP-2 activity. As mentioned earlier, MMP-2 is profibrogenic because of its involvement in the degradation of the basal lamina [1]. A substantial down-regulation of MMP-3 and -13 also occurs. Both are involved in the degradation of fibril-forming collagens, whereas MMP-3 is also an activator of other MMPs [80]. Finally, an

additional HCV protein, E2, is of importance in HCV-related fibrogenesis by way of up-regulation of the destructive metalloproteinase MMP-2 (Figure 1.5C) [81].

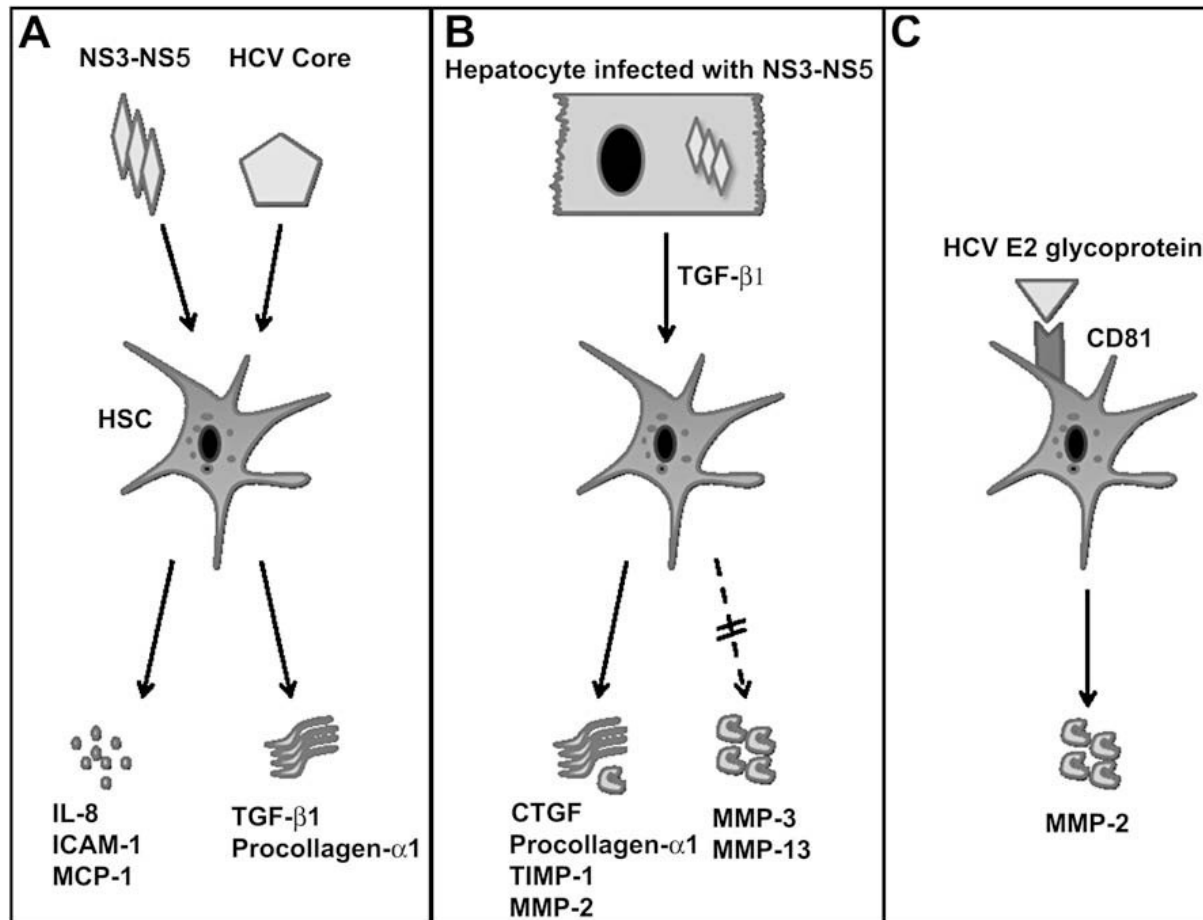


**Figure 1.5 Direct and indirect pro-fibrogenic interactions between the HCV and HSCs.** HCV, Hepatitis C virus; IL, interleukin; ICAM, intercellular adhesion molecule; MCP, monocyte chemoattractant protein; TGF, transforming growth factor; CTGF, connective tissue growth factor; TIMP-1, Tissue Inhibitor of metalloproteinases-1; MMP, matrix metalloproteinase. Adapted from [159]

The liver biopsy of hepatitis C patients is usually interpreted in the Metavir scoring system [82]. The scoring consist of using a grading and staging system. The grade gives an indication of the activity or amount of inflammation and the stage represents the amount of inflammation and the stage the amount of fibrosis.

The grade is assigned a number based on the degree of inflammation, which is usually scored from 0-3 with 0 being no activity and 3 considered severe activity. The amount of inflammation is important because it is considered a precursor to fibrosis.

The fibrosis score is also assigned a number from 0-4:

- 0 = no scarring

- 1 = minimal scarring
- 2 = scarring has occurred and extends outside the areas in the liver that contains blood vessels
- 3 = bridging fibrosis is spreading and connecting to other areas that contain fibrosis
- 4 = cirrhosis or advanced scarring of the liver

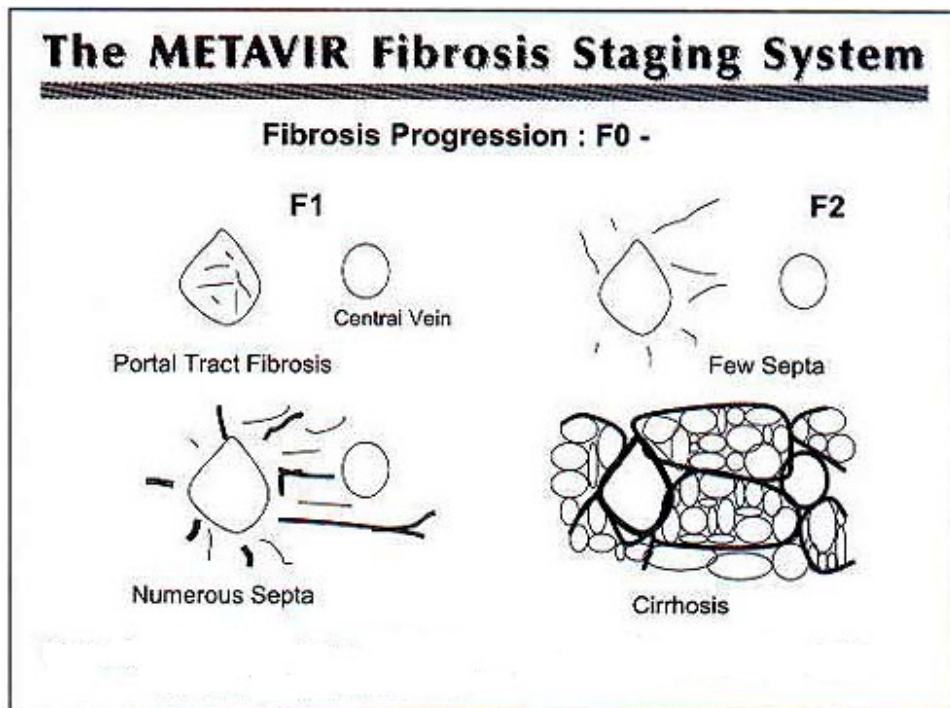


**Figure 1.6 illustration of the METAVIR Fibrosis Staging System.** Adapted from <http://www.msgh.org.my/resources/managementhepatitisc2.htm>

#### 1.1.4 Cholestatic liver disease

In the normal liver, a finely balanced regulation of bile acid uptake, efflux and biosynthesis exists. The farnesoid X receptor (FXR) regulates bile acid biosynthesis and expression of bile salt export pump (BSEP), found on the canalicular membrane of the hepatocyte. In the presence of cholestasis, regardless of etiology, there is a rise in serum bile acids [83]. Cholestatic liver disease include biliary atresia, hereditary forms of cholestasis, primary biliary cirrhosis (PBC) and primary sclerosing cholangitis (PSC).

The pathogenesis of biliary atresia remains poorly understood. The condition manifests in the first few weeks of life with jaundice. Pathologically, the condition is marked by a progressive destruction of the extrahepatic biliary tree. It is not known what causes the inflammation to the extrahepatic ducts, although IFN- $\gamma$  has been identified to play a central role in the progression of biliary atresia and may be a target for treatment [84].

Progressive familial intrahepatic cholestasis, type 1 (PFIC1) is marked by elevated serum bile salts. Patients with PFIC1 have a deficiency of familial intrahepatic cholestasis 1 (FIC-1), a P-type adenosine triphosphatase whose exact function remains poorly defined. FIC-1 expression correlate with FXR activity, thus, patients with an absence of FIC-1 have decreased FXR activity resulting in enhanced ileal resorption of bile salts through increased

expression of ileal lipid binding protein and short heterodimer protein [85]. Rare hereditary forms of cholestasis are Arthrogyrosis-renal dysfunction-cholestasis syndrome [86] and McCune-Albright syndrome [87], both associated with neonatal jaundice.

PBC is an auto-immune disease that develops in genetically susceptible individuals exposed to an environmental trigger or infectious agent that results in loss of immune tolerance to the disease antigen, the dihydrolipoamide acetyltransferase component of pyruvate dehydrogenase complex (PDC-E2). Viral nucleic acids sequences have been cloned from the lymph nodes of patients with PBC suggesting that infection with this virus may be associated with the development of PBC [88, 89]. The identified virus was the human betaretrovirus. Molecular mimicry is another possible mechanism for triggering autoimmunity. There is a short sequence on PDC-E2 that is particularly antigenic because it is exposed on to the molecule's surface. Several groups have implicated exposure to *E.coli* as the source for molecular mimicry and the production of anti-mitochondrial antibodies (AMA) [90]. These AMA are found in 95% of patients with PBC and the pathogenic role of these autoantibodies remains unknown. Additionally, an altered form of PDC-E2 gives rise to breakdown of the B and T cell tolerance to self PDC-E2 and leads to the development of cross-reactivity to native self [91].

In PSC, ICAM-1 plays a potential role in the pathogenesis. Patients with PSC have increased serum levels of soluble ICAM-1 and ICAM-1 is expressed on proliferating bile ducts in late stages of PSC [92]. Animal models suggest that the Mdr2 protein also play an important role in PSC [93]. *Mdr2*<sup>-/-</sup> mice do not secrete phospholipids, leading to high concentrations of free bile salts. This toxic environment weakens tight junctions allowing leakage of bile salts into the portal area, inducing inflammation with neutrophils and CD4 and CD8 positive lymphocytes. Myofibroblasts are activated producing concentric rings of fibrosis. A link with mucoviscidose has been established, patients with PSC have a much higher frequency of mutations in the cystic fibrosis gene product than disease controls [94].

### **1.1.5 Non-alcoholic fatty liver disease**

Non-alcoholic fatty liver disease (NAFLD) is recognized as one of the commonest liver disorders seen by hepatologists [95]. It is estimated that one in three adults has NAFLD. The looming pandemic of obesity and type 2 diabetes coupled with the realization that NAFLD is common in the pediatric population suggests that this prevalence is likely to increase further. Closely associated with the metabolic syndrome, the pathophysiology of NAFLD is centrally related to insulin resistance (IR). The NAFLD spectrum ranges from simple steatosis (fatty liver) to non-alcoholic steatohepatitis (NASH) characterized by liver cell injury, inflammation and fibrosis to cirrhosis, liver failure and hepatocellular carcinoma. Since these histological features are identical to those seen in alcoholic liver disease, the exclusion of excessive alcohol intake, typically less than 20 g per day for women and 30 g per day per men, is required. Post-mortem and liver biopsy in obese cohorts undergoing bariatric surgery have demonstrated that only around 10-20% of even morbidly obese patients develop more than simple steatosis [96, 97].

In recent years, it has become clear that mechanisms of liver injury and fibrosis in NASH are related to free fatty acid (FFA)-induced cytokine, oxidative and endoplasmic reticulum stress-



mediated injury and non-inflammatory mediators of fibrosis [98-100]. TNF $\alpha$  was the first pro-inflammatory cytokine detected in adipose tissue and is involved in the regulation of IR. Increased TNF $\alpha$  is likely the result of metabolic disturbances and caused by lipid products such as FFAs [101]. On the other hand, endotoxin and related products mainly derived from the gut could also represent a trigger for inflammatory responses [102]. Besides TNF $\alpha$ , other cytokines such as IL-6 and C-reactive protein (CRP) also correlate positively with obesity and body mass index (BMI), further proving the concept that obesity and IR might reflect inflammatory conditions [103]. Visceral fat has been demonstrated as an important site for IL-6 secretion in humans. IL-6 production in abdominal adipose tissue is at least 3-times higher compared with subcutaneous adipose tissue, thereby potentially contributing to hepatic IR [104].

Another important cytokine in the context of NAFLD is adiponectin. It is secreted primarily from adipose tissue, however weight loss causes an increase in circulating adiponectin levels [105]. Pro-inflammatory cytokines such as TNF $\alpha$  and IL-6 suppress transcription of adiponectin, but adiponectin itself has an inhibitory effect on TNF $\alpha$  and IL-6 synthesis providing it anti-inflammatory properties [106, 107]. Conversely and adding to this property, adiponectin induces the expression of IL-10, a key anti-inflammatory cytokine, and IL-1 receptor antagonist [108, 109]. By such a pathway, adiponectin could not affect macrophage function which is the primary source of IL-10, but could furthermore limit overwhelming TNF $\alpha$  synthesis in human adipose tissue.

Several years ago, the 'two-hit hypothesis' was put forward to explain the development of NAFLD and the progression from simple steatosis to NASH [110]. It was proposed that the accumulation of lipids in the hepatocytes due to insulin resistance represents the 'first hit' and is the key pathogenic factor for the development of hepatic steatosis. The 'second hit' leads to hepatocyte injury, inflammation and fibrosis, possibly related to expression of pro-inflammatory cytokines as outlined above. Other important mechanisms of the 'second hit' not yet discussed are the appearance of oxidative stress and mitochondrial dysfunction.

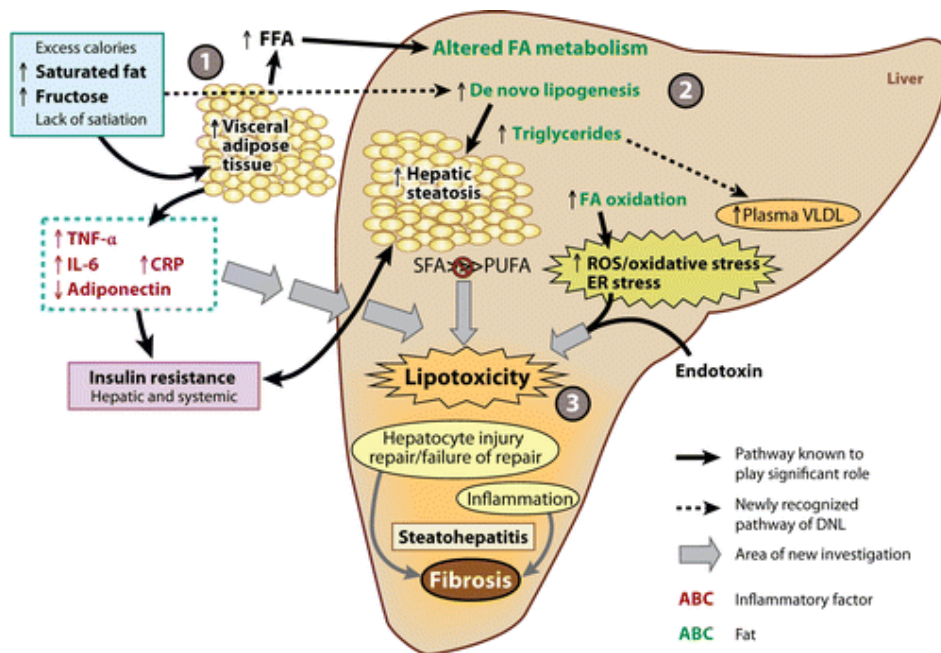


**Figure 1.7 Overview of the pathogenesis of non-alcoholic steatohepatitis with indication of recent findings and new fields of investigation.** TNF, tumor necrosis factor; IL, interleukin; CRP, C-reactive protein; FFA, Free Fatty Acids; FA, Fatty Acid; VLDL, very low density lipoproteins; ROS, reactive oxygen species; ER, endoplasmic reticulum; SFA, saturated fatty acids; PUFA, poly-unsaturated fatty acids. Adapted from [160].

Triglyceride accumulation might induce cytotoxicity either directly or through sensitization to other agents, as steatosis increases the vulnerability of the liver to oxidative stress. Multiple sources of oxidative stress have been identified and include mitochondrial dysfunction, hepatic cytochrome CYP2E1, beta-oxidation by peroxisomes in mitochondria and recruitment of inflammatory cells [111]. One of the consequences of oxidative stress is the activation of HSCs, leading to fibrogenesis. Reactive aldehydes induce nuclear translocation of JNK in HSCs and induce expression of TGF- $\beta$ 1 and MCP-1 [112].

The second hit hypothesis is currently being reconsidered (Figure 1.7). The accumulation of fat in the form of triglycerides is viewed as a less harmful way to cope with the overflow of fatty acids associated with the metabolic alterations underlying fatty liver. In predisposed subjects, this process leads to accumulation of FFAs and to lipids that are more toxic to cells, such as ceramids, leading to lipotoxicity and resulting in chronic liver damage [113]. In conclusion, it is clear that HSC fibrogenesis and NASH have several partners in common. All inflammatory mediators that influence hepatic lipid metabolism have been summarized in Table 1.3.

The altered glucose metabolism also contributes to HSC proliferation because insulin targets different signaling pathways involved in fibrogenesis. Insulin resistance will induce the expression of insulin receptors and receptors for insulin-like growth factor-I, both are mitogenic for HSCs via activation of phosphatidylinositol 3-kinase and ERK [114]. CTGF not only mediates HSC activation and extracellular matrix production, but it also mediates the profibrogenic activity of TGF- $\beta$ 1 [115]. Another group of possible profibrogenic factors involved in the progress of NASH are the receptor for advanced glycation end products (RAGE), exclusively expressed by HSCs [116].

**Table 1.3 Inflammatory mediators that influence hepatic lipid metabolism**

Mediator	Effect on inflammation	Effect on hepatic lipid metabolism	Net effect on hepatic lipids	Effect on insulin sensitivity
Adiponectin	Blocks TNF $\alpha$ synthesis and release	Via <b>AMPK</b> : opposes lipogenesis  Via <b>PPAR-<math>\alpha</math></b> : stimulates oxidation pathways	Decrease	Increase sensitivity (opposes insulin resistance)
PPAR- $\alpha$	Anti-inflammatory (blocks NF-kappaB activated gene transcription)	Stimulates oxidation pathways	Decreases	Increased sensitivity
IL-1 $\beta$	Inflammatory mediator	Downstream effects on cholesterol turnover favoring accumulation	Potentially increases cholesterol	Not shown
MCP-1	Activates macrophage recruitment, TNF $\alpha$ synthesis and release	Stimulates lipogenesis	Possible increase (shown <i>in vitro</i> )	Not shown
TNF- $\alpha$	Mediates, propogates inflammation (via NF-kappaB, IL-6); suppresses adiponectin expression	Stimulates lipogenesis; impairs mitochondrial $\beta$ -oxidation and MTTP-dependent formation of VLDL	Not shown	Suspected mediator of insulin resistance
IL-6	Pro-inflammatory, but hepatoprotective/proproliferative on hepatocytes	Stimulates lipogenesis	Increases	Impairs insulin receptor signaling
Oxidative stress	Activates redox-sensitive pathways: JNK, NF-kappaB, PKC	Decreases VLDL formation/secretion	Expected to increase	Impaired via JNK-serine/threonine phosphorylation of insulin receptor
ER Stress	ROS generation; JNK activation	Stimulates lipogenesis	Causal association not shown	Impaired via JNK-serine/threonine phosphorylation of insulin receptor
Endotoxin	TLR4-dependent activation of NF-kappaB	Possible downstream effects via TNF $\alpha$ and IL-6	Possible worsening of steatosis severity	Not shown

AMPK, AMP protein kinase; ER, endoplasmic reticulum; IL: interleukin; JNK, c-Jun N-terminal protein kinase; MCP-1, monocyte-chemoattractant protein-1; MTTP, microsomal triglyceride transport protein; PPAR- $\alpha$ , peroxisome proliferation activated receptor- $\alpha$ ; PKC, protein kinase C; ROS, reactive oxygen species; TLR, Toll-like receptor; TNF $\alpha$ , tumor necrosis factor- $\alpha$ ; VLDL, very low density lipoprotein. Adapted from [158]

The histological scoring diagnosis system that is used for non-alcoholic fatty liver disease is the Kleiner and Brunt classification [117]. In contrast to the METAVIR-score used in HCV-patients, fibrosis staging is subdivided. Fibrosis scores for stage 1 were extended to include a distinction between delicate (1A) and dense (1B) perisinusoidal fibrosis, and to detect portal-only fibrosis, without perisinusoidal fibrosis (1C). Minimal steatosis (score 0) (under 5%) was separated from mild (5%-33%) steatosis (score 1), moderate (>33%-66%) steatosis (score 2) and severe (>66%) steatosis (score 3). Evaluation of ballooning was limited to three categories (none, few and many) and correspond to a respective score of 0, 1 and 2. Lobular inflammation was assessed semi-quantitatively as the number of inflammatory foci at a magnification of 200x. Four categories can be distinguished, no foci (score), <2 foci per 200x field (score 1), 2-4 foci per 200x field (score 2) and >4 foci per 200x field (score 3). The summed score of the three latter characteristics provide an NAFLD activity score (NAS) [118-120]. Cases with NAS of 0 to 2 are largely considered as patients with simple steatosis; on the other hand cases with scores of  $\geq 5$  are diagnosed as steatohepatitis. Cases with activity scores of 3 and 4 are considered as being part of an intermediate stage and are called borderline NASH patients.

Pediatric cases use the same classification, although inter-observer agreement in scoring the features was lower. Pediatric cases include a significant proportion with only periportal fibrosis [121-123]. This feature is considered unusual in adults, although it has been reported [124]. Pediatric biopsy specimen also showed less lobular inflammation, less ballooning, and only rare Mallory's hyaline when compared to adult cases.

### **1.1.6 Hepatocellular carcinoma**

Hepatocellular carcinoma (HCC) is a malignant tumor arising from hepatocytes. Worldwide, it ranks fifth among the solid tumors and it is the third cause of cancer-related mortality in males with ~500 000 deaths per year [125]. It is most prevalent in Asia and Africa. In Africa, HCC is mostly related to chronic HBV infection, in Asia to hepatitis B or C. The incidence in Europe and the USA is considerably lower with an annual incidence between 1-10 per 100 000, but it is rising mainly due to HCV infection [126]. More recently, NASH is emerging as another important risk factor for HCC [127]. In more than 80% of the cases, HCC is associated with cirrhosis or advanced fibrosis [128, 129]. In the absence of cirrhosis, aflatoxins (mostly combined with HBV), genetic disorders (such as Tyrosinosis) and particular drugs (e.g. anabolic steroids) are known risk factors associated with HCC [130].

Although cirrhosis is associated with the development of HCC, the molecular basis for the cancer-promoting effect of cirrhosis remains far from clear. It is hypothesized that the process of recurrent liver cell necrosis and regeneration with increased cell turn-over, renders hepatocytes more sensitive to the adverse effects of other mutagenic agents. Both genetic and epigenetic changes may occur, eventually leading to the subsequent formation of dysplastic foci, nodules and finally hepatocellular carcinoma [131, 132]. From a pathophysiological perspective, oxidative stress represents an important pathway by which viruses or other risk factors exert their carcinogenic properties.

Oxidative stress is caused by an imbalance between the production of ROS and the ability to detoxify these reactive intermediates or to easily repair the resulting damage. ROS are

involved in the transcription of a large series of cytokines and growth factors, which in turn, can contribute to further production of ROS. Hepatocyte mitochondria and cytochrome P450 enzymes, endotoxin-activated Kupffer cells and neutrophils represent the main sources of free radicals. These free radicals will alter the redox state, and the cellular tissue damage may be potentiated by an associated decrease of antioxidant and energetic reserves [133]. To counteract the effect of oxidative stress, cells have developed two important defense mechanisms: redox active sulphydryl systems including glutathione and thioredoxine and enzymatic systems including superoxide dismutase, catalase and glutathione peroxidase [134]. There is considerable evidence that redox signaling mechanisms function in cell regulation and growth control [135].

Hepatocarcinogenesis is a multistep process in which a number of mutational genetic alterations accumulate in a cell. It involves the transition of a normal cell via the so called initiated cell to a pre-neoplastic lesion that develops into malignant tumor [136] (see figure 1.8)

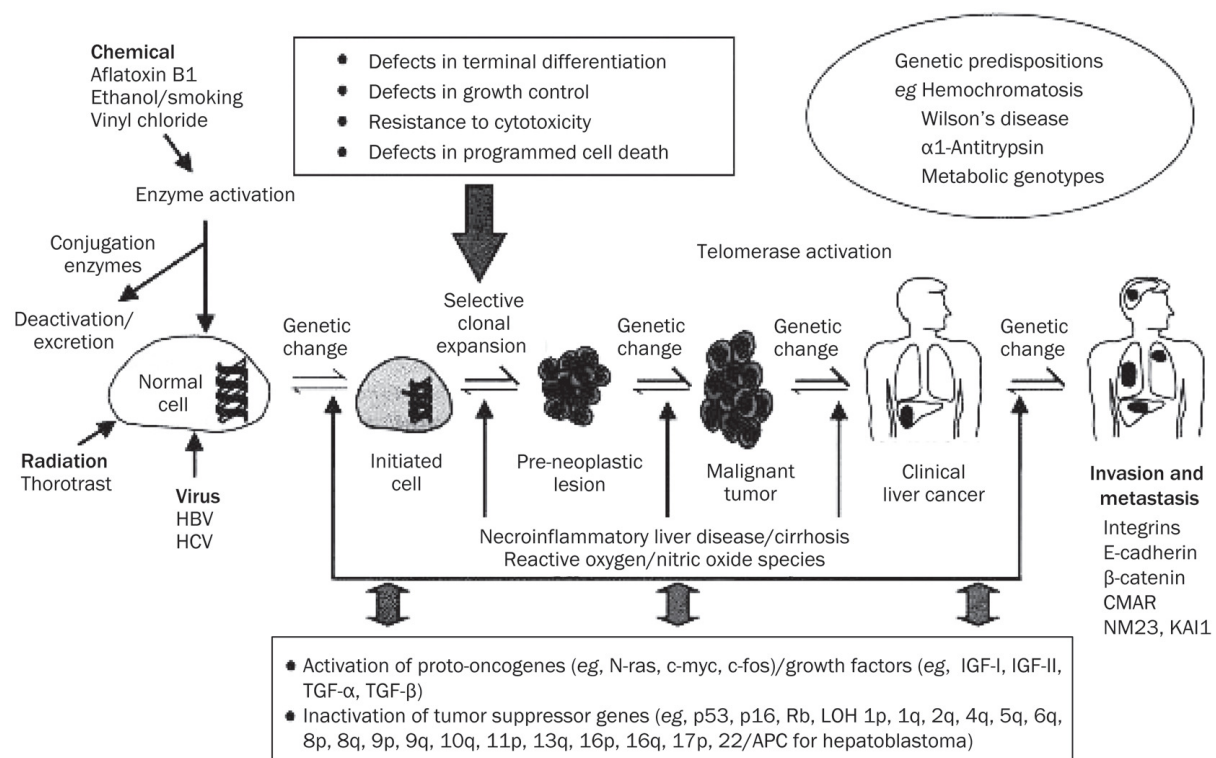


**Figure 1.8. Schematic representation of the multistep process of hepatocarcinogenesis.**

HBV, Hepatitis B virus; HCV, Hepatitis C virus; CMAR, cellular adhesion regulatory molecule; IGF, insulin-like growth factor; TGF, transforming growth factor; APC, adenomatous polyposis coli.

Adapted from [162].

Over recent years, it has become clear that the tumor environment plays an important role in tumorigenesis and tumor progression [137]. Cancer cells are not as autonomous as once thought, they depend on angiogenesis, inflammatory cells and fibroblasts [138, 139]. In the cirrhotic liver, there is an abundance of fibroblasts and there is emerging evidence that some

are cancer associated fibroblasts [140]. In HCC, the progression of malignant hepatocytes frequently depends on TGF- $\beta$ 1 provided by fibroblasts and macrophages. This TGF- $\beta$ 1 is one of the factors that can induce an Epithelial-to-Mesenchymal Transition (EMT) [141]. In EMT, there is a destabilization of adherent junctions [142] and the cells develop more invasive properties [143]. The tumor microenvironment is also influenced by hypoxia and angiogenesis as will be outlined in the next paragraphs.

As indicated, angiogenesis is a key mechanism in HCC. The hypervascularity found in all chronic liver disease facilitates the progression from small dysplastic nodules, through neoplastic lesions to large HCC-tumors [144]. HCC display rapid growth and are consequently in need of a high oxygen and nutrient supply; hypoxia of cancer cells is therefore the main eliciting factor of angiogenesis. It has been shown that chronic exposure to hypoxia leads to an adaptive gene expression profile which influences the aggressive behavior of tumor cells and ensures that cancer cells meet the high demands of oxygen and nutrients. To this end, tumors secrete a number of angiogenic growth factors, such as Vascular Endothelial Growth Factor (VEGF), Platelet Derived Growth Factor (PDGF), Placental Growth Factor (PlGF) and TGF- $\beta$ 1. Different types of angiogenesis occur in HCC ranging from sprouting and intussusceptive angiogenesis to vasculogenesis, vasculogenic mimicry, vessel co-option and lymphangiogenesis. The family of VEGF ligands and their receptors play an important part in almost all of these mechanisms as illustrated in Figure 1.9

In sprouting angiogenesis, the mechanisms of hypoxia that induce angiogenesis are similar to those found in regeneration after partial hepatectomy. The X protein of HBV has been shown to increase the transcriptional activity and protein level of Hypoxia-Inducible Factor-1 (HIF-1) [145]. Hypoxia stimulates angiogenesis through up-regulation of VEGF gene expression by at least two distinct molecular mechanisms: activation of VEGF gene transcription and stabilization of VEGF mRNA [146]. Angiotensin/Tie-2 is also an important pathway in regulating angiogenesis of HCC, although it is not up-regulated by hypoxia [147]. VEGF/Ang-driven sprouting angiogenesis is considered to be the main mechanism of neovascularization in HCC. Intussusceptive angiogenesis is an alternative mode of angiogenesis that consists of microvascular remodeling by transcapillary pillar formation; it relies much less on endothelial cell proliferation. Growth of these endothelial cells leads to sinusoidal multiplication by successive fusion and partitioning of the existing vascular lumens [148]. As stated above, most of HCCs originate from cirrhosis, which undergoes chronic hypoxia and VEGFR-2 levels were down-regulated in both tumor and adjacent tissue [147], preferring intussusceptive angiogenesis, although direct evidence is absent.

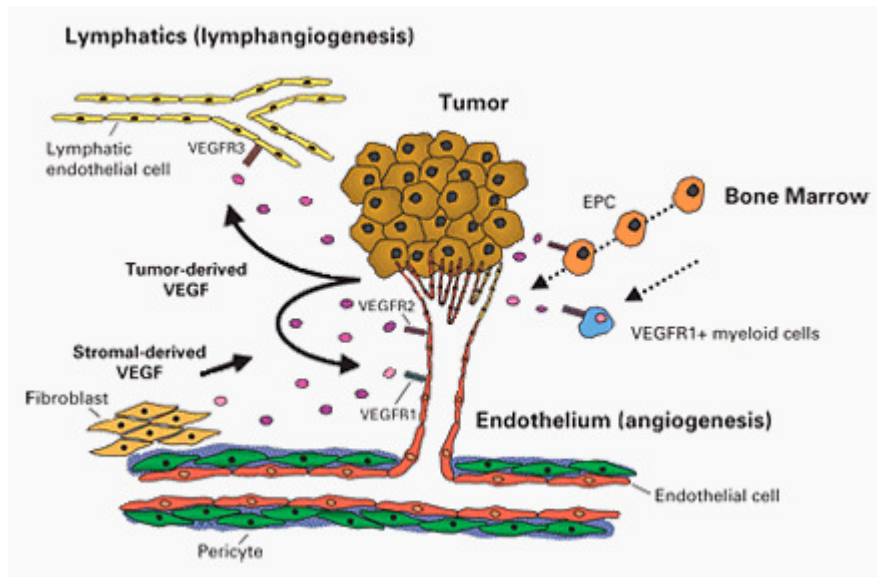


**Figure 1.9 The role of the VEGF family of ligands and receptors in different forms of tumor angiogenesis.** VEGF, vascular endothelial growth factor; VEGFR, vascular endothelial growth factor receptor; EPC, endothelial progenitor cells. Adapted from [163].

Vasculogenesis in HCC has been shown to involve vessel changes in which the formation of blood vessels is due to the arrival and differentiation of endothelial progenitor cells (EPCs) generated from bone marrow [150]. However, the exact mechanisms for recruitment and homing of EPCs to liver cirrhosis or liver cancer are currently unclear. In vasculogenic mimicry, tumor cells de-differentiate to an endothelial phenotype and form tube-like structures. This provides tumor cells with a secondary circulation system of vasculogenic structures lined by tumor cells, independent of angiogenesis [151]. The presence of vasculogenic mimicry is associated with a high tumor grade, invasion and metastasis. Yet again, the exact mechanisms underlying mimicry still need to be clarified. A fifth mechanism through which tumor cells try to supply themselves of oxygen and nutrients is vessel co-option. This occurs when tumor cells can grow along existing vessels without evoking an angiogenic response. It has been reported that a subset of tumors rapidly co-opt existing host vessels to form an initially well-vascularized tumor mass in which the co-opted vessels will undergo a widespread regression, leading to a secondary avascular tumor and massive tumor cell apoptosis, but the remaining tumor is ultimately rescued by robust angiogenesis at the tumor margin [152]. The co-opted vessels display striking and specific up-regulation of Ang-2 [152, 153]. In the early stage, there is minimal up-regulation of VEGF, and elevated Ang-2 expression at tumor periphery is associated with robust angiogenesis. Finally, tumor-associated lymphangiogenesis is also involved in the neovascularization of HCC. The lymphatic microvessel density showed a trend towards association with reduced survival and represents a prognostic factor for disease-free survival, indicating that the role of lymphangiogenesis for tumor progression in HCC is related to the risk of recurrence rather than to local tumor growth [154]. Lymphangiogenesis is mainly regulated by the VEGFR-3 system [155, 156].

The importance of angiogenesis in HCC is also demonstrated by the fact that sorafenib is the only drug that has shown to prolong overall survival of patients with advanced HCC.

Sorafenib is a multi-targeted tyrosine kinase inhibitor with both anti-angiogenic and anti-proliferative effects. However, still this drug has a lot of side-effects and seriously affects quality of life of patients. Other anti-angiogenic multi-targeted tyrosine kinase inhibitors, in particular sunitinib and pazopanib, show promising activity in various stages of clinical trials. Finally, there is an urgent need to identify biomarkers that may guide the rational use of sorafenib and other targeted agents in the treatment of patients with advanced HCC [157]. Our research into *N*-glycosylated based biomarker might potentially comply with this request.

### 1.1.7 References

- [1] Friedman S. Molecular regulation of hepatic fibrosis, an integrated cellular response to tissue injury. *J Biol Chem* 2000;275:2247-2250.
- [2] Guyot C, Lepreux S, Combe C, Doudnikoff E, Bioulec-Sage P, Balalaud C, et al. Hepatic fibrosis and cirrhosis: the (myo)fibroblastic cell subpopulations involved. *Int J Biochem Cell Biol* 2006;38:135-151.
- [3] Jungermann K, Katz N. Functional specialization of different hepatocyte populations. *Physiol Rev* 1989;69:708-764.
- [4] Usynin I, Panin L. Mechanisms determining phenotypic heterogeneity of hepatocytes. *Biochemistry (Mosc)* 2008;73:367-380.
- [5] Gottlieb R. Bilirubin formation and the reticulo-endothelial system. *Can Med Assoc J* 1934;30:365-367.
- [6] Bajor A, Gillberg P, Abrahamsson H. Bile acids: short and long term effects in the intestine. *Scand J Gastroenterol* 2010;45:645-654.
- [7] Kamisako T, Kobayashi Y, Takeuchi K, Ishihara T, Higuchi K, Tanaka Y. Recent advances in bilirubin metabolism research: the molecular mechanism of hepatocyte bilirubin transport and its clinical relevance. *J Gastroenterol* 2000;35:659-664.
- [8] Iyanagi T, Emi Y, Ihushiro S. Biochemical and molecular aspects of genetic disorders of bilirubin metabolism. *Biochim Biophys Acta* 1998;1407:137-184.
- [9] Gourly G. Bilirubin metabolism and kernicterus. *Adv Pediatr* 1997;44:173-229.
- [10] Hass P. Differentiation and diagnosis of jaundice. *ACCN Clin Issues* 1989;10:433-441.
- [11] Okolicsanyi L, Cavestro G, Guatti-Zuliani C. Hyperbilirubinemia: does it matter? *Can J Gastroenterol* 1999;13:663-8.
- [12] Friedman S. Liver fibrosis – from bench to bedside. *J Hepatol* 2008;38:S38-S53.
- [13] Fattovich G, Giustina G, Degos F, Tresmolada F, Diodati G, Almasio P, et al. Morbidity and mortality in compensated cirrhosis type C: a retrospective follow-up study of 384 patients. *Gastroenterology* 1997;112:463-472.
- [14] Friedman S, Maher J, Bissell D. Mechanisms and therapy of hepatic fibrosis: report of the AASLD Single Topic Basic Research Conference. *Hepatology* 2000;32:1403-1408.
- [15] Wallace K, Burt A, Wright M. Liver fibrosis. *Biochem J* 2008;411:1-18.
- [16] Jiang J, Venugopal S, Serizawa N, Chen X, Scott F, Li Y, et al. NOX2 plays a key role in stellate cell activation and liver fibrogenesis in vivo. *Gastroenterology* 2010;139:1375-1384.
- [17] Théret N, Musso O, L'Helgoualc'h A, Clément B. Activation of Matrix Metalloproteinase-2 from hepatic stellate cells requires interactions with hepatocytes. *Am J Pathol* 1997;150:51-58.



- [18] Reeves H, Friedman S. Activation of hepatic stellate cells – A key issue in liver fibrosis. *Front Biosci* 2002;7:d808-d826.
- [19] Henderson N, Iredale J. Liver fibrosis: cellular mechanisms of progression and resolution. *Clin Sci* 2007;112:265-280.
- [20] Novobrantseva T, Majeau G, Amatucci A, et al. Attenuated liver fibrosis in the absence of B cells. *J Clin Invest* 2005;115:3072-3082.
- [21] Hintermann E, Bayer M, Pfeilschifter J, Luster A, Christen U. CXCL10 promotes liver fibrosis by prevention of NK cell mediated hepatic stellate cell inactivation. *J Autoimmun* 2010;35:424-435.
- [22] Melhem A, Muhamma N, Biskara A, Alvarez C, Ilan Y, Bishara T, et al. Anti-fibrotic activity of NK cells in experimental liver injury through killing of activated HSC. *J Hepatol* 2006;45:60-71.
- [23] Prosser C, Yen R, Wu Y. Molecular therapy for hepatic injury and fibrosis: Where are we? *World J Gastroenterol* 2006;12:509-515.
- [24] Adachi T, Togashi H, Suzuki A, Kasai S, Ito J, Sugahara K, et al. NAD(P)H oxidase plays a crucial role in PDGF-induced proliferation of hepatic stellate cells. *Hepatology* 2005;41:1272-1281.
- [25] Friedman S, Wei S, Blaner W. Retinol release by activated rat hepatic lipocytes: regulation by Kupffer cell-conditioned medium and PDGF. *Am J Physiol Gastrointestinal Liver Physiol* 1993;264:G947-G952.
- [26] Li J, Kurula R, Wilson A, Gao X, Zhang Y, et al. Inhibition of Endothelin-1 mediated contraction of hepatic stellate cells by FXR ligands. *PLoS ONE* 2010;5:e13955.
- [27] Gressner A, Weiskirchen R, Breitkopf K, Dooley S. Roles of TGF-beta in hepatic fibrosis. *Front Biosci* 2002;7:d793-d807.
- [28] Benyon R, Arthur M. Extracellular matrix degradation and the role of hepatic stellate cells. *Semin Liver Dis* 2001;3:373-384.
- [29] Czaja M, Geerts A, Xu J, Schmiedeberg P, Yu Y. Monocyte chemoattractant protein 1 (MCP1) expression occurs in toxic rat liver and human liver disease. *J Leukoc Biol* 1994;55:120-126.
- [30] Mühlbauer M, Bosserhoff A, Hartmann A, Thasler E, Weiss T, Herfarth H, et al. A novel MCP-1 gene polymorphism is associated with hepatic MCP-1 expression and severity of HCV-related liver disease. *Gastroenterology* 2003;125:1085-1093
- [31] Pares A, Caballeria J, Bruguera M, Torres M, Rodes J. Histological course of alcoholic hepatitis. Influence of abstinence, sex and extent of hepatic damage. *J Hepatol* 1986;2:33-42.
- [32] Stewart S, Jones D, Day C. Alcohol liver disease: new insights into mechanisms and preventative strategies. *Trends Mol Med* 2001;7:408-13.
- [33] Morgan T, Mandayan S, Jamal M. Alcohol and hepatocellular carcinoma. *Gastroenterology* 2004;127:S87-97.
- [34] Stickel F, Schuppan D, Hahn E, Sutz H. Cocarcinogenic effects of alcohol in hepatocarcinogenesis. *Gut* 2002;51:132-9.
- [35] Crabb D, Matsumoto M, Chang D, You M. Overview of the role of alcohol dehydrogenase and aldehyde dehydrogenase and their variants in the genesis of alcohol-related pathology. *Proc Nutr Soc* 2004;63:49-63.
- [36] Wan Y, Poland R, Lin K. Genetic polymorphism of CYP2E1, ADH2 and ALDH2 in Mexican-Americans. *Genet Test* 1998;2:79-84.
- [37] Zakhari S, Li T. Determinants of alcohol use and abuse: impact of quantity and frequency patterns on liver disease. *Hepatology* 2007;46:2032-9.

- [38] Niemela O, Parkkila S, Yla-Herttuala S, Villanueva J, Ruebner B, Halsted C. Sequential acetaldehyde production, lipid peroxidation, and fibrogenesis in micropig model of alcohol-induced liver disease. *Hepatology* 1995;22:1208-14.
- [39] Sladek N, Manthey C, Maki P, Zhang Z, Landkamer G. Xenobiotic oxidation catalyzed by aldehyde dehydrogenases. *Drug Metab Rev* 1989;20:697-720.
- [40] Liu C, Russell R, Seitz H, Wang X. Ethanol enhances retinoic acid metabolism into polar metabolites in rat liver via induction of cytochrome P4502E1. *Gastroenterology* 2001;120:179-89.
- [41] Wang X. Alcohol, vitamin A, and cancer. *Alcohol* 2005;35:251-8.
- [42] Bataller R, Schwabe R, Choi Y, Yang L, Paik Y, Lindquist J, et al. NADPH oxidase signal transduces angiotensin II in hepatic stellate cells and is critical in hepatic fibrosis. *J Clin Invest* 2003;112:1383-1394.
- [43] Lefkowitz J. Morphology of alcoholic liver disease. *Clin Liver Dis* 2005;9:37-53.
- [44] Lavanchy D. Hepatitis B virus epidemiology, disease burden, treatment and current and emerging prevention and control measures. *J Viral Hepat* 2004;11:97-107.
- [45] Mahoney F. Update on diagnosis, management, and prevention of hepatitis B virus infection. *Clin Microbiol Rev* 1999;12:351-366.
- [46] Lee W. Hepatitis B virus infection. *N Eng J Med* 1997;337:1733-45.
- [47] Alter M. Epidemiology of hepatitis C. *Hepatology* 1997;26:62S-65S.
- [48] Maneerat Y, Wilairatana P, Pongponratn E, Puthavathana P, Chaisri U, Kurathong S, et al. Herpes simplex virus type-2, cytomegalovirus and Epstein-Barr virus infection in acute non A to E hepatitis Thai patients. *Asian Pac J Allergy Immunol* 1997;15:147-51.
- [49] Takeuchi O, Akira S. Innate immunity to virus infection. *Immunol Rev* 2009;227:75-86.
- [50] Kepler T, Chan C. Spatiotemporal programming of a simple inflammatory process. *Immunol Rev* 2007;216:153-163.
- [51] Martinon F, Tschopp J. NLRs join TLRs as innate sensors of pathogens. *Trends Immunol* 2005;26:447-454.
- [52] Bowie A, Unterholzner L. Viral evasion and subversion of pattern-recognition receptor signaling. *Nat Rev Immunol* 2008;8:911-922.
- [53] Sobao Y, Tomiyama H, Sugi K, Tokunaga M, Veno T, Suito S, et al. The role of hepatitis B virus-specific memory CD8 T cells in the control of viral replication. *J Hepatol* 2002;36:105-115.
- [54] Rehmann B, Fowler P, Sidney J, Person J, Redeker A, Brown M, et al. The cytotoxic T lymphocyte response to multiple hepatitis B virus polymerase epitopes during and after acute viral hepatitis. *J Exp Med* 1995;181:1047-1058.
- [55] Zinkernagel R, Haenseler E, Leist T, Cerny A, Hengartner H, Althage A. T cell-mediated hepatitis in mice infected with lymphocytic choriomeningitis virus. Liver cell destruction by H-2 class I-restricted virus-specific cytotoxic T cells as a physiological correlate of the 51Cr-release assay? *J Exp Med* 1986;164:1075-1092.
- [56] Recher M, Lang K, Mavarini A, Hunziker L, Lang P, Fink K, et al. Extralymphatic virus sanctuaries as a consequence of potent T-cell activation. *Nat Med* 2007;13:1316-23.
- [57] Banchereau J, Briere F, Caux C, Davoust J, Lebecque S, Liu Y, Pulendran B, Palucka K. Immunobiology of dendritic cells. *Annu Rev Immunol* 2000;18:767-811.

- [58] Battegay M, Backmann M, Burkhart C, Viville S, Benoist C, Mathis D, et al. Antiviral immune response of mice lacking MHC Class II or its associated invariant chain. *Cell Immunol* 1996;167:115-121.
- [59] Recher M, Lang K, Henziker L, Freigang S, Eschli B, Harris N, et al. Deliberate removal of T cell help improves virus-neutralizing antibody production. *Nat Immunol* 2004;5:934-942.
- [60] Brooks D, Trifilo M, Edelmann K, Teyton L, McGavern D, Oldstone M. Interleukin-10 determines viral clearance of persistence in vivo. *Nat Med* 2006;12:1301-1309.
- [61] Ejnaes M, Filippi C, Martinic M, Ling E, Togher L, Crotty S, et al. Resolution of a chronic viral infection after interleukin-10 receptor blockade. *J Exp Med* 2006;203:2461-2472.
- [62] Dai C, Chuang W, Chang W, Chen S, Lee L, Hscek M, et al. Polymorphisms in the interferon-gamma gene at position +874 in patients with chronic hepatitis C treated with high dose interferon-alpha and ribavirin. *Antiviral Res* 2005;67:93-97.
- [63] Kurabayashi M, Takeyoshi I, Yoshimari D, Koibuchi Y, Ohki T, Matsumoto K, et al. No donor ameliorates ischemia-reperfusion injury of the rat liver with iNOS attenuation. *J Invest Surg* 2005;18:193-200.
- [64] Venkatraman A, Shiva S, Wigley A, Vlasova E, Chhieng D, Bailey S, et al. The role of iNOS in alcohol-dependent hepatotoxicity and mitochondrial dysfunction in mice. *Hepatology* 2004;40:565-573.
- [65] Bao X, Cui J, Wu Y, Han X, Gao C, Hua Z, et al. The roles of endogenous reactive oxygen species and nitric oxide in triptolide-induced apoptotic cell death in macrophages. *J Mol Med* 2007;85:85-98.
- [66] Dimmeler S, Zeiher A. Nitric oxide – an endothelial cell survival factor. *Cell Death Differ* 1999;6:964-968.
- [67] Taylor E, Megson I, Haslett C, Rossi A. Nitric oxide: a key regulator of myeloid inflammatory cell apoptosis. *Cell Death Differ* 2003;10:418-430.
- [68] Eum H, Park S, Lee S. Role of nitric oxide in the expression of hepatic vascular stress genes in response to sepsis. *Nitric oxide* 2007;17:126-133.
- [69] Ito Y, Abril E, Bethea N, McCuskey R. Role of nitric oxide in hepatic microvascular injury elicited by acetaminophen in mice. *Am J Physiol Gastrointest Liver Physiol* 2004;286:G60-G67.
- [70] Kim S, Lee S. Expression of hepatic stress genes following ischemia/reperfusion and subsequent endotoxemia. *Arch Pharm Res* 2004;27:769-775.
- [71] Spengler U, Nattermann J. Immunopathogenesis in hepatitis C virus cirrhosis. *Clin Sci* 2007;112:141-155.
- [72] Mengshol J, Golden-Mason L, Rosen H. Mechanisms of disease: HCV-induced liver injury. *Nat Clin Pract Gastroenterol Hepatol* 2007;4:622-634.
- [73] Bantel H, Lügering A, Heidemann J, Volkmann X, Poremba C, Strassburg C, et al. Detection of apoptotic response activation in sera from patients with chronic HCV infection as associated with fibrotic liver injury. *Hepatology* 2004;40:1078-1087.
- [74] Bantel H, Lügering A, Poremba C, Lügering N, Held J, Domschke W, et al. Caspase activation correlates with the degree of inflammatory liver injury in chronic hepatitis C virus infection. *Hepatology* 2001;34:758-767.
- [75] Canbay A, Taimr P, Torok N, Higuchi H, Friedman S, Gores G. Apoptotic body engulfment by a human stellate cell line is profibrogenic. *Lab Invest* 2003;83:655-63.

- [76] Bantel H, Schulze-Osthoff K. Apoptosis in hepatitis C virus infection. *Cell Death Differ* 2003;10(Suppl1):S48-S58.
- [77] Bataller R, Paik Y, Lindquist J, Lemasters J, Brenner D. Hepatitis C virus core and nonstructural proteins induce fibrogenic effects in hepatic stellate cells. *Gastroenterology* 2004;126:529-540.
- [78] Lalor P, Shields P, Grant A, Adams D. Recruitment of lymphocytes to the human liver. *Immunol Cell Biol* 2002;80:52-64.
- [79] Schulze-Krebs A, Preimel D, Popov Y, Bartenschlager R, Lohmann, Pinzani M, et al. Hepatitis C virus-replicating hepatocytes induce fibrogenic activation of hepatic stellate cells. *Gastroenterology* 2005;129:246-258.
- [80] Benyon R, Arthur M. Extracellular matrix degradation and the role of hepatic stellate cells. *Semin Liver Dis* 2001;21:373-384.
- [81] Mazzocca A, Sciammetta S, Carloni V, Cosmi L, Annunziato F, Harada T, et al. Binding of hepatitis C virus envelope protein E2 to CD81 up-regulates matrix metalloproteinase-2 in human stellate cells. *J Biol Chem* 2005;280:11329-11339.
- [82] Bedossa P, Poynard T. An algorithm for the grading of activity in chronic hepatitis C. The METAVIR Cooperative Study Group. *Hepatology* 1996;24:289-293.
- [83] Anwer M. Cellular regulation of hepatic bile acid transport in health and cholestasis. *Hepatology* 2004;39:581-590.
- [84] Shivakumar P, Campbell K, Sabla G, Miethke A, Tiao G, McNeal M, et al. Obstruction of extrahepatic bile ducts by lymphocytes is regulated by IFN-gamma in experimental biliary atresia. *J Clin Invest* 2004;114:332-339.
- [85] Chen F, Ananthanurayanan M, Emre S, Neimark E, Bull L, Knisely A, et al. Progressive familial intrahepatic cholestasis, type 1, is associated with decreased farnesoid X receptor activity. *Gastroenterology* 2004;126:756-764.
- [86] Gissen P, Johnson C, Morgan M, Stapelbroek J, Forshew T, Cooper W, et al. Mutations in VPS33B, encoding a regulator of SNARE-dependent membrane fusion, cause arthrogyrosis-renal dysfunction-cholestasis (ARC) syndrome. *Nat Genet* 2004;36:400-404.
- [87] Lumbroso S, Paris F, Sultan C. Activating Gsa mutations analysis of 113 patients with signs of McCune-Albright Syndrome – a European collaborative study. *J Clin Endocrin Metab* 2004;89:2107-2113.
- [88] Xu L, Sukalian M, Shen Z. Cloning the human betaretrovirus proviral genome from patients with primary biliary cirrhosis. *Hepatology* 2004;39:151-156.
- [89] Selmi C, Ross S, Ansari A. Lack of immunological or molecular evidence for a role of mouse mammary tumor retrovirus in primary biliary cirrhosis. *Gastroenterology* 2004;127:493-501.
- [90] Bogdanos D, Baum H, Grasso A, Okamoto M, Butler P, Ma Y, et al. Microbial mimics are major targets of cross reactivity with human pyruvate dehydrogenase in primary biliary cirrhosis. *J Hepatol* 2004;40:31-39.
- [91] Plamer J, Robe A, Burt A, Kirby J, Jones D. Covalent modifications as a mechanism for the breakdown of immune tolerance to pyruvate dehydrogenase complex in the mouse. *Hepatology* 2004;39:1538-1592.
- [92] Yang X, Cullen S, Li J, Chapman R, Jewell D. Susceptibility to primary sclerosing cholangitis is associated with polymorphisms of intercellular adhesion molecule-1. *J Hepatol* 2004;40:375-279.
- [93] Fickert P, Fuchsbichler A, Wagner M, Zollner G, Kasu A, Tilg H, Krause R, et al. Regurgitation of bile acids from leaky bile ducts causes sclerosing cholangitis in *Mdr2* (Abcb4) knockout mice. *Gastroenterology* 2004;127:261-274.

- [94] Blanco P, Zaman M, Junaido O, Sheth S, Yantiss R, Nasser I, et al. Induction of colitis in *cfr-* results in bile duct injury. *Am J Physiol Gastrointest Liver Physiol* 2004;287:G491-G496.
- [95] Neuschwander-Tetri B, Caldwell S. Nonalcoholic steatohepatitis: summary of an AASLD single topic conference. *Hepatology* 2003;37:1202-1219.
- [96] Wanless I, Lentz J. Fatty liver hepatitis (steatohepatitis) and obesity: an autopsy study with analysis of risk factors. *Hepatology* 1990;12:1106-1110.
- [97] Dixon J, Bhatel P, O'Brian P. Non-alcoholic fatty liver disease: predictors of non-alcoholic steatohepatitis and liver fibrosis in the severely obese. *Gastroenterology* 2001;121:91-100.
- [98] Murra F, Gastadelli A, Svegliati Baroni G, Tell G, Tiribelli C. Molecular basis and mechanisms of progression of non-alcoholic steatohepatitis. *Trends Mol Med* 2008;14:72-81.
- [99] Day C. Pathogenesis of steatohepatitis. *Best Pract Res Clin Gastroenterol* 2002;16:663-678.
- [100] Day C. From fat to inflammation. *Gastroenterology* 2006;130:207-210.
- [101] Hotamisligil G, Shargill N, Spiegelman B. Adipose expression of tumor necrosis factor- $\alpha$ : direct role in obesity-linked insulin resistance. *Science* 1993;259:87-91.
- [102] Li L, Yang S, Lin H, Huang J, Watkins P, Moser A, et al. Probiotics and antibodies to TNF inhibit inflammatory activity and improve nonalcoholic fatty liver disease. *Hepatology* 2003;37:343-50.
- [103] Uysel K, Weisbrock S, Marino M, Hotamisligil G. Protection from obesity-induced insulin resistance in mice lacking TNF- $\alpha$  function. *Nature* 1997;389:610-614.
- [104] Fontana L, Eagon J, Trujillo M, Scherer P, Klein S. Visceral fat adipokine secretion is associated with systemic inflammation in obese humans. *Diabetes* 2007;56:1010-1013.
- [105] Hotta K, Funahashi T, Arita Y, Takahashi M, Matsuda M, Okamoto Y, et al. Plasma concentrations of a novel, adipose-specific protein, adiponectin, in type 2 diabetic patients. *Arterioscler Thromb Vasc Biol* 2000;20:1595-1599.
- [106] Fasshauer M, Kralisch S, Kleir M, Lessner U, Bluher M, Klein J, et al. Adiponectin gene expression and secretion is inhibited by interleukin-6 in 3T3-L1 adipocytes. *Biochim Biophys Res Commun* 2003;301:1045-1050.
- [107] Maeda M, Shimomura I, Kishida K, Nishizawa H, Matsuda M, Nagaretani H, et al. Diet-induced insulin resistance in mice lacking adiponectin/ACRP30. *Nat Med* 2002;8:731-737.
- [108] Wolf A, Wolf D, Rumpold H, Enrich B, Tilg H. Adiponectin induces the anti-inflammatory cytokines IL-10 and IL-1RA in human leukocytes. *Biochem Biophys Res Commun* 2004;323:630-635.
- [109] Kumada M, Kihara S, Orechi N, Kobayashi H, Okamoto Y, Ohashi K, et al. Adiponectin specifically increased tissue inhibitor of metalloproteinase-1 through interleukin-10 expression in human macrophages. *Circulation* 2004;109:2046-2049.
- [110] Day C, James O. Steatohepatitis: a tale of two 'hits'? *Gastroenterology* 1998;114:842-845.
- [111] Mantena S, King A, Andrinya K, Eccleston H, Bailey S. Mitochondrial dysfunction and oxidative stress in the pathogenesis of alcohol- and obesity-induced fatty liver diseases. *Free Radic Biol Med* 2008;44:1259-1272.
- [112] Parola M, Robino G. Oxidative stress-related molecules and liver fibrosis. *J Hepatol* 2001;35:297-306.
- [113] Jou J, Choi S, Diehl A. Mechanisms of disease progression in nonalcoholic fatty liver disease. *Semin Liver Dis* 2008;28:370-379.

- [114] Svegliati Baroni G, Ridolfi F, Di Sario A, Lasini A, Marucci L, Gaggiotti G, et al. Insulin and insulin-like growth factor-1 stimulate proliferation and type I collagen accumulation by human hepatic stellate cells: differential effects on signal transduction pathways. *Hepatology* 1999;29:1743-1751.
- [115] Grotendorst G. Connective tissue growth factor: a mediator of TGF-beta action on fibroblasts. *Cytokine Growth Factor Rev* 1997;8:171-179.
- [116] Fehrenbach H, Weiskirchen R, Kasper M, Gressner A. Up-regulated expression of the receptor for advanced glycation end products in cultured rat hepatic stellate cells during trans-differentiation to myofibroblasts. *Hepatology* 2001;34:943-952.
- [117] Kleiner D, Brunt E, Van Natta M, Behling C, Contos M, Cummings O, et al. Design and validation of a histological scoring system for nonalcoholic fatty liver disease. *Hepatology* 2005;41:1313-1321.
- [118] Park H, Shima T, Yamaguchi K, Mitsuyoshi H, Minami M, Yasui K, et al. Efficacy of long-term ezetimibe therapy in patients with nonalcoholic fatty liver disease. *J Gastroenterol* 2011;46:101-107.
- [119] Fotiadu A, Gagalis A, Akriadiadis E, Kotoula V, Sinakos E, Karkavelas G, et al. Clinicopathological correlations in a series of adult patients with non-alcoholic fatty liver disease. *Pathol Int* 2010;68:87-92.
- [120] Patton H, Yates K, Unalp-Arida A, Behling C, Huang T, Rosenthal P, et al. Association between metabolic syndrome and liver histology among children with nonalcoholic fatty liver disease. *Am J Gastroenterol* 2010;105:2093-2102.
- [121] Roberts E. Steatohepatitis in children. *Best Pract Res Clin Gastroenterol* 2002;16:749-765.
- [122] Baldrige A, Perezatayde A, Graemecook F, Higgings C, Lavine J. Idiopathic steatohepatitis in childhood: a multicenter retrospective study. *J Pediatr* 1995;127:700-704.
- [123] Rashid M, Roberts E. Nonalcoholic steatohepatitis in children. *J Pediatric Gastroenterol Nutr* 2000;30:48-53.
- [124] Ratzui V, Giral P, Charlotte F, Bruckert E, Thibault V, Theodorou I, et al. Liver fibrosis in overweight patients. *Gastroenterology* 2000;118:1117-1123.
- [125] Parkin D, Bray F, Ferlay J, Pisani P. Global cancer statistics, 2002. *CA Cancer J Clin* 2005;55:74-108.
- [126] El-Seray H, Mason A. Rising incidence of hepatocellular carcinoma in the United States. *N Eng J Med* 1999;340:745-750.
- [127] Llovet J, Burroughs A, Bruix J. Hepatocellular carcinoma. *Lancet* 2003;362:1907-1917.
- [128] Guyot C, Lepreux S, Combe C, Doudnikoff E, Bioulac-Sage P, Balulaud C, et al. Hepatic fibrosis and cirrhosis: the (myo)fibroblastic cell subpopulations involved. *Int J Biochem Cell Biol* 2006;38:135-151.
- [129] Sangiovanni A, Del Nimmo E, Fasani R, De Fazio C, Ronchi G, Romeo R, et al. Increased survival of cirrhotic patients with a hepatocellular carcinoma detected during surveillance. *Gastroenterology* 2004;126:1005-1014.
- [130] Bosch F, Ribes J, Diaz M, Cléres R. Primary liver cancer: worldwide incidence and trends. *Gastroenterology* 2004;127(5 Suppl 1):S5-S16.
- [131] Kojiro M, Roskams T. Early hepatocellular carcinoma and dysplastic nodules. *Semin Liver Dis* 2005;5:133-142.
- [132] Roskams T, Libbrecht L, Desmet V. Progenitor cells in diseased human liver. *Semin Liver Dis* 2003;23:385-396.

- [133] Okuda M, Li K, Beard M, Skowalter L, Scholle F, Lemon S, et al. Mitochondrial injury, oxidative stress, and antioxidant gene expression are induced by hepatitis C virus core protein. *Gastroenterology* 2002;122:366-375.
- [134] Nakamura H, Nakamura K, Yodoi J. Redox regulation of cellular activation. *Annu Rev Immunol* 1997;15:351-369.
- [135] Nkubyo Y, Ziegler T, Gu L, Watson W, Jones D. Glutathione and thioredoxin redox during differentiation in human colon epithelial (Caco-2) cells. *Am J Physiol Gastrointest Liver Physiol* 2002;283:G1352-G1359.
- [136] Hussain S, Zondervan P, Ijzermans J, Schalm S, De Man R, Krestin G, et al. Benign versus malignant hepatic nodules: MR imaging findings with pathologic correlation. *Radiographics* 2002;22:1023-1036.
- [137] Witz I. The tumor microenvironment: the making of a paradigm. *Cancer Microenviron* 2009;2:9-17.
- [138] Mantovani A, Allavena P, Sica A, Balkwill F. Cancer-related inflammation. *Nature* 2008;454:436-444.
- [139] Kalluri R, Zeisberg M. Fibroblasts in cancer. *Nat Rev Cancer* 2006;6:392-401.
- [140] Mazzoca A, Fransvea E, Dituri F, Lupo L, Antonari S, Giannelli G. Down-regulation of connective tissue growth factor by inhibition of transforming growth factor beta blocks the tumor-stroma cross-talk and tumor progression in hepatocellular carcinoma. *Hepatology* 2010;51:523-534.
- [141] Van Zijl F, Mair M, Csiszar A, Schneller D, Zulchner G, Huber H, et al. Hepatic tumor-stroma crosstalk guides epithelial to mesenchymal transition at the tumor edge. *Oncogene* 2009;28:4022-4033.
- [142] Lin C, Lin C, Chen K, Wu J, Huang S, Wang S. Macrophage activation increases the invasive properties of hepatoma cells by destabilization of the adherens junction. *FEBS Lett* 2006;580:3042-3050.
- [143] Kokkinos M, Wafai R, Wong M, Newgreen D, Thompson E, Waltham M. Vimentin and epithelial-mesenchymal transition in human breast cancer-observations in vitro and in vivo. *Cells Tissues Organs* 2007;185:191-203.
- [144] Coulon S, Heindryckx F, Geerts A, Van Steenkiste C, Colle I, Van Vlierberghe H. Angiogenesis in chronic liver disease and its complications. *Liver Int* 2010 [Epub ahead of print].
- [145] Moon E, Jeong C, Jeong J, Kim K, Yu D, Murakami S, et al. Hepatitis B virus X protein induces angiogenesis by stabilizing hypoxia-inducible factor-1 alpha. *FASEB J* 2004;18:382-384.
- [146] Van Marschall Z, Cramer T, Hocher M, Finkenzeller G, Wiedenmann B, Rosewicz S. Dual mechanism of vascular endothelial growth factor upregulation by hypoxia in human hepatocellular carcinoma. *Gut* 2001;48:87-96.
- [147] Saginachi K, Tanaka S, Taguchi K, Aischima S, Shimada M, Tsuneyoshi M. Angiopoietin switching regulates angiogenesis and progression of human hepatocellular carcinoma. *J Clin Pathol* 2003;56:854-860.
- [148] Djonv V, Schmid M, Tschanz S, Burri P. Intussusceptive angiogenesis: its role in embryonic vascular network formation. *Cirr Res* 2000;86:286-292.
- [149] Zeng W, Gouw A, Van Den Heuvel M, Zweis P, Zondervan P, Poppema S, et al. The angiogenic make-up of human hepatocellular carcinoma does not favor vascular endothelial growth factor/angiopoietin driven sprouting neovascularization. *Hepatology* 2007;46:840-848.
- [150] Ho J, Pang R, Lau C, Sun C, Yu W, Fan S, et al. Significance of circulating endothelial progenitor cells in hepatocellular carcinoma. *Hepatology* 2006;44:836-843.

- [151] Haniotis A, Folberg R, Hess A, Seftor E, Gardner L, Pe'er J, et al. Vascular channel formation by human melanoma cells in vivo and in vitro: vasculogenic mimicry. *Am J Pathol* 1999;155:739-752.
- [152] Holash J, Maisonpierre P, Compton D, Boland P, Alexander C, Zagzag D, et al. Vessel co-option, regression, and growth in tumors mediated by angiopoietins and VEGF. *Science* 1999;284:1994-1998.
- [153] Holash J, Wiegand S, Yancopoulos G. New model of tumor angiogenesis: dynamic balance between vessel regression and growth mediated by angiopoietins and VEGF. *Oncogene* 1999;18:5356-5362.
- [154] Thelen A, Jonas S, Benckert C, Weichert W, Schott E, Botcher C, et al. Tumor-associated lymphangiogenesis correlates with prognosis after resection of human hepatocellular carcinoma. *Ann Surg Oncol* 2009;16:1222-1230.
- [155] Thelen A, Scholz A, Benckert C, Van Marschall Z, Schroder M, Wiedenmann B, et al. VEGF-D promotes tumor growth and lymphatic spread in a mouse model of hepatocellular carcinoma. *Int J Cancer* 2008;122:2471-2481.
- [156] Ohtani O, Ohtani Y. Lymph circulation in the liver. *Anat Rec (Hoboken)* 2008;29:643-652.
- [157] Yau T, Pang R, Chan P, Poon R. Molecular targeted therapy of advanced hepatocellular carcinoma beyond sorafenib. *Expert Opin Pharmacother* 2010;11:2187-2198.
- [158] Tilg H, Day C. Management strategies in alcoholic liver disease. *Nat Clin Prac Gastroenterol Hepatol* 2007;4:24-34.
- [159] Van der Poorten D, George J. Disease-specific mechanisms of fibrosis: hepatitis C virus and non-alcoholic steatohepatitis. *Clin Liver Dis* 2008;12:805-824.
- [160] Tiniakos D, Vos M, Brunt E. Nonalcoholic fatty liver disease: pathology and pathogenesis. *Annu Rev Pathol* 2010;5:145-171.
- [161] Larter C, Chitturi S, Heydet D, Farrell G. A fresh look at NASH pathogenesis. Part 1: the metabolic movers. *J Gastroenterol Hepatol* 2010;25:672-690.
- [162] Wang X, Hussain S, Huo T, Wu C, Forgues M, Hofseth Z, et al. Molecular pathogenesis of human hepatocellular carcinoma. *Toxicology* 2002;181-181:43-47.
- [163] Hicklin D, Ellis L. The role of the vascular endothelial growth factor pathway in tumor growth and angiogenesis. *J Clin Oncol* 2005;23:1011-1027.



### 1.2.1 General introduction and biosynthesis

In eukaryotic cells, secreted and membrane proteins are frequently modified with complex glycan structures. These arise as a consequence of three distinct types of modifications: *N*-linked glycosylation of asparagines [1], *O*-linked glycosylation of serine and threonine [2] and glycosylphosphatidyl inositol derivatization of the carboxyl-terminal carboxyl groups [3]. However, it is now firmly established that both Bacteria and Archaea are also capable of protein glycosylation [4, 5]. In this thesis, we will focus on the *N*-glycosylation of serum proteins in higher eukaryotes, in specific of mice and humans. The modification of proteins with *N*-linked glycans is of particular interest because *N*-glycosylation is essential for cell viability, it involves a multitude of enzymes, and at least half of the genes functioning in this biosynthetic pathway have been conserved through evolution. Important is that *N*-glycosylation is the principal posttranslational modification of serum proteins making it suitable for biomarker discovery, mainly because alterations in the abundance of particular *N*-glycans reflect an altered physiological state. *N*-linked carbohydrates play roles in diverse biological processes such as protein folding and conformation, stability, and targeting to subcellular and extracellular sites, as well as cell-matrix and cell-cell interactions [6].

The physiological significance of *N*-glycosylation has long been recognized. As a consequence of these basic properties, protein *N*-glycosylation is implicated in functions related to development and homeostasis. *N*-glycoproteins are highly regulated during growth and differentiation [7], and alterations in protein *N*-glycosylation patterns correlate with developmental programs [8, 9]. The developmental importance of *N*-glycosylation is reflected in such functions as morphogenesis, proliferation and apoptosis.

The reactions of the protein *N*-glycosylation pathway occur along the secretory pathway and entail many enzymes localized in the endoplasmic reticulum (ER) and the Golgi apparatus. Biosynthesis of *N*-glycoproteins is initiated with the dolichol (Dol) pathway in the endoplasmic reticulum [1]. The precursor oligosaccharide GlcNAc<sub>2</sub>Man<sub>9</sub>Glc<sub>3</sub> is assembled on the polyisoprenol carrier lipid, Dol-PP, through a stepwise addition of monosaccharides in a series of reactions catalyzed by glycosyltransferases. All ER glycosyltransferases are transmembrane proteins. The first seven sugars are transferred from the sugar nucleotides UDP-GlcNAc and GDP-Man at the cytosolic side of the ER. The heptasaccharide is then translocated to the lumen of the ER, the subsequent reactions encompass the transfer of four mannoses residues from Dol-P-Man and three glucoses moieties from Dol-P-Glc. The mature oligosaccharide is transferred as a unit from the dolichol carrier to the asparagines residues of polypeptides, within an Asn-X<sub>aa</sub>-Ser/Thr consensus sequence, X<sub>aa</sub> being any amino acid except proline [10] in a reaction catalyzed by the enzyme oligosaccharyltransferase (OST) [11] (Figure 2.1, Figure 2.3).

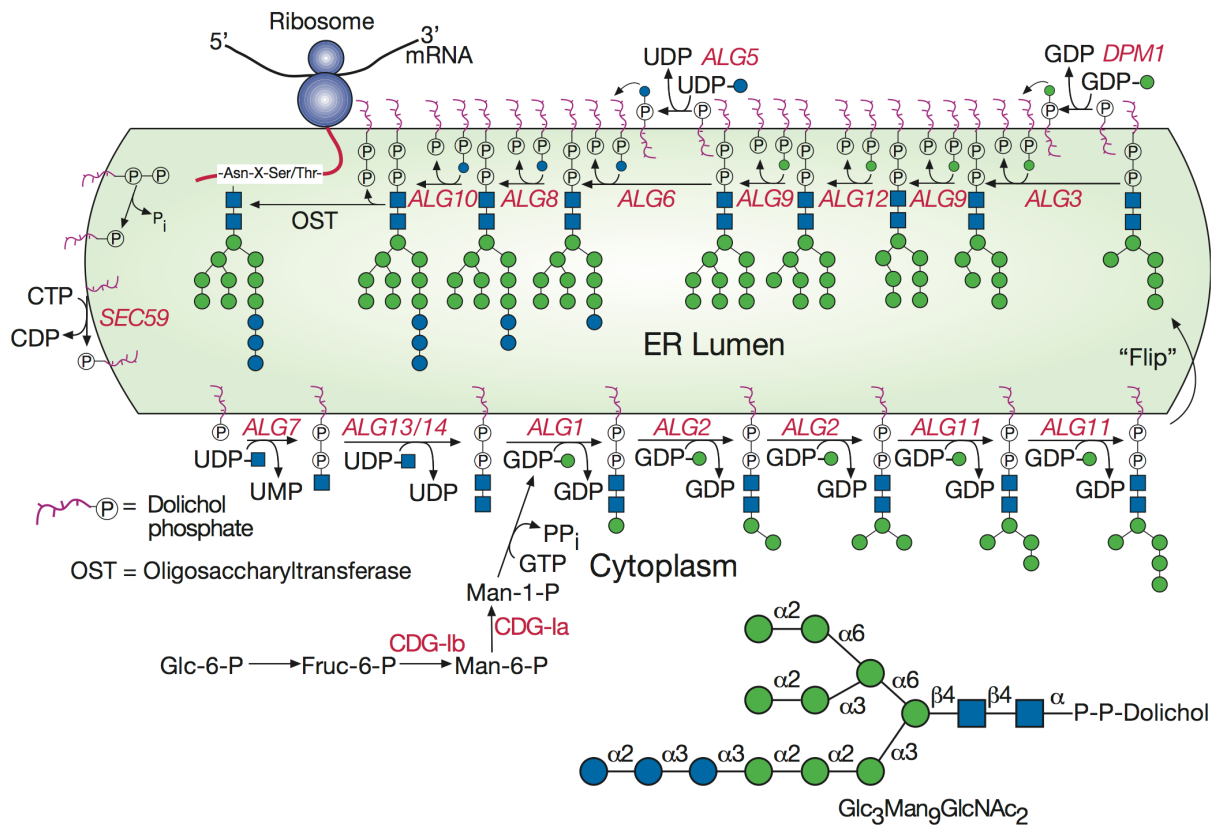


**Figure 2.1 Synthesis of dolichol-P-P-GlcNAc<sub>2</sub>Man<sub>9</sub>Glc<sub>3</sub> in endoplasmic reticulum (dolichol pathway).**  
Adapted from [21].

Not all potential glycosylation sites in proteins that enter the ER are modified. For instance, 10% of proline-free consensus sites in glycoproteins are not modified *in vivo*, whereas other sites are frequently modified incompletely, with the Asn-X<sub>aa</sub>-Thr sites being preferential acceptors to Asn-X<sub>aa</sub>-Ser [12]. Moreover, secondary structure also influences the *in vivo* efficiency of N-glycosylation, and sites located less than 12-14 residues from a transmembrane segment of a protein are typically not modified. Also, sites close to the C-terminus of a protein are not derivatized as effectively.

The transfer of the precursor oligosaccharide to protein is followed by a series of trimming reactions involving the removal of the three glucoses and one mannose via the action of  $\alpha$ -glucosidases I and II and  $\alpha$ -1,2-mannosidase. In yeast, the removal of mannose is restricted to a single  $\alpha$ -1,2-mannose from the central arm of the oligosaccharide, but it can include the action of several mannosidases in higher eukaryotes. A monitoring system has been identified that assists in glycoprotein folding in the ER. Typically, unfolded and misfolded proteins are retained in the ER until they attain their native conformation [13]. An enzyme, UDP-Glc:glycoprotein transferase, catalyzes re-glycosylation of the deglycosylated oligosaccharide on denatured proteins. Therefore, there is a balance between the opposing activities of glucosidases I and II and UDP-Glc:glycoprotein. The re-glycosylated proteins are bound and retained in the ER chaperone calnexin until they attain appropriate conformations. In addition to calnexin, molecular chaperones that function in the proper folding of ER N-glycoproteins include calreticullin and the binding protein, Bip or Grp78.

These proteins are all essential effectors of ER stress, a collective term for conditions interfering with the function of ER [14]. These conditions can include heat shock, inhibition of *N*-glycosylation, and all situations leading to protein misfolding in the ER. In response to this, an unfolded protein response (UPR) is initiated [15] (Figure 2.2). UPR uses an evolutionarily conserved signaling pathway during which the signal of unfolded proteins activates a set of ER-located sensors:

1. The PERK kinase (or eIF2 kinase): it phosphorylates a subunit of the eIF2 that leads to attenuation of general protein synthesis.
2. A special kinase family, carrying an endonuclease activity (involving Ire1a and b) is also activated and in mammals, it initiates gene expressional changes by processing the mRNA of the transcription factor XBP1. XBP1 then translocates to the nucleus and induces a wide range of ER located chaperones, involving members of the glucose regulated protein (Grp) family (Grp78, Grp94). These chaperones play a role in protecting the cell by preventing protein aggregation (keeping the unfolded proteins in a folding-competent state) and by binding and keeping  $\text{Ca}^{2+}$  in the ER lumen.
3. Beside PERK and Ire1, there is a third ER-stress sensor molecule, called ATF6. ATF6 is a transcription factor and it is essential for XBP mRNA expression and chaperone induction upon ER stress.

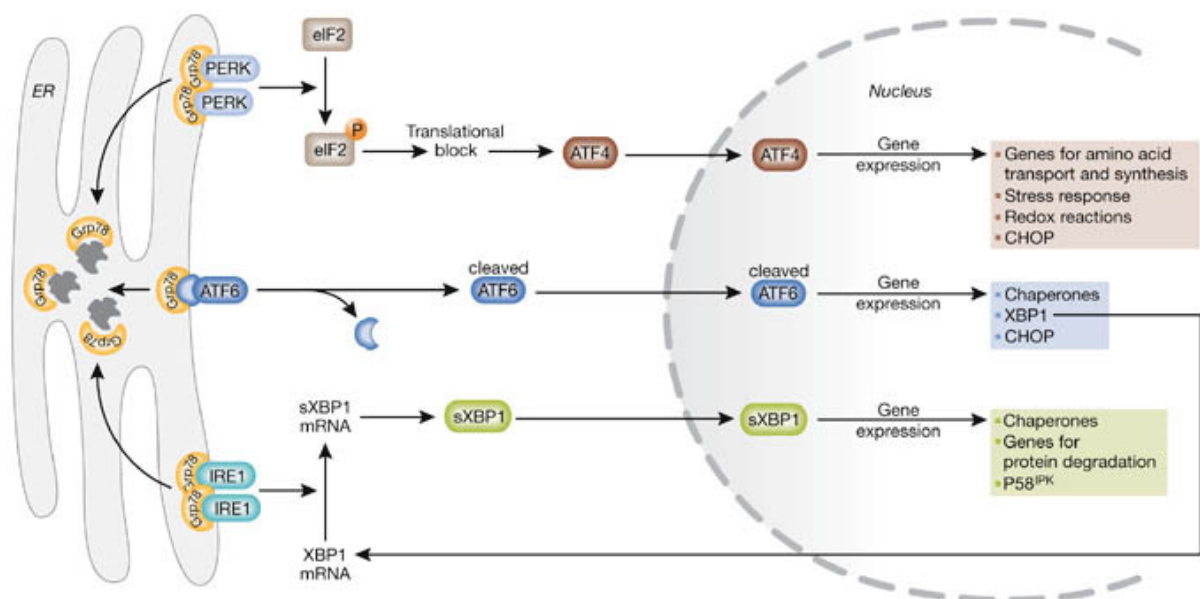


**Figure 2.2 The unfolded protein response.** ER, endoplasmic reticulum; PERK, protein kinase RNA-like endoplasmic reticulum kinase; eIF2A: eukaryotic initiation factor 2A; ATF: activating transcription factor; CHOP, CCAAT/enhancer binding protein (C/EBP) homologous protein; Grp: glucose regulated protein; (s)XBP-1: spliced X-box protein-1; mRNA, messenger RNA; IRE-1, inositol requiring enzyme-1. Adapted from [22].

In summary, stress conditions lead to decreased rate of protein translation to prevent further accumulation of unfolded proteins. Simultaneously, transcription factors are activated in order to induce the expression of the ER-resident chaperones to deal with accumulated protein aggregates. Furthermore, the ER-specific protein-degrading apparatus becomes activated and eliminates denatured proteins. This co-ordinated response halts the build up of proteins, allows time for the elimination of unfolded proteins, and re-establishes cellular homeostasis. However, if the stress cannot be resolved, the cell dies by apoptosis [16].

The processing steps in the Golgi cisternae generate mature *N*-linked oligosaccharide structures. In contrast to reactions of the dolichol pathway, which are highly conserved in eukaryotes, the mature oligosaccharides differ quite significantly across the species. The oligosaccharide chain of mature yeast *N*-linked glycoproteins either consist of a high-mannose “mature core” of 9-13 mannose residues, or they may contain extended branched mannan outer chains consisting of up to 200 residues [17, 18]. The types of mature *N*-linked oligosaccharides synthesized in higher eukaryotes predominantly involve high-mannose, complex and mixed types of structures [1]. In human serum, complex-type *N*-linked glycans are the most abundant glycans accounting for ~96% of total glycans identified, while hybrid and high mannose type glycans comprise the remaining ~4%. [19].

In addition to the trimming reactions in the ER, further removal of three  $\alpha$ -1,2-mannoses in the Golgi generates a structure  $\text{GlcNAc}_2\text{Man}_5$ . This structure serves a precursor to hybrid and complex *N*-glycans in higher eukaryotes. In the medial Golgi compartment, *N*-acetylglucosaminyltransferase I (GnT-I) transfers GlcNAc from UDP-GlcNAc to Man residue. GnT-I is the key enzyme in the biosynthesis of complex-type chains. Subsequently, Golgi  $\alpha$ -mannosidase II removes one  $\alpha$ -1,3- and one  $\alpha$ -1,6-linked mannose to yield  $\text{GlcNAc}_2\text{Man}_3\text{GlcNAc}$ . The fucosyltransferase that attaches fucose in the  $\alpha$ -1,6-linkage to the asparagine-bound GlcNAc in the core has strict requirement for the prior action of the GnT-I enzyme. After the removal of two  $\alpha$ -mannose residues, the second GlcNAc is transferred from UDP-GlcNAc to the Man 1>6 arm by GnT-II to create a biantennary structure. Another GnT-II transfers a GlcNAc to the central, core-bound mannose residue to yield a bisecting GlcNAc. The presence of the bisecting GlcNAc residue at the early stages of processing interferes with the removal of the  $\alpha$ -mannose residues and the action of GnT-II and  $\alpha$ -1,6-fucosyltransferase, and leads to the formation of hybrid-type structures. The latter product can then be extended by the branching *N*-acetylglucosaminyltransferases to generate bi-, tri-, and tetra-antennary structures, which in turn can be terminated with different sugars including galactose (Gal), *N*-acetylgalactosamine (GalNAc), *N*-acetylglucosamine (GlcNAc), fucose and sialic acid residues, therefore forming mature complex oligosaccharides. In general, a strict order of reactions in the synthesis of *N*-linked glycans is observed [20]. An overview of the reactions occurring in the Golgi apparatus can be found in figure 2.3.

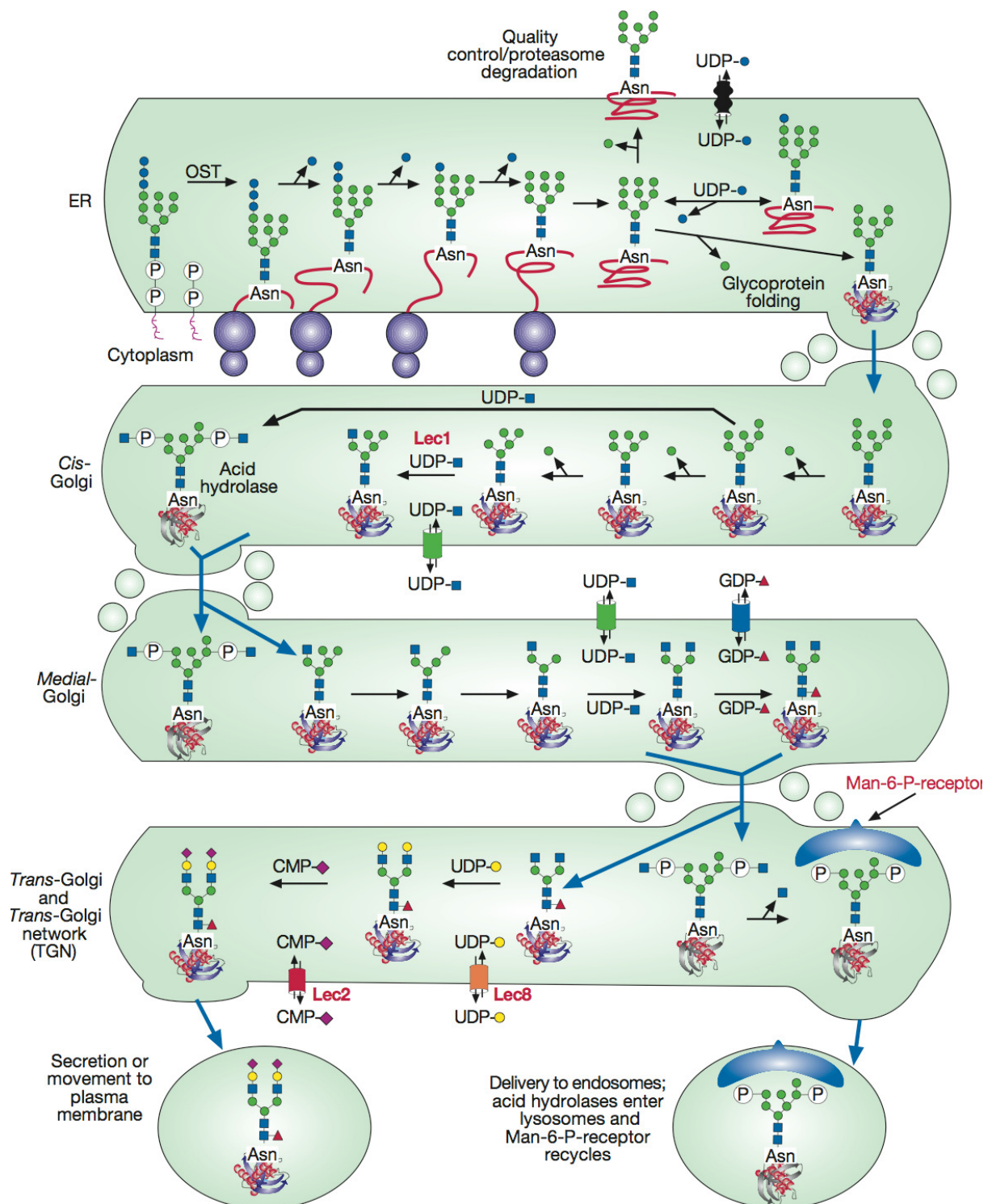


**Figure 2.3. Overview of the processing and maturation steps of an N-glycan in the endoplasmic reticulum and Golgi-apparatus in higher eukaryotes.** Asn, asparagine; OST, oligosaccharyltransferase; UDP, uridine diphosphate; GDP, guanosine diphosphate; CMP, cytidine monophosphate; Man-6-P, mannose-6-phosphate. Adapted from [21].

## 1.2.2 Glycomic techniques

In comparison to genomics and proteomics – where automated synthesis, amplification, expression and characterization have become routine, the tools available for study of glycomics are few. This necessitated the development of unique tools that are currently reaching a reasonable level of sophistication for use by non-specialists [23-25]. The enormous diversity of structures that can be created using a limited number of monosaccharides building blocks coupled with its non template-driven nature has made the task of system-wide glycan profiling a challenging task (Figure 2.4) [26]. A major obstacle for the advancement of glycomics has been the lack of sensitive and easy-to-use high-throughput analytical tools. In this section, a short overview of the different glycomic techniques will be given.

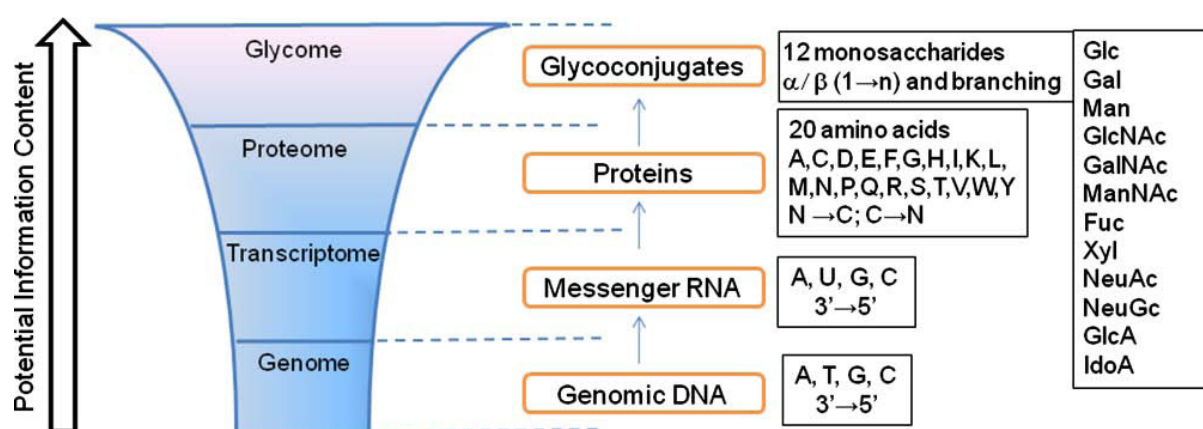


**Figure 2.4 Complexity and diversity of mammalian glycome.** The glycome represents the largest class of posttranslationally modified molecules. The information flow from genome to glycome increases exponentially. Adapted from [65].

### 1.2.2.1 Glycomics and mass spectrometry

Mass spectrometry provides a rapid and sensitive tool for component analysis. Mass spectrometry has therefore emerged as a central tool for glycomics analysis. It is also a precise tool for structural elucidation resulting in significant progress towards understanding the role of the glycome in many biological systems [27].

Mass spectrometers capable of glycan analysis typically employ either matrix-assisted laser desorption/ionization (MALDI) or electrospray ionization (ESI) with or without chromatographic separation. High mass accuracy instruments such as time-of-flight (TOF), ion cyclotron resonance (ICR), and Orbitrap mass analyzers are useful for glycan detection because low mass error are often required for exact mass annotation. Lower performance instruments can make glycan analysis challenging by causing false assignments due to high uncertainties associated with their measurements [28]. Tandem MS can be used to remedy false assignments by providing structural information and glycan compositions. Structural elucidation can be obtained using glycan fragments, exact mass and exoglycosidase digestion.

Although there are many groups studying glycans with mass spectrometry, there are some common features to their chemical processes. Glycans are generally isolated from glycoprotein containing samples by first cleaving off the *N*-glycans with peptide *N*-glycosidase F (PNGase F) and then purifying them with solid phase extraction or high performance liquid chromatography (HPLC). Samples are often concentrated with vacuum centrifuges or lyophilizers before mass spectrometry analysis. The glycans may be derivatized (e.g. methylation, permethylation) to improve ionization and stability of ions in the mass spectrometer. The latter is particularly important with fucosylated and sialylated glycans. Even with the 'soft' ionization sources of electrospray and less 'soft' MALDI, there is still urge to modify sialic acids for stability. As sialylated glycans make up the most abundant species in human serum, they can suppress other less abundant components such as the high mannose glycans. These methods have the additional benefit of positive ion detection of sialylated glycans concurrently with the neutral glycans [29].

Many of the biological sources of glycoproteins, including serum, contain levels of salts that are too high for mass spectrometric analysis because the excess decreases the ionization of the desired analyte. Desalting is often accomplished by filtration [30], dialysis [31], cation exchange resin [32] or carbon-based column adsorption [28, 33].

It has been suggested that a disadvantage of MS glycomic analysis is that it can not distinguish between isomeric structures. However, the ability of ion trap instrumentation to facilitate  $MS^n$  experiments especially on glycans which have been derivatised by permethylation, is allowing unambiguous structural information of isomeric glycans [34]. Additionally, informatic tools are well developed for MS glycomic analysis. Especially in glycomics, the large amount of data places a great burden upon the researcher and annotation of MS data is extremely important [35]. There are several databases of complex glycan structural data, a few prominent publically available examples are:

- the Consortium for Functional Glycomics' (CFG) relational database (<http://www.functionalglycomics.org/glycomics/common/jsp/firstpage.jsp>)
- the Japan Consortium for Glycobiology and Glycotechnology DataBases (JCGGDB) ([http://jcg gdb.jp/index\\_en.html](http://jcg gdb.jp/index_en.html)),
- Glycoscience.de (<http://www.dkfz.de/spec/glycosciences.de/sweetdb/index.php>)
- EuroCarbDB (<http://www.ebi.ac.uk/eurocarb/home.action>)

An example of an MALDI-TOF mass spectrum is given in figure 2.4

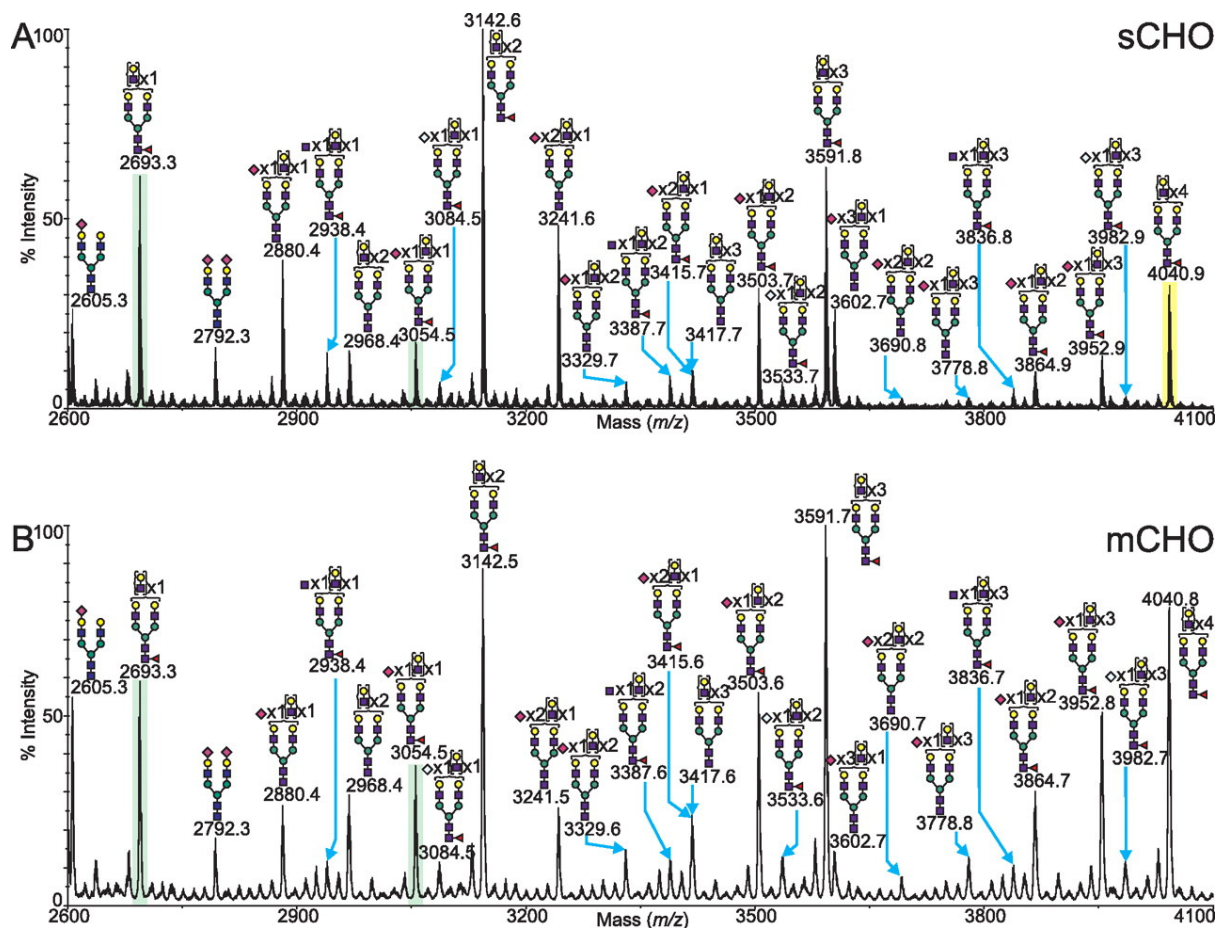


**Figure 2.4 MALDI-TOF MS profiles of the permethylated *N*-glycans derived from wild type CHO cells grown in suspension (A) and wild type CHO cells grown in monolayer (B).**  
Adapted from [66].

### 1.2.2.2

### Glycomics and high performance liquid chromatography

A major problem in glycomic investigation is the structural heterogeneity of glycans representing often complex mixtures of closely related isomeric compounds. For this reason, HPLC has proved to be of great value in profiling and separation of glycans because of the wide range of adsorbents and solvent systems available as well as the speed and reproducibility of separation [36].

In normal phase (NP) HPLC, glycans are retained due to hydrophilic interaction with the stationary phase and the elution times generally increase with size [37]. By comparison with elution positions of glucose isomers (dextran ladder) and distinct oligosaccharide standards, the elution times of individual glycans can be used to predict possible structures. NP-HPLC has been used for underivatized as well as 2-aminopyridine (PA) and 2-aminobenzamide (2-AB) labeled glycans, including also acidic sugar chain species [38, 39]. Reverse phase (RP)-HPLC separates sugars on the basis of their hydrophobicity, i.e., glycans are eluted in the order of decreasing molecular weight, but derivatization with a hydrophobic label (such as PA or 2-AB) is required [39, 40] (Figure 2.5). Likewise, permethylated oligosaccharides may be also employed [41]. Sugar chains that co-elute in NP-HPLC can be often separated by RP-HPLC which can be used, for example, to distinguish between bisected and non-



bisected complex-type structures. Therefore, the two methods are complementary as they allow two structures which co-elute on one system to be resolved on then other [40].

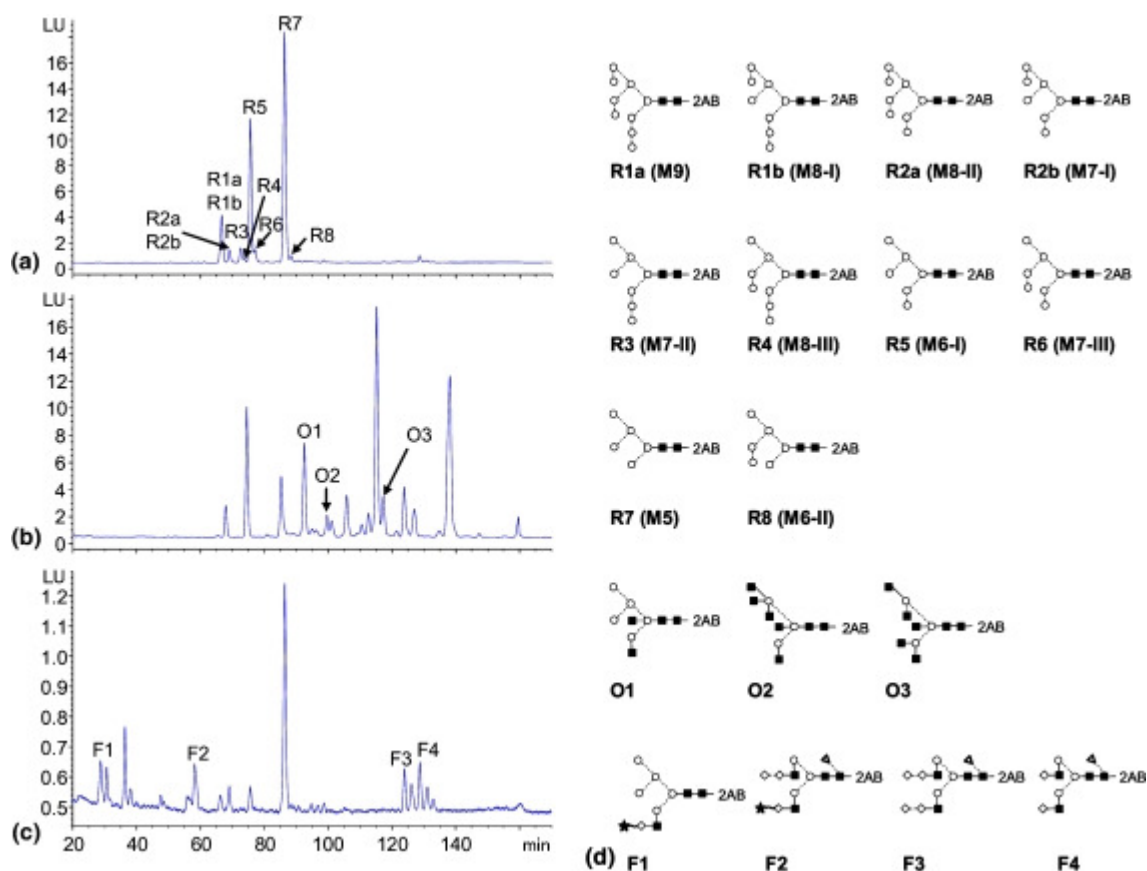


**Figure 2.5 Reverse phase HPLC with fluorescence detection of 2-AB labeled glycans released from (a) 10 µg RNase B, (b) 30 µg ovalbumin and (c) 30 µg fetuin. The structures of the labeled oligosaccharide peaks are shown in (d). Adapted from [67].**

A HPLC method that deserves special attention in the context of glycosylation research is high performance anion-exchange chromatography (HPAEC). Usually electro-chemical detection (pulsed amperometric detection (PAD)) is applied for the analysis after HPAEC separation. In contrast to classic anion-exchange chromatography, HPAEC is performed at a pH of approximately 13. Under these conditions, hydroxyl groups on glycans are partially deprotonated, resulting in a partial negative charge, which is then used for the separation of the glycans. Glycans with a reduced end exhibit less retention than reducing-end glycans, as they lack the anomeric hydroxyl group which is a major contributor to the partial negative charge. Under these conditions, a charge based separation of native glycans as well as glycans derivatized with a neutral label can be achieved. The introduction of labels providing an additional charge leads to an increase in retention times, but a change or enhancement in selectivity is not to be expected [36].

The advantage in comparison to MS is that it can separate and detect oligosaccharides without any derivatization and yet offers excellent resolution and a high sensitivity with a detection limit in the 300 fmol region [42]. In addition, it allows an easier automatization (with

liquid chromatography autosampler) and there is a less cumbersome sample handling. On the other hand, when using MALDI-TOF MS, there is no need for oligosaccharide standards and the time spent on analysis is substantially shorter compared to HPAEC-PAD [43].

### 1.2.2.3 Glycomics and capillary electrophoresis

In capillary electrophoresis (CE), charged analytes are separated according to their migration velocity in an electric field placed across the ends of a capillary column. Since the separation mechanism in CE is different from that of HPLC, both techniques are complementary [44]. The benefits of CE are high separation efficiency and speed of analysis. Charged carbohydrates, such as sulfated or sialylated oligosaccharides, can be separated directly based on their electric charge/molecular size ratio [45]. For neutral glycan mixtures, CE separation requires the conversion into charged species via labeling with a charged fluorophore like ANTS, APTS or 2-AA [46, 47]. A higher charge causes faster analyses and better resolution, making ANTS and APTS the most effective agents for CE analysis of glycans. Labeling of *N*-glycans with APTS under mild reductive amination conditions was shown to preserve sialic acid and fucose residues and allowed a successful profiling also in the case of heavily sialylated *N*-glycans [48].

The technique used in this thesis for the analysis of protein-linked *N*-glycans is DNA sequencer-assisted fluorophore-assisted capillary electrophoresis (DSA-FACE) [49]. Advantages are robustness, high throughput, high sensitivity and reliable quantification of *N*-linked glycans. Moreover, the protocol resolves isobaric glycan stereoisomers which is much more difficult with mass spectrometry. The protocol starts with the denaturation of the glycoproteins and dot-blotting them on a polyvinylidene fluoride (PVDF) membrane-lined 96-well filtration plate. Renaturation is prevented by reductive amination with the advantage that all reagents used are removed by extensive washing without any tube transfers. Subsequently, the *N*-glycans are released with PNGase F in a minimum volume of low-molarity buffer. After vacuum evaporation, the *N*-glycans are labeled with APTS. A problem in using PVDF membranes is their low binding capacity of ~10 µg of glycoprotein. However, the detection limit of laser-induced fluorescence of APTS-labeled sugars is in the low femtomolar range. Moreover, a cleanup step using size-exclusion chromatography over Sephadex G10 packed in 96-well plates is introduced after the APTS labeling. As a consequence, only 10-100 fmol of unlabeled glycans is sufficient for analysis. The clean-up step removes >90% of the free APTS label and effectively desalts the sample, while recovering >70% of the labeled glycans. Finally, the presence of sialic acids on the glycans adds an extra negative charge on the structures, which is a disadvantage in many CE-based methods. Moreover, sialic acids add to the enormous heterogeneity of the glycans and a desialylation reaction is performed to add to the readability in complex mixtures (Figure 2.6).

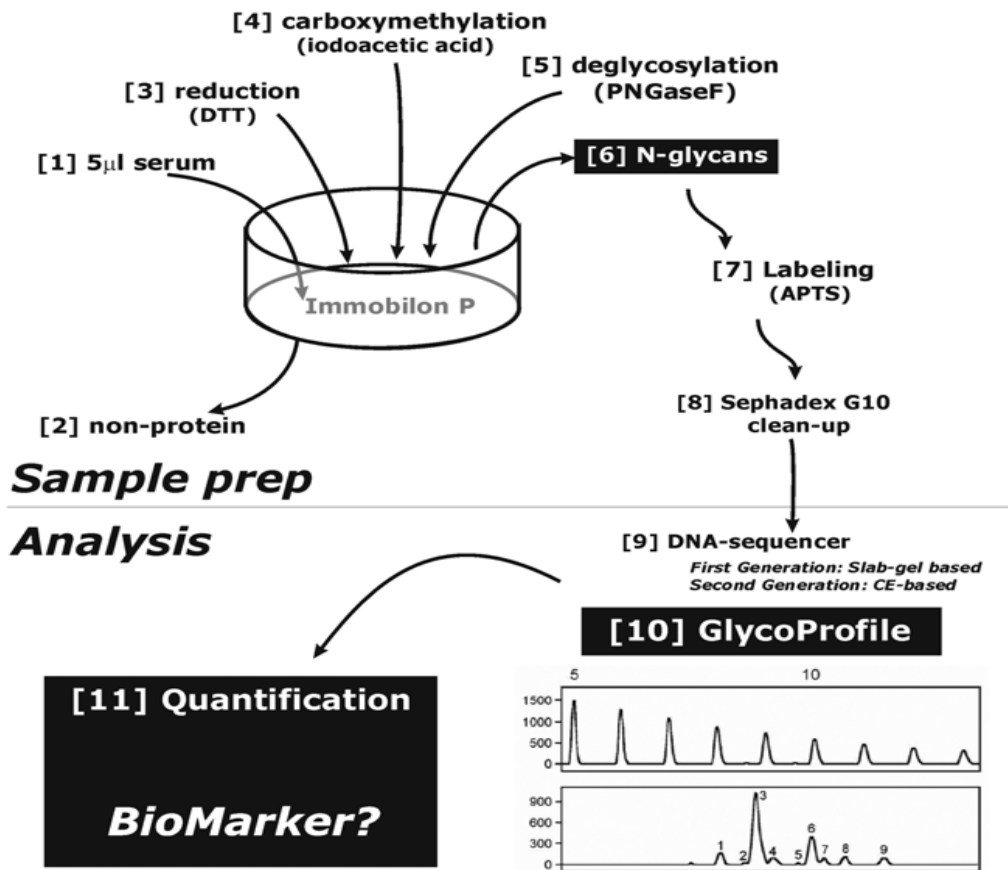


**Figure 2.6 Overview of the DSA-FACE protocol.** DDT, dithiothreitol; PNGase F, peptide *N*-glycosidase F, APTS, 8-aminopyrene-1,3,6-trisulfonic acid. Adapted from [68].

#### 1.2.2.4

#### Glycomics and lectin-based microarrays

Lectins are carbohydrate-binding proteins that are non-enzymatic and not products of an immune response [50]. Lectins have been an invaluable tool in carbohydrate analysis and their utilization in microarray-based technologies has created new opportunities to effectively profile glycan variations on a global scale. A microarray consists of discrete probes immobilized as high-density spots onto a solid support such as glass or nitrocellulose. When challenged with a fluorescent analyte, multiple binding events are observed simultaneously making it a high-throughput technique which provides rapid results [51].

In general, however, the glycan-lectin interaction is relatively weak in comparison to antigen-antibody interactions. Therefore, once bound to a lectin on an array, some glycans may dissociate during the washing process, and this often results in a significant reduction in signal intensity. To circumvent this problem, a lectin microarray based on the principle of evanescent-field fluorescence detection was developed [52]. Lectins that are frequently used in lectin-based microarrays are *Concanavalin A* (Con A), *Arachis hypogaea* (PNA) and *Aleuria auantia* (AAL). These lectins are potentially useful for the diagnosis of HCC patients. An increase of multi-antennary and fucosylated glycans are well documented glycomic alterations in HCC (see further). AAL will specifically bind fucosylated proteins and Con A is specific for biantennary glycans. Therefore, supernatants from liver cancer cell lines, such as

HuH7 (HCC) and HepG2 (hepatoblastoma), will show an increased binding to the AAL lectin, whereas a reduced binding to the Con A lectin will be observed [53, 54].

#### 1.2.2.5 Glycomics and nuclear magnetic resonance

Nuclear magnetic resonance (NMR) spectroscopy is one of the principal techniques used to obtain physical, chemical, electronic and structural information about molecules. NMR is the property that magnetic nuclei have in a magnetic field and applied electromagnetic (EM) pulse will cause the nuclei to absorb energy from the EM pulse and radiated the energy back out. The energy radiated back out is at a specific resonance frequency which primarily depends on the strength of the magnetic field, but also other factors. The title of this section is somewhat misleading, because this sophisticated method is not used for high-throughput glycomic research, but rather for structural insights into carbohydrate-protein interactions [55]. Protein-carbohydrate interactions play crucial roles in numerous biological mechanisms, including intracellular and intercellular routing processes, endocytosis of deleterious glycoconjugates and inflammation [56].

NMR spectrometry is able to detect the binding of ligands to receptors. Several NMR parameters change upon the interaction between molecules. Recently, many NMR methods have been developed to screen collections of compounds, including carbohydrate libraries, for binding to protein receptors [57, 58]. In addition, NMR can also provide structural details of these biologically significant carbohydrate-protein interactions. An important practically application of this technology is found in the field of glycomimetics. This field has attracted considerable attention as potential carbohydrate-based drugs with enhanced chemical and biological stability. For example, a series of GM1 (ganglioside) analogues in which the sialic acid moieties are replaced with the simpler  $\alpha$ -hydroxyl acids have been prepared as part of a strategy to design inhibitors for the cholera toxin [59].

NMR can identify new ligands for receptor, for example the binding of sucrose octasulphate by the natural killer cell receptor NKR-P1A [60], but it can also go a step further in which the epitope of the ligand recognized by the receptors is revealed [61]. Detailed mapping of the ligand helps in the understanding of the binding specificity of the receptor, as shown for the inactive member of the trans-sialidase family from the protozoan *Trypanosoma cruzi*, which is responsible for Chagas' disease [62]. Finally, a topic that is of major interest is the understanding of the structural features at the glycosidic linkages that regulate the three-dimensional structure of glycoproteins. A few studies have been reported that aim to dissect the effect of single and multiple glycosylation on the topology and presentation of the polypeptide chain [63, 64]. An overview of the all the methods used for glycan analysis is given in Table 2.1.

**Table 2.1 Compilation of methods commonly used for glycan analysis**

<b>Method</b>	<b>Structural data obtained</b>	<b>Amount of sample</b>	<b>Labeling required</b>	<b>Advantages</b>	<b>Disadvantages</b>
Mass spectrometry	Composition (Hex, HexNAc, dHex), sequence, branching, partial linkage information	fmole-pmole	No*	High-throughput, sensitive	Quantification difficult
HPAEC-PAD	Structural identification by comparison with reference compounds	Fmole	Yes	Easy automatization and sample handling	No direct structural proof
DSA-FACE	Structural identification by exoglycosidase treatment	Fmole	Yes	High-throughput, sensitive, quantification	No direct structural proof
Lectin affinity microarray	Identification of structural epitopes	fmole-pmole	Yes	High-throughput	Only partial characterization of glycan structures
NMR	Complete structure	Nmole	No	non-destructive	No high-throughput method

\*Labeling is not required, but may enhance ionization; HPAEC-PAD, high performance anio-exchange chromatography pulsed amperometric detection; DSA-FACE, DNA sequencer-assisted fluorophore-assisted capillary electrophoresis, NMR, nuclear magnetic resonance.

### 1.2.3

## ***N*-glycosylation in disease**

#### 1.2.3.1

#### The role of *N*-glycosylation in receptor responses

In the study of disease, the levels of receptor ligands and their downstream signaling pathways have received considerable attention, but less clear are the determinants of receptor availability at the cell surface. In recent years, it became clear that *N*-glycosylation plays an important role in this. The remodeling of *N*-glycans in the Golgi is sensitive to metabolism and when combined with gene-encoded differences in *N*-glycan number per protein, glycoprotein concentrations at the cell surface can be differentially regulated according to their affinities for endogenous lectins [69].

In this context, a lot of research has been done on the epidermal growth factor receptor (EGFR), a cell surface transmembrane glycoprotein. In normal conditions, the receptor is restrained from self-association and activation and additional extrinsic mechanisms of restraint are in place [70]. One of these is galectin binding to the *N*-glycans on EGFR. Galectins are redox-sensitive proteins produced in the cytosol, they bind to the *N*-acetylglucosamine of many glycoproteins at the cell surface [71]. In breast cancer, galectin binding to EGFR slows lateral diffusion and loss to coated-pit endocytosis [72]. In human glioblastomas, an activation mutation in EGFR deletes part of the extracellular domain, removing four of 12 *N*-glycan sites and increasing ligand-independent dimerization [73]. Caveolin1 (Cav1) clusters in cholesterol-rich rafts and binds to EGFR and other signaling proteins resulting in loss of responsiveness to growth factors [74]. Therefore, Cav 1 acts as a tumor suppressor. However, up-regulation of *N*-glycan branching in mouse mammary tumor cells acts dominantly to protect EGFR from Cav1 suppression [72].

The  $\alpha$  and  $\beta$  subunits of the T cell receptor (TCR) are *N*-glycosylated on at least seven Asn-X-Ser/Thr sites [75]. On naive cells, galectin-3 binds to the TCR and prevents spontaneous TCR oligomerization in the absence of antigen, thereby blocking recruitment of CD4-Lck to TCR and its transfer to lipid microdomains [76]. It will also prevent CD8 binding, thereby insulating against complex formation and it will increase the threshold to TCR agonists [77]. Mice that are deficient in the branching enzyme GnT-V or  $\beta$ -1,3-*N*-acetylglucosaminyltransferase ( $\beta$ 3GnT2), an enzyme that extends the  $\beta$ 1,6 branches with poly-*N*-acetylglucosamine, drops the barrier to TCR clustering and auto-immune disease *in vivo* [78, 79]. Selective removal of specific *N*-glycosylation sites from TCR also enhances receptor diffusion, multimerization and activation [80].

Remarkably, the number of glycosylation sites varies considerably between different glycoproteins. Receptor kinases that stimulate growth and proliferation such as insulin receptor, EGFR and platelet-derived growth factor receptor (PDGFR) have approximately five times more glycosylation sites and more sites per 100 amino acids than receptors that mediate organogenesis, differentiation and arrest (such as Tie1, Musk, Ltk) [69]. These observations suggest that *N*-glycan numbers per peptide is a conserved and functionally significant feature of receptor kinases. This also explains the importance of *N*-glycan alterations in cancer.

1.2.3.2

Congenital disorders of glycosylation

Congenital disorders of glycosylation (CDG) are caused by defects in *N*-glycan biosynthesis and provide insight into the functions of *N*-glycans in humans. Type I CDGs are deficiencies in various enzymes in the biosynthetic pathway for  $\text{Glc}_3\text{Man}_9\text{GlcNAc}_2\text{-PP-dolichol}$ , the donor for *N*-glycan addition. As a result, in CDG, usage of *N*-glycosylation sites is reduced [81] (Figure 2.7)

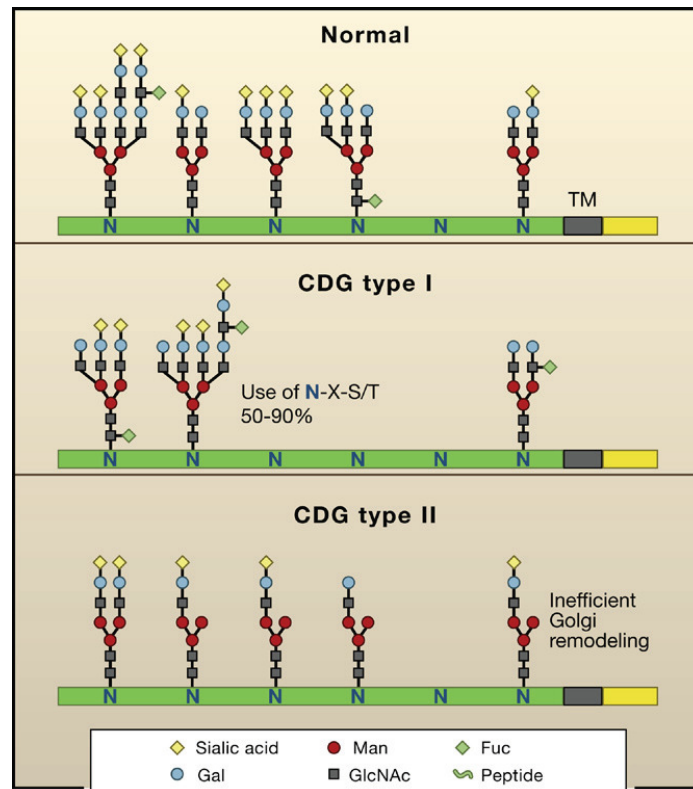


**Figure 2.7 Congenital disorders of glycosylation and glycoforms.** Glycoprotein glycoforms differ based on *N*-glycan structures present at each NXS/T site (not all sites are occupied). CDG type I alters glycoform distribution and CDG type II are deficiencies in Golgi remodeling or glycoprotein trafficking. CDG, congenital disorder of glycosylation. Adapted from [110].

CDG-Ib is a deficiency in phosphomannose isomerase (PMI) that decreases the supply of guanosine diphosphate mannose (GDP-Man) for dolichol-PP-oligosaccharide synthesis. Unlike most CDGs, the symptoms of CDG-Ib including failure to thrive, coagulopathy, protein-losing enteropathy and liver fibrosis, can be improved by supplementation of the diet with mannose [82]. Low glucose conditions impair  $\text{Glc}_3\text{Man}_9\text{GlcNAc}_2\text{-PP-dolichol}$  biosynthesis, giving rise to smaller intermediates and incomplete *N*-glycosylation. The resulting UPR activates PERK, which inhibits general translation by phosphorylating eIF2 $\alpha$ , and this allows  $\text{Glc}_3\text{Man}_9\text{GlcNAc}_2\text{-PP-dolichol}$  and *N*-glycosylation levels to recover [83]. Fibroblasts from patients with type I CDG displayed similar but moderate induction of PERK kinase, suggesting that ER and metabolic stress may be a common feature of CDG-I [84].

Patients with defects in the Golgi and secretory pathway are classified as having type II CDG, which is characterized by reduced branching or extension to the *N*-glycans. The clinical phenotypes of type I and II CDG are often similar, but type II patients can also suffer from psychomotor retardation, ataxia, seizures and retinopathy. These deficiencies arise from loss-of-function mutations in genes related to remodeling: GnT-II (CDG-IIa),  $\alpha$ -glucosidase I (CDG-IIb), GDP-fucose Golgi transporter (CDG-IIc) and  $\beta$ -1,4-galactosyltransferase (CDG-IIId) [81]. Leukocyte adhesion deficiency type II (LAD II) is caused by a mutation in the Golgi GDP-Fucose transporter that reduces cell surface fucosylated glycans, and patients suffer recurrent infection due to a deficiency in selectin ligands. The fucose salvage pathway has the capacity to generate very high concentrations of GDP-Fuc, sufficient to overcome a partial defect in Golgi GDP-Fuc transport in patients [85].

Liver symptoms are involved in most patients with CDG. An overview of the subtypes in which an impact on liver function is described in literature, although most liver symptoms occur in CDG type I patients. Diminished liver function has been reported in two patients and two siblings with CDG-IId [86, 87]. In one of these patients, hepatomegaly, bile lakes and liver fibrosis were observed. Histologically, the liver showed bile duct malformation, which were defined by the persistence of an excess of embryological bile duct structures in ductal plate configuration [86]. Furthermore, in three CDG-Ic patients, liver biopsies revealed abnormal lysosomal inclusions in hepatocytes [88], but no bile duct abnormalities. CDG-Ih is characterized by a severe hepato-intestinal phenotype with elevated liver enzymes and hepatomegaly [89, 90]. Liver biopsy was performed in one patient, showing multiple, cystic, dilated intra- and extrahepatic bile ducts. The patients also developed cholestasis and diffuse renal microcysts [90]. In one neonate patient with CDG-IIb, progressive hepatomegaly was observed and the patients died after 74 days. Post mortem light microscopy of the liver revealed dilatation and proliferation of the bile ducts. Furthermore, the liver displayed progressive cholangiofibrosis, steatosis, cholestasis and the appearance of bile thrombi in hepatocytes and bile ducts [91].

### 1.2.3.3 Glyco-biomarkers of cancer and chronic inflammation

In addition to its diagnostic properties in liver diseases, that will be discussed in section 1.4, *N*-glycosylation has especially been useful for the diagnosis of cancer and chronic inflammation. Obviously, both are associated with liver diseases and there will be some overlapping features.

Two of the most well characterized glycosylation changes in the *N*-linked serum glycome of cancer patients are the degree of branching (indicated by the number of GlcNAcs attached to the chitobiose core) and the levels of sialyl Lewis x (SLe<sup>x</sup>) structures [92, 93]. The SLe<sup>x</sup> epitope consists of a sialic acid residue  $\alpha$ 2,3-linked to galactose with fucose  $\alpha$ 1,3 fucose linked to GlcNAc. These glycan biomarkers have also been identified as markers for chronic inflammation [94, 95]. Tumors and tumor microenvironments are rich sources of cytokines and in late stages of tumor progression, the serum of cancer patients can present markers of chronic inflammation. These glycosylation changes correlate with the level of CRP in stage four ovarian cancer patients [92]. In 90% of patients, resection of the tumor in non small-cell lung cancer leads to postsurgical reduction in the level of SLe<sup>x</sup> in the serum glycome, with 60% reaching normal levels [96]. SLe<sup>x</sup> has long been established as being vital for the



process of leukocyte extravasation from the blood stream. SLe<sup>x</sup> is a ligand for endothelial-selectin (E-selectin) which expressed exclusively on endothelial cells in response to inflammatory stimuli [97]. Leukocytes, which display SLe<sup>x</sup> epitopes, exploit this interaction to adhere to the endothelium and initiate rolling. Following integrin interactions, the cells extravasate from the blood stream. SLe<sup>x</sup> levels are significantly higher on metastatic cancer cells [98] and can be exploited to aid metastasis [99].

Obviously, individual serum proteins, that are primarily produced by the liver, also contain both glycan alterations in oncogenic and inflammatory conditions. Immunoglobulin G is an abundant serum protein in humans that is not produced by the liver, but released by plasma cells in response to antigens that activate B-cells. Most *N*-glycans on IgG are biantennary, whereas multi-antennary glycans on IgG are rare [100]. Especially the galactose content of the IgG glycoforms is known to vary in cancer and inflammation. The completely agalactosylated glycoforms (IgG-G0) are elevated in cancer patients and they have been shown to increase with tumor progression [92, 101]. Hyperfucosylation has also been identified, but this could be the result of the increase in agalactosylated glycoforms which are also all fucosylated. Although present in cancer, increase of IgG-G0 were especially found in chronic inflammatory conditions such as rheumatoid arthritis (RA), Crohn's disease, systemic lupus erythematosus and tuberculosis [102, 103]. In RA, the level of IgG-G0 is more than two SDs above those of aged matched healthy controls [102, 104], correlates with disease activity and is directly associated with pathogenesis in a mouse model [105]. Interestingly, the elevation of IgG-G0 is reversible and levels in RA patients who go into remission during pregnancy generally fall into normal range in the third trimester [105].

The reduction in galactosylation of IgG glycans is not a consequence of elevated IgG synthesis by B cells, as there is no correlation between the serum concentration of IgG and IgG-G0 in patients with RA, suggesting the glycosylation machinery is sufficient to deal with the increased protein trafficking [103]. The increase of IgG-G0 has been associated with lowered galactosyltransferase (GalT) activity [106, 107]. There is a linear correlation between B and T cell GalT activity and IgG-G0 levels in RA serum [108]. However, other studies have not identified a difference in the level of GalT within B cells from RA patients and suggest that the reduced GalT activity may arise from a reduced activity of the enzyme [109]. The factors that contribute to the reduced GalT activity in the plasma cell subset remain to be established.

## 1.2.4 References

- [1] Kornfeld R, Kornfeld S. Assembly of asparagine-linked oligosaccharide. *Ann Rev Biochem* 1985;54:631-664.
- [2] Hounsell E, Davies M, Renouf D. O-linked protein glycosylation structure and function. *Glycoconj J* 1996;13:19-26.
- [3] Udenfriend S, Kodukula K. How glycosylphosphatidylinositol-anchored membrane proteins are made. *Ann Rev Biochem* 1995;64:591-593.
- [4] Szymanski C, Wren B. Protein glycosylation in bacterial mucosal pathogens. *Nat Rev Microbiol* 2005;3:225-237.

- [5] Abu-Qarn M, Eichler J, Sharon N. Not just for Eukarya anymore: protein glycosylation in Bacteria and Archaea. *Curr Opin Struct Biol* 2008;18:544-550.
- [6] Varki A. Biological roles of oligosaccharides: all of the theories are correct. *Glycobiology* 1993;3:97-130.
- [7] Gu J, Isaji T, Sata Y, Kariya Y, Fukuda T. Importance of N-glycosylation on alpha5beta1 integrin for its biological functions. *Biol Pharm Bull* 2009;32:780-785.
- [8] Habibi-Babadi N, Su A, de Carvalho C, Colavita A. The N-glycanase png-1 acts to limit axon branching during organ formation in *Caenorhabditis elegans*. *J Neurosci* 2010;30:1766-1776.
- [9] Dennis J, Granorsky M, Warren C. Protein glycosylation in development and disease. *Bioessays* 1999;21:412-421.
- [10] Lehle L, Bause E. Primary structural requirements for N- and O-glycosylation of yeast mannoproteins. *Biochim Biophys Acta* 1984;700:246-250.
- [11] Silberstein S, Gilmore R. Biochemistry, molecular biology, and genetics of the oligosaccharyltransferase. *FASEB J* 1996;10:849-858.
- [12] Gavel Y, Van Heijne G. Sequence differences between glycosylated and non-glycosylated Asn-X-Thr/Ser acceptor sites: implications for protein engineering. *Protein Eng* 1990;3:433-442.
- [13] Herbert D, Simons J, Peterson J, Helenius A. Calnexin, calreticulin, and Bip/Kar2p in protein folding. *Cold Spring Harbor Symposia on Quantitative Biology* 1995;60:405-415.
- [14] Xu C, Bailly-Maitre B, Reed J. Endoplasmic reticulum stress: cell life and death decisions. *J Clin Invest* 2005;115:2656-2664.
- [15] Hotamisligil G. Endoplasmic reticulum stress and the inflammatory basis of metabolic disease. *Cell* 2010;140:900-917.
- [16] Hampton R. ER stress response: getting the UPR hand on misfolded proteins. *Curr Biol* 2000;10:R518-521.
- [17] Ballou L, Hitzeman R, Lewis M, Ballou C. Vanadate-resistant yeast mutants are defective in protein glycosylation. *Proc Natl Acad Sci USA* 1991;88:3209-3212.
- [18] Trimble R, Atkinson P. Structural heterogeneity in the Man<sub>8-13</sub>GlcNAc oligosaccharides from log-phase *Saccharomyces* yeast: a one- and two-dimensional <sup>1</sup>H NRM spectroscopic study. *Glycobiology* 1992;2:57-75.
- [19] Chu C, Niñonuevo M, Clowers B, Perkins P, An H, Yin H, et al. Profile of native N-linked glycan structures from human serum using high performance liquid chromatography on a microfluidic chip and time-of-flight mass spectrometry. *Proteomics* 2009;9:1939-1951.
- [20] Kukuruzinska M, Lennon K. Protein N-glycosylation: molecular genetics and functional significance. *Crit Rev Oral Biol Med* 1998;9:415-448.
- [21] Stanley P, Schachter H, Taniguchi N. N-glycans. In: Varki A, Cummings R, Esko J, Freeze H, Stanley P, Bertozzi C, Hart G, Etzler M. *Essentials of Glycobiology*, 2nd edition. Cold Spring Harbor (NY): *Cold Spring Laboratory Press*, 2009.
- [22] Szegezdi E, Logue S, Gorman A, Samali A. Mediators of endoplasmic reticulum stress-induced apoptosis. *EMBO Rep* 2006;7:880-885.
- [23] Bertozzi C, Kiessling L. Chemical glycobiology. *Science* 2001;291:2357-2364.
- [24] Pilobello K, Mahal L. Deciphering the glycode: the complexity and analytical challenge of glycomics. *Curr Opin Chem Biol* 2007;11:300-305.
- [25] Prescher J, Bertozzi C. Chemical technologies for probing glycans. *Cell* 2006;126:851-854.

- [26] Gabius H, Siebert H, André S, Jiménez-Barbero J, Rüdiger H. Chemical biology of the sugar code. *ChemBiochem* 2004;5:740-764.
- [27] Park Y, Lebrilla C. Application of Fourier transform ion cyclotron resonance mass spectrometry to oligosaccharides. *Mass Spectrom Rev* 2005;24:232-264.
- [28] Kronewitter S, An H, de Leoz M, Lebrilla C, Miyamoto S, Leiserowitz G. The development of retrosynthetic glycan libraries to profile and classify the human serum N-linked glycome. *Proteomics* 2009;9:2986-2994.
- [29] An H, Kronewitter S, de Leoz M, Lebrilla C. Glycomics and disease markers. *Curr Opin Chem Biol* 2009;13:601-607.
- [30] Woosly B, Kim Y, Kolli V, Wello L, King D, Poe R, et al. Glycan analysis of recombinant *Aspergillus niger* endo-polygalacturonase A. *Carbohydr Res* 2006;341:2370-2378.
- [31] Merry A, Neville D, Royle L, Mattheus B, Harvey D, Dwek R, et al. Recovery of intact 2-aminobenzamide-labeled O-glycans released from glycoproteins by hydrazinolysis. *Anal Biochem* 2002;304:91-99.
- [32] Botelho J, Atwood J, Cheng L, Abvarez-Manilla G, York W, Orlando R. Quantification by isobaric labeling (QUIBL) for the comparative glycomic study of O-linked glycans. *Int J Mass Spectrom* 2008;278:137-142.
- [33] An H, Miyamoto S, Lancaster K, Kirmiz C, Li B, Lam K, et al. Profiling of glycans in serum for the discovery of potential biomarkers for ovarian cancer. *J Proteome Res* 2006;5:1626-1635.
- [34] Devakumar A, Mechuf Y, Kang P, Novotny M, Reilly J. Identification of isomeric N-glycan structures by mass spectrometry with 157 nm laser-induced photofragmentation. *J Am Soc Mass Spectrom* 2008;19:1027-1040.
- [35] North S, Hitchen P, Haslam S, Dell A. Mass spectrometry in the analysis of N-linked and O-linked glycans. *Curr Opin Struct Biol* 2009;19:498-506.
- [36] Geyer H, Geyer R. Strategies for analyses of glycoprotein glycosylation. *Biochim Biophys Acta* 2006;1764:1853-1869.
- [37] Royle L, Mattu T, Hart E, Langridge J, Merry A, Murphy M. An analytical and structural database provides a strategy for sequencing O-glycans from microgram quantities of glycoprotein. *Anal Biochem* 2002;304:70-90.
- [38] Wuhrer M, Koeleman C, Deelder A, Hokke C. Normal-phase nanoscale liquid chromatography-mass spectrometry of underivatized oligosaccharides at low-femtomole sensitivity. *Anal Chem* 2004;76:833-838.
- [39] Kuraya M, Hase S. Analysis of pyridylaminated O-linked sugar chains by two-dimensional sugar mapping. *Anal Biochem* 1996;233:205-211.
- [40] Rudd P, Colominas C, Royle L, Murphy M, Hart E, Merry H, et al. A high-performance liquid chromatography based strategy for rapid, sensitive sequencing of N-linked oligosaccharide modifications to proteins in sodium dodecyl sulphate polyacrylamide electrophoresis gel bands. *Proteomics* 2001;1:285-294.
- [41] Delaney J, Louros P. Liquid chromatography ion trap mass spectrometric analysis of oligosaccharides using permethylated derivatives. *Rapid Commun Mass Spectrom* 2001;15:325-334.
- [42] Davies M, Hounsell E. Carbohydrate chromatography: towards yoctomole sensitivity. *Biomed Chromatogr* 1996;10:285-289.
- [43] Grey C, Edebrink P, Krook M, Jacobsson S. Development of a high performance anion exchange chromatography analysis for mapping of oligosaccharides. *J Chromatogr B* 2009;877:1827-1832.

- [44] Jorgenson J. Electrophoresis. *Anal Chem* 1986;58:143A-760A.
- [45] Hermentin P, Doengas R, Witzel R, Hokke C, Vliegenthart J, Kamerling H, et al. A strategy for the mapping of N-glycans by high-performance capillary electrophoresis. *Anal Biochem* 1994;221:29-41.
- [46] Chiesa C, O'Neill R. Capillary zone electrophoresis of oligosaccharides derivatized with various aminonaphthalene sulfonic acids. *Electrophoresis* 1994;15:1132-1140.
- [47] Guttman A, Pritchett T. Capillary gel electrophoresis separation of high mannose types oligosaccharides derivatized by 1-aminopyrene-3,6,8-trisulfonic acid. *Electrophoresis* 1995;16:1905-1911.
- [48] Chen F, Evangelista R. Profiling glycoprotein N-linked oligosaccharide by capillary electrophoresis. *Electrophoresis* 1998;19:2639-2644.
- [49] Laroy W, Contreras R, Callewaert N. Glycome mapping on DNA sequencing equipment. *Nat Prot* 2006;1:397-405.
- [50] Lis H, Sharon N. Lectins: carbohydrate-specific proteins that mediate cellular recognition. *Chem Rev* 1998;98:637-674.
- [51] Hsu K, Mahal L. Sweet tasting chips: microarray-based analysis of glycans. *Curr Opin Chem Biol* 2009;13:427-432.
- [52] Kuno A, Uchiyama N, Koseki-Kuno S, Ebe Y, Takashima S, Yamada M, et al. Evanescent -field fluorescence-assisted lectin microarray: a new strategy for glycan profiling. *Nat Methods* 2005;2:851-856.
- [53] Ito H, Kuno A, Sawaki H, Sogabe M, Ozaki H, Tanaka Y, et al. Strategy for glycoproteomics: identification of glycol-alteration using multiple glycan profiling tools. *J Proteome Res* 2009;8:1358-1367.
- [54] Ishiyuro T, Sakaguchi H, Fukui M, Sugitachi I. Serum alpha-fetoprotein subfractions in hepatic malignancies identified by different reactivities with concanavalin A, lentil lectin or phytohemagglutinin E. *Jpn J Surg* 1986;16:16-21.
- [55] Kogelberg H, Solis F, Jiménez-Barbero J. New structural insights into carbohydrate-protein interactions from NMR spectroscopy. *Curr Opin Struct Biol* 2003;13:646-653.
- [56] Engering A, Geijtenbeek T, Van Kooyk Y. Immune escape through C-type lectins in dendritic cells. *Trends Immunol* 2002;23:480-485.
- [57] Pellecchia M, Sem D, Wüthrich K. NMR in drug discovery. *Nat Rev Drug Discov* 2002;1:211-219.
- [58] Stockman B, Dalvit C. NMR screening techniques in drug discovery and drug design. *Prog Nucl Magn Reson* 2002;41:187-231.
- [59] Bernardi A, Potenza D, Capelli A, Garcia-Herrero A, Cañada F, Jiménez-Barbero J. Second-generation mimics of ganglioside GM1 oligosaccharide: a three-dimensional view of their interactions by NMR and computational methods. *Chem Eur J* 2002;8:4598-4612.
- [60] Kogelberg H, Frenkiel T, Birdsall B, Chai W, Maskett F. Binding of sucrose octasulphate to the C-type lectin-like domain of the recombinant natural killer cell receptor NKR-P1A observed by NMR spectroscopy. *Chembiochem* 2002;3:1072-1077.
- [61] Kooistra O, Herfurth L, Lüneberg E, Frosch M, Petus T, Zähringer U. Epitope mapping of the O-chain polysaccharide of *Legionella pneumophila* serogroup 1 lipopolysaccharide by saturation-transfer-difference NMR spectroscopy. *Eur J Biochem* 2002;269:573-582.
- [62] Todeschini A, Girard M, Wieruszkeski J, Nunes M, Doskeis R, Medonça-Previato L, et al. Transsialidase from *Trypanosoma cruzi* binds host T-lymphocytes in a lectin manner. *J Biol Chem* 2002;277:45962-45968.

- [63] Grinstead J, Koganty R, Krantz M, Longenecker B, Campbell A. Effect of glycosylation on MUC-1 humoral immune recognition: NMR studies of MUC-1 glycopeptide-antibody interactions . *Biochemistry* 2002;41:9946-9961.
- [64] Kindahl L, Sandstorm C, Craig A, Norberg T, Kenne L. H-1 NMR studies on the solution conformation of contulakin-G and analogues. *Can J Chem* 2002;80:1022-1031.
- [65] Gupta G, Surolia A, Srinivana-Gopalan S. Lectin microarrays for glycomic analysis. *OMICS* 2010;14:419-436.
- [66] North S, Huang H, Sundaram S, Jang-Lee J, Etienne A, Trollope A, et al. Glycomics profiling of Chinese hamster ovary cell glycosylation mutants reveals N-glycans of a novel size and complexity. *J Biol Chem* 2010;285:5759-5775.
- [67] Chen X, Flynn G. Gas-phase oligosaccharide nonreducing end (GONE) sequencing and structural analysis by reverse phase HPLC/mass spectrometry with polarity switching. *J Am Soc Mass Spectrom* 2009;20:1821-1833.
- [68] Laroy W, Contreras R. Glycoprofiling by DNA sequencer-aided fluorophore-assisted carbohydrate electrophoresis: new opportunities in diagnosing and following disease. In: Appasani K, Southern E. Bioassays: from basics to diagnostics. *Humana Press*, 2007
- [69] Lau K, Partridge E, Grigorian A, Slivescu C, Reinhold V, Demetriou M, et al. Complex N-glycan number and degree of branching cooperate to regulate cell proliferation and differentiation. *Cell* 2007; 129:123-134.
- [70] Klein P, Mattoon D, Lemmon M, Schlessinger J. A structure-based model for ligand binding and dimerization of EGR receptors. *Proc Natl Acad Sci USA* 2004; 101:929-934.
- [71] Patnaik S, Potvin B, Carlsson S, Sturm D, Leffler H, Stanley P. Complex N-glycans are the major ligands for galactin-1, and -3, and -8 in Chinese hamster ovary cells. *Glycobiology* 2006;16:305-317.
- [72] Lajoie P, Partridge E, Geray G, Goetz J, Pawling J, Lagana A, et al. Plasma membrane domain organization regulates EGFR signalling in tumor cells. *J Cell Biol* 2007;179:341-356.
- [73] Fernandes H, Cohen S, Bishayee S. Glycosylation-induced conformational modification positively regulates receptor-receptor association: a study with an aberrant epidermal growth factor receptor (EGFRvIII/DeltaEGFR) expressed in cancer cells. *J Biol Chem* 2001;276:5375-6383.
- [74] Okamoto T, Sehlegel A, Scherer P, Lisanti M. Caveolins, a family of scaffolding proteins for organizing "preassembled signaling complexes" at the plasma membrane. *J Biol Chem* 1998;273:5419-5422.
- [75] Rudd P, Wormald M, Stanfield R, Huang M, Mattsson M, Speir J, et al. Roles for glycosylation of cell surface receptors involved in cellular immune recognition. *J Mol Biol* 1999;293:351-366.
- [76] Grigorian A, Torossian S, Demetrou M. T-cell growth, cell surface organization, and the galectin-glycoprotein lattice. *Immunol Rev* 2009;230:232-246.
- [77] Demotte N, Stroobant V, Courtoy P, Van der Smissen P, Colau D, Luescher I, et al. Restoring the association of the T cell receptor with CD8 reverses anergy in human tumor-infiltrating lymphocytes. *Immunity* 2008;28:414-424.
- [78] Demetriou M, Granosky M, Quaggin S, Dennis J. Negative regulation of T-cell activation and autoimmunity by Mgat5 N-glycosylation. *Nature* 2001;409:733-739.
- [79] Togayachi A, Kozono Y, Ishida H, Abe S, Suzuki N, Tsunoda Y, et al. Polylysosamine on glycoproteins influences basal levels of lymphocyte and macrophage activation. *Proc Natl Acad Sci USA* 2007;104:15829-15834.

- [80] Kuball J, Hauptrock B, Malina V, Antunes E, Voss R, Wolf M, et al. Increasing functional avidity of TCR-redirected T cells by removing defined N-glycosylation sites in the TCR-constant domain. *J Exp Med* 2009;206:463-475.
- [81] Jaeken J, Matthijs G. Congenital disorders of glycosylation: a rapidly expanding disease family. *Annu Rev Genomics Hum Genet* 2007;8:261-278.
- [82] Freeze H. Disorder in protein glycosylation and potential therapy: tip of an iceberg? *J Pediatr* 1998;133:593-600.
- [83] Shang J, Gao N, Kaufman R, Ron D, Harding H, Lehrman M. Translation attenuation by PERK balances ER glycoprotein synthesis with lipid-linked oligosaccharide flux. *J Cell Biol* 2007;176:605-616.
- [84] Lecca M, Wagner U, Patrignani A, Berber E, Hennet T. Genome-wide analysis of the unfolded protein response in fibroblasts from congenital disorders of glycosylation type-I patients. *FASEB J* 2005;19:240-242.
- [85] Marquardt T, Lühnk, Srikrishna G, Freeze H, Harms E, Vestweber D. Correction of leukocyte adhesion deficiency type II with oral fucose. *Blood* 1999;94:3976-3985.
- [86] Sun L, Ekland E, Chang W, Wang C, Cohen J, Freeze H. Congenital disorder of glycosylation Id presenting with hyperinsulinemic hypoglycemia and islet cell hyperplasia. *J Clin Endocrinol Metab* 2005;90:4371-4375.
- [87] Kranz C, Sun L, Ekland E, Krasnewich D, Casey J, Freeze H. CDG-Id in two siblings with partially different phenotypes. *Am J Med Genet A* 2007;143A:1414-1420.
- [88] Grunwald S, De Vos R, Jaeken J. Abnormal lysosomal inclusions in liver hepatocytes but not in fibroblasts in congenital disorders of glycosylation (CDG). *J Inherit Metab Dis* 2003;26:49-64.
- [89] Chantret I, Dancourt J, Dupre T, Delenda C, Backer S, Vuillaumier-Barrot S, et al. A deficiency in dolichyl-P-glucose: Glc1Man9GlcNAc2-PP-dolichyl alpha3-glycosyltransferase defines a new subtype of congenital disorders of glycosylation. *J Biol Chem* 2003;278:9962-9971.
- [90] Schollen E, Frank C, Keldermans L, Reyntjes R, Grubenmann C, Clayton P, et al. Clinical and molecular features of three patients with congenital disorders of glycosylation type 1h (CDG-1h) (Alg8 deficiency). *J Med Genet* 2004;41:550-556.
- [91] De Praeter C, Gewig G, Bause E, Nuytinck L, Vliegthart J, Breuer W, et al. A novel disorder caused by defective biosynthesis of N-linked oligosaccharides due to glucosidase I deficiency. *Am J Hum Genet* 2000;66:1744-1756.
- [92] Saldova R, Royle L, Radcliffe C, Hamid U, Evans R, Arnold J, et al. Ovarian cancer is associated with changes in glycosylation in both acute-phase proteins and IgG. *Glycobiology* 2007;17:1344-1356.
- [93] Dage J, Ackermann B, Halsall H. Site localization of sialyl Lewis(x) antigen on alpha1-acid glycoprotein by high performance liquid chromatography-electrospray mass spectrometry. *Glycobiology* 1998;8:755-760.
- [94] Brinkman-van der Linden E, de Haan P, Havenaar E, van Dijk W. Inflammation-induced expression of sialyl Lewis X is not restricted to alpha1-acid glycoprotein but also occurs to a lesser extent on alpha1-antichymotrypsin and haptoglobin. *Glycoconj J* 1998;15:177-182.
- [95] van Dijk W, Havenaar E, Brinkman-van der Linden E. Alpha1-acid glycoprotein (orosomuroid): pathophysiological changes in glycosylation in relation to its function. *Glycoconj J* 1995;12:227-233.
- [96] Mizuguchi S, Inoue K, Iwata T, Nishida T, Izumi M, Tsukioka T, et al. High serum concentrations of sialyl Lewis (x) predict multilevel N2 disease in nonsmall-cell lung cancer. *Ann Surg Oncol* 2006;13:1010-1018.

- [97] Bevilacqua M, Stenglin S, Gimbrone M, Seed B. Endothelial leukocyte adhesion molecule 1: an inducible receptor for neutrophils related to complement regulatory proteins and lectins. *Science* 1989;243:1160-1165.
- [98] Kurebayashi, Nomura T, Hirono M, Okulo S, Udagawa K, Shiiki S, et al. Combined measurement of serum sialyl Lewis X with serum CA15-3 in breast cancer patients. *Jpn J Clin Oncol* 2006;36:150-153.
- [99] Witz I. The involvement of selectins and their ligands in tumor-progression. *Immunol Lett* 2006;104:89-93.
- [100] Kobata A. The N-linked sugar chains of human immunoglobulin G: their unique pattern, and their functional roles. *Biochim Biophys Acta* 2008;1780:472-478.
- [101] Kanoh Y, Mashiko T, Danbara M, Takayama Y, Ohtani S, Egawa S, et al. Changes in serum IgG oligosaccharide chains with prostate cancer progression. *Anticancer Res* 2004;24:3135-3139.
- [102] Parekh R, Dwek R, Sutton B, Fernandes B, Leung A, Stanworth D, et al. Association of rheumatoid arthritis and primary osteoarthritis with changes in the glycosylation pattern of total serum IgG. *Nature* 1985;316:452-457.
- [103] Parekh R, Isenberg D, Rook G, Roitt I, Dwek R, Rademacher T. A comparative analysis of disease-associated changes in the galactosylation of serum IgG. *J Autoimmun* 1989;2:101-114.
- [104] Parekh R, Roitt I, Isenberg D, Dwek R, Rademacher T. Age-related galactosylation of the N-linked oligosaccharides of human serum IgG. *J Exp Med* 1988;167:1731-1736.
- [105] Rook G, Steele J, Brealey R, Whyte A, Isenberg D, Sumar N, et al. Changes in IgG glycoform levels are associated with remission of arthritis during pregnancy. *J Autoimmun* 1991;4:779-794.
- [106] Roitt I, Dwek R, Parekh R, Rademacher T, Alavi A, Axford J, et al. Changes in carbohydrate structure in IgG in rheumatoid arthritis. *Reanti Prog Med* 1988;79:314-317.
- [107] Axford J, Mackenzie L, Lydard P, Hay F, Isenberg D, Roitt I, et al. Reduced B-cell galactosyltransferase activity in rheumatid arthritis. *Lancet* 1987;2:1486-1488.
- [108] Axford J, Sumar N, Alavi A, Isenberg D, Young A, Badman K, et al. Changes in normal glycosylation mechanisms in autoimmune rheumatic disease. *J Clin Invest* 1992;89:1021-1031.
- [109] Keusch J, Lydard P, Berger E, Delves P. B lymphocyte galactosyltransferase protein levels in normal individuals and in patients with rheumatoid arthritis. *Glycoconj J* 1998;15:1093-1097.
- [110] Dennis J, Nabi I, Demetriou M. Metabolism, cell surface, and disease. *Cell* 2009;139:1229-1241.

### 1.3.1 Liver biopsy: limitations and complications

Liver biopsy is invasive and can cause significant complications. Nearly 30% of patients report having substantial pain after liver biopsy, and some experience serious complications such as pneumothorax, bleeding, or puncture of the biliary tree. In very rare cases, patients die of intraperitoneal bleeding. The mortality is about 1 in 10 000 [1, 2]. Performing liver biopsies generally has substantial socio-economic cost, since the patients must be observed for bleeding complications. Moreover, due to its invasive nature, it can not be used repeatedly in follow-up.

Furthermore, hepatic pathology, particularly fibrosis, is not always uniformly distributed. Surgical wedge biopsy provides adequate tissue volume to overcome this problem. Needle biopsy, on the other hand, provides a much smaller volume of tissue (1/50 000 of total mass) [2]. As examples of the resulting sampling errors that can occur, consider the two most common chronic liver diseases: hepatitis C and fatty liver disease. Regev *et al* performed laparoscopically guided biopsy of the right and left hepatic lobes in a series of 124 patients with chronic hepatitis C [3]. Biopsy samples from the right and left lobes differed in the intensity of inflammation in 24.2% of the cases and in the intensity of fibrosis in 33.1%. Differences of more than one grade of inflammation or stage of fibrosis were uncommon. However, in 14.5%, cirrhosis was diagnosed in one lobe, but not in the other. In a study with non-alcoholic fatty liver disease, Ratziu *et al* found that none of the features characteristic of non-alcoholic steatohepatitis were highly concordant in paired liver biopsies [4]. Finally, in a study of 10 000 liver biopsies, Bedossa demonstrated that only 65% of the biopsies with a length of 15 mm and 75% of biopsies with a length of 25 mm the stage of fibrosis was correctly diagnosed [5]. In our experience, the length of needle biopsies rarely exceed 15 mm. Clearly, needle liver biopsy is far from an ideal test.

Increasingly, liver diseases can be diagnosed precisely with imaging techniques, serum markers, or both. It is foreseen that liver biopsy will play a lesser role in diagnosis in the near future.

### 1.3.2 Imaging techniques

A central limitation of the imaging techniques is that they appear to perform better in the detection of advanced stages of liver disease. Therefore, imaging techniques have great value in the detection of cirrhosis and especially HCC, but the sensitivity of detection is usually lower in fibrotic livers. In addition, much more imaging techniques can be used to diagnose HCC and these techniques are therefore discussed separately.



The basic principle of transient elastography is that propagation velocity of a wave through a homogeneous tissue is proportional to its elasticity (stiffness). The elasticity has been demonstrated to correlate to the amount of fibrosis in the liver [6]. The transducer is placed over the liver and transmits a low-frequency (50 Hz) wave that propagates through the liver and the velocity of the wave is then measured by pulse-echo ultrasound. If the liver is fibrotic, the elastic waves propagate more rapid than in a normal liver [7]. In 5-10% of patients, valid measurements can not be obtained due to overweight (25% of patients with a BMI>30 can not be scanned), narrow intercostal space and ascites [8]. Studies have shown high intraobserver and interobserver agreement (interclass correlation coefficient 0.96-0.98% and 0.89-0.98) [9].

In 2003, a first study of transient elastography was published [7]. In total, 91 patients with chronic hepatitis C were examined with liver biopsy as well as liver elasticity measurements. The study demonstrated good correlation between histological grading and liver elasticity. Transient elastography was 99% effective in detecting cirrhosis and 88% effective in detecting fibrosis. Many studies have followed after this initial investigation with similar good results, although the very high area under curve (AUC) could not be reproduced. Important is that optimal cut-off values are not the same for cirrhosis of different etiology. The optimal cut-off values in HBV patients was lower than for HCV patients. In contrast, the optimal cut-off value for patients with cirrhosis because of alcohol abuse or NASH was higher [10]. The correlation between liver stiffness values and liver biopsies does not seem to be affected by steatosis [11]. Finally, transient elastography also correlates with the presence of portal hypertension and related complications such as esophageal varices [12].

However, it has been demonstrated that liver stiffness measurement is unsuitable for detecting fibrosis in patients with acute hepatitis [13, 14]. There are speculations that measurement of liver stiffness may be misleading in patients with chronic liver diseases during intermittent flares of liver inflammation. It is still unclear to which degree transient elastography may replace liver biopsies. Castera *et al* suggested that 77% of all liver biopsies (viral hepatitis) could be avoided by transient elastography combined with biomarkers [15].

A technique that appears even more promising is magnetic resonance elastography [16]. The technique is similar to that used in ultrasound elastography in that it uses a vibration device to induce a shear wave in the liver. However, in this case, the wave is detected by a modified magnetic resonance imaging machine, and a color-coded image is generated that depicts the wave velocity, and hence stiffness, throughout the organ. Studies have shown a magnetic resonance scoring system that distinguishes Child-Pugh grade A cirrhosis from other grades to be 93% sensitive and 82% specific [17]. The strength of this technique is that the separation of values for varying stages of fibrosis is very good and considerable better in comparison to ultrasound elastography [18].

Four imaging techniques are frequently used in the assessment of liver cancer. Contrast-enhanced ultrasound (CEUS), computed tomography (CT), magnetic resonance imaging (MRI) and positron emission tomography (PET). These four are discussed shortly in the following two paragraphs. Imaging of the liver vasculature is an important part of HCC imaging owing to the very strong neo-angiogenesis in hepatocarcinogenesis.

CEUS makes use of ultrasound contrast agents (UCAs). UCAs used in diagnostic ultrasound are characterized by a microbubble structure, consisting of gas bubbles stabilized by a shell [19]. Microbubbles sizes typically range from 3 to 5  $\mu\text{m}$  and on intravenous injection remain in the vascular compartment for several minutes, being small enough to avoid filtration by the lungs and too large to enter the interstitial fluid. These compounds demonstrate strong non-linear harmonic responses when insonated with low acoustic pressure and generate specific signals without being destroyed when insonated at low mechanical index, thus allowing continuous real-time imaging [19]. For CT, a 'dual-phase' technique is commonly employed with image acquisition in the hepatic arterial dominant phase and in the portal venous-dominant phase. The 'triple-phase' technique includes an early arterial phase, imaged 18-25s following bolus injection of contrast [20]. In contrast to CT, lesion/liver contrast is higher for MRI than with CT and the flexibility and range of pulse sequences available in MRI provide a significant advantage over CT. Hepatobiliary MRI uses several magnetic resonance pulse sequences, each of which produces images that provide unique information about the liver and the biliary tree [21]. Finally, PET has the advantage over cross-sectional anatomical imaging of providing whole body imaging, allowing the detection of multifocal and metastatic disease. There are many radiopharmaceuticals based on labeled short-lived positron-emitters, of which, the most widely used is the fluorinated glucose derivative  $^{18}\text{F}$ -fluorodeoxyglucose, but this does not work in all patients [22].

Despite technical improvements in all imaging techniques, difficulties remain in detecting small ( $\leq 2$  cm) lesions in the cirrhotic liver. A recent prospective study comparing imaging findings with pathological examination of the transplanted liver in a pre-transplant population, found that ultrasound, MRI and CT had similar sensitivities for HCC detection on a lesion-by-lesion basis, although ultrasound performed slightly better on a patient-by-patient basis [23]. PET failed to detect any of the pathologically proven HCC lesions. Currently, ultrasound is recommended in the screening of patients at risk of HCC [24]. In experienced hands, ultrasound can detect 80-90% of lesions 3-5 cm in diameter and has 60%-80% sensitivity in the detection of lesions of 1 cm [25, 26]. In cases of elevated AFP with no nodule visible on ultrasound, CT is recommended to investigate the possibility of infiltrative HCC. In a prospective study comparing CT findings and pathological examination of the transplanted liver in large pre-transplant population with cirrhosis, CT detected tumor in only 44% of patients in whom HCC was found at pathological examination [27]. In contrast to other imaging techniques, the sensitivity of MRI in the detection of HCC decreases in cases with advanced cirrhosis [28], and the presence of ascites can generate significant artifacts. Additional difficulties can arise in distinguishing well-differentiated HCC from regenerative and dysplastic nodules [29].

### 1.3.3 Serum markers

#### 1.3.3.1 Serum markers for fibrosis/cirrhosis

Serum markers of liver fibrosis progression can be divided into Class I and Class II biomarkers of fibrosis. The markers of Class I directly represent the intensity of fibrogenesis or fibrinolysis. Frequently, they involve costly laboratory tests and are the result of translation of fibrogenic mechanisms into clinical application. Therefore, their selection is hypothesis-driven. Class II biomarkers are empirically derived indexes which include proteins, enzymes, coagulation factors, and other various biochemical and cytological markers often combined into mathematical formula. They usually represent the stage of fibrosis or the extent of fibrotic transformation of liver parenchyma. These two groups of biomarkers are useful for different purposes, Class I are generally (but not always) more sensitive in determining intensity of fibrogenesis, or grade of the disease, Class II markers could help us estimate the extent of fibrosis or stage of the disease [30]. Due to the large number of these biomarkers, they are summarized in two tables with the focus on the relatively few markers which gained limited clinical importance. For the Class II markers, only the liver fibrosis scoring systems are given [31].

**Table 3.1 Class I biomarkers of liver fibrogenesis**

	Specimen			Method
	Serum	Urine	Liver biopsy	
<i>Extracellular matrix-related enzymes</i>				
Prolyl hydroxylase	+	-	+	RIA, radioenzymatic
Monoamine-oxidase	+	-	(+)	Enzymatic
Lysl oxidase	+	-	+	RIA
Lysyl hydroxylase	+	-	-	RIA
Galactosylhydroxyllysyl-glucosyltransferase	+	-	+	RIA
Collagen peptidase	+	-	+	Enzymatic
N-acetyl-b-D-glucosaminidase	+	+	+	Enzymatic
<i>Collagen fragments and split products</i>				
Type-I-procollagen				
N-terminal propeptide (PINP)	+	-	+	ELISA
C-terminal propeptide (PICP)	+	-	+	RIA
Type-III-procollagen				
Intact procollagen	+	-	-	RIA
N-terminal propeptide (PIIINP)				
Complete propeptide (Col 1-3)	+	-	-	RIA
Globular domain of propeptide (Col-1)	+	-	-	RIA
Type IV-collagen				
NC1-fragment (C-terminal) crosslinking domain (PIVP)	+	+	-	RIA, ELISA

7S domain ("7S collagen")	+	+	-	RIA
Type VI-collagen	+	+	+	RIA
<i>Glycoproteins and matrix-metalloproteinase (inhibitors)</i>				
Laminin, P1-fragment	+	-	-	RIA, EIA
Undulin	+	-	-	EIA
Vitronectin	+	-	-	EIA
Tenascin	+	-	-	ELISA
YKL-40	+	-	+	RIA/ELISA
(pro) MMP-2	+	-	-	ELISA
Tissue inhibitor of metalloproteinases (TIMP-1, TIMP-2)	+	-	-	ELISA
sICAM-1 (soluble intercellular adhesion molecule, sCD54)	+	-	-	ELISA
<i>Glycosaminoglycans</i>				
Hyaluronic acid (hyaluronan)	+	-	-	Radioligand assay/ ELISA
<i>Molecular mediators</i>				
Transforming growth factor beta (TGF- $\beta$ )	+	-	-	ELISA
Connective tissue growth factor (CTGF, CCN2)	+	?	-	ELISA

MMP, matrix metalloproteinase; RIA, radioimmunoassay; ELISA, enzyme linked immunosorbant assay; EIA, enzyme immunoassay. Adapted from [30].

**Table 3.2 Liver fibrosis scoring systems**

Index	Parameters	Type of chronic liver disease	Sensitivity (%)	Specificity (%)	Reference
<i>Liver fibrosis scoring systems using standard laboratory tests</i>					
Sheth index (De Ritis)	AST/ALT ratio	HCV	53	100	[32]
Bonacini-index	ALT/AST-ratio, INR, platelet count	HCV	46	98	[33]
Pohl-score	AST/ALT-ratio, platelet count	HCV	41	99	[34]
Forns-index	Age, platelet count, GMT, cholesterol	HCV	94	51	[35]
WAI-index (APRI)	AST, platelet count	HCV	89	75	[36]
Testa-index	Platelet count/spleen diameter-ratio	HCV	78	79	[37]
FIB-4	Platelet count, AST, ALT, age	HCV/HIV	70	74	[38]

*Liver fibrosis scoring systems using non-standard laboratory tests*

PGA-index	Prothrombin time, GMT, apolipoprotein	A1 mixed	91	81	[39]
PGAA-index	Prothrombin time, GMT, apolipoprotein A1, $\alpha$ 2-macroglobulin	Alcohol	79	89	[40]
Fortunato-index	Fibronectin, prothrombin time, PCHE, ALT, Mn-SOD, $\beta$ -NAG	HCV		94	[41]
FibroTest (Fibro-score)	Haptoglobin, $\alpha$ 2-macroglobulin, apolipoprotein A1, GGT, bilirubin	HCV	75	85	[42]
ActiTest	FibroTest+ALT	HCV			[43]
Sud-index (fibrosis probability index, FPI)	Age, AST, cholesterol, insulin resistance (HOMA), past alcohol intake	HCV	96	44	[44]

*Liver fibrosis scoring systems using Class I fibrosis markers*

Patel-index	Hyaluronic acid, TIMP-1, $\alpha$ 2-macroglobulin	HCV	77	73	[45]
Leroy-score	PIIINP, MMP-1	HCV	60	92	[46]
Rosenberg-score (ELF score)	PIINP, hyaluronic acid, TIMP-1	Mixed	90	41	[47]
Fibrometer test	Platelet count, prothrombin index, AST, $\alpha$ 2-macroglobulin, hyaluronic acid, urea, age	Mixed	81	84	[48]
Hepascore	Bilirubin, GMT, hyaluronic acid, $\alpha$ 2-macroglobulin, age, gender	HCV	63	89	[49]

---

AST, aspartate aminotransferase; ALT, alanine aminotransferase; HCV, hepatitis C virus; INR, international normalized ratio; GMT, gamma-glutamyl transferase; APRI, aminotransferase to platelet ratio; HIV, human immunodeficient virus; PCHE, pseudocholesterase; Mn-SOD, Mn superoxide dismutase;  $\beta$ -NAG, beta-N-acetylglucosaminidase; HOMA, Homeostatic Model Assessment; TIMP-1, Tissue inhibitor for matrix metalloproteinases. Adapted from [31].

### 1.3.3.2 Serum markers for hepatocellular carcinoma

In analogy with the markers for fibrosis/cirrhosis, the list of serum markers for hepatocellular carcinoma is extensive. Therefore, a short discussion of the most important (clinically relevant) markers is given.

*$\alpha$ -fetoprotein* is a unique marker that is used in clinical practice in combination with hepatic echography in the screening of cirrhotic patients to discover HCC, but other markers have been studied to reach an earlier diagnosis. Moreover, cirrhotic patients can show a transient AFP elevation that is associated with hepatocyte regeneration as a consequence of liver necroinflammation [50]. Persistent AFP elevations is found in some of these patients. In this case, *Lens culinaris* reactive AFP (AFP-L3%) measurement may be of help in the HCC

diagnosis. AFP-L3% is the product of  $\alpha$ -1,6-fucosyltransferase; this enzyme is higher in HCC tissues than in peritumoral tissues [51]. Therefore, AFP-L3% is considered more specific than AFP in HCC diagnosis.

Eighty percent of the patients with small HCC-lesions show no increased AFP concentration. Sensitivity of AFP even decreases from 52% to 25% when tumour diameter is respectively >3 cm and <3 cm, suggesting a correlation between serum AFP concentration and tumour size [52]. So far, no universally accepted guidelines have been formulated. AFP also has a role in monitoring the response to treatment in HCC. A decrease in serum AFP concentration with a half-time of <5 days and a normalization to an AFP serum concentration of <10  $\mu$ g/l is one criterion to assess treatment effectiveness [53]. However, this criterion can only be applied when serum AFP concentration is elevated prior to treatment. In HCC patients where serum AFP is not increased before therapy, AFP has a limited value for assessing treatment response [54]. Table 3.3 summarizes diagnostic values of serum AFP levels using different cut-off values.

**Table 3.3 Summary of diagnostic values of alpha-fetoprotein levels for detecting HCC**

Cut-off value ( $\mu$ g/l)	Sensitivity (%)	Specificity (%)	Reference
20	55-60	88-90	[55, 56, 57]
50	47	96	[58]
100	31.2	98.8	[55]
200	22.4	99.4	[55]
400	17.1	99.4	[55]

Adapted from [61]

The following markers act as a diagnostic aid for HCC. *Des-gamma-carboxyprothrombin* is an abnormal prothrombin identified as a biomarker for HCC diagnosis. *Squamous cell carcinoma antigen* (SCCA) expression is more increased in premalignant dysplastic nodules than in HCC [58]. Smaller HCC show a higher SCCA expression than larger ones: decreased SCCA expression is correlated with progression of tumor size while increased SCCA expression in surrounding non-tumoral tissues of larger HCC is a marker for neoplastic transformation. *Serum proteomics* is used for the serologic recognition of protein profiles associated with cancer. Proteomic approach can accurately identify clinical HCC in cirrhotic patients. *Golgi Protein 73* is considered a possible marker for HCC; in fact it shows a specificity of 75% and a sensitivity of 69% [59].

The following markers determine prognosis in HCC. *Glypican-3* (GPC3) expression is less frequently observed in well-differentiated HCC than in moderately and poorly differentiated HCC. GPC3-positive patients show a lower survival than GPC3-negative patients. *Vascular endothelial growth factor* (VEGF) positively regulates tumor neovascularization. HCC patients with overexpression of VEGF have a lower survival rate. The increase of *P-aPKC-1* expression is correlated with more aggressive tumoral behavior, it is considered a prognostic factor for the survival of HCC patients. *Chromogranin A* is used to evaluate neuroendocrine differentiation of HCC and it may be of help in the therapeutic approach. The overexpression of hepatic *transforming growth factor  $\beta$ 1* is found in HCC and is correlated with carcinogenesis, progression, and prognosis of HCC [59].

Finally, particular markers can aid in monitoring therapy in advanced HCC. *Hepatocyte growth factor* is considered a useful marker for evaluating the possible complications arising

after curative hepatic resection. *Serum anti-p53* correlated positively with a poor prognosis and a shorter survival. It is used in the planning of HCC therapy [60]. *E-cadherin* and  $\beta$ -*catenin* are reduced in poorly differentiated cancer and their expression is correlated with metastasis development.

### 1.3.4 References

- [1] Rockey D, Caldwell S, Goodman Z, Nelson R, Smith A. American Association for the Study of Liver Diseases. Liver biopsy. *Hepatology* 2009;49:1017-1044.
- [2] Bravo A, Sheth S, Chopra S. Liver biopsy. *N Eng J Med* 2001;344:495-500.
- [3] Regev A, Berko M, Jeffers L, Milikowski C, Molina E, Pyrsopoulos M, et al. Sampling error and intraobserver variation in liver biopsy in patients with chronic HCV infection. *Am J Gastroenterol* 2002;97:2614-2618.
- [4] Ratziu V, Charlotte F, Hertier A, Gombert S, Giral P, Bruckert E, et al. LIDO study group. Sampling variability of liver biopsy in nonalcoholic fatty liver disease. *Gastroenterology* 2005;128:1098-1906.
- [5] Bedossa P, Dargère D, Paradis V. Sampling variability of liver fibrosis in chronic hepatitis C. *Hepatology* 2003;39:239-244.
- [6] Yeh W, Li P, Jeng Y, Hsu H, Kuo P, Li M, et al. Elastic modules measurements of human liver and correlation with pathology. *Ultra Med Bio* 2002;28:467-474.
- [7] Sandrin L, Fourquet B, Hasquenoph J, Yon S, Fournier C, Mal F, et al. Transient elastography: a new noninvasive method for assessment of hepatic fibrosis. *Ultra Med Bio* 2003;29:1705-1713.
- [8] Castéra L, Forns X, Alberti A. Non-invasive evaluation of liver fibrosis using transient elastography. *J Hepatol* 2008;48:835-847.
- [9] Franquelli M, Rigamonti C, Casazza G, Conte D, Donato M, Ronchi G, et al. Reproducibility of transient elastography in the evaluation of liver fibrosis in patients with chronic liver disease. *Gut* 2007;56:968-973.
- [10] Ganne-Carié N, Ziol M, de Lédinghen V, Douvin C, Marcellin P, Castéra L, et al. Accuracy of liver stiffness for the diagnosis of cirrhosis in patients with chronic liver diseases. *Hepatology* 2006;44:1511-1517.
- [11] Ziol M, Handra-Luca A, Kettanach A, Christidis C, Mal F, Kazemi F, et al. Noninvasive assessment of liver fibrosis by measurement of stiffness in patients with chronic hepatitis C. *Hepatology* 2005;41:48-54.
- [12] Vizzutti F, Arena U, Romanelli R, Rega L, Foschi M, Colanrande S, et al. Liver stiffness measurement predicts severe portal hypertension in patients with HCV-related cirrhosis. *Hepatology* 2007;45:1290-1297.
- [13] Sagir A, Erhardt A, Schmitt M, Häussinger D. Transient elastography is unreliable for detection of cirrhosis in patients with acute liver damage. *Hepatology* 2008;47:592-595.
- [14] Arena U, Vizzutti F, Corti G, Ambu S, Stasi C, Bresci S, et al. Acute viral hepatitis increases the liver stiffness values measured by transient elastography. *Hepatology* 2008;47:380-384.
- [15] Castéra L, Vergniol J, Foucher J, Le Bail B, Chanteloup E, Haaser M, et al. Prospective comparison of transient elastography, FibroTest, APRI, and liver biopsy for the assessment of fibrosis in chronic hepatitis C. *Gastroenterology* 2005;128:343-350.
- [16] Talawalkar J. Elastography for detecting hepatic fibrosis: options and considerations. *Gastroenterology* 2008;135:299-302.

- [17] Ito K, Mitchell D, Hann H, Kim Y, Fujita T, Okazaki H, et al. Viral-induced cirrhosis: grading of severity using MR imaging. *AJR Am J Roentgenol* 1999;173:591-596.
- [18] Huwart L, Sempoux C, Vicaut E, Salamek H, Annet L, Danse E, et al. Magnetic resonance elastography for the noninvasive staging of liver fibrosis. *Gastroenterology* 2008;135:32-40.
- [19] Cosgrove C, Eckersley R. Contrast-enhanced ultrasound: basic physics and technology overview. In: Cencioni R. Enhancing the role of ultrasound with ultrasound contrast agents. Pisa: Springer, 2006:3-14.
- [20] Foley W, Mallisee T, Hohenwarter M, Wilson C, Quiroz F, Taylor A. Multiphase hepatic CT with a multirow detector CT scanner. *AJR Am J Roentgenol* 2000;175:679-685.
- [21] Semelka R, Helmberger T. Contrast agents for MR imaging of the liver. *Radiology* 2001;218:27-38.
- [22] Meikle S, Dahlbom M. Positron emission tomography (PET). In: Ell P, Gambhir S. Nuclear medicine in clinical diagnosis and treatment. Edinburgh: Churchill Livingstone, 2004:187-1843.
- [23] Glockner J. Hepatobiliary MRI: current concepts and controversies. *J Magn Reson Imaging* 2007;25:681-695.
- [24] Ryder S. Guidelines for the diagnosis and treatment of hepatocellular carcinoma (HCC) in adults. *Gut* 2003;52 Suppl3:iii1-iii8.
- [25] Colombo M, de Franchis R, Del Ninno E, Sangiovanni A, De Fazio C, Tommasini M, et al. Hepatocellular carcinoma in Italian patients with cirrhosis. *N Eng J Med* 1991;325:675-680.
- [26] Okuda K. Early recognition of hepatocellular carcinoma. *Hepatology* 1986;6:729-738.
- [27] Peterson M, Baron R, Marsh J, Oliver J, Confer S, Hunt L, et al. Pretransplantation surveillance for possible hepatocellular carcinoma in patients with cirrhosis: epidemiology and CT-based tumor detection rate in 430 cases with surgical pathologic correlation. *Radiology* 2000;217:743-749.
- [28] Teefey S, Hildebolt C, Dehdashti F, Siegel B, Peters M, Heiken J, et al. Detections of primary hepatic malignancy in liver transplant candidates: prospective comparison of CT, MR imaging, US, and PET. *Radiobiology* 2003;226:533-542.
- [29] Hussain S, Zondervan P, Ijzerman J, Schalm S, de Man R, Krestin G. Benign versus malignant hepatic nodules: MR imaging findings with pathologic correlation. *Radiographics* 2002;22:1023-1039.
- [30] Gressner A, Gao C, Gressner O. Non-invasive biomarkers for monitoring the fibrogenic process in liver: a short survey. *World J Gastroenterol* 2009;15:2433-2440.
- [31] Jarcuska P, Janicko M, Veseling E, Jarcusko P, Skladany L. Circulating markers of liver fibrosis progression. *Clin Chem Acta* 2010;411:1009-1017.
- [32] Sheth S, Flamm S, Gordon F, Chopra S. AST/ALT ratio predicts cirrhosis in patients with chronic hepatitis C virus infection. *Am J Gastroenterol* 1998;93:44-48.
- [33] Bonacini M, Hadi G, Govindarajan S, Lindsay K. Utility of a discriminant score for diagnosing advanced fibrosis or cirrhosis in patients with chronic hepatitis C virus infection. *Am J Gastroenterol* 1997;92:1302-1304.
- [34] Pohl A, Behling C, Oliver D, Kilani M, Monson P, Hassanein T. Serum aminotransferase levels and platelets counts as predictors of degree of fibrosis in chronic hepatitis C virus infection. *Am J Gastroenterol* 2001;96:3142-3146.
- [35] Forns X, Ampurdanes S, Ilovet J, Aponte J, Quinto J, Martinez-Bauer E, et al. Identification of chronic hepatitis C patients with hepatic fibrosis by a simple predictive model. *Hepatology* 2002;36:986-992.



- [36] Wai C, Greenson J, Fontana R, Kalbfleisch J, Marrero J, Conjeevareem H, et al. A simple noninvasive index can predict both significant fibrosis and cirrhosis in patients with chronic hepatitis C. *Hepatology* 2003;38:518-526.
- [37] Testa R, Testa E, Giannini E, Barro P, Milazzo S, Isola L, et al. Noninvasive ratio indexes to evaluate fibrosis staging in chronic hepatitis C: role of platelet count/spleen diameter ratio index. *J Intern Med* 2006;260:142-150.
- [38] Sterling R, Lissen E, Clumeck N, Sola R, Correa M, Montaner J, et al. Development of a simple noninvasive index to predict significant fibrosis in patients with HIV/HCV coinfection. *Hepatology* 2006;43:1317-1325.
- [39] Poynard T, Aubert A, Bedossa P, Abella A, Naveau S, Paraf F et al. A simple biological index for detection of alcoholic liver disease in drinkers. *Gastroenterology* 1991;100:1397-1402.
- [40] Naveau S, Poynard T, Benattur C, Bedossa P, Chaput J. Alpha-2 macroglobulin and hepatic fibrosis. Diagnostic Interest. *Dig Dis Sci* 1994;39:2426-2432.
- [41] Fortunato G, Castaldo G, Oriani G, Cerini R, Intrievi M, Molinavo E, et al. Multivariate discriminant function based on six biochemical markers in blood can predict the cirrhotic evolution of chronic hepatitis. *Clin Chem* 2001;47:1696-1700.
- [42] Imbert-Bismut F, Ratziu V, Pieroni L, Charlotte F, Benhamou Y, Poynard T. Biochemical markers of liver fibrosis in patients with hepatitis C virus infection: a prospective study. *Lancet* 2001;357:1069-1075.
- [43] Poynard T, McHutchinson J, Manns M, Myers R, Albrecht J. Biochemical surrogate markers of liver fibrosis and activity in a randomized trial of peginterferon alpha-2b and ribavirin. *Hepatology* 2003;38:481-492.
- [44] Sud A, Hui J, Farrele G, Bandara P, Kench J, Feng C, et al. Improved prediction of fibrosis in chronic hepatitis C using measures of insulin resistance in a probability index. *Hepatology* 2004; 1239-1247.
- [45] Patel K, Gordon S, Jacobson I, Hézode C, Oh E, Smith K, et al. Evaluation of a panel of non-invasive serum markers to differentiate mild from moderate-to-advanced liver fibrosis in chronic hepatitis C patients. *J Hepatol* 2004;41:935-942.
- [46] Leroy V, Monier F, Bottari S, Trocme C, Strm N, Hilleret M, et al. Circulating matrix metalloproteinases 1, 2, 9 and their inhibitors TIMP-1 and TIMP-2 as serum markers of liver fibrosis in patients with chronic hepatitis C: comparison with PIIINP and hyaluronic acid. *Am J Gastroenterol* 2004;99:271-279.
- [47] Rosenberg W, Voelker M, Thiel R, Becha A, Burt A, Schuppan D, et al. Serum markers detect the presence of liver fibrosis: a cohort study. *Gastroenterology* 2004;127:1704-1713.
- [48] Cales P, Oberti F, Michalak S, Hubert-Fouchard I, Rousselet M, Konaté A, et al. A novel panel of blood markers to assess the degree of liver fibrosis. *Hepatology* 2008;42:1373-1381.
- [49] Adams L, Bulsara M, Rossi E, DeBoer B, Spears D, George J. Hepascore: an accurate validated predictor of liver fibrosis in chronic hepatitis C infection. *Clin Chem* 2005;51:1867-1873.
- [50] Liauw Y, Tai D, Chen T, Chu M, Huang M. Alpha-fetoprotein changes in the course of chronic hepatitis: relation to bridging hepatic necrosis and hepatocellular carcinoma. *Liver* 1986;6:133-137.
- [51] Noda K, Myoshi E, Uozumi M, Yanagidani S, Ikeda Y, Gao C, et al. Gene expression of alpha1-6 fucosyltransferase in human hepatoma tissues: a possible implication for increased fucosylation of alpha-fetoprotein. *Hepatology* 1998;28:944-952.
- [52] Saffroy R, Pham P, Reffas M, Takka M, Lemoine A, Debuire B. New perspectives and strategy research biomarkers for hepatocellular carcinoma. *Clin Chem Lab Med* 2007;45:1169-1179.

- [53] Han S, Yoo S, Choi S, Hwang E. Actual half-life of alpha-fetoprotein as a prognostic tool in pediatric malignant tumors. *Pediatr Surg Int* 1997;12:599-602.
- [54] Bruix J, Sherman M, Llovet J, Beaugrand M, Lencioni R, Burroughs A, et al. Clinical management of hepatocellular carcinoma. Conclusions of the Barcelona-2000 EASL conference. European Association for the Study of the Liver. *J Hepatol* 2001;35:421-430.
- [55] Trevisani F, D'Intino P, Morselli-Labate A, Mazzella G, Accogli E, Caraceni P, et al. Serum alpha-fetoprotein for diagnosis of hepatocellular carcinoma in patients with chronic liver disease: influence of HBsAg and anti-HCV status. *J Hepatol* 2001;139:570-575.
- [56] Gambarin-Gelwan M, Wolf D, Shapiro R, Schwartz M, Min A. Sensitivity of commonly available screening tests in detecting hepatocellular carcinoma in cirrhotic patients undergoing liver transplantation. *Am J Gastroenterol* 2000;95:1535-1538.
- [57] Cedrone A, Covino M, Caturelli E, Pompili M, Aliotta A, Trombino C, et al. Utility of alpha-fetoprotein (AFP) in the screening of patients with virus-related chronic liver disease: does different viral etiology influence AFP levels in HCC? A study in 350 western patients. *Hepatogastroenterology* 2000;47:1654-1658.
- [58] Guido M, Roskams T, Pontisso P, Fassan M, Thung S, Giaconelli L. Squamous cell carcinoma antigen in human liver carcinogenesis. *J Clin Pathol* 2008;61:445-447.
- [59] Malaguarnera G, Giordano M, Paladina I, Berretta M, Cappellani A, Malaguarnera M. Serum markers of hepatocellular carcinoma. *Dig Dis Sci* 2010;55:2744-2755.
- [60] Wu T, Hsieh Y, Wu C, Hsieh Y, Huang C, Liu J. Overexpression of protein kinase C alpha mRNA in human hepatocellular carcinoma: a potential marker of disease prognosis. *Clin Chim Acta* 2007;382:54-58.
- [61] Debruyne E, Delanghe J. Diagnosis and monitoring hepatocellular carcinoma with alpha-fetoprotein: new aspects and applications. *Clin Chim Acta* 2008;395:19-26.

# Chapter 1.4

## ***“Alteration of protein glycosylation in liver diseases”***

**Bram Blomme**<sup>1</sup>, Christophe Van Steenkiste<sup>1</sup>, Nico Callewaert<sup>2,3</sup>, Hans Van Vlierberghe<sup>1</sup>

<sup>1</sup>Department of Hepatology and Gastroenterology, Ghent University Hospital, Ghent, Belgium

<sup>2</sup>Unit for Molecular Glycobiology, Department for Molecular Biomedical Research, VIB, Ghent University, Ghent, Belgium

<sup>3</sup>Department of Biochemistry, Physiology and Microbiology, Ghent University, Ghent, Belgium

**Journal of Hepatology 2009; 50(3): 592-603**

Special article

## Alteration of protein glycosylation in liver diseases<sup>☆</sup>

Bram Blomme<sup>1</sup>, Christophe Van Steenkiste<sup>1</sup>, Nico Callewaert<sup>2,3</sup>, Hans Van Vlierberghe<sup>1,\*</sup>

<sup>1</sup>Department of Hepatology and Gastroenterology, Ghent University Hospital, B-9000 Ghent, Belgium

<sup>2</sup>Unit for Molecular Glycobiology, Department for Molecular Biomedical Research, VIB, Ghent University, Ghent, Belgium

<sup>3</sup>Department of Biochemistry, Physiology and Microbiology, Ghent University, Ghent, Belgium

Chronic liver diseases are a serious health problem worldwide. The current gold standard to assess structural liver damage is through a liver biopsy which has several disadvantages. A non-invasive, simple and non-expensive test to diagnose liver pathology would be highly desirable. Protein glycosylation has drawn the attention of many researchers in the search for an objective feature to achieve this goal. Glycosylation is a posttranslational modification of many secreted proteins and it has been known for decades that structural changes in the glycan structures of serum proteins are an indication for liver damage. The aim of this paper is to give an overview of this altered protein glycosylation in different etiologies of liver fibrosis / cirrhosis and hepatocellular carcinoma. Although individual liver diseases have their own specific markers, the same modifications seem to continuously reappear in all liver diseases: hyperfucosylation, increased branching and a bisecting *N*-acetylglucosamine. Analysis at mRNA and protein level of the corresponding glycosyltransferases confirm their altered status in liver pathology. The last part of this review deals with some recently developed glycomic techniques that could potentially be used in the diagnosis of liver pathology.

© 2008 European Association for the Study of the Liver. Published by Elsevier B.V. All rights reserved.

**Keywords:** Glycosylation; Liver fibrosis; Hepatocellular carcinoma; Glycomics; Bio-marker

Associate Editor: M.P. Manns

<sup>☆</sup> The authors declare that they do not have anything to disclose regarding funding from industries or conflict of interest with respect to this manuscript.

\* Corresponding author.

E-mail address: Hans.Vanvlierberghe@UGent.be (H.V. Vlierberghe).

**Abbreviations:** ER, endoplasmic reticulum; Asn, asparagine; Ser, serine; Thr, threonine; GlcNAc, *N*-acetylglucosamine; HCC, hepatocellular carcinoma; ALD, alcoholic liver diseases; CDT, carbohydrate-deficient transferrin; ST6GalI,  $\beta$ -galactoside  $\alpha$ 2,6 sialyltransferase; TSA, total sialic acid; FSA, free sialic acid; Hp, haptoglobin; Con A, Concanavalin A; Apo E, Apolipoprotein E; GnT-III, *N*-acetylglucosaminyltransferase III; LAL, lysosomal acid lipase; HPLC, high performance liquid chromatography; MALDI-TOF, matrix assisted laser desorption/ionization time-of-flight; AGP,  $\alpha$ 1-acid glycoprotein; GnT-V, *N*-acetylglucosaminyltransferase V; HBx, HBV x-protein;  $\alpha$ 1-6 FT,  $\alpha$ 1-6 fucosyltransferase; LCA, lens culinaris agglutinin; E-PHA, Phaseolus vulgaris: erythroagglutinating; L-PHA, Phaseolus vulgaris: leuco-agglutinating; AAT,  $\alpha$ -1-antitrypsin; TF, transferrin; DEN, diethylnitrosamine; DSA-FACE, DNA sequencer-assisted fluorescence-assisted carbohydrate electrophoresis; IgG, immunoglobulin G.

### 1. Introduction

Over the years it has become apparent that changes in protein glycosylation play an important role in the pathogenesis and progression of various liver diseases. In order to comprehend the relationship between glycosylation and liver diseases, some basic insight into this complex phenomenon is necessary. Therefore, a short introduction is provided, which covers basic biochemical aspects of glycosylation (see Fig. 1).

In general, glycosylation consists of co- and post-translational modification steps, in which individual glycans are added to proteins translated into the endoplasmic reticulum (ER), forming oligosaccharide chains. This is an enzyme-directed and a site-specific process. Two types of protein glycosylation exist: *N*-glycosylation to the amide nitrogen of asparagine (Asn) side chains and *O*-glycosylation to the hydroxyl groups of serine (Ser) and threonine (Thr) side chains. Most proteins in human serum contain one or more *N*-linked glycans, with the exception of albumin and C-reactive

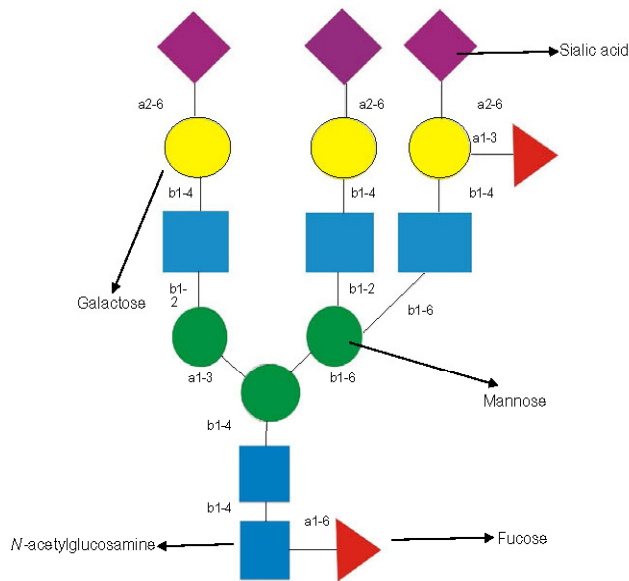


**Fig. 1.** *N*-Glycan with indication of the individual monosaccharides and the different binding types between the monosaccharides. a1–3: alpha 1–3 binding; a1–6: alpha 1–6 binding; a2–6: alpha 2–6 binding; b1–2: beta 1–2 binding; b1–4: beta 1–4 binding; b1–6: beta 1–6 binding.

protein. *O*-glycans are found in mucins, which are abundantly present on mucosal surfaces and saliva. Most modifications of glycosylation in liver diseases that have been studied affect *N*-glycosylated proteins and these will primarily be discussed. The *N*-oligosaccharide chain is attached to asparagine occurring in the tripeptide sequence Asn-X-Ser, in which X could be any amino acid except proline [1–4].

The biosynthesis of *N*- and *O*-glycans take place in the ER and the Golgi apparatus and it can be roughly divided in three steps [5]. The first step in *N*-glycosylation is carried out in the ER and consists of the formation of an oligosaccharide-lipid complex containing three glucoses, nine mannoses and two *N*-acetylglucosamines (GlcNAc). The lipid portion (dolichol) acts

as a carrier molecule. The second step is the transfer of the oligosaccharide portion to a growing nascent polypeptide and the simultaneous removal of the three glucose residues and 1 mannose residue. The premature glycoprotein is then mediated to the Golgi apparatus where residual monosaccharides are removed until a (mannose)<sub>5</sub>(GlcNAc)<sub>2</sub> heptasaccharide chain is formed. From here on, specific glycosyltransferases (Table 1 and [9–11]) and glycosidases will further modify the core-structure by adding or removing monosaccharides, respectively [6]. Glycosyltransferases make use of nucleotides sugars (donors) in order to incorporate monosaccharides into the *N*-glycan. Glycosidases on the other hand, catalyze the hydrolysis of the glycosidic linkage. In addition, glycans can have various branches (2–5) and are termed bi-, tri-, tetra- and penta-antennary, respectively. The enzymatic addition and removal of monosaccharides allow the formation of glycans with various length, composition and structure [7,8].

The functional role(s) of the *N*-linked carbohydrate moieties of glycoproteins is/are often not well understood. However, glycosylation is a necessity in the correct folding of certain proteins. Aberrant protein folding affects various physiochemical and functional properties of proteins: protein stability, protein solubility, protein inter-/intracellular transport and half-life in blood. The opposite can also be true. Carbohydrate moieties on glycoproteins also fulfill a role in intercellular contact and communication, which is an important aspect of host immunity as well as cancer [12–15].

The liver contains various receptors on sinusoidal and hepatocyte surfaces. A lot of proteins that bind to these receptors rely on their carbohydrate moieties. Besides changes in glycosylation patterns, the changes in receptor concentration and distribution also occur in various chronic liver diseases (cirrhosis, hepatocellular carcinoma (HCC) and alcoholic liver diseases

**Table 1**  
Glycosyltransferases that are important in the modification of *N*-glycans on serum proteins.

Glycosyltransferase family	Mammalian glycosyltransferases	Substrate specificity
Fucosyltransferases [9]	$\alpha$ 1,2-Fucosyltransferase*	$\alpha$ 1,2 Linkage to the terminal Gal residue in <i>N</i> - or <i>O</i> -glycans
	$\alpha$ 1,3/4-Fucosyltransferase*	$\alpha$ 1,3 or $\alpha$ 1,4 Linkage to GlcNAc in GlcNAc-Gal structures
	$\alpha$ 1,6-Fucosyltransferase	$\alpha$ 1,6 Linkage to the innermost (core) GlcNAc in <i>N</i> -glycans
<i>N</i> -Acetylglucosaminyltransferases [10]	<i>N</i> -Acetylglucosaminyltransferase III	GnT-III catalyzes the addition of GlcNAc via $\beta$ 1-4 linkage to the $\beta$ -mannose core of <i>N</i> -glycans
	<i>N</i> -Acetylglucosaminyltransferase IV*	GnT-IV catalyzes the formation of GlcNAc- $\beta$ 1-4 branches at the Man $\alpha$ 1-3 side of the trimannosyl core of <i>N</i> -glycans
	<i>N</i> -Acetylglucosaminyltransferase V	GnT-V catalyzes the formation of GlcNAc- $\beta$ 1-6 branches at the Man $\alpha$ 1-6 side of the trimannosyl core of <i>N</i> -glycans
Sialyltransferases [11]	$\alpha$ 2,6-Sialyltransferase*	ST6GalII mediates the transfer of sialic acid residue with an $\alpha$ 2,6-linkage to a terminal Gal residue
	$\alpha$ 2,3-Sialyltransferase*	ST3GalII mediates the transfer of sialic acid to a Gal residue of a terminal Gal $\beta$ 1-3GalNAc oligosaccharide

\* Different glycosyltransferases of this class are known.

**Table 2**  
Commonly used lectins for the study of altered glycan structures in chronic liver diseases [20].

Lectin	Common name	Specificity	Application
Canavalia ensiformis (Concanavalin A, Con A)	Jack Bean	Man/Glc (Man > Glc > GlcNAc)	Con A has been extensively used in the isolation and structural studies of glycoconjugates and it has some clinical uses such as crossed affinity immunoelectrophoresis
Lens culinaris (LCA)	Lentil	Man/Glc (Man > Glc > GlcNAc)	<i>Lens</i> lectin is used for the isolation and analysis of glycoproteins. It is also a useful tool for the determination of the degree of fucosylation of alpha-fetoprotein and the histochemical staining of glycoconjugates
Lotus tetragonolobus (LTA)	Asparagus pea	Fuc ( $\alpha$ -L-Fuc)	The <i>Lotus</i> lectins have specifically been used for the recognition of fucosylated glycans
Phaseolus vulgaris: erythroagglutinating (E-type, E-PHA)	Kidney bean	Complex (Gal $\beta$ (1,4)GlcNAc $\beta$ (1,2)Man)	Especially used for the identification of glycans with a bisecting modification
Phaseolus vulgaris: leuco- agglutinating (L-type, L-PHA)	Kidney bean	Complex (Gal $\beta$ (1,4)GlcNAc $\beta$ (1,2) [Gal $\beta$ (1,4)GlcNAc $\beta$ (1,6)]Man)	As L-PHA is reactive with $\beta$ (1,6) branched structures of trimannosyl core asparagine-linked glycans which are highly selective markers of the metastatic potential of tumor cells, this lectin is used in cancer diagnosis

(ALD)). This leads to an accumulation of certain glycoproteins in the circulation [16,17].

In the following sections we will discuss the role of glycosylation in liver fibrosis and its relation to various liver pathologies (ALD, hepatitis B, bile-related diseases and obesity) and its role in HCC. The last section will deal with analytical advances in glycoresearch in recent years which now allows the rapid and detailed mapping of the complex mixtures present within biofluid samples.

## 2. Alteration of glycosylation in fibrosis – cirrhosis

The gold standard to assess liver fibrosis is through a liver biopsy, which involves the removal of a small liver sample. It is well known that this procedure is accompanied by several complications. Changes in glycosylation of serum proteins have been extensively used as a non-invasive alternative and this has resulted in the development of sensitive and discriminating clinical tests for diagnostic purposes. The rationale for these tests is that the majority of glycosylated serum proteins are synthesized by the liver and in all major liver diseases, changes in this glycosylation occur.

While early glycome studies were confined to the study of sialylation patterns, glycomics has evolved ever since [18]. In the past two decades, the main way of investigating glycosylation was by using lectins [19,20]. These lectins bind with a particular glycan structure (core-fucosylated glycans, complex glycans,...) (Table 2). Today, with the advent of high-throughput glycomic techniques, we are progressing towards a system biology approach comprising genomics and proteomics in order to draw general conclusions about a particular pathology.

### 2.1. Alcoholic liver disease

Carbohydrate-deficient transferrin (CDT) is the most used marker of chronic alcohol abuse. Human serum transferrin is a glycoprotein synthesized by the liver and involved in iron transport between sites of absorption and delivery [21]. Chronic ethanol intake alters the normal microheterogeneity pattern of transferrin as a consequence of changes in the sialic acid contents [22,23] (See Table 3 for an overview of the assays that were used to investigate the glycan status). A decreased level of dolichol has been observed in rats fed ethanol [24]. The abnormal terminal sialylation can be explained by a decrease in  $\beta$ -galactoside  $\alpha$ 2,6 sialyltransferase (ST6GalII) mRNA and protein expression and/or an increase in hepatocyte membrane associated sialidase observed during chronic alcohol abuse [25–27]. Oxidation products of ethanol such as acetaldehyde interfere with the *N*-glycan biosynthesis and/or transfer by binding the involved enzymes. Therefore, CDT is likely the result of changes in glycosylation during biosynthesis and catabolism. Although CDT is recognized as a marker of chronic alcohol consumption, the reliability of this marker is largely dependent on the analytical fractionation method (capillary electrophoresis). Alterations in glycosylation and lack of clinical analytical standard methods might contribute to the discrepancy and sensitivity of CDT in clinical settings [28,29].

Desialylation is the most important alteration observed in ALD. Besides transferrin, many other proteins are known to be desialylated in ALD including orosomucoid,  $\alpha$ 1-antitrypsin, ceruloplasmin [30]. Therefore, the overall serum desialylation pattern was studied in which serum total sialic acid (TSA) and serum free sialic

Table 3

Overview of the main assays used to investigate the glycan status at protein or genetic level in different etiologies of chronic liver diseases.

Etiologies			
Alcoholic liver diseases	Fatty liver diseases bile related diseases Viral liver diseases Hepatocellular carcinoma		
HPAEC-PAD [32] CIAE with Con A [34]	MALDI-TOF MS [41]	DSA-FACE [94]	DSA -FACE [95] CIAE with Con A [60,61,68,71,77], LCA [52,53,60,63,64,68] HPLC [60,64,67,69] Enzyme Assay of $\alpha$ 1-6 FT [59,62], GnT-I [73], GnT-III [62,71,73,79,80,82], GnT-IV [62,80,82], GnT-V [62,77,79,80,82,83], ST [49] Lectin Blotting with Con A [72], LCA [59], E-PHA [72,74], L-PHA [84] Allo A [66] RT-PCR [69,72,77] Northern Blot [59,72,74,79,82,84] Affinity Column Chromatography [54,66,70] Lectin-Affinity Electrophoresis Con A [55], LCA [55,59], E-PHA [55], Allo A [55] <i>In situ</i> hybridization [48] Immunocytochemical determination [82,84]
HPLC [37] Enzyme Assays for GT [24,36,37], MT [37], ST [37]	HPLC [38] Enzyme Assay for GnT-III [39] and $\alpha$ 1,6FT [40]	HPLC [100] Enzyme Assay of GnT-III [42,44], GnT-IV [42,43], GnT-V [42,43], GT [42] Lectin FLISA [100]	
Assays used	Fucose-binding lectin coupled to Sepharose beads [33] RT-PCR [27] Northern Blot [25] Chromatofocusing [23]	Lectin Blotting with E-PHA [38,39], L-PHA [39], AAL [40,41], AOL [41], Con A [41], SSA [41], MAM [41]  Northern Blot [38,39]	
		RT-PCR [44,45] Northern Blot [42,43,45]  FACS analysis [42,43]	

acid (FSA) were studied as potential markers of alcohol abuse [31]. Both TSA and FSA were significantly increased during alcohol abuse, but as markers, they have a low sensitivity (46%) and negative predictive value (27%). Consequently, the clinical utility for screening alcoholic patients is limited.

In terms of changes in glycosylation status, haptoglobin (Hp) has also been proposed as a candidate marker of ALD, especially alcoholic cirrhosis [32,33]. This hemoglobin-scavenger showed two major changes in glycosylation: increased branching and increased fucosylation (hyperfucosylation i.e. the increased presence of fucose residues in the glycan structure). Hyperfucosylation is predominantly present at the  $\alpha$ 1,3 position linked to the subterminal GlcNAc instead of the core fucose position. The activity of  $\alpha$ 1,3 fucosyltransferase in blood is directly associated with elevated Hp concentrations. Changes in branching were less frequent but still significant in ALD. This was determined by an increased *N*-acetylglucosamine content of the Hp molecule (mol/mol Hp). However, these alterations were not specific for alcoholic cirrhosis and were also observed in cases of primary biliary cirrhosis and chronic alcohol abusers, but were absent in chronic active hepatitis. Besides haptoglobin, other glycoproteins are known to exhibit an increased branching during alcoholic liver disease:  $\alpha$ 1 acid glycoprotein,  $\alpha$ 2-HS-glycoprotein and transferrin [34]. In the alcoholic groups, the proportion of Con A-unreactive subpopulations of these glycoproteins increased.

The Golgi apparatus plays an important role in the alteration of glycosylation patterns of all liver diseases.

This is especially well studied in ALD [35,36]. Characteristic is the significant accumulation of hepatic protein caused by impaired glycosylation and glycoprotein trafficking. An example of impaired glycosylation is a decrease in the activity of galactosyltransferase [36]. A proposed explanation for this reduced Golgi functioning is the deficient polymerization of microtubular protein as a downstream consequence of hepatic acetaldehyde accumulation due to ethanol oxidation [35].

A study by Ghosh et al. [37] summarized the previously mentioned alterations of *N*-glycosylation in an experimental rat model of ALD: decreased enzyme activities of mannosyltransferase and galactosyltransferase, lowered intracellular dolichol concentration, strong decreased synthesis and activity of ST6GalI. In addition to these findings, an increase of 30% in liver weight was observed compared to the body weight of this rat model. This is due to a significant accumulation of hepatic lipids and proteins, which leads to fatty liver and even steatosis. The novelty of this study is that they also showed an alteration in *O*-glycosylation. The protein apolipoprotein E was used as a model to study this. As in *N*-glycosylation, an impairment of mannosylation and sialylation was shown. The relative ratio of labeled sugar to leucine incorporation (glycosylation index) showed a 50% decrease for relative mannosylation of Apo E molecule at both the microsomal and Golgi level. Glycan structures on apolipoprotein E were hypothesized to play a role in the association between this apolipoprotein and high density lipoproteins (HDL) and very low density lipoproteins. The observed impairment (namely in mannosylation and sialylation of the protein

molecule) might be responsible for the defective clearance of HDL and therefore lead to a defective cholesterol transport to the liver and subsequent hepatic lipid accumulation. Apolipoproteins and their attached glycans are also involved in the development of a fatty liver, which is discussed in the next section.

## 2.2. Fatty liver diseases

Transgenic mice that specifically express *N*-acetylglucosaminyltransferase III (GnT-III) in the liver had hepatocytes with a swollen oval-like morphology, with many lipid droplets [38,39]. GnT-III transfers a GlcNAc residue to the trimannoside core of *N*-glycans. The aberrant glycosylation of apolipoprotein-B (increased level of bisecting GlcNAc) disturbs the function of this protein and causes a decrease in the release of lipoproteins and an accumulation of apolipoprotein-B in the liver. These transgenic mice showed microvesicular fatty alterations with abnormal lipid accumulation in the hepatocytes. Beside apolipoprotein-B, apolipoprotein A-1 was also significantly increased in liver tissue in these mice. These studies reveal that glycosylation is a factor in the regulation of lipoprotein metabolism and that an aberrant *N*-glycan structure can modify certain biochemical parameters of lipid metabolism in the liver.

Not only GnT-III, but also ectopic expression of  $\alpha$ 1,6 fucosyltransferase causes steatosis in the liver and kidney [40]. Similarly, numerous small vacuoles filled with lipid droplets were histologically observed. In contrast to the studies with GnT-III, a significant increase in cholesterol esters and triglycerides was observed. Crucial in this model was the lowered activity of lysosomal acid lipase (LAL), caused by an increased fucosylation of this enzyme. The accumulation of inactive LAL might contribute to the lipid accumulation observed in the lysosomes of the liver.

## 2.3. Bile-related liver diseases

Fucosylation of *N*-glycans on glycoproteins seems to be the most important alteration in bile-related liver diseases. An increase in fucosylation of biliary glycoproteins was reported by Nakawaga et al. [41] who analyzed the oligosaccharide structure by used 2D mapping HPLC (high performance liquid chromatography) and MALDI-TOF (matrix assisted laser desorption/ionization time-of-flight) mass spectrometry in bile and serum. The binding of biliary glycoproteins to a lectin which recognizes fucose residues, was enhanced and specific glycoproteins ( $\alpha$ 1-antitrypsin,  $\alpha$ 1-acid glycoprotein and haptoglobin) were stronger fucosylated in bile opposite serum of patients with gallbladder stones. It was suggested that fucosylation of glycoproteins could be a possible signal for secretion into bile ducts in the liver.  $\alpha$ 1-6 fucosyltransferase (Fut8)-deficient mice

showed decreased levels of  $\alpha$ 1-antitrypsin and  $\alpha$ 1-acid glycoprotein (AGP) in bile and were relocated to the liver of Fut8-deficient mice [41]. To date, no other study has confirmed these results in an experimental setting.

## 2.4. Viral liver diseases

Among the viral liver diseases, the hepatitis B virus (HBV) infection has been most extensively investigated in search of changes in glycosylation. Alteration in glycosylation between HBV and HCC show many similarities, because of the correlation of long-term HBV-infection and the increased risk of HCC. GnT-III is likely to play a prominent role in the alteration of glycosylation in these viral infected population.

An *in vitro* experiment using human hepatoblastoma cell line (Huh6) transfected with the hepatitis B viral genome (HB611) showed a specific decrease in GnT-III activity opposite the untransfected Huh6 cell line [42]. Glycosyltransferases other than GnT-III were unaltered. Subsequent Northern blot analysis showed that this difference was due to a decreased transcript of GnT-III. GnT-III and GnT-V are known to compete for the same substrate and by suppressing GnT-III, HBV might therefore push the hepatoblastoma cells towards a more malignant phenotype with branched complex-type *N*-linked oligosaccharides proteins. On the other hand the GnT-III gene was transfected into the HB611 cell line, which resulted in decreased secretion of HBV-related proteins and a marked suppression of HBV-related mRNAs [43]. This suggests a possible anti-viral role for this enzyme in *in vivo* circumstances. These results indicate that some glycoproteins whose oligosaccharide structures are changed by overexpression of GnT-III suppress HBV protein expression. This might be a unique approach to prevent HBV replication.

However, contradictory results exist concerning GnT-III expression observed in HBV-transfected hepatocyte cell lines [44,45]. For instance, in contrast to the hepatoblastoma cell line, a HBV-transfected fetal hepatocyte cell line showed an increased GnT-III expression. In addition, HBV x-protein (HBx)-transfected cell line showed a much stronger GnT-III expression in contrast to hepatocarcinoma cells and the GnT-III-transfected cell line [46]. This result suggests strong GnT-III promoter enhancing activity for the HBx-gene. These HBx-transfected cells also showed an accumulation of aberrant glycosylated apolipoprotein B's (increased levels of bisecting GlcNAc), triglyceride and cholesterol. These findings were supported by the previous mentioned transgenic mice in fatty liver diseases. The observed discrepancy between these studies is caused by the difference in experimental setting (used cell line, transfected genes). It is therefore unclear whether GnT-III exhibits a positive or negative influence on the HBV infection.



One of the few reports where differences in glycosylation could serve as a discriminating factor between liver diseases was performed by Anderson et al. [46]. They used AGP as the model protein to test this. Hyperfucosylation (predominantly  $\alpha$ 1-3) occurred in all liver diseases, especially in hepatitis B and C virus infected patients, but an additional *N*-acetylgalactosamine was detected in the majority of hepatitis C patients as determined by high performance anion exchange chromatography analysis. This is unexpected because this monosaccharide is rarely present in *N*-glycans.

### 3. Alteration of glycosylation in hepatocellular carcinoma

Alterations to the normal function of the glycosylation machinery are increasingly recognized as an indication of malignant cellular transformation. In relation to HCC, glycosyltransferases are most intensively studied. Three glycosyltransferases are considered crucial: *N*-acetylglucosaminyltransferase V (GnT-V), *N*-acetylglucosaminyltransferase III (GnT-III) and  $\alpha$ 1-6 fucosyltransferase ( $\alpha$ 1-6FT). These enzymes have been suggested in the development of fibrosis, but the relation with HCC is much clearer and well documented. The activity of these three enzymes is significantly altered in hepatoma tissues or serum of HCC patients and suggest a subsequent change in glycan structures.

Some evidence can also be found that the expression of ST6GalII is up-regulated in human HCC patients and in a transgenic mouse model of HCC [47–49]. We already mentioned this enzyme in ALD where it was down-regulated. It seems that ST6GalII is differently regulated in cirrhosis and HCC.

#### 3.1. Fucosyltransferases

The best known marker in HCC is the elevated serum concentration of fucosylated  $\alpha$ -fetoprotein (AFP) and this has become a standard in cancer diagnostics over the years. The presence of molecular variants of AFP with different carbohydrate chains has first been demonstrated by reactions with lectins such as concanavalin A and lentil lectin (*Lens culinaris* agglutinin) [50].

It is known that the serum AFP concentration levels also increase in benign liver diseases such as acute hepatitis and cirrhosis. Therefore, the serum AFP concentration alone is of little use in the differential diagnosis of HCC and benign liver diseases [51]. Consequently, it is important to develop a method that distinguishes between HCC and non-neoplastic liver diseases [52,53]. The fucosylation index could be a possible aid to achieve this goal. Fucosylated AFPs are specifically recognized by the lentil lectin and were determined by crossed immunoaffino-electrophoresis as the lentil lectin reactive fraction in total AFP. The fucosylation index is then the

percentage of the lentil lectin reactive fraction in total AFP. A highly significant increase in fucosylation index was observed in cirrhotic patients after the development of HCC. This index is useful in the early detection of HCC, especially in patients with cirrhosis which are at risk of developing HCC in the following years.

Similar results were obtained by other research groups in patients with low serological levels of AFP [54,55]. The latter study determined AFP using different lectins: Con A, LCA-A, E-PHA and allo A. The AFP bands separated with different lectins in this study appear to have sugar-chain heterogeneity with little overlap. The presence of this tumor heterogeneity forms the basis for the combined evaluation of tumor markers. A fraction of AFP obtained with the lectin *Lens culinaris* agglutinin A (AFP-L3) and another fraction of AFP obtained with lectin erythroagglutinating phytohemagglutinin (AFP-P4) were simultaneously analyzed and resulted in a very high sensitivity (97%) and specificity (99,7%) in monitoring the evolution of HCC in cirrhotic patients. However, when AFP-L3 is evaluated individually, it is known to have a high specificity but not enough sensitivity to be considered a surveillance tool for HCC [56]. Because AFP-L3 has been related to tumors with rapid growth, larger size, portal vein invasion and metastasis [57,58], its utility may be more of a prognostic marker for HCC rather than for a screening test. In addition to the increase in fucosylation patterns, mRNA of the responsible enzyme  $\alpha$ 1-6FT was shown to be enhanced in proportion to the enzymatic activity in HCC patients [59].

Besides an increment in fucosylation, formation of new antennae is also a characteristic feature of the carbohydrate chains of AFP from patients with neoplastic liver diseases [60]. Fucosylated tri-antennary, tetra-antennary and penta-antennary glycans attached to transferrin synthesized by the human hepatocarcinoma cell line Hep G2 have been reported by Campion et al. [61]. Ohno et al. provided additional results which confirmed these findings *in vitro* [62]. AFPs were purified from 2 different hepatoma cell lines (Hep G2 and HuH-7) and a hepatoblastoma cell line (HuH-6). Simultaneously, the activities of  $\alpha$ 1-6FT, GnT-III and GnT-V were assayed in these cell lines. Fucosylated biantennary structure and  $\alpha$ 1-6FT were most frequently detected in all three cell lines. In addition, Hep G2 cells contained a high level of GnT-V, which catalyzes the formation of a triantennary structure, while GnT-III was elevated in HuH-6 cells. These data indicate that the sugar structures of AFP in these cell lines correlate well with the activities of  $\alpha$ 1-6FT, GnT-III and GnT-V.

Besides AFP,  $\alpha$ 1-antitrypsin (AAT) is known to express fucosylated biantennary glycans distinctive for HCC. Similar to AFP, the percentage of reactive species with the lectin *Lens culinaris* agglutinin was shown to be significantly higher in HCC than in benign liver diseases

and normal controls [63]. Further structural analysis on the AAT-attached glycans was performed and it was shown that the fucosylated biantennary glycans were increased two-fold opposite non-fucosylated glycans [64]. Under normal circumstances, non-fucosylated biantennary glycans are the most abundant glycans on AAT [65]. Therefore, an increment in fucosylation on AAT is a characteristic of patients with HCC. Transferin (TF) also shows significant changes in glycosylation patterns (fucosylation) but shows too many structural variation in contrast to AFP and AAT [66–68]. Both glycoproteins are useful alternatives in case of low AFP-levels in order to detect HCC. Although, in contrast to APF, LCA-reactive AAT and TF are not able to discriminate between HCC and liver cirrhosis.

Very recently, a study appeared that links *N*-glycan alterations to drug resistance in HCC. Especially  $\alpha$ 1–6 FT was overexpressed in drug-resistant cell lines and the glycomics analysis showed high core-fucosylation [69]. This further emphasizes the existence and importance of fucosylation anomalies occur in HCC.

### 3.2. *N*-acetylglucosaminyltransferases

#### 3.2.1. *N*-acetylglucosaminyltransferase III

*N*-acetylglucosaminyltransferase III adds a “bisecting” GlcNAc in  $\beta$ 1,4 linkage to the  $\beta$ -linked mannose Asn-linked core structure. This enzyme was determined in hepatic nodules of humans and rats and the GnT-III activity in these nodules were shown to be significantly higher in contrast to its surrounding and the control liver [70–72]. These studies suggest a possible correlation between the GnT-III activity and the precancerous stage of hepatocarcinogenesis. The activity of GnT-III in serum samples of HCC patients was determined by HPLC and it was significantly higher up-regulated in these patients in contrast to patients showing liver cirrhosis, chronic hepatitis and healthy controls. The GnT-III activity could be useful in HCC treatment follow-up because GnT-III activity is significantly reduced in HCC following percutaneous ethanol infection therapy and/or transcatheter arterial chemoembolization [71].

GnT-III exerts different (pathological) activity in an experimental mouse and rat model [70,73]. Hepatic tumor formation in the mouse model was not accompanied by an increase in GnT-III activity nor glycoproteins expression showing a bisecting GlcNAc. They could also show that in *Mgat3*<sup>-/-</sup> mice (GnT-III coding gene) initiation of hepatic neoplasms was normal, but progression was severely retarded. A glycoprotein with the bisected GlcNAc synthesized outside of the liver might act as a necessary growth factor in tumor progression. Moreover, diethylnitrosamine (DEN) induced HCC in transgenic mice (*Mgat3* <sup>$\Delta/\Delta$</sup> , carrying a deletion in the *Mgat3* gene) remained unaltered by high levels of GnT-III in the liver. Ectopic expression of the *Mgat3*

gene in the liver followed by DEN induced HCC and subsequent phenobarbital (PB) treatment did not result in significant changes in the number of tumors or liver weight [74]. The retarded tumor progression in the *Mgat3*<sup>-/-</sup> mice was showed a decrease in hepatocyte proliferation rather than an increase in hepatocyte apoptosis [75]. When the glycoprotein factor lacks the bisecting GlcNAc, it can not exert its normal function. The growth factor acting glycoprotein with the bisecting GlcNAc has still to be identified.

#### 3.2.2. *N*-acetylglucosaminyltransferase V

$\beta$ 1-6-GlcNAc branching providing by GnT-V is directly associated with metastasis [76] and might serve as marker for tumor invasiveness in HCC patients [77]. GnT-V is coded on the *Mgat5* gene which is regulated by the Ras signaling pathway. This pathway is commonly up-regulated in various tumor cells [78]. In analogy with  $\alpha$ 1-6 fucose,  $\beta$ 1-6 branching is also a molecular signal that exerts a particular biological function. Phosphorylation is another posttranslational modification and its importance in inter-/intracellular signal transduction is well known. It seems that glycosylation might have a similar signaling function.

Both GnT-III and GnT-V activity are increased in HCC, but the activity of GnT-III is much more prominent than GnT-V [79–81]. As previously mentioned, both glycosyltransferases compete for the same substrate. An increase in GnT-III activity might suppress GnT-V activity and subsequent GlcNAc  $\beta$ 1–6 branching. In several cancers it has been shown that GnT-III counteracts tumor progression, while GnT-V promotes it [44,76]. Moreover, it is known that GnT-III and GnT-V activity undergo opposing changes during different stages of the cell cycle in a hepatoma cell line [82]. These changes might be the result of a change in regulatory mechanisms of the cell cycle. The peak activity of GnT-III (during G0/G1) coincided with the lowest activity of GnT-V during G0/G1-stage while the opposite is seen during G2/M-stage.

A progressive increase in GnT-V was observed during HCC and was likely correlated with the TNM-classification of HCC. GnT-V activity in advanced HCC was clearly up-regulated opposite early HCC [83]. However, these findings were contradicted by the study of Ito et al. which showed a reversed expression level in early and advanced stages of HCC [84].

## 4. From glycoproteomics to glycomics

Glycosylation has evolved from simple surface glycans for the discrimination of blood types to glycans determining tumor progression. Given the importance of glycans in various biological activities (e.g. liver diseases) and the restriction of genomics and proteomics,

glycomics has emerged among other – omics domains. The glycome can be defined as the complete set of glycan structures present in specific cells, tissues or organisms. The dynamic nature of these post-translational modifications and their complex regulation indicate that direct mapping of the total pathologic changes to glycans may be more informative than characterizing the glycans on individual proteins [85,86]. Glycomic analysis also overcomes the problem of microheterogeneity of single proteins. Individual proteins mostly do not have one characteristic alteration in liver pathology (what would be favorable in clinical testing), but multiple transitions.

Many previous analyses have been performed with the technology also commonly used in proteomics. For instance, two-dimensional gel electrophoresis of serum from alcoholic patients with or without liver cirrhosis resulted in microheterogeneity among Hp, AAT and TF proteins in these patients [87]. Further analysis using lectin blotting showed common changes in glycosylation as an early indication or result of excessive alcohol consumption. A similar approach was used by Henry et al. [88] in the study of carbohydrate deficiency syndrome. In addition, mass spectrometry provides glycan structure information based on fragmentation patterns and the mass of the different sugar components.

Nowadays, *N*-glycans are enriched by peptide-*N*-glycosidase and are investigated in a protein-independent way. The *N*-glycan fraction can either be analyzed by mass spectrometry or by normal phase high performance liquid chromatography (NP-HPLC) using lectin-affinity column. NP-HPLC provides *N*-glycan profile, visualized as an electroferogram. Improvement has been made in the *N*-glycan profiling using DNA sequencer-assisted fluorophore-assisted carbohydrate electrophoresis (DSA-FACE) [89]. An important advantage of this technology is that the results can be combined and compared with those obtained from MALDI-TOF of the same analytes on at least the same level of sensitivity. For a clear overview of the used techniques in glycomics we refer to the following reviews [90–93].

Based on recurring, unique glycan characteristics in various liver diseases, *N*-glycan study (*N*-glycome) has become an interesting research field in search of useful carbohydrate biomarkers. Using the DSA-FACE approach, Callewaert et al. were able to successfully discriminate non-cirrhotic from cirrhotic patients based on their serological *N*-glycome [94]. The electroferogram particularly showed an increase in agalacto sugar and decrease in tri-antennary sugar. The logarithmic ratio of the peak heights of a biantennary, core-fucosylated and bisecting GlcNAc modified sugar (increased in cirrhosis) and a triantennary sugar (decreased in cirrhosis) showed to have a good diagnostic value for the recognition of cirrhosis (AUC = 0,87, specificity = 100% and sensitivity = 75%) and was renamed the GlycoCirrho-Test. The main disadvantage of this technique is that

it can not be used as a follow-up tool, a significant difference could only be observed between F0–F3 and F4. In addition, Liu et al. were able to diagnose HCC based on the log ratio of two identified peaks following DSA-FACE on patient sera. A fucosylated tri-antennary glycan was increased in contrast to a bisecting biantennary glycan in HCC and this is consistent with previous findings on GnT-V and GnT-III activity in HCC. This test was named GlycoHCCTest in analogy with GlycoCirrhoTest and showed an accuracy similar to AFP (~80%) [95]. However, the individual variation in the blood serum profiles was still rather high. Therefore, more extensive *N*-glycan profiling studies on individuals should be carried out, including longitudinal samples over long periods.

In addition to this study, *N*-glycome profile studies have emerged using MALDI-TOF mass spectrometry (MS). The main idea behind this approach is the reduction of analysis time and sample used for analysis [96,97]. Although mainly used in the structural analysis of glycans, quantitative profiling is also possible [96–99]. In this regard, Morelle et al. [97] studied total serum *N*-glycome of cirrhotic patients applying mass spectrometry for both purposes: MALDI-TOF MS for mass profiling and electrospray ionization ion-trap MS for structural characterization. However, the results of this approach were limited to 26 different identified glycans (normally over a hundred) due to isobaric glycan compounds, which cannot be distinguished. Besides similarity with the findings of Callewaert et al. (increase in bisecting GlcNAc and core fucosylation), Morelle et al. discovered an interesting group of neutral oligosaccharides. Mass spectrometry-based are, however, less suitable for diagnostics, because of the low reproducibility.

Serum is an obvious choice to study the *N*-glycome in association with liver disease, because a large portion of these *N*-glycans originate from serum proteins and are produced in the liver. However, serum also consists largely of immunoglobulins (Ig), especially IgG. IgG is produced in B-cells and are also glycosylated; therefore the whole serum *N*-glycome might be biased by these IgG-related glycan structures [94]. Metha et al. [100] took this to the next level and clearly showed that the major serum glycoprotein containing altered glycosylation as a function of cirrhosis is not a liver-derived protein at all. It was rather IgG (produced by B-cells) that was specifically reactive to the alpha-Gal epitope. However, in healthy subjects, this only constitutes ~1% of total serum IgG. Moreover, this epitope is absent in humans, but is abundantly synthesized by bacteria.

## 5. General conclusions

We have clearly shown that glycosylation changes in liver pathology. Although liver diseases of different

etiology have their own markers (e.g. CDT in alcoholic liver disease or AFP in HCC), the alterations of glycosylation of these proteins are quite uniform. In other words, the same type of alterations seems to continuously reappear in the different types of chronic liver diseases: increased fucosylation, increased branching and increased bisecting GlcNAc modified glycans. The activities of the glycosyltransferases that are responsible for these alterations ( $\alpha$ 1–6 FT, GnT-V and GnT-III, respectively) are extensively studied and are known to be significantly elevated in liver pathology.

Clinical tests based on these altered glycan structures have been studied intensively, but only a few have made it into clinical practice. An important reason is that although the methods used for determining the altered sugar chain moieties are reliable, they are also time consuming. With the advent of new technologies that enable simple and rapid screening methods, we are getting a step closer to finding the holy grail of hepatic clinical testing, a non-invasive test that can replace a liver biopsy. However, a combination of markers and techniques will probably be necessary to achieve this goal.

#### Acknowledgement

The authors thank Kin Jip Cheung for editing the manuscript. BB is a recipient of a scholarship GOA BOFF07/GOA/017 of the University Ghent Research Fund (BOF).

#### References

- [1] Ploegh H, Neeffes JJ. Protein glycosylation. *Curr Opin Cell Biol* 1990;2:1125–1130.
- [2] Hebert DN, Garman SC, Molinari M. The glycan code of the endoplasmic reticulum: asparagine-linked carbohydrate as protein maturation and quality-control tags. *Trends in Cell Biol* 2005;15:364–370.
- [3] Kornfeld S. Diseases of abnormal protein glycosylation: an emerging area. *J Clin Invest* 1998;101:1293–1295.
- [4] Lis H, Sharon N. Protein glycosylation: structural and functional aspects. *Eur J Biochem* 1993;218:1–27.
- [5] Schachter H. The subcellular sites of glycosylation. *Biochem Soc Symp* 1974;40:57–71.
- [6] Paulson JC, Colley KJ. Glycosyltransferases: structure, localization, and control of cell type-specific glycosylation. *J Biol Chem* 1989;264:17615–17618.
- [7] Spiro RG. Protein glycosylation: nature, distribution, enzymatic formation, and disease implications of glycopeptide bonds. *Glycobiology* 2002;12:43R–56R.
- [8] Burda P, Aebi M. The dolichol pathway of N-linked glycosylation. *Biochem Biophys Acta* 1999;1426:239–257.
- [9] Javaud C, Dupuy F, Maftah A, Julien R, Petit JM. The fucosyltransferase gene family: an amazing summary of the underlying mechanisms of gene evolution. *Genetica* 2003;118:157–170.
- [10] Taniguchi N, Miyoshi E, Ko JH, Ikeda Y, Ihara Y. Implication of N-acetylglucosaminyltransferases III and V in cancer: gene regulation and signaling mechanism. *Biochim Biophys Acta* 1999;1455:287–300.
- [11] Harduin-Lepers A, Vallejo-Ruiz V, Krzewinski-Recchi MA, Samyn-Petit B, Julien S, Delannoy P. The human sialyltransferase family. *Biochimie* 2001;83:727–737.
- [12] Zhao Y, Takahashi M, Gu J, Miyoshi E, Matsumoto A, Kitazume S, et al. Functional roles of N-glycans in cell signaling and cell adhesion in cancer. *Cancer Sci* 2008;99:1304–1310.
- [13] Varki A. Biological roles of oligosaccharides: all of the theories are correct. *Glycobiology* 1993;3:97–130.
- [14] Dwek RA. Glycobiology: 'towards understanding the function of sugars'. *Biochem Soc Trans* 1995;23:1–25.
- [15] Taniguchi N, Miyoshi E, Gu J, Honke K, Matsumoto A. Decoding sugar functions by identifying target glycoproteins. *Curr Opin Struct Biol* 2006;16:561–566.
- [16] Sawamura T, Nakada H, Hazama H, Shiozaki Y, Sameshima Y, Tashiro Y. Hyperasialoglycoproteinemia in patients with chronic liver-diseases and or liver-cell carcinoma: asialoglycoprotein receptor in cirrhosis and liver-cell carcinoma. *Gastroenterology* 1984;87:1217–1221.
- [17] Burgess JB, Baenziger JU, Brown WR. Abnormal surface distribution of the human asialoglycoprotein receptor in cirrhosis. *Hepatology* 1992;15:702–706.
- [18] Martinez J, Barsigian C. Carbohydrate abnormalities of N-linked plasma glycoproteins in liver-disease. *Lab Invest* 1987;57:240–257.
- [19] Turner GA. N-glycosylation of serum proteins in disease and its investigation using lectins. *Clin Chim Acta* 1992;208:149–171.
- [20] Van Damme EJM, Peumans WJ, Bardocz S, Pusztai A. Handbook of plant lectins: properties and biomedical applications. Amsterdam: John Wiley & Sons; 1998.
- [21] De Jong G, Van Dijk JP, Van Eijk HG. The biology of transferrin. *Clin Chim Acta* 1990;190:1–46.
- [22] Flahaut C, Michalski JC, Danel T, Humbert MH, Klein A. The effects of ethanol on the glycosylation of human transferrin. *Glycobiology* 2003;13:191–198.
- [23] Storey EL, Anderson GJ, Mack U, Powell LW, Halliday JW. Desialylated transferrin as a serological marker of chronic excessive alcohol ingestion. *Lancet* 1987;1:1292–1294.
- [24] Cottalasso D, Domenicotti C, Traverso N, Pronzato MA, Nanni G. Influence of chronic ethanol consumption on toxic effects of 1,2-dichloroethane: glycolipoprotein retention and impairment of dolichol concentration in rat liver microsomes and Golgi apparatus. *Toxicology* 2002;178:229–240.
- [25] Rao M, Lakshman MR. Chronic ethanol consumption leads to destabilization of rat liver  $\beta$ -galactoside-sialyltransferase mRNA. *Metabolism* 1999;48:797–803.
- [26] Xin Y, Lasker JM, Lieber CS. Serum carbohydrate-deficient transferrin: mechanism of increase after chronic alcohol intake. *Hepatology* 1995;22:1462–1468.
- [27] Gong M, Garige M, Hirsch K, Lakshman MR. Liver Gal beta 1,4GlcNAc alpha 2,6-sialyltransferase is down-regulated in human alcoholics: possible cause for the appearance of asialo-conjugates. *Metabolism* 2007;56:1241–1247.
- [28] Liu YS, Xu GY, Cheng DQ, Li YM. Determination of serum carbohydrate-deficient transferrin in the diagnosis of alcoholic liver disease. *Hepatobiliary Pancreat Dis Int* 2005;4:265–268.
- [29] Stadheim LM, O'Brien JF, Lindor KD, Gores GJ, McGill DB. Value of determining carbohydrate-deficient transferrin isoforms in the diagnosis of alcoholic liver disease. *Mayo Clin Proc* 2003;78:703–707.
- [30] Tsutsumi M, Wang JS, Takada A. Microheterogeneity of serum glycoproteins in alcoholics: is desialo-transferrin the marker of chronic alcohol-drinking or alcoholic liver-injury. *Alcohol Clin Exp Res* 1994;18:392–397.
- [31] Chrostek L, Cylwik B, Korcz W, Krawiec A, Koput A, Supronowicz Z, et al. Serum free sialic acid as a marker of alcohol abuse. *Alcohol Clin Exp Res* 2007;31:996–1001.

- [32] Mann AC, Record CO, Self CH, Turner GA. Monosaccharide composition of haptoglobin in liver-diseases and alcohol-abuse large changes in glycosylation associated with alcoholic liver-disease. *Clin Chim Acta* 1994;227:69–78.
- [33] Chambers W, Thompson S, Skillen AW, Record CO, Turner GA. Abnormally fucosylated haptoglobin as a marker for alcoholic liver-disease but not excessive alcohol-consumption or Nonalcoholic liver-disease. *Clin Chim Acta* 1993;219:177–182.
- [34] Jezequel M, Seta NS, Corbic MM, Feger JM, Durand GM. Modifications of concanavalin a patterns of alpha-1-acid glycoprotein and alpha-2-Hs glycoprotein in alcoholic liver-disease. *Clin Chim Acta* 1988;176:49–57.
- [35] Matsuda Y, Takada A, Takase S, Sato H. Accumulation of glycoprotein in the Golgi-apparatus of hepatocytes in alcoholic liver injuries. *Am J Gastroenterol* 1991;86:854–860.
- [36] Guasch R, Renaupiqueras J, Guerri C. Chronic ethanol-consumption induces accumulation of proteins in the liver Golgi-apparatus and decreases galactosyltransferase activity. *Alcohol Clin Exp Res* 1992;16:942–948.
- [37] Ghosh P, Liu QH, Lakshman MR. Long-term ethanol exposure impairs glycosylation of both *N*- and *O*-glycosylated proteins in rat-liver. *Metabolism* 1995;44:890–898.
- [38] Ihara Y, Yoshimura M, Miyoshi E, Nishikawa A, Sultan AS, Toyosawa S, et al. Ectopic expression of *N*-acetylglucosaminyltransferase III in transgenic hepatocytes disrupts apolipoprotein B secretion and induces aberrant cellular morphology with lipid storage. *Proc Natl Acad Sci USA* 1998;95:2526–2530.
- [39] Lee J, Song EY, Chung TW, Kang SK, Kim KS, Chung TH, et al. Hyperexpression of *N*-acetylglucosaminyltransferase-III in liver tissues of transgenic mice causes fatty body and obesity through severe accumulation of Apo A-I and Apo B. *Arch Biochem Biophys* 2004;426:18–31.
- [40] Wang W, Li W, Ikeda Y, Miyagawa JI, Taniguchi M, Miyoshi E, et al. Ectopic expression of alpha1,6 fucosyltransferase in mice causes steatosis in the liver and kidney accompanied by a modification of lysosomal acid lipase. *Glycobiology* 2001;11:165–174.
- [41] Nakagawa T, Uozumi N, Nakano M, Mizuno-Horikawa Y, Okuyama N, Taguchi T, et al. Fucosylation of *N*-glycans regulates the secretion of hepatic glycoproteins into bile ducts. *J Biol Chem* 2006;281:29797–29806.
- [42] Miyoshi E, Nishikawa A, Ihara Y, Hayashi N, Fusamoto H, Kamada T, et al. Selective suppression of *N*-acetylglucosaminyltransferase-III activity in a human hepatoblastoma cell-line transfected with hepatitis-B virus. *Cancer Res* 1994;54:1854–1858.
- [43] Miyoshi E, Ihara Y, Hayashi N, Fusamoto H, Kamada T, Taniguchi N. Transfection of *N*-acetylglucosaminyltransferase-III gene suppresses expression of hepatitis-B virus in a human hepatoma-cell line, Hb611. *J Biol Chem* 1995;270:28311–28315.
- [44] Shim JK, Lee YC, Chung TH, Kim CH. Elevated expression of bisecting *N*-acetylglucosaminyltransferase-III gene in a human fetal hepatocyte cell line by hepatitis B virus. *J Gastroenterol Hepatol* 2004;19:1374–1387.
- [45] Kang SK, Chung TW, Lee JY, Lee YC, Morton RE, Kim CH. The hepatitis B virus x protein inhibits secretion of apolipoprotein B by enhancing the expression of *N*-acetylglucosaminyltransferase III. *J Biol Chem* 2004;279:28106–28112.
- [46] Anderson N, Pollacchi A, Hayes P, Therapondos G, Newsome P, Boyter A, et al. A preliminary evaluation of the differences in the glycosylation of alpha-1-acid glycoprotein between individual liver diseases. *Biomed Chromatogr* 2002;16:365–372.
- [47] Cao Y, Merling A, Crocker PR, Keller R, Schwartz-Albiez R. Differential expression of beta-galactoside alpha 2,6 sialyltransferase and sialoglycans in normal and cirrhotic liver and hepatocellular carcinoma. *Lab Invest* 2002;82:1515–1524.
- [48] Dall'Olio F, Chiricolo M, D'Errico A, Gruppioni E, Altissimi A, Fiorentino M, et al. Expression of beta-galactoside alpha 2,6 sialyltransferase and of alpha 2,6-sialylated glycoconjugates in normal human liver, hepatocarcinoma, and cirrhosis. *Glycobiology* 2004;14:39–49.
- [49] Pousset D, Piller V, Bureaud N, Monsigny M, Piller F. Increased alpha 2,6 sialylation of N-glycans in a transgenic mouse model of hepatocellular carcinoma. *Cancer Res* 1997;57:4249–4256.
- [50] Bayard B, Kerckaert JP. Characterization and isolation of nine rat alpha-fetoprotein variants by gel electrophoresis and lectin affinity chromatography. *Biochem Biophys Res Commun* 1977;77:489–495.
- [51] Karvountzis GG, Redeker AG. Relation of alpha-fetoprotein in acute hepatitis to severity and prognosis. *Ann Intern Med* 1974;80:156–160.
- [52] Aoyagi Y, Suzuki Y, Isemura M, Nomoto M, Sekine C, Igarashi K, et al. The fucosylation index of alpha-fetoprotein and its usefulness in the early diagnosis of hepatocellular-carcinoma. *Cancer* 1988;61:769–774.
- [53] Aoyagi Y, Saitoh A, Suzuki Y, Igarashi K, Oguro M, Yokota T, et al. Fucosylation index of alpha-fetoprotein, a possible aid in the early recognition of hepatocellular-carcinoma in patients with cirrhosis. *Hepatology* 1993;17:50–52.
- [54] Du MQ, Hutchinson WL, Johnson PJ, Williams R. Differential alpha-fetoprotein lectin binding in hepatocellular-carcinoma diagnostic utility at low serum levels. *Cancer* 1991;67:476–480.
- [55] Taketa K, Sekiya C, Namiki M, Akamatsu K, Ohta Y, Endo Y, et al. Lectin-reactive profiles of alpha-fetoprotein characterizing hepatocellular-carcinoma and related conditions. *Gastroenterology* 1990;99:508–518.
- [56] Sterling RK, Jeffers L, Gordon F, Sherman M, Venook AP, Reddy KR, et al. Clinical utility of AFP-L3% measurement in North American patients with HCV-related cirrhosis. *Am J Gastroenterol* 2007;102:2196–2205.
- [57] Li D, Mallory T, Satomura S. AFP-L3: a new generation of tumor marker for hepatocellular carcinoma. *Clin Chim Acta* 2001;313:15–19.
- [58] Yamashiki N, Seki T, Wakabayashi M, Nakagawa T, Imamura M, Tamai T, et al. Usefulness of lens culinaris agglutinin A-reactive fraction of alpha-fetoprotein (AFP-L3) as a marker of distant metastasis from hepatocellular carcinoma. *Oncol Rep* 1999;6:1229–1232.
- [59] Noda K, Miyoshi E, Uozumi N, Yanagidani S, Ikeda Y, Gao CX, et al. Gene expression of alpha 1-6 fucosyltransferase in human hepatoma tissues: a possible implication for increased fucosylation of alpha-fetoprotein. *Hepatology* 1998;28:944–952.
- [60] Aoyagi Y, Suzuki Y, Igarashi K, Saitoh A, Oguro M, Yokota T, et al. Carbohydrate structures of human alpha-fetoprotein of patients with hepatocellular carcinoma: presence of fucosylated and non-fucosylated triantennary glycans. *Br J Cancer* 1993;67:486–492.
- [61] Campion B, Leger D, Wieruszkeski JM, Montreuil J, Spik G. Presence of fucosylated triantennary, tetraantennary and pentaantennary glycans in transferrin synthesized by the human hepatocarcinoma cell line Hep G2. *Eur J Biochem* 1989;184:405–413.
- [62] Ohno M, Nishikawa A, Koketsu M, Taga H, Endo Y, Hada T, et al. Enzymatic basis of sugar structures of alpha-fetoprotein in hepatoma and hepatoblastoma cell lines: correlation with activities of alpha 1-6 fucosyltransferase and *N*-acetylglucosaminyltransferases III and V. *Int J Cancer* 1992;51:315–317.
- [63] Sekine C, Aoyagi Y, Suzuki Y, Ichida F. The reactivity of alpha-1-antitrypsin with lens-culinaris agglutinin and its usefulness in the diagnosis of neoplastic diseases of the liver. *Br J Cancer* 1987;56:371–375.

- [64] Saitoh A, Aoyagi Y, Asakura H. Structural analysis on the sugar chains of human alpha 1-antitrypsin: presence of fucosylated biantennary glycan in hepatocellular carcinoma. *Arch Biochem Biophys* 1993;303:281–287.
- [65] Hodges LC, Laine R, Chan SK. Structure of the oligosaccharide chains in human alpha-1-protease inhibitor. *J Biol Chem* 1979;254:8208–8212.
- [66] Yamashita K, Koide N, Endo T, Iwaki Y, Kobata A. Altered glycosylation of serum transferrin of patients with hepatocellular carcinoma. *J Biol Chem* 1989;264:2415–2423.
- [67] Matsumoto K, Maeda Y, Kato S, Yuki H. Alteration of asparagine-linked glycosylation in serum transferrin of patients with hepatocellular carcinoma. *Clin Chim Acta* 1994;224:1–8.
- [68] Suzuki Y, Aoyagi Y, Mori S, Suda T, Naitoh A, Isokawa O, et al. Microheterogeneity of serum transferrin in the diagnosis of hepatocellular carcinoma. *J Gastroenterol Hepatol* 1996;11:358–365.
- [69] Kudo T, Nakagawa H, Takahashi M, Hamaguchi J, Kamiyama N, Yokoo H, et al. *N*-glycan alterations are associated with drug resistance in human hepatocellular carcinoma. *Mol Cancer* 2007;6:32.
- [70] Narasimhan S, Schachter H, Rajalakshmi S. Expression of *N*-acetylglucosaminyltransferase-III in hepatic Nodules during rat-liver carcinogenesis promoted by orotic-acid. *J Biol Chem* 1988;263:1273–1281.
- [71] Mori S, Aoyagi Y, Yanagi M, Suzuki Y, Asakura H. Serum *N*-acetylglucosaminyltransferase III activities in hepatocellular carcinoma. *J Gastroenterol Hepatol* 1998;13:610–619.
- [72] Song EY, Kang SK, Lee YC, Park YG, Chung TH, Kwon DH, et al. Expression of bisecting *N*-acetylglucosaminyltransferase-III in human hepatocarcinoma tissues, fetal liver tissues, and hepatoma cell lines of Hep3B and HepG2. *Cancer Invest* 2001;19:799–807.
- [73] Bhaumik M, Harris T, Sundaram S, Johnson L, Guttenplan J, Rogler C, et al. Progression of hepatic neoplasms is severely retarded in mice lacking the bisecting *N*-acetylglucosamine on *N*-glycans: evidence for a glycoprotein factor that facilitates hepatic tumor progression. *Cancer Res* 1998;58:2881–2887.
- [74] Yang XP, Bhaumik M, Bhattacharyya R, Gong S, Rogler CE, Stanley P. New evidence for an extra-hepatic role of *N*-acetylglucosaminyltransferase III in the progression of diethylnitrosamine-induced liver tumors in mice. *Cancer Res* 2000;60:3313–3319.
- [75] Yang XP, Tang J, Rogler CE, Stanley P. Reduced hepatocyte proliferation is the basis of retarded liver tumor progression and liver regeneration in mice lacking *N*-acetylglucosaminyltransferase III. *Cancer Res* 2003;63:7753–7759.
- [76] Dennis JW, Laferte S, Waghorne C, Breitman ML, Kerbel RS. Beta-1-6 branching of Asn-linked oligosaccharides is directly associated with metastasis. *Science* 1987;236:582–236585.
- [77] Yanagi M, Aoyagi Y, Suda T, Mita Y, Asakura H. *N*-acetylglucosaminyltransferase V as a possible aid for the evaluation of tumor invasiveness in patients with hepatocellular carcinoma. *J Gastroenterol Hepatol* 2001;16:1282–1289.
- [78] Dennis JW, Granovsky M, Warren CE. Glycoprotein glycosylation and cancer progression. *Biochim Biophys Acta* 1999;1473:21–34.
- [79] Miyoshi E, Nishikawa A, Ihara Y, Gu JG, Sugiyama T, Hayashi N, et al. *N*-acetylglucosaminyltransferase-III and *N*-acetylglucosaminyltransferase-V messenger-RNA levels in Lec rats during hepatocarcinogenesis. *Cancer Res* 1993;53:3899–3902.
- [80] Nishikawa A, Gu J, Fujii S, Taniguchi N. Determination of *N*-acetylglucosaminyltransferase-III, *N*-acetylglucosaminyltransferase-IV and *N*-acetylglucosaminyltransferase-V in normal and hepatoma tissues of rats. *Biochim Biophys Acta* 1990;1035:313–318.
- [81] Koenderman AH, Koppen PL, Koeleman CA, van den Eijnden DH. *N*-acetylglucosaminyltransferase III, IV and V activities in Novikoff ascites tumour cells, mouse lymphoma cells and hen oviduct. Application of a sensitive and specific assay by use of high-performance liquid chromatography. *Eur J Biochem* 1989;181:651–655.
- [82] Guo HB, Jiang AL, Ju TZ, Chen HL. Opposing changes in *N*-acetylglucosaminyltransferase-V and -III during the cell cycle and all-trans retinoic acid treatment of hepatocarcinoma cell line. *Biochim Biophys Acta* 2000;1495:297–307.
- [83] Yao M, Zhou DP, Jiang SM, Wang QH, Zhou XD, Tang ZY, et al. Elevated activity of *N*-acetylglucosaminyltransferase V in human hepatocellular carcinoma. *J Cancer Res Clin Oncol* 1998;124:27–30.
- [84] Ito Y, Miyoshi E, Sakon M, Takeda T, Noda K, Tsujimoto M, et al. Elevated expression of UDP-*N*-acetylglucosamine: alpha-mannoside beta1,6 *N*-acetylglucosaminyltransferase is an early event in hepatocarcinogenesis. *Int J Cancer* 2001;91:631–637.
- [85] Bosques CJ, Raguram S, Sasisekharan R. The sweet side of biomarker discovery. *Nat Biotechnol* 2006;24:1100–1101.
- [86] Raman R, Raguram S, Venkataraman G, Paulson JC, Sasisekharan R. Glycomics: an integrated systems approach to structure-function relationships of glycans. *Nat Methods* 2005;2:817–824.
- [87] Gravel P, Walzer C, Aubry C, Balant LP, Yersin B, Hochstrasser DF, et al. New alterations of serum glycoproteins in alcoholic and cirrhotic patients revealed by high resolution two-dimensional gel electrophoresis. *Biochem Biophys Res Commun* 1996;220:78–85.
- [88] Henry H, Froehlich F, Perret R, Tissot JD, Eilers-Messerli B, Lavanchy D, et al. Microheterogeneity of serum glycoproteins in patients with chronic alcohol abuse compared with carbohydrate-deficient glycoprotein syndrome type I. *Clin Chem* 1999;45:1408–1413.
- [89] Laroy W, Contreras R, Callewaert N. Glycome mapping on DNA sequencing equipment. *Nat Protoc* 2006;1:397–405.
- [90] Turnbull JE, Field RA. Emerging glycomics technologies. *Nat Chem Biol* 2007;3:74–77.
- [91] Miyamoto S. Clinical applications of glycomic approaches for the detection of cancer and other diseases. *Curr Opin Mol Ther* 2006;8:507–513.
- [92] Morelle W, Michalski JC. Glycomics and mass spectrometry. *Curr Pharm Des* 2005;11:2615–2645.
- [93] Pilobello KT, Mahal LK. Deciphering the glycode: the complexity and analytical challenge of glycomics. *Curr Opin Chem Biol* 2007;11:300–305.
- [94] Callewaert N, Van Vlierberghe H, Van Hecke A, Laroy W, Delanghe J, Contreras R. Noninvasive diagnosis of liver cirrhosis using DNA sequencer-based total serum protein glycomics. *Nat Med* 2004;10:429–434.
- [95] Liu XE, Desmyter L, Gao CF, Laroy W, Dewaele S, Vanhooren V, et al. *N*-glycomic changes in hepatocellular carcinoma patients with liver cirrhosis induced by hepatitis B virus. *Hepatology* 2007;46:1426–1435.
- [96] Kam RKT, Poon TCW, Chan HLY, Wong N, Hui AY, Sung JY. High-throughput quantitative profiling of serum *N*-glycome by MALDI-TOF mass spectrometry and *N*-glycomic fingerprint of liver fibrosis. *Clin Chem* 2007;53:1254–1263.
- [97] Morelle W, Flahaut C, Michalski JC, Louvet A, Mathurin P, Klein A. Mass spectrometric approach for screening modifications of total serum *N*-glycome in human diseases: application to cirrhosis. *Glycobiology* 2006;16:281–293.
- [98] Stahl B, Thurl S, Zeng JR, Karas M, Hillenkamp F, Steup M, et al. from human milk as revealed by matrix-assisted laser

- desorption/ionization mass spectrometry. *Anal Biochem* 1994;223:218–226.
- [99] Harvey DJ. Quantitative aspects of the matrix-assisted laser-desorption mass-spectrometry of complex oligosaccharides. *Rapid Commun Mass Spectrom* 1993;7:614–619.
- [100] Mehta AS, Long RE, Comunale MA, Wang M, Rodemich L, Krakover J, et al. Increased levels of galactose-deficient anti-Gal immunoglobulin G in the sera of hepatitis C virus-infected individuals with fibrosis and cirrhosis. *J Virol* 2008;82:1259–1270.

# **Chapter 2:**

# **Aim and outline of**

# **the thesis**

---



Approximately 10% of the world population is affected by a liver disease. For diagnosis, grading and treatment, an invasive technique is currently used (percutaneous liver biopsy). As already outlined in the introduction, this technique has several disadvantages. The procedure is involved with serious complications (low risk of intraperitoneal hemorrhage and/or pneumothorax, high risk of pain). Furthermore, the sampling error with under or overestimation of the fibrotic grade is an inherent problem of this technique. Finally, a liver biopsy is expensive. In Europe, the total cost is estimated at 1250 euro for each intervention.

Research into non-invasive alternatives is therefore necessary. Our research group already detected significant differences in serum protein *N*-glycosylation between patients with and without cirrhosis and we developed a technology that can measure these alterations at clinical relevant high-throughput. For this purpose, a multi-capillary DNA sequencer is used as glycan analytical tool. With this technology, compensated cirrhosis can be distinguished from pre-cirrhotic fibrosis with a specificity of more than 95% and a sensitivity that varies between 60-80%.

This thesis is part of a GOA-project (“Gemeenschappelijk Onderzoek Actie”). The common goal of the GOA-project was to translate the collected knowledge and developed technology to a clinical format. This was performed in different fields: clinical chemistry, endocrinology and glycobiology. The work in this thesis represents the research performed in the field of hepatology in which still a lot of questions were unanswered. In general, this research was conducted according to two major questions in which the initial results were further explored in depth.

1. The initial study (Callewaert *et al.* Nat Med 2004) was predominantly performed in viral hepatitis C patients. Do these alterations also occur in the other major etiologies of chronic liver disease (alcoholic, cholestatic, viral hepatitis B and non-alcoholic fatty liver disease)? Furthermore, what is the influence of particular co-morbidities of chronic liver disease (portal hypertension, jaundice) on the *N*-glycan alterations (**Chapter 3.1**)?
  - a. Identified differences seen in humans can be validated in mouse models with the advantage that the influence of particular variables on *N*-glycan alteration can be investigated independently of each other. Examples are the partial portal vein ligation (PPVL) model (portal hypertension); common bile duct ligation model (hyperbilirubinemia) and the CCl<sub>4</sub> model (alcoholic micronodular cirrhosis) (**Chapter 3.1**).
  - b. Serum proteins are produced by the liver and B cells. The liver produces the majority of the serum proteins, but B cells are responsible for the production of an important group of serum glycoproteins, the immunoglobulins. The impact of the liver on *N*-glycan alterations in mouse models of chronic liver diseases can be studied independently of B cells by using B cell deficient mice (**Chapter 3.2**).
  - c. In addition to the fibrotic/cirrhotic mouse models, we wanted to investigate the *N*-glycan alterations in a mouse model of hepatocellular carcinoma (HCC). This mouse model is induced by chronic injections with diethylnitrosamine (DEN). Our lab does a lot of research into anti-angiogenic compounds as

treatment of HCC. A very promising compound is a murine monoclonal antibody directed against the placental growth factor (anti-PlGF) which significantly improved tumor burden and mortality in the DEN-induced HCC mouse model. We examined if *N*-glycosylation patterns could be used as a non-invasive follow-up tool to evaluate the efficacy of anti-PlGF (**Chapter 3.3**).

2. A second important objective was to develop a biomarker that can distinguish between patients with steatosis and patients with non-alcoholic steatohepatitis (NASH). We already observed a gradual increase of agalactosylated glycans, glycans that lack the galactose in the glycan structure and are uniquely present on IgG, in augmenting fibrotic stages of HCV-patients. As the distinction between steatosis and NASH patients is mainly inflammation-dependent, we investigated whether the agalacto-IgG component could distinguish both patient populations. The biomarker was developed in a population of patients that were scheduled for bariatric surgery. This population included no patients with advanced fibrosis. Fibrosis is attended by its own specific glycomic alterations and could therefore interfere with the development of a marker that is specific for NASH. This glycomarker was subsequently validated in a large, independent population including patients that were diagnosed with non-alcoholic fatty liver disease (NAFLD) through a percutaneous liver biopsy without surgery (**Chapter 3.4**).
  - a. As a continuation of this research, we examined pediatric NAFLD patients to investigate if similar features applied to this population and if therefore the same biomarker can be used to distinguish steatotic from NASH patients in children under 19 (**Chapter 3.5**).
  - b. Finally, an investigation was performed into the mechanism of undergalactosylation in non-alcoholic steatohepatitis. There are strong indications that endoplasmic stress (ER) stress (unfolded protein response) plays an important part in this. This was examined by isolating plasma cells from the leukocyte population in NAFLD patients. Plasma cells are the B cell subset that produces the immunoglobulins. The RNA fraction was subsequently extracted from the plasma cells and several important ER stress genes were evaluated by qPCR analysis (**Chapter 3.6**).

# **Chapter 3:**

# **Results**

---

# Chapter 3.1

## ***“Impact of elevation of total bilirubin level and etiology of the liver disease on serum N-glycosylation patterns in mice and humans”***

**Bram Blomme**<sup>1</sup>, Christophe Van Steenkiste<sup>1</sup>, Jacques Vanhuyse<sup>2</sup>, Isabelle Colle<sup>1</sup>, Nico Callewaert<sup>3,4</sup>, Hans Van Vlierberghe<sup>1</sup>

<sup>1</sup>Department of Hepatology and Gastroenterology, Ghent University Hospital, Ghent, Belgium

<sup>2</sup>Department of Pathology, Ghent University Hospital, Ghent, Belgium

<sup>3</sup>Unit for Molecular Glycobiology, Department for Molecular Biomedical Research, VIB, Ghent, Belgium

<sup>4</sup>Department of Biochemistry, Physiology and Microbiology, Ghent University, Ghent, Belgium

**American Journal of Physiology: Gastrointestinal and Liver Physiology 2010; 298:  
G615-G624**

# Impact of elevation of total bilirubin level and etiology of the liver disease on serum *N*-glycosylation patterns in mice and humans

Bram Blomme,<sup>1</sup> Christophe Van Steenkiste,<sup>1</sup> Jacques Vanhuyse,<sup>2</sup> Isabelle Colle,<sup>1</sup> Nico Callewaert,<sup>3,4</sup> and Hans Van Vlierberghe<sup>1</sup>

<sup>1</sup>Department of Hepatology and Gastroenterology, Ghent University Hospital; <sup>2</sup>Department of Pathology, Ghent University Hospital; <sup>3</sup>Unit for Molecular Glycobiology, Department for Molecular Biomedical Research, Vlaams Instituut voor Biotechnologie, Ghent University; and <sup>4</sup>Department of Biochemistry, Physiology and Microbiology, Ghent University, Ghent, Belgium

Submitted 9 October 2009; accepted in final form 31 December 2009

**Blomme B, Van Steenkiste C, Vanhuyse J, Colle I, Callewaert N, Van Vlierberghe H.** Impact of elevation of total bilirubin level and etiology of the liver disease on serum *N*-glycosylation patterns in mice and humans. *Am J Physiol Gastrointest Liver Physiol* 298: G615–G624, 2010. First published January 7, 2010; doi:10.1152/ajpgi.00414.2009.—The GlycoFibroTest and GlycoCirrhoTest are noninvasive alternatives for liver biopsy that can be used as a follow-up tool for fibrosis patients and to diagnose cirrhotic patients, respectively. These tests are based on the altered *N*-glycosylation of total serum protein. Our aim was to investigate the impact of etiology on the alteration of *N*-glycosylation and whether other characteristics of liver patients could have an influence on *N*-glycosylation. In human liver patients, no specific alteration could be found to make a distinction according to etiological factor, although alcoholic patients had a significant higher mean value for the GlycoCirrhoTest. Undergalactosylation did not show a significantly different quantitative alteration in the cirrhotic and non-cirrhotic population of all etiologies. Importantly, patients with an elevation of total bilirubin level (>2 mg/dl) had a strong increase of glycans modified with  $\alpha$ 1–6 fucose. The fucosylation index was therefore significantly higher in fibrosis/cirrhosis and hepatocellular carcinoma patients with elevated total bilirubin levels irrespective of etiology. Furthermore, in a multiple linear regression analysis, only markers for cholestasis significantly correlated with the fucosylation index. In mouse models of chronic liver disease, the fucosylation index was uniquely significantly increased in mice that were induced with a common bile duct ligation. Mice that were chronically injected with CCl<sub>4</sub> did not show this increase. Apart from this difference, common changes characteristic to fibrosis development in mice were observed. Finally, mice induced with a partial portal vein ligation did not show biological relevant changes indicating that portal hypertension does not contribute to the alteration of *N*-glycosylation.

biomarker; glycomics;  $\alpha$ 1–6 fucose; DSA-FACE; hyperbilirubinemia

LIVER FIBROSIS IS CHARACTERIZED by the replacement of liver tissue by fibrous scar tissue and the development of regenerative nodules, leading to progressive loss of liver function (22). The “golden” standard to assess progression of liver fibrosis is a liver biopsy (1, 10), but it is associated with several complications such as intraperitoneal hemorrhage (~1%), puncture of the gallbladder, pneumothorax (both <0.5%), and in very rare cases even death (0.01–0.001%) (18, 20). Because of these limitations, there is an increasing demand for noninvasive serum tests and imaging techniques to assess the stage of liver

fibrosis. In this regard, interest is raised in serum *N*-glycan profiles as potential indicator of liver disease.

The majority of serum proteins are produced by the liver and nearly all of these proteins are *N*-glycosylated, a noticeable exception being albumin. Recently, a new technological platform, DNA sequencer-assisted-fluorophore-assisted capillary electrophoresis (DSA-FACE) (14), has been developed to assess glycan structures. This has led to the discovery of a noninvasive test characteristic for end-stage cirrhosis, the GlycoCirrhoTest. This test is defined by the logarithmic proportion of the peak heights of a biantennary,  $\alpha$ 1–6 fucosylated, and bisecting *N*-acetylglucosamine (GlcNAc) modified sugar (NA2FB, increased in cirrhosis) and a triantennary sugar (NA3, decreased in cirrhosis) in the electropherogram (3).

NA2FB represents the increase of bisecting GlcNAc-modified glycans in cirrhotic patients, and NA3 represents the decrease of multiantennary glycans in the serum of cirrhotic patients. This is associated with the upregulation of *N*-acetylglucosaminyltransferase III (GnT-III, responsible for bisecting GlcNAc-modified glycans) and the competitive decrease of *N*-acetylglucosaminyltransferase V (GnT-V, responsible for multiantennary glycans) in regenerative nodules, and these occur per definition only in the cirrhotic stage.

Undergalactosylation (UGS), the increase of agalacto glycans in serum, is also an important feature in the glycosylation patterns of liver patients. These glycans, which lack one or both galactoses, progressively increase with Metavir stage (2), and they can be predominantly found on immunoglobulin G (IgG) (21). UGS of IgG forms the basis of the GlycoFibroTest. Finally, it was shown that the increased abundance of an  $\alpha$ 1–3 fucosylated glycan, NA3Fb, is associated with the development of hepatocellular carcinoma (HCC) in hepatitis B (HBV) patients (15).

Callewaert et al. (3) showed the potential of glycome research in biomarker discovery. Complementary to this study, we wanted to investigate the impact of etiology on *N*-glycosylation patterns. Therefore, we examined five patient populations of different etiology: cholestatic, HBV, hepatitis C (HCV), alcoholic, and nonalcoholic steatohepatitis (NASH) patients and one control population of healthy volunteers. Importantly, it was observed that patients with an elevation in serum total bilirubin level (>2 mg/dl) had a significant increase of peak height of glycans modified with  $\alpha$ 1–6 fucose. Therefore, the fucosylation index (FI), defined as the percentage of  $\alpha$ 1–6 fucosylated glycans in the glycome of serum proteins, was significantly elevated in fibrosis/cirrhosis patients with increased levels of total bilirubin. An increase of the FI

Address for reprint requests and other correspondence: H. Van Vlierberghe, Dept. of Hepatology and Gastroenterology, Ghent Univ. Hospital, B-9000 Ghent, Belgium (e-mail: hans.vanvlierberghe@ugent.be).

Table 1. Anthropomorphic data and liver tests in the different etiologies of chronic liver disease and control group

	Fibrosis/Cirrhosis Patient Etiologies					
	Cholestatic	HBV	HCV	Alcoholic	NASH	Control
Age, yr	45.2 ± 15.6	45.1 ± 16.4	53.9 ± 16.1	59.2 ± 9.2	46.2 ± 12.2	46.6 ± 12.8
Weight, kg	72.9 ± 14.8	80.3 ± 15.5	72.9 ± 13.6	80 ± 18.5	89.4 ± 23.7	ND
Sex, men/women	10/5	13/7	21/11	22/9	11/6	10/5
F0-F1	ND	ND	5/32 (15.6%)	ND	ND	NA
F2	ND	ND	3/32 (9.4%)	ND	ND	NA
F3	ND	ND	3/32 (9.4%)	ND	ND	NA
F4	4/15 (26.7%)	9/20 (45%)	21/32 (65.6%)	23/31 (74.2%)	4/17 (23.5%)	NA
Bilirubin, mg/dl	1.34 ± 1.5	1.04 ± 0.93	1.02 ± 1	1.79 ± 1.4	5.3 ± 14.4	0.2 ± 0.16
AST, U/l	45.6 ± 39.6	31.2 ± 15.9	68.3 ± 42.8	43.6 ± 26.3	34.8 ± 38.4	8.6 ± 5.7
ALT, U/l	55.5 ± 52.1	33.1 ± 31.2	76.8 ± 81.5	31.3 ± 19.2	36.1 ± 58.1	10.6 ± 3.9
GGT, U/l	202.3 ± 439	24.8 ± 13.7	89.3 ± 73.2	117.5 ± 115.8	98 ± 127.1	29.2 ± 24

HBV, hepatitis B; HCV, hepatitis C; NASH, nonalcoholic steatohepatitis; AST, aspartate aminotransferase; ALT, alanine aminotransferase; GGT,  $\gamma$ -glutamyl transferase; ND, not determined; NA, not applicable.

has especially been linked with HCC patients (6, 17), and, therefore, we also tested some HCC serum samples with normal (0–1 mg/dl) and elevated (>2 mg/dl) total bilirubin serum level. Moreover, patients with a strong elevation of total bilirubin level were excluded in the original studies (3, 21, 15).

To confirm the results of the human data, we investigated the N-glycosylation patterns of two mouse models of chronic liver disease, common bile duct ligation (CBDL) and subcutaneous injections with carbon tetrachloride (CCl<sub>4</sub>). In addition, a mouse model for a pure portal hypertension (PHT) without liver damage, partial portal vein ligation (PPVL), was also evaluated.

## MATERIALS AND METHODS

**Human liver patients.** Five patient populations of at least 15 patients each were assembled (Table 1). Each group had a specific etiology: cholestasis ( $n = 15$ ), HBV ( $n = 20$ ), HCV ( $n = 32$ ), alcoholic ( $n = 31$ ), and NASH ( $n = 17$ ). The cholestatic group consisted of 1 patient with progressive familial intrahepatic cholestasis, 9 patients with primary sclerosing cholangitis, and 5 patients with primary biliary cirrhosis. Most of the alcoholic patients kept to a regime of alcohol abstinence at the time of analysis; there was only one active drinker (>21 alcoholic consumptions/wk). The majority of HBV patients (70%) were on treatment. We also included a control group of 16 healthy volunteers and a HCC group of 16 patients (Table 2). The volume of the tumor in a HCC patient was calculated on the basis of the diameter (>1 cm) of the nodule(s) reported by the radiologist on CT scan. In the case of multiple nodules, the different diameters

were counted up. Subsequently, the formula to calculate the volume of a sphere ( $4/3\pi r^3$ ) was used to assess tumor volume. Medical records of these patients were reviewed. Liver tests, Metavir stage if determined by biopsy, other underlying diseases or conditions, and clinical manifestations were assessed. All patients and volunteers signed an informed consent, and the protocol was approved by the ethical committee of the Ghent University Hospital. Serum samples of patients and controls were taken fasted.

The concentration of bile acids in serum was spectrophotometrically determined on a Hitachi 912 analyzer (Diagnostica; Boehringer Mannheim, Ingelheim, Germany) by use of a commercial kit (Trinity Biotech, Co. Wicklow, Ireland). The alanine aminotransferase activity (ALT), aspartate aminotransferase activity (AST),  $\gamma$ -glutamyl transferase (GGT), alkaline phosphatase (AP), C-reactive protein (CRP), total bilirubin, and total protein were analyzed by routine photometric test on a Hitachi 747 analyzer (Diagnostica, Boehringer Mannheim).

**Animal models.** Male C57Bl/6 mice (25–30 g) were purchased from Harlan Laboratories (Horst, The Netherlands). The mice were kept under constant temperature and humidity in a 12-h controlled light-dark cycle. The Ethical Committee of experimental animals at the faculty of Medicine and Health Sciences, Ghent University, Belgium, approved the protocols.

The mouse model for a pure PHT without liver damage was induced by PPVL (7). The surgical procedure was performed under sterile conditions. Mice were anesthetized under isoflurane inhalation (Forene; Abbott, Brussels, Belgium). A midline abdominal incision was performed and the portal vein was separated from the surrounding tissue. A ligature (silk cut 5-0) was tied around both portal vein and adjacent 27-gauge blunt-tipped needle. Subsequent

Table 2. Anthropomorphic data and liver tests in the different etiologies of HCC patients

	Etiologies of HCC Patients			
	HBV	HCV	Alcoholic	NASH
<i>n</i>	2	4	8	2
Age, yr	72 ± 12.7	76.3 ± 7.6	64.7 ± 16	65.5 ± 78
Weight, kg	54.5 ± 7.8	69.5 ± 17.7	73.8 ± 18.1	83 ± 8.9
Sex, men/women	1/1	3/1	5/3	1/1
Bilirubin, mg/dl	3.4 ± 4.1	1.85 ± 1.6	5.1 ± 6.9	0.6 ± 0
AST, U/l	76 ± 84.9	73.5 ± 30.4	70.1 ± 59.3	31.5 ± 17.7
ALT, U/l	44.5 ± 40.3	64 ± 24.2	35 ± 20.1	37 ± 14.1
GGT, U/l	99 ± 46.7	217.3 ± 193.4	164.4 ± 83.4	136 ± 161.2
AFP, ng/ml	1,009 ± 1422	133.1 ± 208.9	10027 ± 24416.4	140.1 ± 195.1
MELD score	13.9 ± 5.8	11.7 ± 3.4	14.2 ± 8.4	7.2 ± 0.1
Milan criteria, within/outside	1/1	3/1	5/3	1/1

HCC, hepatocellular carcinoma; MELD, Model for End-Stage Liver Disease.

removal of the needle yielded a calibrated stenosis of the portal vein. Mice were euthanized at 7 and 14 days after PPVL ( $n = 8$  in each group).

The portal venous pressure was measured in PPVL and Sham mice. The portal vein was cannulated through an ileocolic vein with a 24-gauge catheter (Becton Dickinson, Erebodegem-Aalst, Belgium), which was advanced into the portal vein and connected to a highly sensitive pressure transducer (Powerlab, ADInstruments, Spechbach, Germany). The external zero reference point was placed at the midportion of the animal.

The mouse model for a secondary biliary cirrhosis is CBDL (13). The surgical procedure was performed under sterile conditions. Under isoflurane inhalation anesthesia, a midline abdominal incision was made and the common bile duct was isolated. The common bile duct was occluded with a double ligature of a nonresorbable suture (silk cut 5-0). The first ligature was made below the junction of the hepatic ducts and the second was made above the entrance of the pancreatic duct. The common bile duct was sectioned between the two ligatures. Mice were euthanized 1, 3, 4, 5, and 6 wk after CBDL ( $n = 8$  in each group). Sham-operated mice were used as control group for the CBDL and PPVL model ( $n = 8$  in each group).

Finally, the third mouse model was induced by chronic subcutaneous administration of  $\text{CCl}_4$  (Merck, Darmstadt, Germany) twice weekly (1:1 dissolved in olive oil; 1 ml/kg) (11), and 5% alcohol was added to drinking water. Mice were euthanized after 1, 3, 6, 10, and 16 wk ( $n = 8$  per group). Control mice for  $\text{CCl}_4$  received a saline solution (1 ml/kg) subcutaneously ( $n = 8$  in each group). No alcohol was added to the drinking water. The time points at which the mice in the different mouse models were euthanized roughly correspond with the semiquantitative Metavir stage (2) as validated in a previous study (8).

Blood samples were taken by puncture of the aorta abdominalis. These samples were centrifuged at 2,000 rpm for 10 min. At least 200  $\mu\text{l}$  of serum was taken off the clot and the ALT, AST, and total bilirubin were analyzed as described for the human samples. The remaining serum volume was used for the analysis of the *N*-glycan profiles and to perform two ELISAs for the determination of the serum IgG and serum amyloid A concentration (Immunology Consultants Laboratory, Newburg, OR). The ELISAs were run according to manufacturer's instructions and all analyses were done in duplicate.

Histopathology of the mouse liver was performed by staining with 0.1% picrosirius red. Microscopic evaluation was carried out blinded by two independent investigators (J. Vanhuyse and B. Blomme). Scoring of the liver tissues was done to determine the stage of fibrosis, and this was expressed according to the Metavir score (2) with the emphasis on the fibrosis and not on activity.

**Serum protein *N*-glycome sample processing.** The 96-well on-membrane deglycosylation method (14) was used to prepare 8-amino-pyrene-1,3,6-trisulfonate (APTS)-labeled *N*-glycans from 5  $\mu\text{l}$  serum. Samples were finally reconstituted in 5  $\mu\text{l}$  Milli-Q water and analyzed by DSA-FACE.

To get an idea about the structures of the glycans present in the mouse profiles, exoglycosidase array sequencing was applied. Batches (0.5  $\mu\text{l}$ ) of APTS-labeled *N*-glycans were subjected to digestion with different mixtures of exoglycosidases in 5 mM  $\text{NH}_4\text{Ac}$  (pH 5). The enzymes used were *Arthrobacter ureafaciens* sialidase, *Streptococcus pneumoniae*  $\beta$ -1,4-galactosidase, jack bean  $\beta$ -*N*-acetylhexosaminidase, and bovine kidney  $\alpha$ -fucosidase. After complete digestion (overnight at 37°C), the samples were evaporated to dryness, reconstituted in 10  $\mu\text{l}$  water, and analyzed by DSA-FACE.

**Data processing.** We quantified the heights of 11 peaks that were detectable in all mouse and human samples (Fig. 1) to obtain a numerical description of the profiles and analyzed these data with SPSS 15.0 software (SPSS, Chicago, IL). First, the sum of the peak heights of all the peaks were calculated (total intensity) and then the peak heights were normalized to the total intensity of the measured peaks (expressed as percentage of the total intensity).

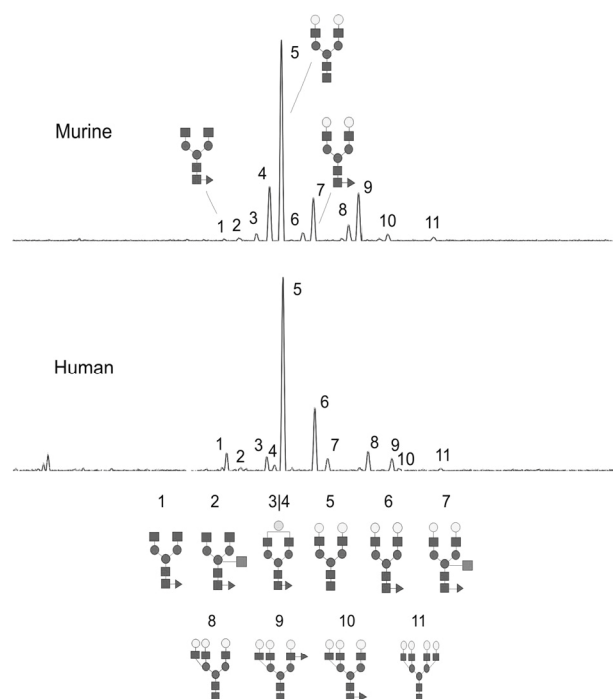


Fig. 1. *Top*: typical desialylated *N*-glycan profile from a control C57Bl/6 mouse total serum protein. *Bottom*: typical desialylated *N*-glycan profile from a healthy human control total serum protein. The glycan structures of all the peaks in the human profile are known: Peak 1 indicates an agalacto  $\alpha$ 1–6 fucosylated biantennary glycan (NGA2F), peak 2 indicates an agalacto  $\alpha$ 1–6 fucosylated bisecting biantennary glycan (NGA2FB), peaks 3 and 4 indicate a single agalacto  $\alpha$ 1–6 fucosylated biantennary glycan (NG1A2F), peak 5 indicates a bigalacto biantennary glycan (NA2), peak 6 indicates a bigalacto  $\alpha$ 1–6 fucosylated biantennary glycan (NA2F), peak 7 indicates a bigalacto  $\alpha$ 1–6 fucosylated bisecting biantennary glycan (NA2FB), peak 8 indicates a triantennary glycan (NA3), peak 9 indicates a  $\alpha$ 1–3 fucosylated triantennary glycan (NA3Fb), peak 10 indicates a  $\alpha$ 1–6 fucosylated triantennary glycan (NA3Fc), and peak 11 indicates a tetra-antennary glycan (NA4). The symbols used in the structural formulas are as follows: open circle,  $\beta$ -linked galactose; square,  $\beta$ -linked *N*-acetylglucosamine; shaded circle,  $\alpha$ / $\beta$ -linked mannose; triangle,  $\alpha$ -1,3/6-linked fucose. The structures of the peaks in the mouse profile were obtained after exoglycosidase digests. The 3 glycans indicated in the murine profile were clearly deduced from the exoglycosidase digests (data not shown).

All mouse data were analyzed with Mann-Whitney *U*-test (control vs. treated). The human data were statistically processed as appropriate for the study design (independent sample *t*-test, single-factor ANOVA, Kruskal-Wallis test, and multiple linear regression). A *P* value less than 0.05 was considered significant in all analyses.

## RESULTS

*Alcoholic patients have a significant higher mean value for the GlycoCirroTest.* The analysis was done on cirrhotic HCV ( $n = 21$ ) and cirrhotic alcoholic patients ( $n = 23$ ). The relative percentage of NA2FB was significantly higher in the alcoholic group compared with the HCV group ( $8.9 \pm 2.8$  vs.  $6.4 \pm 2.4\%$ ) ( $P = 0.004$ ; two-tailed *t*-test). The relative percentage of NA3 was not significantly different between the two groups ( $P = 0.164$ ; two-tailed *t*-test), although the mean value in the alcoholic group was lower than in the HCV group (2.5 vs. 3.1%). As a consequence, the mean value of the GlycoCirroTest was almost double as high in the alcoholic group compared with the HCV group ( $0.59 \pm 0.33$  vs.  $0.31 \pm 0.26$ ) ( $P = 0.005$ ; two-tailed *t*-test). The cirrhotic patients in the other etiologies also had a mean value that was considerably lower than that of

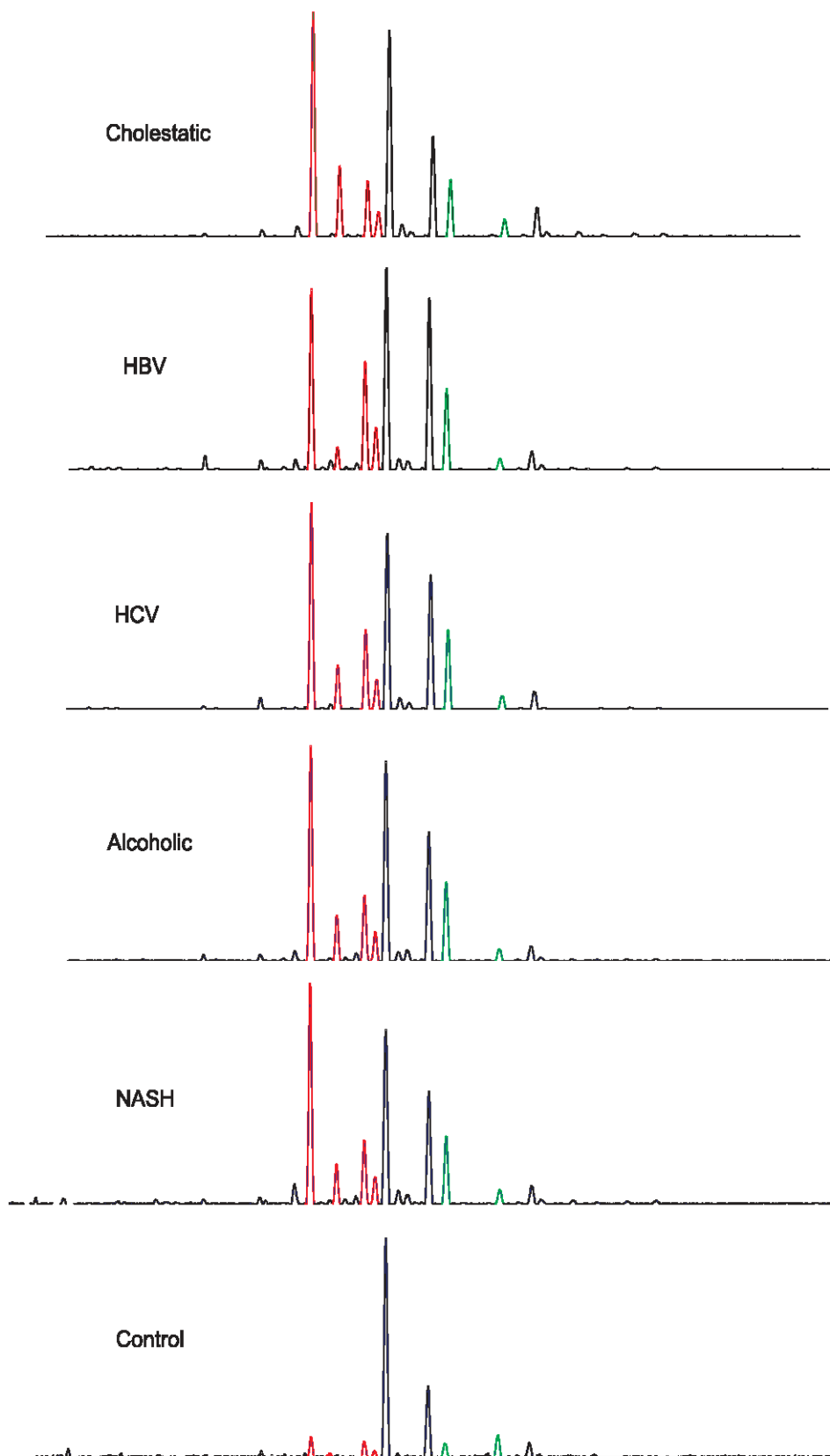


Fig. 2. Comparison of typical cirrhotic *N*-glycan profiles of different etiologies and a typical *N*-glycan profile of a healthy control. The peaks that represent undergalactosylated glycans are in red and the peaks that represent the GlycoCirrhoTest are in green. HBV, hepatitis B; HCV, hepatitis C; NASH, nonalcoholic steatohepatitis.

alcoholic patients: cholestatic  $0.26 \pm 0.2$ ,  $n = 4$ , and HBV  $0.3 \pm 0.39$ ,  $n = 9$ . These latter observations were still substantially higher compared with the control group ( $-0.03 \pm 0.15$ ) (Fig. 2). The value for NASH patients ( $0.5 \pm 0.57$ ,  $n = 4$ ) was also quite high. Our data set, in all etiologies together, had an area under the receiver operating characteristic curve (AUROC) of 0.81

for the discrimination between F0–F3 and F4, which was similar to the original study (3). More informative was the AUROC in the individual etiologies: cholestatic (0.77), HBV (0.72), HCV (0.68), alcoholic (0.96), and NASH (0.83). Finally, we found significant correlations between scores of the GlycoCirrhoTest and various markers of chronic liver disease:



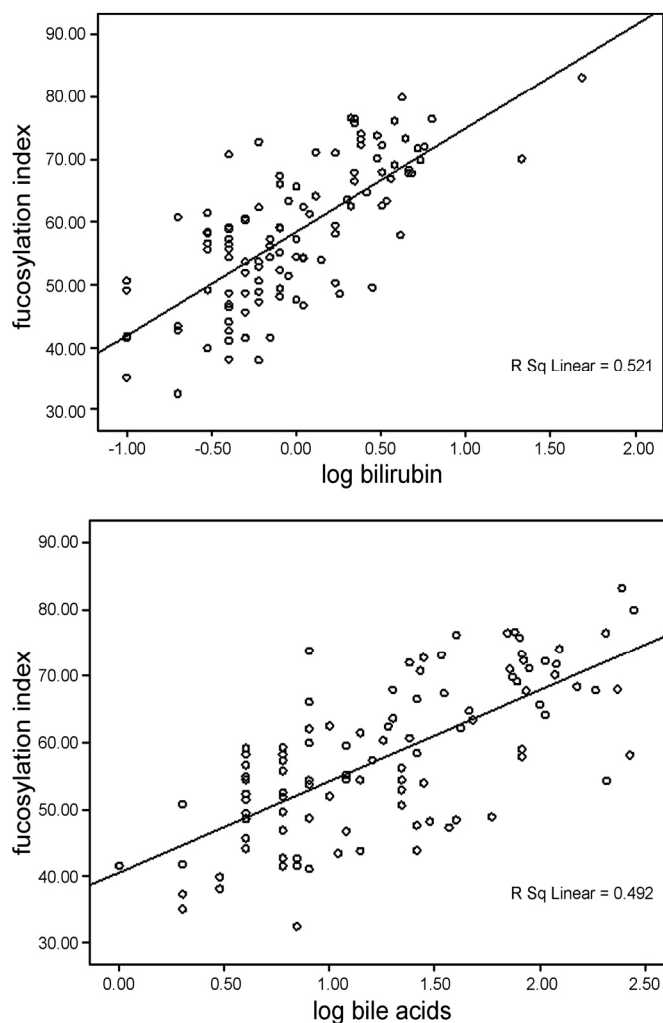


Fig. 3. Scatter dots of the correlation between the logarithmically transformed bilirubin and serum bile acid concentration with the fucosylation index.

GGT, AST, total bilirubin, AP, and bile acids ( $P < 0.001$ ; Spearman rank test) and ALT ( $P = 0.018$ ; Spearman rank test). This was expected because the GlycoCirrhoTest only displays an increase in score in the cirrhotic stage as these parameters were also seen to be elevated at this stage. In contrast, there was no correlation between scores of the GlycoCirrhoTest and viral load in HBV and HCV patients ( $P = 0.347$ ; Spearman rank test).

No significantly different quantitative alteration in undergalactosylation score between all etiologies. UGS score was defined as  $\{[2 \times (\text{peak}1 + 2)] + \text{peak} 3 + \text{peak} 4\} / \{[2 \times (\text{peak}1 + \text{peak}2 + \text{peak}3 + \text{peak}4 + \text{peak}5 + \text{peak}6 + \text{peak}7)] + [3 \times (\text{peak}8 + \text{peak}9 + \text{peak}10)] + (4 \times \text{peak}11)\}$  (expressed in %) (20).

In the noncirrhotic group (F1–F3), there was no significant difference in UGS score between the etiologies as determined by pairwise comparisons using Scheffé’s tests (single-factor ANOVA). The HCV and alcoholic liver disease group showed the highest mean level of UGS score (0.24 and 0.23, respectively), followed by HBV (0.2), cholestatic liver disease, (0.18), and NASH (0.16) ( $P = 0.322$ ).

The classification according to Metavir stage was possible for the HCV-population (Table 1). We were able to reproduce the linear increase of UGS score in increasing Metavir stage: F1 0.15, F2 0.25, F3 0.29, and F4 0.32.

In cirrhotic patients, again no significant difference in UGS score between the etiologies was seen ( $P = 0.054$ , Kruskal-Wallis  $H$ -test). Mean UGS score was highest in cirrhotic NASH patients (0.35), followed by alcoholic (0.34) and HCV (0.32) patients. Cholestatic (0.23) and HBV (0.17) patients had a clearly lower, although not significant, mean level of UGS score.

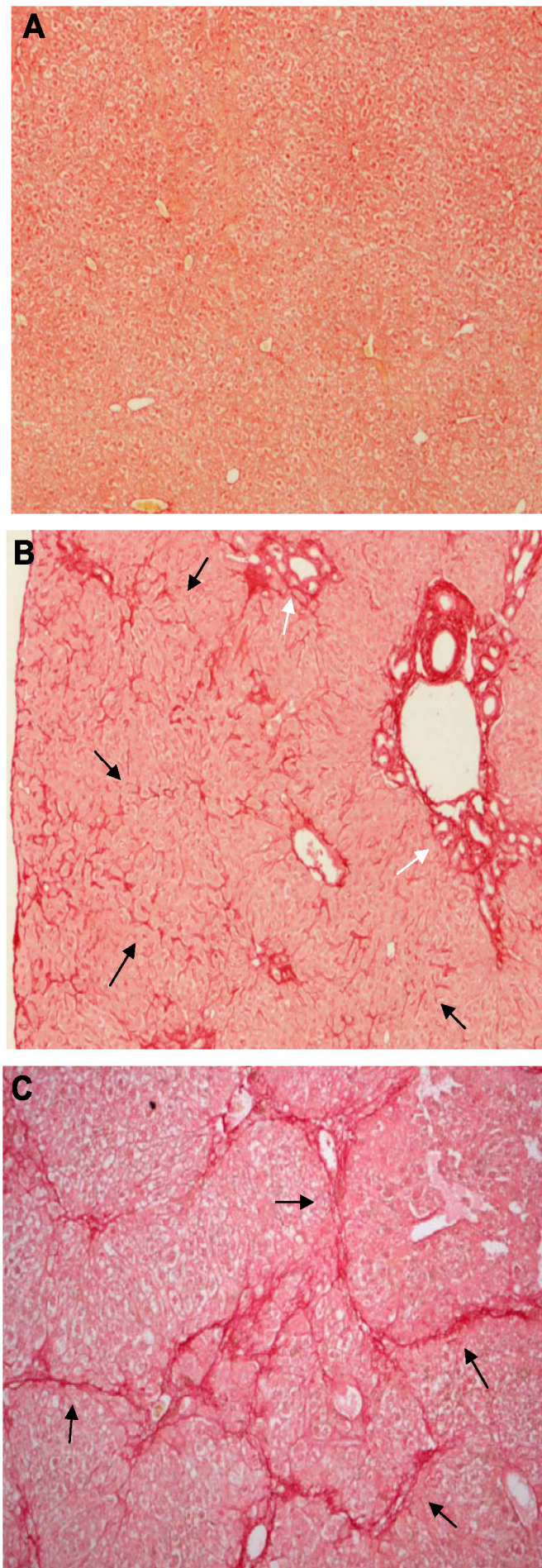
Fucosylation index is significantly increased in fibrosis/cirrhosis and HCC patients with an elevation of total bilirubin level. It was observed that the FI of liver patients with an elevation in total bilirubin level (70%) was significantly higher than the FI of liver patients with normal total bilirubin levels (52.9%) ( $P < 0.001$ ; two-tailed  $t$ -test). The increase in  $\alpha 1$ –6 fucosylation was clearly not linked to etiology (single-factor ANOVA,  $P = 0.254$ ), only to an elevation in total bilirubin level. The FI was comparable in the progression of F1 to F3 in HCV patients (0.5, 0.58, and 0.52, respectively), but it was clearly elevated in the cirrhotic stage (0.7). Patients with the syndrome of Gilbert had a normal FI. The degree of  $\alpha 1$ –3 fucose did not differ significantly between patients with normal and elevated bilirubin levels ( $P = 0.687$ ; two-tailed  $t$ -test).

We also tested other markers of liver damage (AST, ALT, GGT, AP, CRP, and total protein) to investigate whether these did not confound our results. Only AST and AP were also significantly elevated in the group with increased FI ( $P = 0.001$  and  $P = 0.034$ , respectively; two-tailed  $t$ -test).

Table 3. Laboratory tests: CBDL-sham and CCl<sub>4</sub>-saline

	CBDL					Sham				
	1 wk	3 wk	4 wk	5 wk	6 wk	1 wk	3 wk	4 wk	5 wk	6 wk
AST, U/l	586 ± 417‡	377 ± 101‡	326 ± 75‡	477 ± 239‡	422 ± 201‡	87 ± 16	102 ± 52.5	71 ± 12	82 ± 34	136 ± 52
ALT, U/l	694 ± 662‡	246 ± 38‡	206 ± 65‡	296 ± 118‡	284 ± 141‡	66 ± 39	46 ± 18	41 ± 12	38 ± 10	68 ± 44
TBiln, mg/dl	13.1 ± 6.2‡	24.8 ± 4.9‡	20.7 ± 5.7‡	17.6 ± 4.6‡	22.9 ± 4.6‡	0.11 ± 0.04	0.13 ± 0.04	0.12 ± 0.02	0.16 ± 0.04	0.19 ± 0.03
	CCl <sub>4</sub>					Saline				
	1 wk	3 wk	6 wk	10 wk	16 wk	1 wk	3 wk	6 wk	10 wk	16 wk
AST, U/l	112 ± 42	215 ± 159†	78 ± 44	122 ± 61	98 ± 26*	89 ± 21	81 ± 23	72 ± 21	87 ± 81	67 ± 29
ALT, U/l	87 ± 52	68 ± 24†	51 ± 30	77 ± 28*	88 ± 34†	81 ± 59	41 ± 16	38 ± 6.9	47 ± 15	28 ± 10
TBiln, mg/dl	0.2 ± 0.06	0.17 ± 0.05†	0.22 ± 0.08*	0.21 ± 0.15*	0.19 ± 0.02	0.2 ± 0.2	0.12 ± 0.01	0.15 ± 0.04	0.09 ± 0.04	0.21 ± 0.05

Values are means ± SD;  $n = 8$  subjects per group. CBDL, common bile duct ligation; CCl<sub>4</sub>, carbon tetrachloride; TBiln, total bilirubin. \* $P < 0.05$ ; † $P < 0.01$ ; ‡ $P < 0.001$  compared with sham and saline.



Subsequently, we tested eight HCC patients with an elevation in total bilirubin level and eight HCC patients with normal total bilirubin level. Again, the FI in the HCC group with elevated total bilirubin concentrations was significantly higher (70.8 vs. 48.7%,  $P < 0.001$ ; two-tailed  $t$ -test). Both populations did not differ in  $\alpha$ -fetoprotein level ( $P = 0.35$ ; two-tailed  $t$ -test) but AST was significantly increased in the HCC group with increased FI ( $P < 0.001$ ; two-tailed  $t$ -test) in agreement with the results in the fibrosis/cirrhosis group. There was no significant difference in the other markers (ALT, GGT, AP, CRP, and total protein). Again, the level of  $\alpha$ 1,3-fucose did not differ significantly between HCC patients with normal and elevated bilirubin levels ( $P = 0.585$ ; two-tailed  $t$ -test).

We also analyzed the correlation between the scores of the GlycoHCCTest and tumor volume in HCC patients. There was a clear trend observed between the two variables, but significance was not reached ( $P = 0.054$ ; Spearman rank test). Only one HCC patient showed metastasis and this did not influence the score.

**Serum bile acid concentration.** Serum bile acid concentration was determined in every fibrosis/cirrhosis and HCC patient. Inconsistent data (low total bilirubin-high FI and vice versa) showed consistency in the bile acid data. Cholestatic patients had a mean serum bile acid concentration of  $49.5 \mu\text{mol/l}$  ( $\pm 83.4$ ), HBV patients had a mean value of  $16.2 \mu\text{mol/l}$  ( $\pm 26.1$ ), HCV patients had a mean value of  $38.6 \mu\text{mol/l}$  ( $\pm 53.2$ ), alcoholic patients had a mean value of  $50.2 \mu\text{mol/l}$  ( $\pm 56$ ), NASH patients had a mean value of  $67.2 \mu\text{mol/l}$  ( $\pm 85.4$ ) and HCC patients had a mean value of  $51.5 \mu\text{mol/l}$  ( $\pm 73$ ).

**Only markers for cholestasis correlated significantly with the FI in a multivariate analysis.** The total bilirubin and bile acid data were first logarithmically transformed. The correlation between the FI and the discontinuous variables HCC, cirrhosis (cirrhotic and noncirrhotic), and etiology was determined with a two-tailed Spearman test and a single-factor ANOVA. The correlation with the continuous variables total bilirubin, serum bile acid concentration, AST, and AP was determined with a simple linear regression analysis. The variables AST, total bilirubin, serum bile acid concentration, and cirrhosis correlated significantly with the FI ( $P < 0.001$ ). Scatter dots of the correlation between the (logarithmically transformed) total bilirubin and serum bile acid concentration are seen in Fig. 3.

Subsequently, a multiple linear regression analysis was performed with FI as dependent factor and bilirubin level, serum bile acid concentration, AST, AP, HCC, etiology, and cirrhosis as covariants in the linear model. The (logarithmically transformed) total bilirubin level, (logarithmically transformed) bile acid concentration, and AP correlated significantly with the FI ( $P < 0.001$ ,  $P = 0.001$ , and  $P = 0.029$ , respectively) in the linear model.

Fig. 4. Sirius red staining (objective magnification  $\times 10$ ). A: control mice for  $\text{CCl}_4$  and Sham-operated mice did not develop fibrosis at any time point (Stage 0 or F0). B: typical cirrhotic image of the liver 6 wk after common bile duct ligation (CBDL; black arrows, fibrotic strands; white arrows, bile duct proliferation). C: typical cirrhotic image of the liver chronically injected with  $\text{CCl}_4$  for 16 wk (black arrows, fibrotic strands).

*Laboratory tests and histological analysis of mouse models of chronic liver disease.* Test samples (4 in the PPVL and Sham groups) confirmed earlier reports that there were no changes in AST, ALT, and bilirubin after PPVL induction (6). One week after PPVL induction, the portal venous pressure (PVP) was at a mean of 8.3 mmHg ( $\pm 1.9$ ), and 2 wk after PPVL induction mean PVP rose further to 10.7 mmHg ( $\pm 4$ ). This was significantly higher than sham-operated mice that had a mean PVP of 4.3 mmHg ( $\pm 0.8$ ) ( $P < 0.001$ ) 1 wk after induction and at 2 wk a PVP of 5 mmHg ( $\pm 1.7$ ) ( $P = 0.004$ ). Histological examination revealed no significant fibrosis development in PPVL mice at 1 and 2 wk after induction. They were predominantly scored F0.

After 3 wk of CCl<sub>4</sub> administration, the Sirius red stain demonstrated fibrotic changes in the centrilobular area. After 6 wk the liver architecture demonstrated a reversed lobulation due to development of centrocentral fibrotic linkages, and after 10 wk the reversed lobulation was accentuated with the development of centroportal thin fibrotic septa apart from the centrocentral fibrotic linkages. Finally, after 16 wk, all mice had homogeneous characteristics of cirrhosis. For laboratory tests, see Table 3.

Enlargement of the portal tracts accompanied by dilatation of bile canaliculi and proliferation of the smaller bile ducts appeared as soon as 1 wk after CBDL. After 3 wk, the periportal alterations were accompanied by fibrotic changes to be described as F2 and evolving into F3 after 5 wk of CBDL. After 6 wk, the majority of mice (62.5%) developed cirrhosis with nodular changes in the liver parenchyma. For laboratory tests see Table 3. Typical cirrhotic images of CBDL and CCl<sub>4</sub> mice are seen in Fig. 4.

*N-glycosylation patterns in mouse models of chronic liver disease.* The overall picture of the glycosylation pattern of a PPVL mouse was that of a control sample. One week after PPVL induction, peak 5/NA2 was significantly decreased ( $P = 0.003$ ) and peak 6 was significantly increased ( $P = 0.006$ ) compared with sham mice. Two weeks after induction, when PVP is at its maximum (7), only one peak was significantly altered: peak 9 was significantly increased ( $P = 0.004$ ) compared with Sham mice (Table 4). However, no systematic changes were observed.

In CCl<sub>4</sub> mice, a significant increase in peaks 9 and 11 in the glycosylation pattern was observed starting from the first week

of CCl<sub>4</sub> treatment. Peak 10 also started to increase significantly in abundance from 6 wk on. After 3 wk of CCl<sub>4</sub>, peak 5/NA2 decreased significantly in abundance and at later time points, its two adjacent peaks (peaks 3 and 4) also decreased significantly in abundance (Fig. 5) (for  $P$  values, see Table 4).

CBDL mice were characterized by the significantly increased abundance of peaks 1, 6, and 7 (Table 4, Fig. 5) in the glycosylation pattern. Peak 1/NGA2F increased significantly already in the first week after CBDL and peaks 6 and 7/NA2F after 3 wk CBDL. Fucosidase digest revealed that these are all fucosylated glycans. CBDL mice also exclusively had a significant lowered abundance of peak 8 and, in common with CCl<sub>4</sub>, a decrease in abundance of peaks 4 and 5/NA2. CBDL mice also showed a significantly elevated peak height of peaks 9, 10, and 11 in agreement with CCl<sub>4</sub> mice. Peak 11 was significantly increased in abundance from an early stage on, but peaks 9 and 10 only in the cirrhotic stage (for  $P$  values, see Table 4).

As a consequence of the increase of fucosylated glycans in CBDL mice, the FI was an excellent marker to distinguish CCl<sub>4</sub> and CBDL mice. This index barely rose above 20% in CCl<sub>4</sub> and control mice, whereas it reaches 30 to 40% in CBDL mice ( $P < 0.001$  in F2, F3, and F4 stages) (Fig. 6). We also analyzed one pure bile mouse sample, and the FI was comparable to a serum sample of a CBDL mouse (42%).

*IgG and SAA concentration in mouse models of chronic liver disease.* Six mice were evaluated at every time point in the CCl<sub>4</sub> and CBDL group and two mice at every time point in the control mice. Both fibrotic mouse models showed a doubling of the IgG concentration in the progression of fibrosis to cirrhosis (from  $\sim 0.5$  mg/ml to  $\sim 1.3$  mg/ml). Apart from an early strong increase in serum amyloid A (SAA) concentration (a mean of 700  $\mu$ g/ml after 3 wk, in the CCl<sub>4</sub> model and a mean of 320  $\mu$ g/ml after 1 wk in the CBDL model) no significant difference in SAA concentration between the CCl<sub>4</sub>, CBDL, and control mice could be observed (baseline value was  $\sim 50$   $\mu$ g/ml).

## DISCUSSION

Alteration of total serum *N*-glycans is indicative for chronic necroinflammatory diseases, and especially in liver diseases it shows great potential as biomarker (3, 15, 21). Our group has made important contributions to this research with a follow-up

Table 4. Mean relative peak height (in %) of the different peaks in the mouse electropherogram-treated control

Group and Time point	Peak 1	Peak 2	Peak 3	Peak 4	Peak 5	Peak 6	Peak 7	Peak 8	Peak 9	Peak 10	Peak 11
<b>CCl<sub>4</sub>-Saline</b>											
Week 1	0.7–0.7	1.4–1.7	1.3–1.8	10–11.4	46.2–47.7	2.6–3.3	13.6–15.2	3.9–3.5	15.3–11.2‡	3–2.7	1.6–1‡
Week 3	0.7–0.8	1.1–1.3	3–2	12.9–12.6	45.4–49.3*	2.6–2.9	12.2–12.7	4.5–3.8	13.8–11.6*	2.4–2.2	1.3–1*
Week 6	1.4–1.4	1.3–1.2	0.7–2.3‡	6.9–12.7‡	49.2–48.3	2.5–2.9	16.2–12.4	2.3–4	15.2–11.7‡	3–2‡	1.4–1*
Week 10	2–2.9	1.2–1.4	0.8–1.6‡	9.3–12.3‡	45.9–48.8	3.2–3.4	14.6–13.2	3–3.2	15.9–10.7‡	2.7–1.8‡	1.5–0.8‡
Week 16	2.7–2.3	1.3–1.6*	0.8–1.1‡	9.2–12.3‡	44.6–50.9‡	2.2–2.5	14.8–13.7	3–2.6	17.2–10.5‡	2.5–1.8‡	1.7–0.8‡
<b>CBDL-Sham</b>											
Week 1	0.9–0.6*	0.9–1.1	4.6–3.7	16.3–15.2	40.9–40.5	3.4–3.3	14–12	4.5–5.9*	11.1–14*	1.7–2.6	1.7–1.4*
Week 3	5.8–1.7‡	1.8–2.5	2.1–2.4	10.1–12.8‡	40–46.6‡	3.6–2.8‡	20.5–13‡	2.5–4‡	9.8–11*	1.9–2.1	2–1‡
Week 4	3.3–2.3*	1.3–1.2	2–1.3	10–10.5	43–51.2‡	3.6–2.9‡	20.2–14.3‡	2.5–2.8*	9.9–11.2	1.9–2	1.7–0.7‡
Week 5	6.5–2.6‡	1.5–1.6	1.7–1.6	9.2–10.6	38.7–47.4‡	3.2–3*	21.3–15.6‡	2.5–3.2*	11.1–11.2	2.4–2.5	1.7–0.9‡
Week 6	3.7–1‡	1.7–1.2	1.3–1.5	10.5–14.9‡	41–48.9‡	3.8–3.5*	20.9–13.2‡	2.5–3.2‡	11.1–9.9*	2.4–2‡	2.1–0.8‡
<b>PPVL-Sham</b>											
Week 1	1.1–1.5	1.2–1.1	4.1–3.3	16–14.8	39–44.4‡	4.6–3.3*	15.2–12.8	4.7–4.4	10.5–11.3	2.6–2.1	1.1–1
Week 2	1.1–1.6	1.2–1.3	1.8–2.2	13.1–14	48.7–49.8	3.5–4	12.3–13.9	3.6–3.5	12–9.2‡	1.7–1.9	1–0.8

\* $P < 0.05$ ; † $P < 0.01$ ; ‡ $P < 0.001$ .

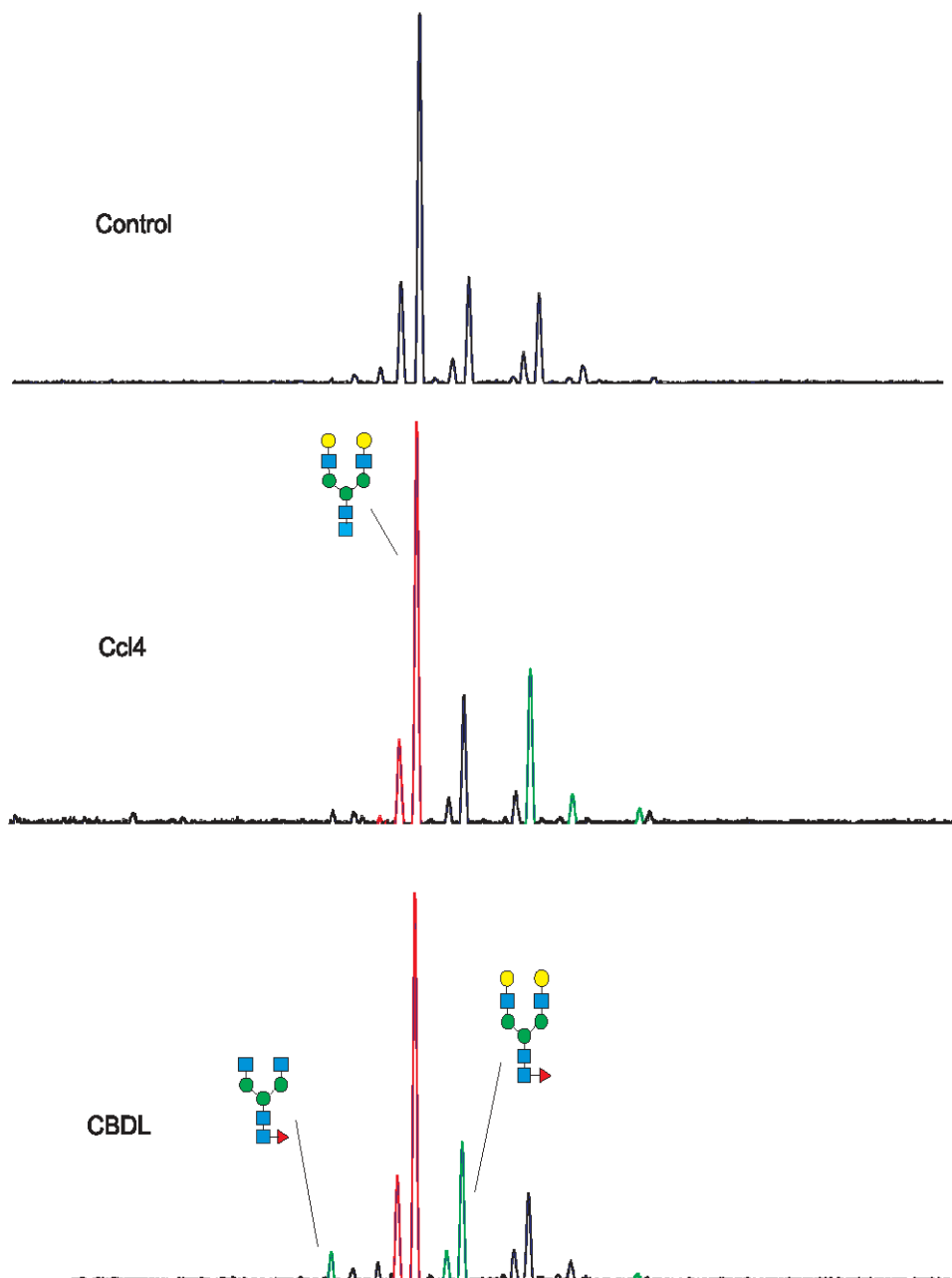


Fig. 5. Comparison of a typical *N*-glycan profile of control, CCl<sub>4</sub> (F2–F4), and CBDL (F2–F4) mice. The peaks that significantly decrease in abundance compared with control mice are in red and those that significantly increase in abundance compared with control mice are in green.

tool for fibrosis (21) and noninvasive tests for cirrhosis and HCC (3, 15).

Alcoholic patients were shown to have a mean value for the GlycoCirrhoTest that was considerably higher than in other liver patients. This could be due to the micronodular fibrotic nature of the liver of alcoholic patients. More nodules correspond to more elevated GnT-III induction in the cirrhotic liver (3). The mean value of NASH patients was also quite high, but this was due to one outlier in a limited number of samples. Nevertheless, the mean value of the cirrhotic patients in all etiologies was significantly and considerably higher than the mean value of the control group. Chen et al. (4) stated that NASH patients had no change in expression of GnT-III and GnT-V and these patients could therefore not be diagnosed with the GlycoCirrhoTest. However, we found that three of our four cirrhotic NASH patients had a high value for the GlycoCirrhoTest, well over the cutoff value for cirrhosis, which implies strong upregulation of GnT-III and concomitant downregulation of GnT-V (Fig. 2).

UGS of IgG in the progression of fibrosis is the feature on which the GlycoFibrotest is mainly based. This article shows that there was no significantly different quantitative alteration in undergalactosylation in the cirrhotic as well as in the noncirrhotic population across all etiologies (Fig. 2). Remarkable was the strong increase of UGS score in cirrhotic NASH patients compared with the noncirrhotic group. The overall higher mean value of UGS in the cirrhotic stage (with the exception of HBV) can be attributed to the linear increase of the mean UGS state of IgG that reaches a maximum in end-stage liver disease (21) as exemplified in HCV patients.

An important finding was that an elevation of total bilirubin is strongly associated with a consequent increase of the FI. In a multiple regression model, a significant correlation was found with the (logarithmically transformed) bile acid concentration and AP. These biochemical variables are markers for liver damage, but specifically for cholestasis.

Increase in fucosylation has especially been linked with HCC and an upregulation of fucosyltransferases in hepatoma

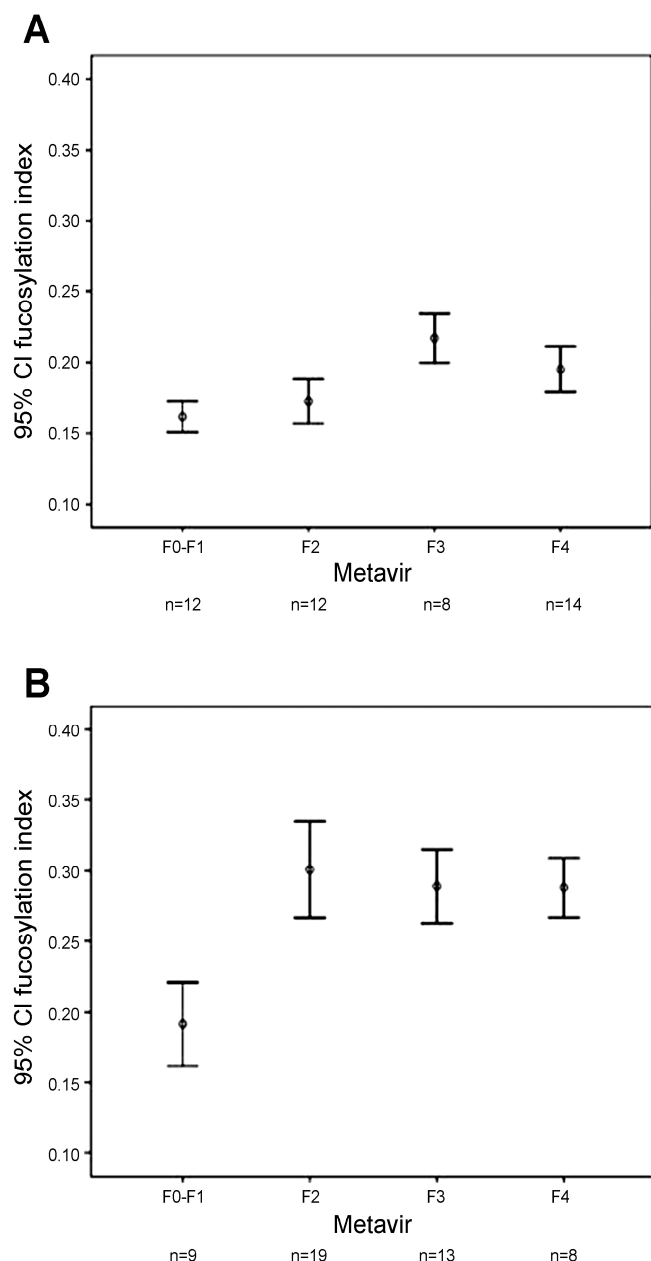


Fig. 6. Error bars represent the evolution of the fucosylation index (FI) in the progression toward cirrhosis. Starting from a F2 stage, the FI is clearly higher in the CBDL mice (B) compared with the CCl<sub>4</sub> mice (A).

tissue was suggested to be the driving force after this increased fucosylation of serum proteins (5, 18). An alternative hypothesis in non-HCC cholestatic patients reasons that  $\alpha$ 1–6 fucosylation of *N*-linked glycans within polarized hepatocytes directs glycoproteins to the basolateral surface and into bile. As a consequence,  $\alpha$ 1–6 fucosylated glycoforms are normally rare in the blood and are enriched in the bile. Thus, if liver cells become depolarized, the  $\alpha$ 1–6 fucosylated glycoforms rise in abundance in the blood (16). The data collected in this study strongly favor the latter hypothesis. Moreover, the presence of high concentrations of bile acids in the serum samples with high FI is a strong confirmation of our data.

In the setting of cholestasis, the basolateral path to the bile ducts is blocked. Therefore, we hypothesize that there is an accumulation of  $\alpha$ 1–6 fucosylated glycoproteins in the hepatocyte. The only exit for these glycoproteins is apically to the space of Disse and eventually to the systemic circulation. In

conclusion,  $\alpha$ 1–6 fucosylation seems to be not a HCC marker, but a marker for hyperbilirubinemia.

Our group has previously shown that  $\alpha$ 1–3 fucose significantly increases in HCC patients (15). However, we could not reproduce this upregulation of  $\alpha$ 1–3 fucose, possibly because we used a mixed HCC population of different etiologies in contrast to the original study that was uniquely performed in HBV patients (15). The  $\alpha$ 1–3 fucose did not differ significantly between patients with normal and elevated bilirubin level, in both fibrosis/cirrhosis and HCC patients.

The mouse models allowed us to investigate some variables independently from each other. The influence of PHT was investigated with PPVL mice. No biologically relevant changes in *N*-glycosylation were observed in the PPVL mice, indicating that PHT does not contribute to the alteration of *N*-glycosylation in liver diseases.

The effect of elevated total bilirubin levels on *N*-glycosylation can be studied with CBDL mice. In analogy with liver patients that had a strong increase in total bilirubin, CBDL mice had a strong increased abundance of all  $\alpha$ 1–6 fucosylated glycans. An additional advantage of mouse models is the easy follow-up of histology and there is also less bias in the histological analysis of the mouse liver. In this respect, we were able to observe that the increase of  $\alpha$ 1–6 fucosylation is an early event in the cholestatic development (Table 3).

CCl<sub>4</sub> mice did not show an increase in total bilirubin level and these mice therefore did not have an increased FI. These mice develop a micronodular fibrosis/cirrhosis with characteristics of an alcoholic cirrhosis, and it is also considered as a model with an important amount of inflammation. However, inflammation did not have an influence on the *N*-glycosylation patterns in these mouse models. Apart from an early peak in SAA concentration, no significant difference was observed and there was no such correlation with the *N*-glycosylation patterns of the mouse models. The hallmarks of CCl<sub>4</sub> mice are an increase of peaks 9, 10, and 11, probably all multiantennary glycans. Again, this occurred very early in the fibrotic development and was not unique to CCl<sub>4</sub> mice because also CBDL mice had a significant increased abundance of these three glycans, albeit later in the fibrotic development. Other common changes with CBDL were a significant decrease in abundance of peak 5/NA2 and its adjacent peak 4.

Some *N*-glycosylation aspects of human liver patients are difficult to study in mouse models. Even if UGS would be present in mouse models, it would be much less pronounced than in humans because the IgG concentration in serum is inherently low at 0.5 to 1.5 mg/dl. Additionally, in mice, glycan modifications that do not exist in humans, especially  $\alpha$ -galactosylation, are present (12). Therefore, the baseline *N*-glycosylation pattern of a control C57Bl/6 mouse will be different than the baseline *N*-glycosylation pattern of a healthy human control (Fig. 1). Moreover, our study strongly suggests that the spectrum of *N*-glycosylation alterations in liver disease is different between mice and humans. In summary, caution is offered when extrapolating mouse data.

In conclusion, we have shown that the GlycoFibroTest and GlycoCirrhoTest can be used in all etiologies as universal noninvasive tests. An important finding was that liver patients with elevated total bilirubin levels have a significant increase of glycans modified with  $\alpha$ 1–6 fucose. When studying fucosylation, a distinction has to be made between an increase of

$\alpha$ 1–6 fucose, which is a marker for hyperbilirubinemia, and an increase of  $\alpha$ 1–3 fucose, which is a marker for HCC, the latter most likely exclusively in HBV patients. Future studies on biomarker discovery based on *N*-glycosylation will have to take into account that an increase of total bilirubin is attended with an increase of  $\alpha$ 1–6 fucosylation in serum.

#### ACKNOWLEDGMENTS

The authors thanks Julien Dupont, Kim Olievier, and Annelies Van Hecke for expert technical assistance and Dieter Vanderschaeghe for editing the manuscript and for helpful discussions.

#### DISCLOSURES

No conflicts of interest are declared by the author(s).

#### REFERENCES

1. Al Knawy B, Shiffman M. Percutaneous liver biopsy in clinical practice. *Liver Int* 27: 1166–1173, 2007.
2. Bedossa P, Poynard T. An algorithm for the grading of activity in chronic hepatitis C. The METAVIR Cooperative Study Group. *Hepatology* 24: 289–293, 1996.
3. Callewaert N, Van Vlierberghe H, Van Hecke A, Laroy W, Delanghe J, Contreras R. Noninvasive diagnosis of liver cirrhosis using DNA sequencer-based total serum protein glycomics. *Nat Med* 10: 429–434, 2004.
4. Chen C, Schmilovitz-Weiss H, Liu XE, Pappo O, Halpern M, Sulkes J, Braun M, Cohen M, Barak N, Tur-Kaspa R, Vanhooren V, Van Vlierberghe H, Libert C, Contreras R, Ben-Ari Z. Serum protein *N*-glycans profiling for the discovery of potential biomarkers for nonalcoholic steatohepatitis. *J Proteome Res* 8: 463–470, 2009.
5. Chen G, Guan M, Su B, Lu Y. mRNA expression of three glycosyltransferases in human hepatoma tissues. *Clin Chim Acta* 313: 77–80, 2001.
6. Comunale MA, Lowman M, Long RE, Krakover J, Philip R, Seholzer S, Evans AA, Hann HW, Block TM, Mehta AS. Proteomic analysis of serum associated fucosylated glycoproteins in the development of primary hepatocellular carcinoma. *J Proteome Res* 5: 308–315, 2006.
7. Fernandez M, Vizzutti F, Garcia-Pagan J, Rodes J, Bosch J. Anti-VEGF Receptor-2 monoclonal antibody prevents portal-systemic collateral vessel formation in portal hypertensive mice. *Gastroenterology* 126: 886–894, 2004.
8. Geerts AM, Vanheule E, Praet M, Van Vlierberghe H, De Vos M, Colle I. Comparison of three research models of portal hypertension in mice: macroscopic, histological and portal pressure evaluation. *Int J Exp Pathol* 89: 251–263, 2008.
9. Gilmore IT, Burroughs A, Murray-Lyon IM, Williams R, Jenkins D, Hopkins A. Indications, methods, and outcomes of percutaneous liver biopsy in England and Wales: an audit by the British Society of Gastroenterology and the Royal College of Physicians of London. *Gut* 36: 437–441, 1995.
10. Grant A, Neuberger J. Guidelines on the use of liver biopsy in clinical practice. *Gut* 45: S1–S11, 1999.
11. Janakat S, Al-Merie H. Optimization of the dose and route of injection, and characterization of the time course of carbo tetrachloride-induced hepatotoxicity in the rat. *J Pharmacol Toxicol Methods* 48: 41–44, 2002.
12. Koike C, Uddin M, Wildman DE, Gray EA, Trucco M, Starzl TE, Goodman M. Functionally important glycosyltransferase gain and loss during catarrhine primate emergence. *Proc Natl Acad Sci USA* 104: 559–564, 2007.
13. Kountouras J, Billing BH, Scheuer PJ. Prolonged bile duct obstruction: a new experimental model for cirrhosis in rat. *Br J Exp Pathol* 65: 305–311, 1984.
14. Laroy W, Contreras R, Callewaert N. Glycome mapping on DNA sequencing equipment. *Nat Protoc* 1: 397–405, 2006.
15. Liu XE, Desmyter L, Gao CF, Laroy W, Dewaele S, Vanhooren V, Wang L, Zhuang H, Callewaert N, Libert C, Contreras R, Chen C. *N*-glycomic changes in hepatocellular carcinoma patients with liver cirrhosis induced by hepatitis B virus. *Hepatology* 46: 1426–1435, 2007.
16. Nakagawa T, Uozumi N, Nakano M, Mizuno-Horikawa Y, Okuyama N, Taguchi T, Gu J, Kondo A, Taniguchi N, Miyoshi E. Fucosylation of *N*-glycans regulates the secretion of hepatic glycoproteins into bile ducts. *J Biol Chem* 281: 29797–29806, 2006.
17. Noda K, Miyoshi E, Uozumi N, Yanagidani S, Ikeda Y, Gao C, Suzuki K, Yoshihara H, Yoshikawa K, Kawano K, Hayashi N, Hori M, Taniguchi N. Gene expression of alpha 1–6 fucosyltransferase in human hepatoma tissues: a possible implication for increased fucosylation of alpha-fetoprotein. *Hepatology* 28: 944–952, 1998.
18. Ohno M, Nishikawa A, Koketsu M, Taga H, Endo Y, Hada T, Higashino K, Taniguchi N. Enzymatic basis of sugar structures of alpha-fetoprotein in hepatoma and hepatoblastoma cell lines: correlation with activities of alpha 1–6 fucosyltransferase and N-acetylglucosaminyltransferases III and V. *Int J Cancer* 51: 315–317, 1992.
19. Piccinino F, Sagnelli E, Pasquale G, Giusti G. Complications following percutaneous liver biopsy: a multicenter retrospective study on 68,276 biopsies. *J Hepatol* 2: 165–173, 1986.
20. Van Beneden K, Coppieters K, Laroy W, De Keyser F, Hoffman IE, Van den Bosch F, Vander Cruyssen B, Drennan M, Jacques P, Rottiers P, Verbruggen G, Contreras R, Callewaert N, Elewaut D. Reversible changes in serum immunoglobulin galactosylation during the immune response and treatment of inflammatory autoimmune arthritis. *Ann Rheum Dis* 68: 1360–1365, 2009.
21. Vanderschaeghe D, Laroy W, Sablon E, Halfon P, Van Hecke A, Delanghe J, Callewaert N. GlycoFibroTest is a highly performant liver fibrosis biomarker derived from DNA sequencer-based serum protein glycomics. *Mol Cell Proteomics* 8: 986–994, 2009.
22. Wallace K, Burt AD, Wright MC. Liver fibrosis. *Biochem J* 411: 1–18, 2008.

# Chapter 3.2

***“Alterations of serum protein N-glycosylation in two mouse models of chronic liver disease are hepatocyte and not B cell driven”***

**Bram Blomme**<sup>1</sup>, Christophe Van Steenkiste<sup>1</sup>, Paolo Grassi<sup>2</sup>, Stuart M Haslam<sup>2</sup>, Anne Dell<sup>2</sup>, Nico Callewaert<sup>3,4</sup>, Hans Van Vlierberghe<sup>1</sup>

<sup>1</sup>Department of Hepatology and Gastroenterology, Ghent University Hospital, Ghent, Belgium

<sup>2</sup>Division of Molecular Biosciences, Faculty of Natural Sciences, Imperial College London, London SW7 2AZ, UK

<sup>3</sup>Unit for Molecular Glycobiology, Department for Molecular Biomedical Research, VIB, Ghent University, Ghent, Belgium

<sup>4</sup>Department of Biochemistry, Physiology and Microbiology, Ghent University, Ghent, Belgium

**Accepted for publication in American Journal of Physiology: Gastrointestinal and Liver Physiology**

## Abstract

**INTRODUCTION:** *N*-glycosylation of immunoglobulin G (IgG) has an important impact on the modification of the total serum *N*-glycome in chronic liver patients. Our aim was to determine the role and magnitude of the alterations in which hepatocytes and B cells are involved in two mouse models of chronic liver disease.

**MATERIALS AND METHODS:** Common bile duct ligation (CBDL) and subcutaneous injections with CCl<sub>4</sub> were induced in B cell deficient and wild type (WT) mice. IgG depletion was performed with beads covered with protein A/G and the depletions were evaluated by SDS-PAGE and Western blot analysis. *N*-glycan analysis was performed by improved DSA-FACE technology. Structural analysis of the mouse serum *N*-glycans was performed by exoglycosidase digests and MALDI-TOF mass spectrometry of permethylated glycans.

**RESULTS:** The alterations seen in B cell deficient mice closely resembled the alterations in WT mice, both in the CBDL and the CCl<sub>4</sub> model. *N*-glycan analysis of the IgG-fraction in both mouse models revealed different changes compared to humans. Overall, the impact of IgG glycosylation on total serum glycosylation was marginal. Interestingly, the amount of fibrosis present in CBDL B cell deficient mice was significantly increased compared to CBDL WT mice, whereas the opposite was true for the CCl<sub>4</sub> model as determined by sirius red staining. However, this had no major effect on the alteration of *N*-glycosylation of serum proteins.

**DISCUSSION:** Alterations of total serum *N*-glycome in mouse models of chronic liver disease are hepatocyte-driven. Undergalactosylation of IgG is not present in mouse models of chronic liver disease.



## 1. Introduction

In humans, immunoglobulin G (IgG) is the most abundant glycoprotein in serum. IgG molecules consist of two Fab and one Fc fragment, which are linked through a flexible hinge region [9]. *N*-glycosylation is present in the CH<sub>2</sub> domain of the Fc fragment and about 30% of the circulating human IgG is also glycosylated in the Fab region. The majority of the Fc glycans are complex biantennary structures, multi-antennary structures are very rare on IgG [13]. This is in contrast to serum proteins synthesized by hepatocytes of which 5% to 15% of the glycans are multi-antennary structures (own data). The relative proportions of the other glycans on IgG are also completely different compared to glycans of liver-produced proteins. Especially agalactosylated glycans, that lack one or both galactoses in the glycan structure, are characteristic for IgG glycosylation and are rarely found on liver-produced proteins [29].

Alteration of *N*-glycosylation of serum proteins have been extensively studied by our group in various pathological states of the liver (GlycoFibroTest, GlycoCirrhoTest and GlycoHCCTest – Table 1). In humans, these glycomic changes can be subdivided in alterations caused by B cells and alterations driven by the liver.

**Table 1: *N*-glycome derived biomarkers in various pathological states of the liver. The combination of these three markers is collectively called the GlycoHepatoTest.**

Marker name	Marker
GlycoFibroTest*	$\log \frac{[NGA2FB]}{[NA3]}$
GlycoCirrhoTest <sup>†</sup>	$\log \frac{[NA2FB]}{[NA3]}$
GlycoHCCTest <sup>‡</sup>	$\log \frac{[NA3F]}{[NA2FB]}$

\*Vanderschaeghe et al. 2009 [29]; <sup>†</sup>Callewaert et al. 2004 [3]; <sup>‡</sup>Liu et al. 2007 [18]

The GlycoFibroTest, that can be used as a follow-up tool for liver fibrosis patients, is mainly determined by IgG *N*-glycosylation. NGA2FB, an agalacto glycan, is present in the nominator. There is a linear increase of agalactosylated glycans (NGA2F and NGA2FB) on IgG in ascending Metavir-stage [1] and we previously found that the correlation of NGA2FB with fibrosis was better than with NGA2F [29]. This result indicates that there is also an increased *N*-acetylglucosaminyltransferase III (GnT-III) activity in B cells during liver fibrosis/cirrhosis and not just only in regenerative liver nodules. This observation was confirmed by Klein *et al* [11, 12].

NA3 is present in the denominator of both the GlycoFibroTest and GlycoCirrhoTest. Biosynthesis of glycoconjugates necessitates the generation of activated monosaccharides. These activated monosaccharides take the form of nucleotide-sugars (e.g. UDP-GlcNAc). The sugar nucleotides are generated starting from non-activated monosaccharides that are either directly taken up from the extracellular environment or generated by the cell's metabolism from other monosaccharides [6]. In hepatocytes, the latter pathway is not present, and the *N*-acetylglucosamine (GlcNAc) formed in these cells comes from lysosomal degradation of plasma glycoproteins that were taken up from the systemic circulation by

surface receptors. This GlcNAc is then reused for the biosynthesis of the *N*-glycans of glycoproteins. As fibrosis progresses, collagen is deposited in the space of Disse and progressively less receptor-mediated uptake by the hepatocyte will be possible. Moreover, NA3 is formed by the GnT-V enzyme and it is known that the  $K_m$  values of GnT-V are much higher compared to those of other GlcNAc transferases [26]. Therefore, if there is a limited supply of GlcNAc, other GlcNAc transferases will consume the introduced GlcNAc more readily and there will be less GlcNAc available for GnT-V to synthesize NA3. These two factors combined, result in a lower NA3 production in ascending Metavir stage.

The GlycoCirrhoTest and GlycoHCCTest are diagnostic tests to respectively distinguish cirrhotic patients from non-cirrhotic patients and patients with hepatocellular carcinoma (HCC) from cirrhotic patients [3,18]. These tests are determined by the competition of the GnT-III and the GnT-V enzyme for the same substrate (tri-mannose core). In cirrhosis, there is an upregulation of GnT-III in regenerative nodules and this enzyme is responsible for the formation of bisecting GlcNAc modified glycans. In this way, an increased abundance of these glycans on liver-produced proteins is observed in the serum of cirrhotic patients. However, it was recently shown that these bisecting glycans were particularly present on IgG and IgA in cirrhotic patients indicating an also strong B cell involvement [11]. In HCC, the opposite occurs. There is an upregulation of the GnT-V enzyme in tumor cells so that the balance is shifted towards more multi-antennary glycans on liver-produced proteins. Next to GnT-V,  $\alpha$ 1-3 fucosyltransferase is also necessary to produce NA3Fb that is significantly increased in HCC-patients. It has previously been shown that the branching fucose modification, that is produced by this enzyme, is strongly associated with HCC [27]. As indicated earlier, B cell involvement in the GlycoHCCTest can also not be excluded because of the presence of NA2FB in the denominator. In summary, B cells are the dominant factor in the alteration of protein glycosylation in human liver patients.

*N*-glycosylation of serum proteins is somewhat species-specific. On IgGs, the major difference with humans is that *N*-glycans on mouse IgGs terminate with *N*-glycolylneuraminic acid instead of *N*-acetylneuraminic acid [24]. On liver-produced proteins, the major difference with humans is the presence of  $\alpha$ 1-3 galactosylated glycoforms. The enzyme that produces these glycoforms is been lost in the evolution towards the human lineage [14]. Furthermore, differences in expression of certain glycosyltransferases (for instance *Mgat3*) also exist between mice and humans. The glycosylation of mice IgG is barely described in literature and the published papers do not indicate the presence of bisected *N*-acetylglucosamine at the difference of human IgG *N*-glycans [20, 21].

We previously did a glycomic research into the alterations that occurred in two mouse models of chronic liver disease, common bile duct ligation (CBDL) and chronic injections with CCl<sub>4</sub> [2]. In summary, we saw an increased abundance of core-fucosylated glycans in CBDL mice and an increased abundance of glycans that are located at the end of the electropherogram in CCl<sub>4</sub> mice, most likely all multi-antennary glycans. Our aim was to elucidate the role and magnitude that *N*-glycosylation of liver-produced proteins plays in these alterations by using B cell deficient mice. In addition, IgGs were captured from the serum of wild type (WT) CBDL and CCl<sub>4</sub> mice and the *N*-glycan fraction thereof was also determined.

## 2. Materials and Methods

### 2.1 mouse models of chronic liver disease

Male B10.129S2(B6)-*Igh-6*<sup>tm1Cgn</sup>/J mice ( $\mu$ MT-mice) were purchased from Jackson Laboratories (Bar Harbor, Maine, USA). B cell development is arrested in these mice at the stage of pre-B cell maturation by a deletion in the heavy chain region of IgM. As a consequence, these mice do not have mature B cells in their blood [10]. This implies that isotype switching from IgM to IgG is not possible and no IgG is present in the serum of these mice. C57Bl/10 control mice were purchased from Harlan Laboratories (Horst, The Netherlands). B cell deficient mice were housed in individually ventilated cages, whereas control mice were kept under normal housing conditions. Both mouse groups underwent a 12 hours controlled light/dark cycle at a constant temperature and humidity. The Ethical Committee of experimental animals at the faculty of Medicine and Health Sciences, Ghent University, Belgium, approved the protocols.

CBDL, CCl<sub>4</sub> and their respective controls were induced in B cell deficient and control mice. The surgical procedure for CBDL was performed under sterile conditions in a laminar flow cabinet. Under isoflurane inhalation, a midline abdominal incision was made and the common bile duct was isolated. The common bile duct was occluded with a double ligature of a non-resorbable suture (silk cut 5-0). The first ligature was made below the junction of the hepatic ducts and the second was made above the entrance of the pancreatic duct. The common bile duct was sectioned between the two ligatures [15]. Mice were sacrificed 6 weeks after CBDL (n=8). In wild type mice, this time point correlates with the cirrhotic stage. Sham-operated mice were used as control group and they were also sacrificed after 6 weeks (n=10) [5].

The second mouse model was induced by chronic subcutaneous (SC) administration of carbon tetrachloride (CCl<sub>4</sub>) (Merck, Darmstadt, Germany) twice weekly (1:1 dissolved in olive oil; 1 ml/kg) [7]. 5% alcohol was added to drinking water. Mice were sacrificed after 16 weeks (n=8). Again, this correlates with the cirrhotic stage in wild type mice as validated in our lab [5]. Control mice received a physiological saline solution (1 ml/kg) subcutaneously. They were sacrificed after 16 weeks (n=10). No alcohol was added to the drinking water.

Body, liver and spleen weight were determined in every mice. Liver and spleen weight were expressed as percentage of body weight (relative liver and spleen weight). Blood samples were taken by placing a catheter in the arteria carotis. These samples were centrifuged at 10 000 rpm for 10 minutes. 200  $\mu$ l serum was taken off the clot for the determination of liver function tests (alanine aminotransferase activity (ALT), aspartate aminotransferase activity (AST) and total bilirubin (Tbiln)) in B cell deficient and control mice. These were analyzed using routine photometric tests on a Hitachi 747 analyser (Diagnostica, Boehringer Mannheim, Ingelheim, Germany). The remaining serum volume was used for N-glycan analysis in B cell deficient and WT mice and for IgG depletion in WT mice. Finally, serum IgG concentration was determined in 4 samples of every B cell deficient group and in 5 samples of every WT group (CBDL, CCl<sub>4</sub> and their respective controls) by an Enzyme-Linked Immuno Sorbant Assay (ELISA) (Immunology Consultants Laboratory Inc – Newburg, OR, USA). The ELISA was run according to manufacturer's instructions and all analyses were done in duplo.

A liver section of about 1 cm in diameter of the left, right and middle lobe was taken for histological examination. Livers were fixed in 4% phosphate buffered formaldehyde solution (Sigma, St. Louis, MO, USA) and embedded in paraffin. From all tissue samples, 5  $\mu$ m tissue sections were cut with a Leica RM 2145 sliding microtome (Leica Microsystems, Nussloch, Germany). The liver tissues sections were stained with 0.1% picosirius red. The amount of fibrosis in the liver correlates with the amount of redness present on a liver tissue section. At an objective magnification of 20x, three regions were randomly chosen per liver tissue section and the amount of redness was electronically quantified using the imaging system Cell<sup>^</sup>D (Olympus, Hamburg, Germany). The mean value of these three regions was taken as a numeric description of the amount of fibrosis.

## 2.2 IgG depletion

Serum samples of wild type mice were depleted using beads covered with protein A/G (Thermo Scientific, Waltham, MA, USA). 100  $\mu$ l serum was diluted with 100  $\mu$ l binding buffer and subsequently incubated with 35  $\mu$ l beads for 1 hour. The mixture was transferred to a 96-well filter plate and centrifuged at 1000g for 15 seconds. The IgG depleted eluate was captured in a microtiterplate. Subsequently, after five wash steps with binding buffer, pure IgG was eluted from the beads with 0.1M glycine pH 2 in the 96-well filter plate. After centrifugation at 1000g for 15 seconds, the eluate is neutralized with 1M Tris pH 8.8. IgG-depleted serum and the IgG fraction were stored at -20 °C for N-glycan analysis.

## 2.3 Proteomic analysis: SDS-PAGE and WB analysis

Serum and IgG-depleted samples were diluted 1/20, the IgG fraction was processed undiluted. The samples were mixed with LDS sample buffer (NuPage; Invitrogen, Seattle, WA) and a sample reducing agent (dithiothreitol, Invitrogen). The proteins were denatured by heating at 70°C for 10 minutes, subsequently loaded into 10% Bis-Tris Gel (Invitrogen) and separated at a voltage of 170V for 1 hour. Finally, the gels were stained with Coomassie blue (Sigma-Aldrich, Bornem, Belgium) for 1h and destained twice for 1h and overnight.

For the Western blot analysis, the proteins were transferred to a nitrocellulose membrane (GE Healthcare, Little Chalfont, Buckinghamshire, United Kingdom) after separation in a 10% Bis-Tris Gel. Membranes were blocked in Tris-buffered saline containing 0.05% Tween and 5% non-fat milk. The membranes were incubated for 1 hour with a secondary antibody (anti-IgG, dilution 1:10 000). Horseradish peroxidase (HRP) detection was carried out with an enhanced chemiluminescence substrate (Roche Diagnostics, Indianapolis, IN).

## 2.4 Glycomic analysis

The N-glycans present in 5  $\mu$ l of serum were released from the proteins with peptide N-glycanase F (PNGase F). Subsequently, the glycans are fluorescently labeled and desialylated (*Arthrobacter ureafaciens* sialidase; Roche, Mannheim, Germany). DNA sequencer-assisted fluorophore-assisted capillary electrophoresis (DSA-FACE) technology was used to profile and analyze the labeled glycans. For an elaborate description of the protocol, we refer to [17]. 11 peaks were present in the electropherogram of every native and IgG-depleted mouse serum sample and 9 peaks were present in the electropherogram of every mouse IgG sample. The peak height of every peak was quantified to obtain a

numerical description of the profiles. These data were analyzed with SPSS 16.0 software (SPSS, Chicago, IL, USA). The peak heights were normalized to the total intensity of the measured peaks (represented as a percentage of the total peak height).

Structural analysis of APTS-labelled serum *N*-glycans was performed by digesting appropriate amounts with exoglycosidases: *Streptococcus pneumoniae*  $\beta$ -1,4-galactosidase, jack bean  $\beta$ -*N*-acetylhexosaminidase, bovine kidney  $\alpha$ -fucosidase (all from Prozyme, San Leandro, CA, USA). DSA-FACE was used to analyze the digestion products.

## 2.5 MALDI-TOF mass spectrometry

### 2.5.1 *Derivatisation of samples*

The released *N*-glycans were purified by chromatography on a Sep-Pak C18 cartridge (Waters Corp. Milford, MA) to separate the released, hydrophilic *N*-glycans from the remaining hydrophobic compounds. The Sep-Pak columns were conditioned by eluting sequentially with 5 ml methanol, 5 ml dilute acetic acid, 5 ml propan-1-ol, and 15 ml dilute acetic acid. Dried samples were resuspended in a small volume of dilute acetic acid, loaded onto the column and eluted stepwise with 5 ml of dilute acetic acid as previously described (8). The purified *N*-glycans were subsequently methylated using the sodium hydroxide permethylation procedure as described previously (8).

Briefly, 5-7 NaOH pellets were ground to fine powder and mixed with 2-3 ml anhydrous dimethylsulfoxide (Romil, UK) before adding to each dried sample. This was followed by the addition of 0.6 ml of methyl iodide and vigorous shaking at room temperature for 15 minutes. Permethyated glycans were extracted with chloroform and then purified by using Sep-Pak C18 cartridges.

The cartridges were successively conditioned with methanol (5 ml), water (5 ml), acetonitrile (5 ml) and water (15 ml). Each sample was dissolved in 200  $\mu$ l of methanol:water (1:1) solution before loading onto the cartridges. The cartridges were washed with 5 ml of water and then eluted sequentially with 3 ml of each 15%, 35%, 50% and 75% acetonitrile solution in water.

35%, 50% and 75% acetonitrile/water fractions were collected and then concentrated with a Savant SpeedVac and subsequently lyophilized.

### 2.5.2 *MS and MS/MS analyses of Permethyated Glycans*

MALDI-TOF data were acquired on a Voyager-DE STR mass spectrometer (Applied Biosystems, Foster City, CA) in the reflectron mode with delayed extraction. Permethyated samples were dissolved in 10  $\mu$ l of matrix (20 mg/ml 2,5-dihydroxybenzoic acid in 70% (v/v) aqueous methanol), spotted onto a target plate, and dried under vacuum.

Further MS/MS analyses of peaks observed in the MS spectra were carried out using a 4800 MALDI-TOF/TOF (Applied Biosystems) mass spectrometer in positive ion mode (M + Na)<sup>+</sup>.

The collision energy was set to 1 kV, and argon was used as collision gas. Samples were dissolved in 10  $\mu$ l of methanol, and 1  $\mu$ l was mixed at a 1:1 ratio (v/v) with 2,5-dihydroxybenzoic acid (20 mg/ml in 70% methanol in water) as matrix.

### 2.5.3

### Analysis of MALDI data

The MS and MS/MS data were processed using Data Explorer 4.9 Software (Applied Biosystems, U.K.). The mass spectra were baseline corrected (default settings) and noise filtered (with correction factor of 0.7), and then converted to ASCII format. The processed spectra were then subjected to manual assignment and annotation with the aid of a glycoinformatics tool known as GlycoWorkBench [4].

Peak picking was done manually, and proposed assignments for the selected peaks were based on molecular mass composition of the <sup>12</sup>C isotope together with knowledge of the biosynthetic pathways.

### 2.6

### Statistical analysis

Data analysis was performed with SPSS version 16.0 (SPSS Inc, Chicago, IL). The data were statistically processed with the Mann-Whitney U-test unless stated otherwise. *P* values less than 0.05 (2-tailed probability) were considered as significant.

## 3.

## Results

### 3.1

### Clinical data

Clinical data of the WT and B cell deficient mice in both models of chronic liver diseases are summarized in Table 2.

**Table 2: Clinical data and liver function tests of B cell deficient and wild type mice**

	<b>CBDL 6w <math>\mu</math>MT</b>	<b>Sham 6w <math>\mu</math>MT</b>	<b>CBDL 6w WT</b>	<b>Sham 6w WT</b>
Body weight (g)	19.6 ( $\pm$ 2.0) $\dagger$	28.9 ( $\pm$ 2.1)	19.9 ( $\pm$ 2.3) $\dagger$	26.0 ( $\pm$ 1.1)
Rel Liver weight (%)	10.3 ( $\pm$ 2.2) $\dagger$	4.6 ( $\pm$ 0.4)	9.5 ( $\pm$ 2.8) $\dagger$	5.2 ( $\pm$ 0.4)
Rel Spleen weight (%)	0.45 ( $\pm$ 0.4) $\dagger$	0.12 ( $\pm$ 0.02)	0.46 ( $\pm$ 0.1)	0.4 ( $\pm$ 0.08)
AST (U/l)	500 ( $\pm$ 447) $\dagger$	43 ( $\pm$ 60)	422 ( $\pm$ 201) $\dagger$	136 ( $\pm$ 52)
ALT (U/l)	264 ( $\pm$ 122) $\dagger$	38.7 ( $\pm$ 11.2)	284.3 ( $\pm$ 141.3) $\dagger$	68 ( $\pm$ 44)
TBiln (mg/dl)	17.0 ( $\pm$ 6.6) $\dagger$	0.06 ( $\pm$ 0.02)	22.9 ( $\pm$ 4.6) $\dagger$	0.19 ( $\pm$ 0.03)
	<b>CCl<sub>4</sub> 16w <math>\mu</math>MT</b>	<b>Saline 16w <math>\mu</math>MT</b>	<b>CCl<sub>4</sub> 16w WT</b>	<b>Saline 16w WT</b>
Body weight (g)	28.9 ( $\pm$ 2.8)	32.0 ( $\pm$ 4.2)	30.3 ( $\pm$ 1.8)*	28.0 ( $\pm$ 3.2)
Rel Liver weight (%)	5.9 ( $\pm$ 0.7) $\ddagger$	4.9 ( $\pm$ 0.4)	5.6 ( $\pm$ 0.4) $\ddagger$	5.0 ( $\pm$ 0.4)
Rel Spleen weight (%)	0.12 ( $\pm$ 0.02)	0.11 ( $\pm$ 0.09)	0.37 ( $\pm$ 0.11)	0.31 ( $\pm$ 0.07)
AST (U/l)	73 ( $\pm$ 37)*	70 ( $\pm$ 81)	98 ( $\pm$ 26)*	67 ( $\pm$ 29)
ALT (U/l)	61 ( $\pm$ 28)*	34 ( $\pm$ 20)	88 ( $\pm$ 34) $\ddagger$	28 ( $\pm$ 10)
TBiln (mg/dl)	0.08 ( $\pm$ 0.02)**	0.09 ( $\pm$ 0.03)	0.19 ( $\pm$ 0.02)	0.21 ( $\pm$ 0.05)

Values are mean ( $\pm$ SD); *n*=8 subjects per group. CBDL, common bile duct ligation; CCl<sub>4</sub>, carbon tetrachloride.  $\mu$ MT: B cell deficient; WT: wild type. \**P*<0.05;  $\ddagger$ *P*<0.01;  $\dagger$ *P*<0.001 compared to control mice in the B cell deficient and WT models. •*P*<0.05, \*\**P*<0.001 (B-cell deficient compared to WT).

### 3.2

#### Histological analysis

CBDL B cell deficient mice showed significantly more fibrosis compared to CBDL WT mice. The mean surface of fibrosis was quantified in CBDL B cell deficient mice as  $41955.6 \mu\text{m}^2$  versus  $32687.4 \mu\text{m}^2$  in CBDL WT mice ( $P=0.04$ , two-tailed  $t$ -test). Interestingly, the  $\text{CCl}_4$  model showed the opposite result, there was significantly more fibrosis present in WT mice chronically injected with  $\text{CCl}_4$  compared to B cell deficient mice chronically injected with  $\text{CCl}_4$ . The mean surface of fibrosis was quantified in  $\text{CCl}_4$  B cell deficient mice as  $19327.1 \mu\text{m}^2$  versus  $26481 \mu\text{m}^2$  in  $\text{CCl}_4$  WT mice ( $P=0.004$ , two-tailed  $t$ -test) (Fig. 1).

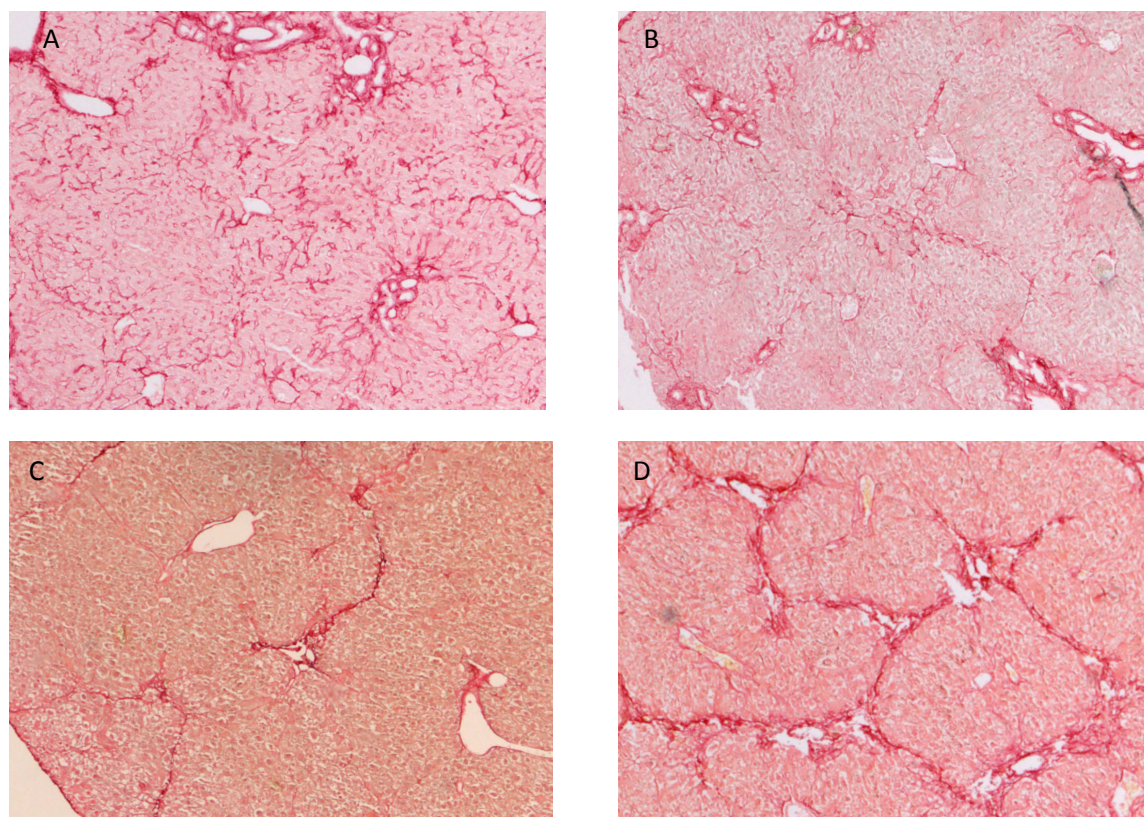


Figure 1. **The B cell deficient state has an opposite effect on the development of fibrosis in CBDL and  $\text{CCl}_4$  mice.** All liver slides were stained with 0.1% picrosirius red. In B cell deficient CBDL mice (A), there was significantly more fibrosis present in the liver compared to CBDL WT mice (B) as determined by sirius red stain values ( $P=0.04$ ). In contrast, in B cell deficient  $\text{CCl}_4$  mice (C), there was significantly less fibrosis present in the liver compared to  $\text{CCl}_4$  WT mice (D) as determined by sirius red stain values ( $P=0.004$ ).

### 3.3

#### IgG concentration in murine serum samples

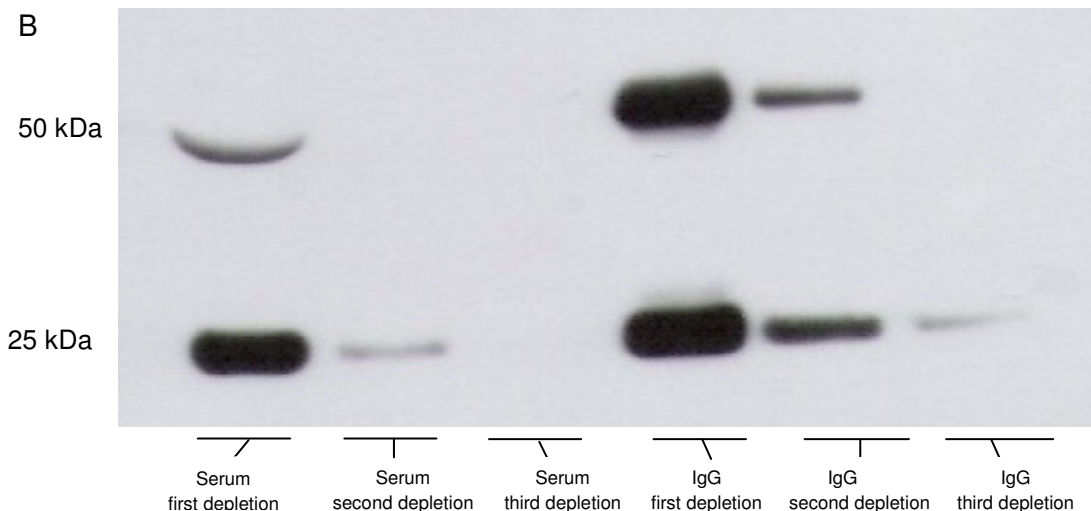
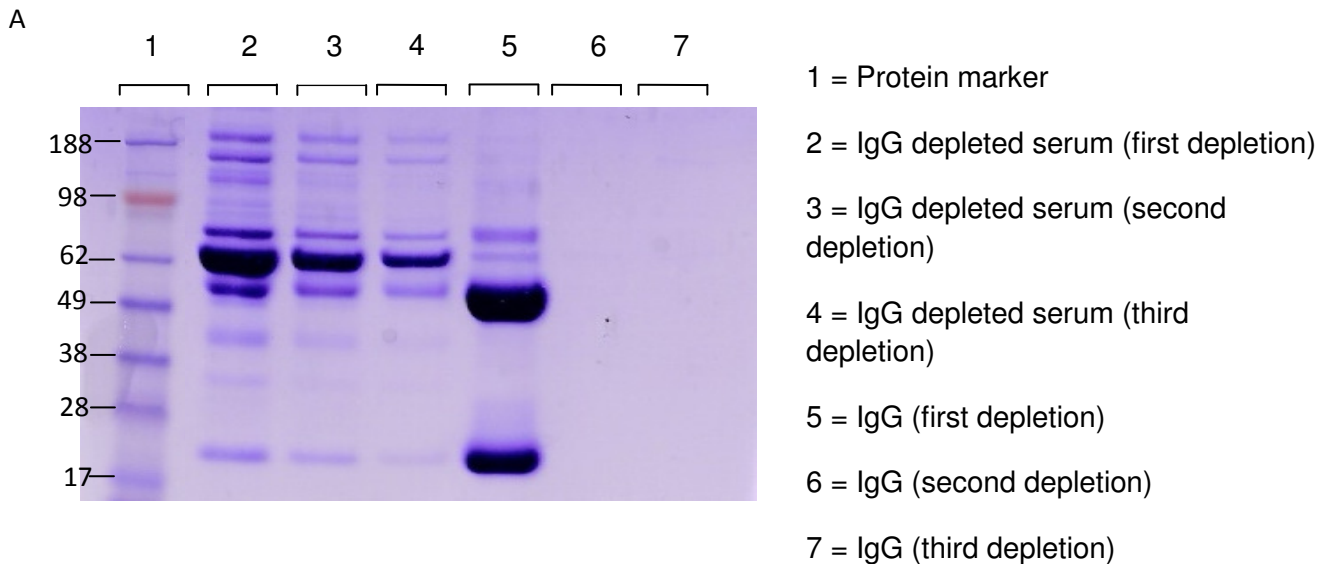
The optical density measured in all B cell deficient mice, irrespective from induced liver damage, rarely exceeded background value. As expected, this indicates that no IgG was present in the serum of B cell deficient mice.

In agreement with our previous study, IgG concentration in WT mice was low in comparison with human serum samples and ranged between 0.5 and 1.5 mg/ml (2). The IgG

concentration was comparable in CBDL, CCl<sub>4</sub> and Sham-operated WT mice (mean value of 0.99 mg/ml ( $\pm$ 0.17), 0.97 mg/ml ( $\pm$ 0.16) and 1.08 mg/ml ( $\pm$ 0.33), respectively), but considerably lower in saline-injected mice (mean value of 0.75 mg/ml ( $\pm$ 0.1)). The relative high IgG concentration in Sham-operated mice can be explained by the invasive character of this procedure and the fact that cholestatic liver damage in mice does not seem to result in further IgG elevation.

### 3.4 Proteomic evaluation of the IgG depletion and the IgG-fraction

Each IgG molecule is a dimer and consists of four polypeptides, two identical heavy (H) chains (MW, 53 kDa) and two identical light (L) chains (MW, 22.5 kDa). The pure IgG-fraction was clearly shown on 1D-PAGE and comparison with native samples revealed that not all IgG was removed from the sample in the first depletion (fig. 2). The definitive answer was given by Western blot analysis, after three consecutive depletions, all samples were IgG-free and very little pure IgG (a fraction of the light chain) could be recovered in the third depletion (fig. 2).





C

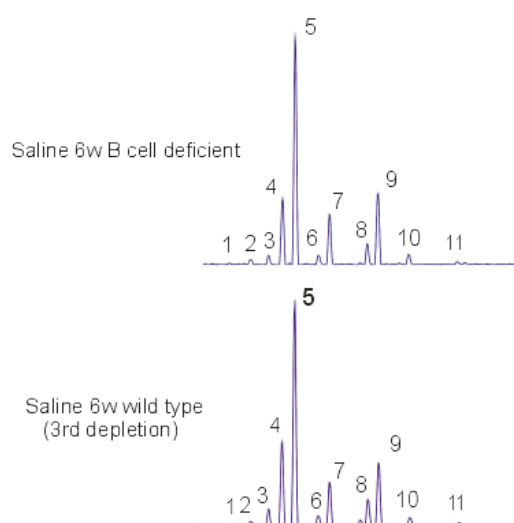


Fig. 2. **SDS-PAGE (A) and Western blot (WB) (B) analysis of the IgG-depletions.** SDS-PAGE revealed that IgG is abundantly captured in the first depletion, and absent in the second and third depletion indicating that the vast majority of IgG is removed from serum in the first depletion. However, WB showed that three depletions are necessary to remove all IgG from serum. The serum *N*-glycosylation pattern of a WT serum sample that was depleted three times was identical to that of a B cell deficient serum sample (C).

### 3.5 Glycomic analysis

#### 3.5.1 *Structural analysis of the mouse serum N-glycans*

Exoglycosidase digests provided structural information on most of the peaks, but it could not unambiguously determine the precise glycan structure (supplemental figures online). In contrast, MALDI-TOF analysis revealed the precise glycan structures of the most abundant peaks in the IgG and total serum electropherogram (fig. 3), but since it is a less sensitive technique compared to capillary electrophoresis, not all peaks present in the electropherogram were detected in the MS spectra. Moreover, structural analysis with MALDI-TOF MS was performed without sialidase digest, therefore, multiple peaks in the total serum MS spectrum correspond to one peak in the total serum electropherogram.

By combining the exoglycosidase digests and MS-data, the following peaks could be deduced in the IgG electropherogram: peak 1 is an agalacto, core- $\alpha$ -1,6-fucosylated biantennary (NGA2F), peaks 3 and 4 are single agalacto, core- $\alpha$ -1,6-fucosylated biantennaries (NG1A2F) and peak 7 is a bigalacto, core- $\alpha$ -1,6-fucosylated biantennary glycan (NA2F). Similarly, the following peaks could be deduced in the total serum electropherogram: peak 1 is an agalacto, core- $\alpha$ -1,6-fucosylated biantennary (NGA2F), peak 5 is a bigalacto, biantennary glycan (NA2), peak 7 is a bigalacto, core- $\alpha$ -1,6-fucosylated biantennary glycan (NA2F) and peak 9 is tri-antennary glycan (NA3). From the latter structure (NA3), it could be deduced that peaks 10 and 11 are also two multi-antennary glycans. The remaining peaks in the IgG and total serum electropherogram could not be

definitely determined, particularly because the precise glycan structure was not assessed by MS-analysis. This was mostly the case for the low abundant peaks in the electropherograms. Importantly, the fucosidase digest confirmed that peaks 1, 6 and 7 are core fucosylated glycans and the MS-analysis also confirmed the absence of bisecting GlcNAc modified glycans in both IgG and total serum electropherogram.

### 3.5.2 *General aspects*

Peak 1 (NGA2F) is a IgG-specific, but not exclusive glycan. In B cell deficient mice, peak 1 is still present, but in very small quantities, whereas it is one of the most abundant glycans on IgG. In WT mice, peak 1 is one of the minor peaks in the electropherogram reflecting the low IgG concentration in serum of mice. In contrast, peaks 8 and 11 were never present on IgG indicating that these glycans only appear on liver-produced protein (fig. 4, 5 and 6). Glycomic analysis was done on the IgG fraction that was captured in the first depletion.

### 3.5.3 *Wild type and B cell deficient mice*

#### 3.5.3.1 *CBDL 6w vs. Sham 6w*

First, we looked at significant *N*-glycan alterations in total serum by comparing WT CBDL mice with WT sham-operated mice. A significant increase in peak height of peaks 1 (NGA2F), 6, 7 (NA2F) and 11 and a significant decrease in peak height of peaks 2, 5 (NA2) and 9 (NA3) were observed.

Subsequently, we compared the peak heights of CBDL B cell deficient mice with the peak heights of Sham-operated B cell deficient mice. In this analysis, specifically the *N*-glycan alterations on liver-produced protein are observed and the pattern of alterations closely reflected those of total serum. A significant increase in peak height of peaks 1 (NGA2F), 6, 7 (NA2F) and 11 and a significant decrease in peak height of peaks 2, 3, 4, 5 (NA2) and 9 (NA3) were observed (fig. 4).

Despite the close resemblance of the glycomic profile between WT and B cell deficient mice, two peaks (peak 2 and 3) were supplementary decreased in the B cell deficient CBDL model. We correlated the relative peak height of these peaks with the sirius stain values to determine if the difference in fibrotic development between the WT and B cell deficient mouse is responsible for the additional alterations. However, no correlation could be found between the sirius red stain values and peaks 2 and 3 (Spearman's rank correlation test,  $P=0.76$  and  $0.42$ , respectively).

The same analysis was performed for all other peaks in the electropherogram, both in the WT and B cell deficient mice. Only in the  $CCl_4$  WT model, we found significant correlations between sirius red stain values and the relative peak heights (see following section).

#### 3.5.3.2 *CCl<sub>4</sub> 16w vs. saline 16w*

In total serum, we observed a significant increase in peak height of peaks 9 (NA3) and 11 and a significant decrease in peak height of peaks 2, 3, 4, 6 and 10. In analogy of CBDL, the pattern of alterations on liver-produced protein closely resembled those of total serum. When comparing  $CCl_4$  injected B cell deficient mice with saline injected B cell deficient mice, we

observed a significant increased peak height of peaks 8, 9 and 11 and a significant decreased peak height of peaks 1 (NGA2F), 2, 3, 4, 6 and 10 (fig. 5).

Similar to the CBDL model, two peaks were supplementary significantly altered in the B cell CCl<sub>4</sub> model. Peak 1 (NGA2F) was additionally significantly decreased and peak 8 was additionally significantly increased. We also examined if these extra alterations were due to the significant less fibrotic development in the B cell deficient CCl<sub>4</sub> model. Again, no correlation could be found between the sirius red stain values and peak 1 (NGA2F) and peak 8 (Spearman's rank correlation,  $P=0,73$  and  $P=0.57$ , respectively).

Surprisingly, many relative peak heights in the CCl<sub>4</sub> WT model correlated very well with the sirius red stain values. There were significant correlations with peak 3 ( $P=0.007$ ), peak 4 ( $P=0.021$ ), peak 5 ( $P=0.007$ ), peak 7 ( $P=0.021$ ), peak 8 ( $P=0.004$ ), peak 9 ( $P=0.028$ ) and peak 11 ( $P=0.028$ ) (Spearman's rank correlation). For the most part, these are also the peaks that were significantly altered in peak height in the CCl<sub>4</sub> model.

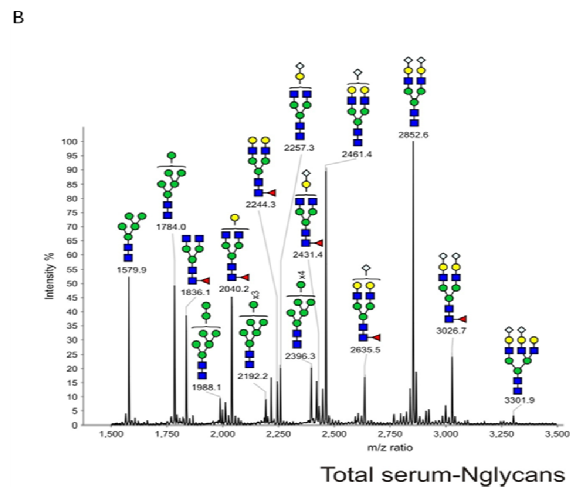
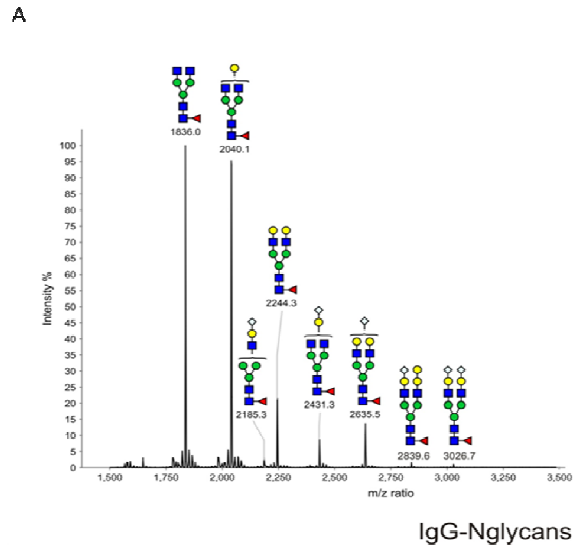
### 3.5.4 *Immunoglobulin G*

#### 3.5.4.1 *CBDL 6w vs. Sham 6w*

We compared the height of the nine peaks in the IgG electropherogram of CBDL mice (n=6) with those of Sham mice (n=8). Only one peak was significantly altered. Peak 2 was significantly increased in the IgG electropherogram of CBDL mice ( $P=0.029$ ) (fig. 6).

#### 3.5.4.2 *CCl<sub>4</sub> 16w vs. saline 16w*

The same analysis was performed on the IgG electropherograms of CCl<sub>4</sub> (n=8) and saline (n=8) injected mice. Three peaks were significantly altered in height. Peak 1 (NGA2F) and peak 2 were significantly decreased on the IgGs of CCl<sub>4</sub> mice ( $P=0.036$  and  $P=0.027$ ). In contrast, peak 3 (NG1A2F) was significantly increased on the IgGs of CCl<sub>4</sub> mice ( $P=0.036$ ) (fig. 6).



**Key:**

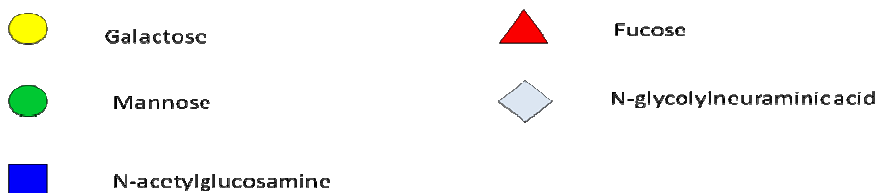


**Figure 3. MALDI-TOF MS of N-glycans released from mouse IgG and Total Serum by PNGase F digestion.** Glycans were permethylated prior to MALDI-TOF analysis. Structures were assigned taking into account the molecular weight value and the fragment ions obtained upon MS/MS analysis.

**A:** Profile of total permethylated N-glycans released from a pool of 72 mice IgG samples. Annotated structures correspond to core fucosylated complex-type biantennary glycans (m/z 1893, 2098, 2301), and core-fucosylated complex-type mono- and biantennary glycans with N-glycolylneuraminic acid as (m/z 2185, 2489, 2693, 2839, 3026) and  $\alpha$ -linked galactose (m/z 2839) as capping sugars..

**B:** Profile of total permethylated N-glycans released from a pool of 60 mice serum samples. Annotated structures correspond to high mannose type N-glycans (m/z 1636 and 1841), core fucosylated complex type biantennary glycans (m/z 1893, 2098, and 2301), complex type mono- and biantennary glycans with N-glycolylneuraminic acid as capping sugar (m/z 2315, 2519, 2910), and core fucosylated complex type mono- and biantennary glycans with N-glycolylneuraminic acid as capping sugar (m/z 2489, 2693 and 3084). One tri-antennary N-glycan was also detected with two N-glycolylneuraminic acid residues at m/z value 3359.

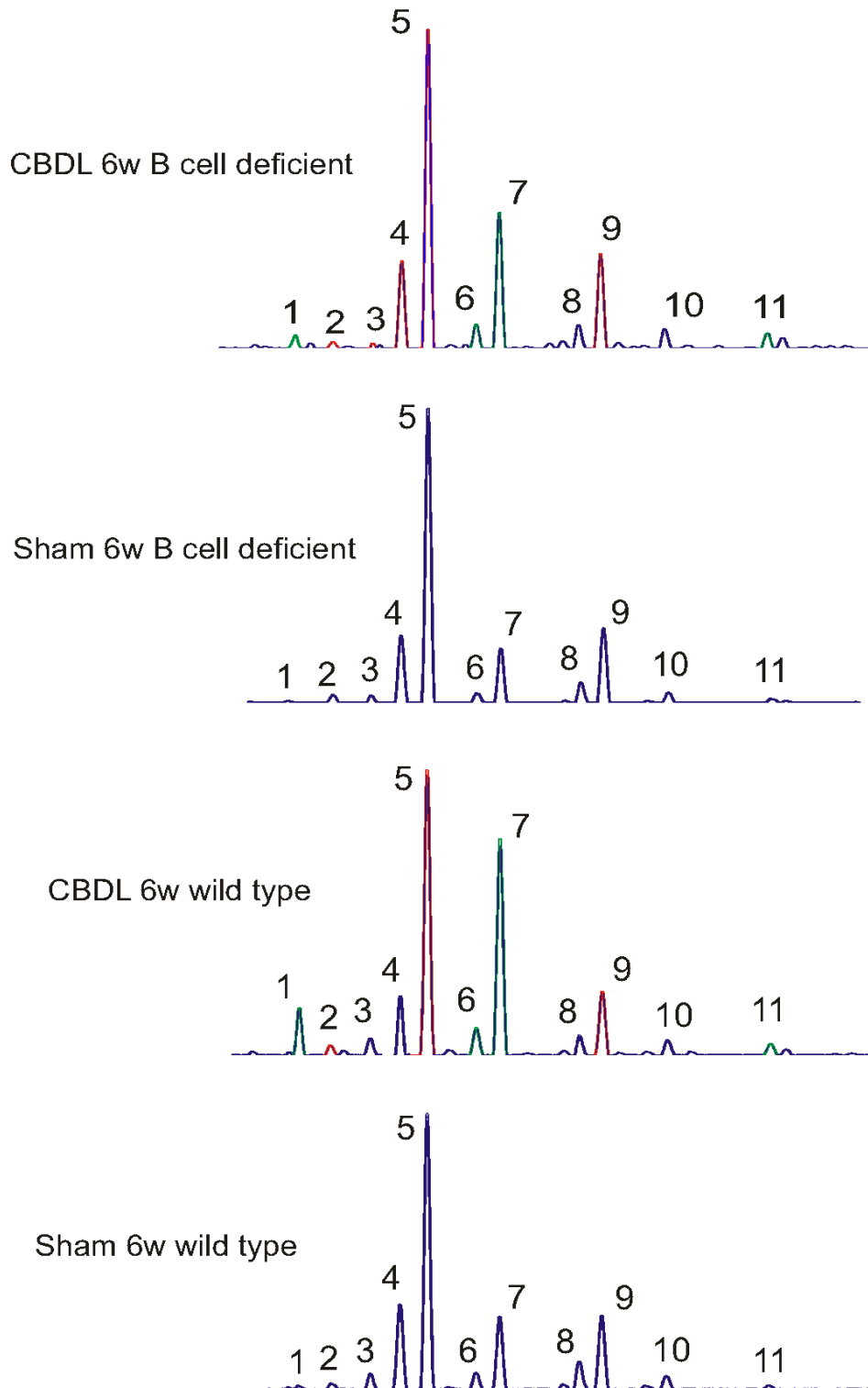


**Figure 4. serum N-glycosylation patterns of the CBDL and Sham model in B cell deficient and wild type mice.** The alterations in B cell deficient mice closely resemble the alterations seen in wild type mice. Green: significantly increased in relative peak height vs. control; red: significantly decreased in relative peak height vs. control.

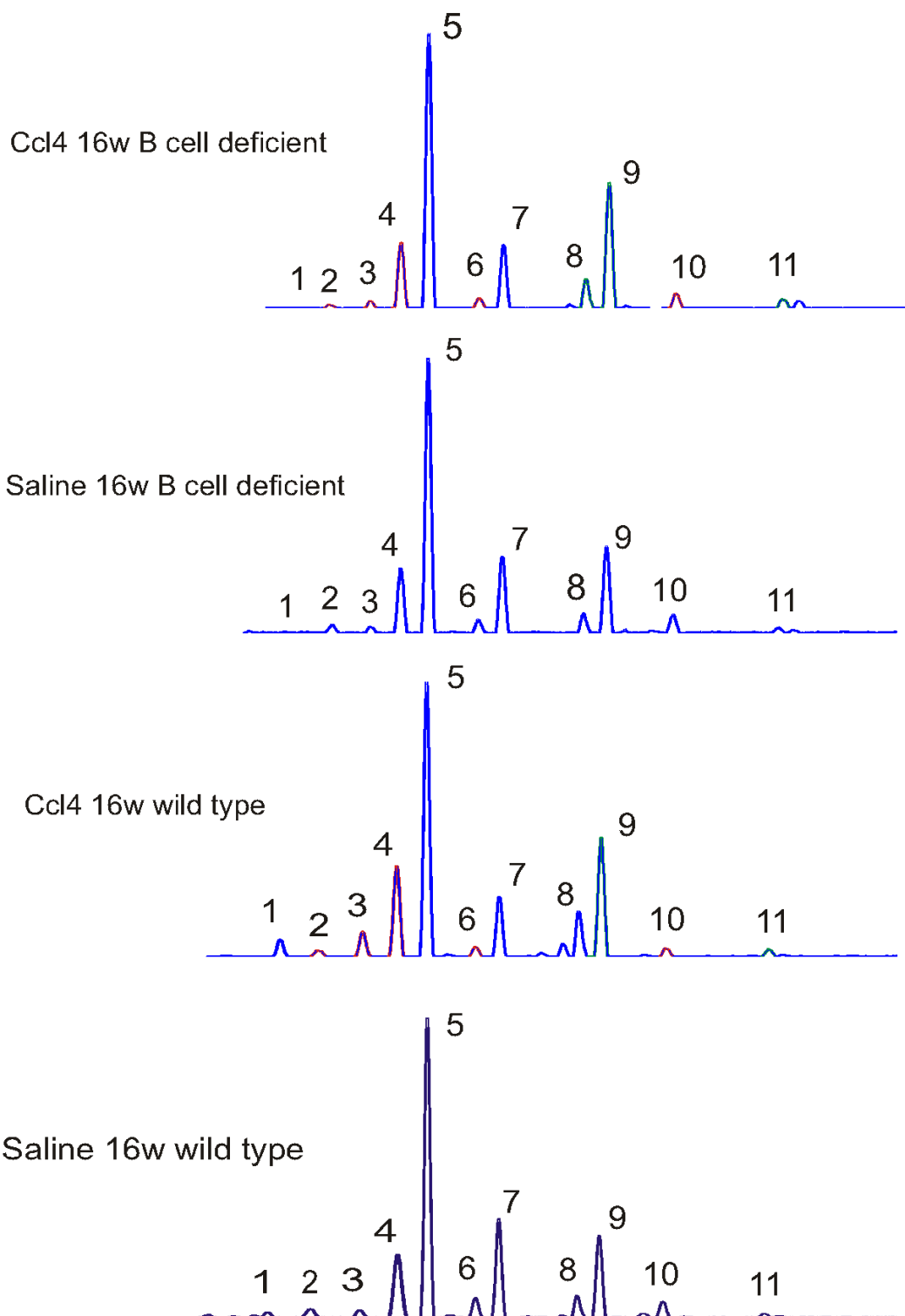


**Figure 5. serum *N*-glycosylation patterns of the CCl<sub>4</sub> and saline model in B cell deficient and wild type mice.** In analogy with the CBDL model, there is little difference between the alterations observed in B cell deficient and wild type mice. Green: significantly increased in relative peak height vs. control; red: significantly decreased in relative peak height vs. control.

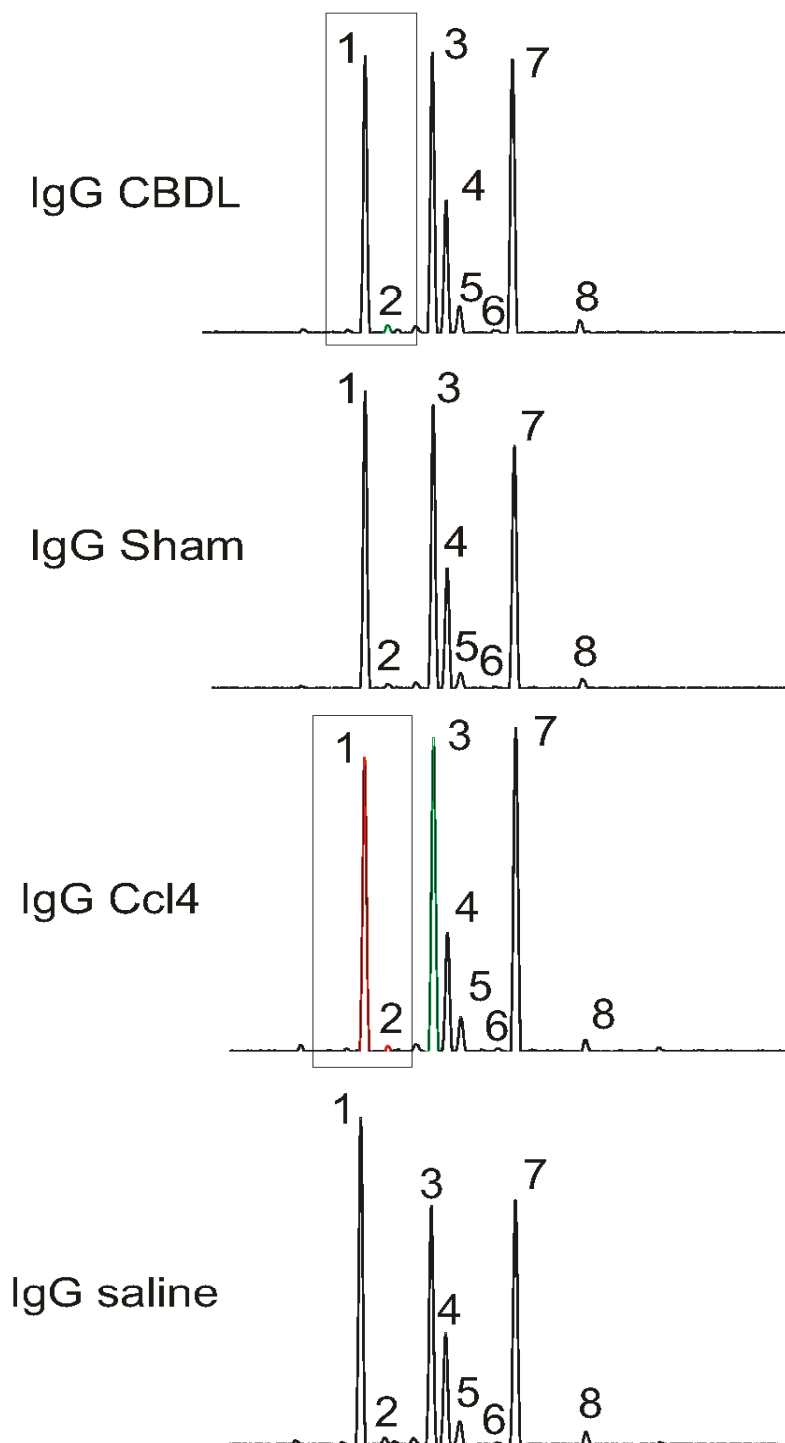


**Figure 6. N-glycosylation patterns of IgG in CBDL, Sham, CCl<sub>4</sub> and saline injected mice.** Significant N-glycan alterations were scarce on IgG in the mouse models of chronic liver diseases. Peak 2 was significantly increased on IgG of CBDL mice compared to Sham mice. Peak 1 and 2 were significantly decreased and peak 3 was significantly increased on IgG of CCl<sub>4</sub> mice compared to saline injected mice. The boxes indicate the agalactosylated glycans in the electropherogram. Although peak 2 is elevated in CBDL mice, it does not contribute considerably to the undergalactosylation status of IgG because of its low abundance. Moreover, these glycans are even significantly decreased in the CCl<sub>4</sub> model.

#### 4. Discussion

*N*-glycan alterations observed in total serum can reflect a changed B cell and/or a changed hepatocyte physiology. In mouse models of chronic liver disease, the dominant factor is clearly the change in hepatocyte *N*-glycan homeostasis. The pattern of *N*-glycan alterations in total serum closely resemble the alterations seen on liver-produced protein, both in the CCl<sub>4</sub> and the CBDL model.

Significant *N*-glycan alterations on IgG were scarce. On IgGs of CBDL mice, only peak 2 was significantly increased. In total serum, peak 2 is not significantly altered, there could be a balanced effect between a decrease on liver-produced protein and an increase on IgGs. There were more significant alterations on IgGs of mice chronically injected with CCl<sub>4</sub>. Peaks 1 and 2 are significantly decreased in peak height and peak 3 is significantly increased in peak height. The decrease of peak 1 and increase of peak 3 are not found in the total serum electropherogram reflecting the low IgG concentration in mice (0.5-1.5 mg/dl) in comparison to humans (8-20 mg/dl) [2].

In general, IgG *N*-glycosylation has a more significant impact in humans than in mice. Not only is there a higher IgG concentration, the number and magnitude of alterations on IgG during liver fibrosis is more elaborate and this clearly has an important influence on the total serum *N*-glycome of cirrhotic patients [11]. Interestingly, undergalactosylation of IgG, an important feature on the IgGs of human liver patients, was not observed in these mouse models of chronic liver disease. This does not necessarily mean that IgG undergalactosylation does not occur in mice. It is well known that undergalactosylation of IgG is also present in rheumatoid arthritis (RA) patients and in contrast to our study, this undergalactosylation could be extrapolated to a mouse model of RA [16, 28].

It must be noted that there are important variations in terminal galactosylation of IgGs between mice and humans. 70% of human IgG oligosaccharides are galactosylated, whereas only ~45% of mouse IgG oligosaccharides contain galactose residues and this was confirmed by the MS-analysis of the pooled IgG fraction [24]. Moreover, the change in agalacto glycans on IgG is functionally important. In the context of undergalactosylation, especially complement-dependent cytotoxicity (CDC) is affected in which less terminal galactose on IgG results in reduced CDC activity. However, undergalactosylation also results in the exposure of terminal GlcNAc residues that have been shown to bind to the serum protein mannose binding protein and activate the alternative complement cascade [25]. To what extent this has an impact on the IgG functionality of CCl<sub>4</sub> and CBDL mice remains to be elucidated.

An interesting observation was the degree of fibrosis present in the mouse models of chronic liver disease induced in B cell deficient mice. In the CCl<sub>4</sub> model, there was significantly less fibrotic development in B cell deficient mice, whereas the opposite situation was present in the CBDL model. In the CCl<sub>4</sub> model, B cells seem to have an impact on fibrosis in an antibody- and T cell-independent manner [23]. The main hypothesis is that macrophages that contribute to recovery from inflammatory scarring are preferentially activated in the absence of B cells. Moreover, soluble factors produced by stimulated B cells can induce collagen synthesis by hepatic stellate cells.



In contrast, in a model of primary biliary cirrhosis, B cell deficient mice developed a more severe form of cholangitis than controls and had a significant greater frequency of activated CD4<sup>+</sup> and CD8<sup>+</sup> T cells in the liver [22]. They also had reduced frequency of Foxp3<sup>+</sup> regulatory T cells in the hepatic CD4<sup>+</sup> T cell population and natural killer T cells in hepatic inflammatory cell infiltrates. In this model, B cells have a suppressive effect on the inflammatory response.

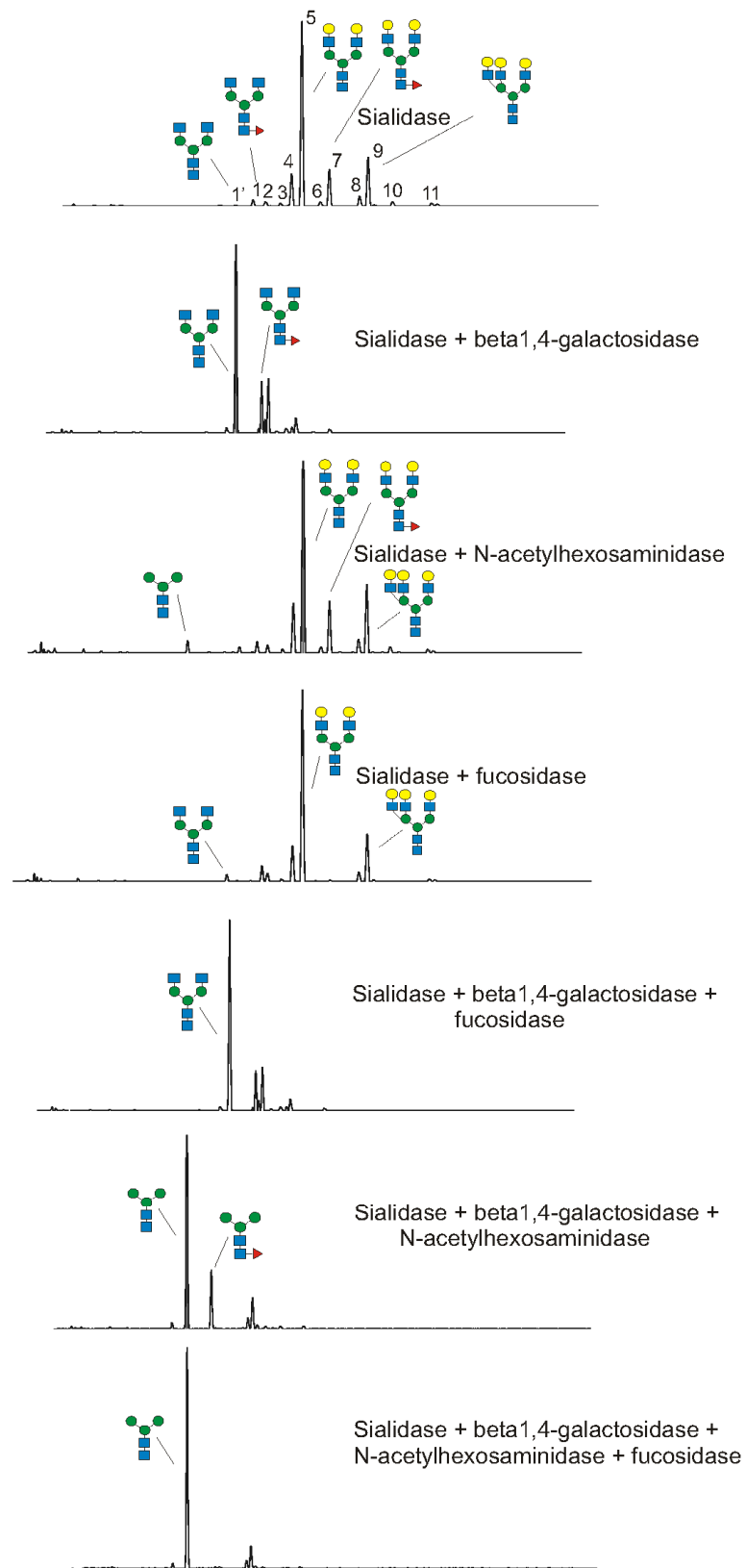
These results indicate that the discrepancy in fibrotic development between the two models can mainly be explained by the interaction between B and T cells. In the CCl<sub>4</sub> model, B cells have an impact on fibrosis independently from T cells, whereas in the CBDL model, the T cell population is significantly altered in the absence of B cells. A detailed clarification of this difference in fibrotic development between the two models falls beyond the scope of this study.

In the B cell deficient CBDL model, peak 2 and 3 are supplementary significantly decreased in comparison to WT mice and in the CCl<sub>4</sub> model, peak 1 and peak 8 were also additionally significantly altered in B cell deficient mice. However, no correlation between the sirius red stain values and the peak heights of these peaks could be observed indicating that the difference in fibrotic development between WT and immunocompromised mice is not responsible for the extra glycomic alterations. In a previous study [2], we established that the majority of *N*-glycan alterations in the CCl<sub>4</sub> and CBDL model were present at an early stage in the fibrotic development. Since we looked at the end-stage of fibrotic development in both models, the impact of these histological differences on *N*-glycan alterations are minimal.

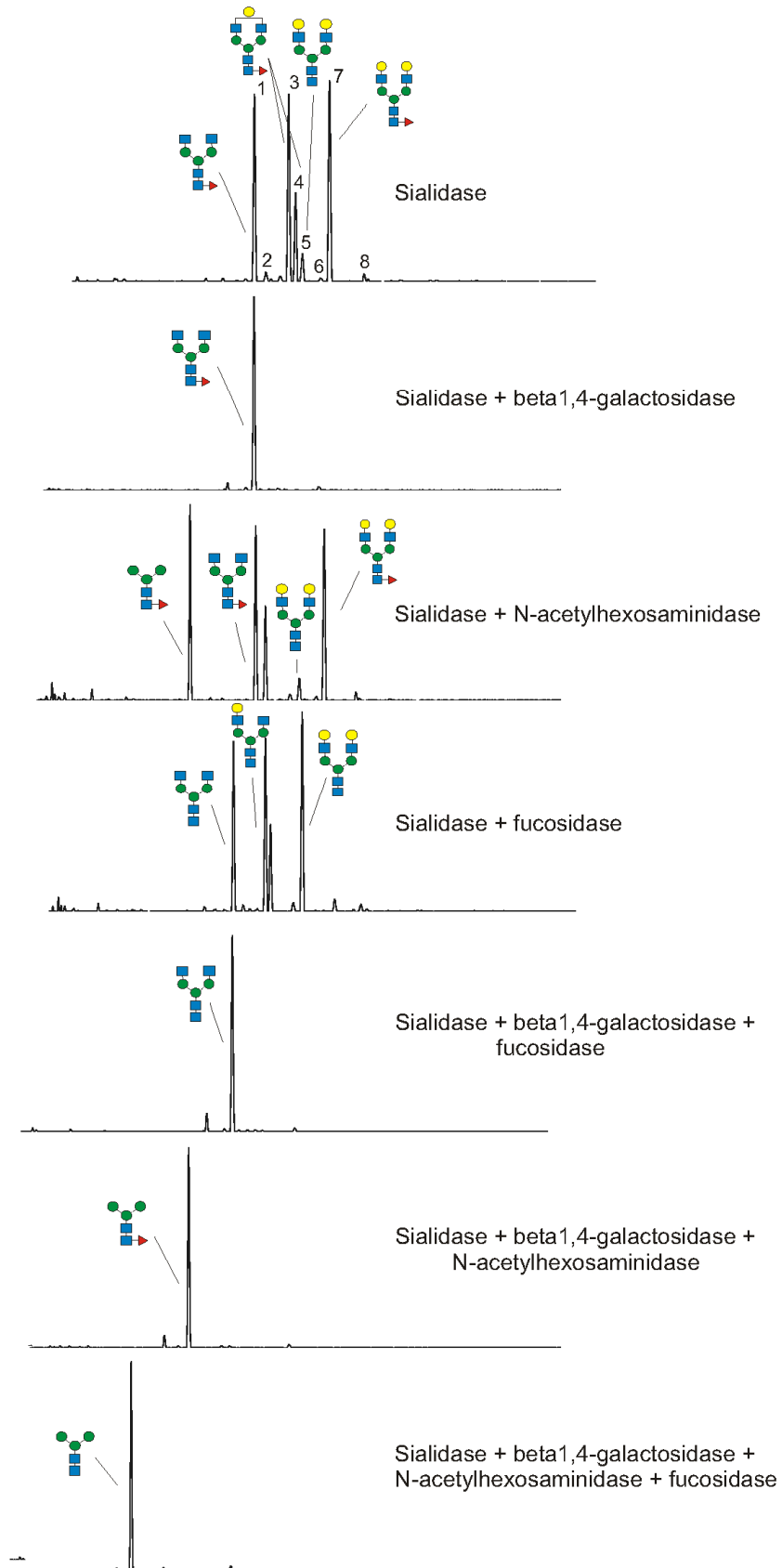
The serum *N*-glycosylation pattern of a WT serum sample that was depleted three times was identical to that of a B cell deficient serum sample. This was an extra confirmation that the B cell deficient mice did not contain IgGs. By combining the data from the B cell deficient mice with the fucosidase digest, it was confirmed that the increase of α1-6 fucosylated glycans (peak 1, 6 and 7) in CBDL mice is hepatocyte and not B cell dependent. This is important because this feature could be extrapolated to human liver patients with hyperbilirubineamia [2]. The most likely hypothesis is that fucosylation of *N*-linked glycans within polarized hepatocytes directs glycoproteins to the apical surface and into bile [19]. In cholestatic conditions, the hepatocyte becomes depolarized and the fucosylated glycoforms end up in the systemic circulation instead of bile. Moreover, the increase of multi-antennary glycans (peaks 9 and 11) in CCl<sub>4</sub> was also confirmed as determined in our previous study [2]. Although another multi-antennary glycan (peak 10) was significantly decreased in CCl<sub>4</sub> mice, this glycan is fucosylated (most likely branch fucosylated) as indicated by the fucosidase digest and this will influence its behavior in chronic liver disease. Finally, in agreement with previous reports [30], we could not identify any bisecting GlcNAc modified glycans in total serum indicating no expression of the *Mgat3* gene in normal liver and B cell. This supports the evidence of a non-hepatic action of GnT-III in promoting hepatocyte proliferation after partial hepatectomy as well as the progression of diethylnitrosamine-induced tumors [30].

In conclusion, alterations of serum protein *N*-glycosylation in mice are mainly hepatocyte driven. Alterations of *N*-glycans on IgG are less abundant and do not reflect an undergalactosylation status. This in combination with the low IgG concentration in mice minimizes the impact of IgG *N*-glycosylation in mouse models of chronic liver disease.

Supplementary data:



Supplemental figure 1. Exoglycosidase digests of mouse total serum N-glycans



Supplemental figure 2. Exoglycosidase digests of mouse immunoglobulin G *N*-glycans

## 5. Acknowledgements

The authors thanks Julien Dupont and Annelies Van Hecke for expert technical assistance. The mass spectrometry work was supported by the Biotechnology and Biological Sciences Research Council (BBF0083091) and Marie Curie Initial Training Network, EuroglycoArrays Project, part of the PF7 People Programme.

## 6. References

- [1] Bedossa P, Poynard T. An algorithm for the grading of activity in chronic hepatitis C. The METAVIR Cooperative Study Group. *Hepatology* 1996;24:289-293.
- [2] Blomme BA, Van Steenkiste C, Vanhuysse J, Colle I, Callewaert N, Van Vlierberghe H. The impact of elevation of total bilirubin level and etiology of the liver disease on serum N-glycosylation patterns in mice and men. *Am J Physiol Gastrointest Liver Physiol* 2010;298:G615-24.
- [3] Callewaert N, Van Vlierberghe H, Van Hecke A, Laroy W, Delanghe J, Contreras R. Noninvasive diagnosis of liver cirrhosis using DNA sequencer-based total serum protein glycomics. *Nature Med* 2004;10:429-434.
- [4] Ceroni A, Maass K, Geyer H, Geyer R, Dell A, Haslam SM. GlycoWorkBench: a tool for the computer-assisted annotation of mass spectra of glycans. *J Proteome Res* 2008;7:1650-1659.
- [5] Geerts AM, Vanheule E, Praet M, Van Vlierberghe H, De Vos M, Colle I. Comparison of three research models of portal hypertension in mice: macroscopic, histological and portal pressure evaluation. *Int J Exp Pathol* 2008;89:251-263.
- [6] Gerardy-Schahn R, Oelmann S, Bakker H. Nucleotide sugar transporters: biological and functional aspects. *Biochimie* 2001;83:775-82.
- [7] Janakat S, Al-Merie H. Optimization of the dose and route of injection, and characterisation of the time course of carbon tetrachloride-induced hepatotoxicity in the rat. *J Pharmacol Toxicol Methods* 2002;48:41-44.
- [8] Jang-Lee J, North S, Sutton-Smith M, Goldberg D, Panico M, Morris H, et al. Glycomic profiling of cells and tissues by mass spectrometry: fingerprinting and sequencing methodologies. *Methods Enzymol* 2006 415:59-86.
- [9] Jefferis R. Antibody therapeutics: isotype and glycoform selection. *Expert Opin Biol Ther* 2007; 7:1401-1413.
- [10] Kitamura D, Roes J, Kuhn R, Rajewsky K. A B cell-deficient mouse by targeted disruption of the membrane exon of the immunoglobulin mu chain gene. *Nature* 1991;350:423-426.
- [11] Klein A, Carre Y, Louvet A, Michalski JC, Morelle W. Immunoglobulines are the major glycoproteins involved in the modifications of total N-glycome in cirrhotic patients. *Proteomics Clin App* 2010;4:379-393.
- [12] Klein A, Michalski JC, Morelle W. Modifications of human total serum N-glycome during liver fibrosis-cirrhosis, it is all about immunoglobulines? *Proteomics Clin Appl* 2010;4:372-378.
- [13] Kobata A. The N-linked sugar chains of human immunoglobulin G: their unique pattern, and their functional roles. *Biochim Biophys Acta* 2008;1780:472-478.

- [14] Koike C, Uddin M, Wildman DE, Gray EA, Trucco M, Starzl TE, et al. Functionally important glycosyltransferase gain and loss during catarrhine primate emergence. *Proc Natl Acad Sci USA* 2007;104:559-564.
- [15] Kountouras J, Billing BH, Scheuer PJ. Prolonged bile duct obstruction: a new experimental model for cirrhosis in the rat. *Br J Exp Pathol* 1984;65:305-311.
- [16] Kotz K, Hansler M, Sauer H, Kaltenhauser S, Hantzschel H. Immunoglobulin G galactosylation deficiency determined by isoelectric focusing and lectin affino blotting in differential diagnosis of rheumatoid arthritis. *Electrophoresis* 1996;17:533-534.
- [17] Laroy W, Contreras R, Callewaert N. Glycome mapping on DNA sequencing equipment. *Nat Protoc* 2006;1:397-405.
- [18] Liu XE, Desmyter L, Gao CF, Laroy W, Dewaele S, Vanhooren V, et al. N-glycomic changes in hepatocellular carcinoma patients with liver cirrhosis induced by hepatitis B virus. *Hepatology* 2007;46:1426-1435.
- [19] Mehta A, Block TM. Fucosylated glycoproteins as markers of liver disease. *Disease Markers* 2008;25:259-265.
- [20] Mizuochi T, Hamako J, Nose M, Titani K. Structural changes in the oligosaccharide chains of IgG in autoimmune MRL/Mp-lpr/lpr mice. *J Immunol* 1990;145:1794-1798.
- [21] Mizuochi T, Hamako J, Titani K. Structures of the sugar chains of mouse immunoglobulin G. *Arch Biochem Biophys* 1987;257:387-394.
- [22] Moritoki Y, Zhang W, Tsuneyama K, Yoshida K, Wakabayashi K, Yang GX, et al. B cells suppress the inflammatory response in a mouse model of primary biliary cirrhosis. *Gastroenterology* 2009;136:1037-1047.
- [23] Novobrantseva TI, Majeau GR, Amatucci A, Kogan S, Brenner I, Casola S, et al. Attenuated liver fibrosis in the absence of B cells. *J Clin Invest* 2005;115:3072-3082.
- [24] Raju TS, Briggs JB, Borge SM, Jones AJ. Species-specific variation in glycosylation of IgG: evidence for the species-specific sialylation and branch-specific galactosylation and importance for engineering recombinant glycoprotein therapeutics. *Glycobiology* 2000;10:477-486.
- [25] Raju TS. Terminal sugars of Fc glycans influence antibody effector functions of IgGs. *Curr Opin Immunol* 2008;20:471-78.
- [26] Sasai K, Ikeda Y, Fujii T, Tsuda T, Taniguchi N. UDP-GlcNAc concentration is an important factor in the biosynthesis of  $\beta$ 1,6-branched oligosaccharides: regulation based on the kinetic properties of N-acetylglucosaminyltransferase V. *Glycobiology* 2002;12:119-27.
- [27] Tanabe K, Deguchi A, Higashi M, Usuki H, Suzuki Y, Uchimura Y, et al. Outer arm fucosylation of N-glycans increases in sera of hepatocellular carcinoma patients. *Biochem Biophys Research Comm* 2008;374:219-225.
- [28] Van Beneden K, Coppieters K, Laroy W, De Keyser F, Hoffman IE, Van den Bosch F, et al. Reversible changes in serum immunoglobulin galactosylation during the immune response and treatment of inflammatory autoimmune arthritis. *Ann Rheum Dis* 2009;68:1360-1365.

[29] Vanderschaeghe D, Laroy W, Sablon E, Halfon P, Van Hecke A, Delanghe J, et al. GlycoFibroTest is a highly performant liver fibrosis biomarker derived from DNA sequencer-based serum protein glycomics. *Mol Cell Proteomics* 2009;8:986-994.

[30] Yang X, Tang J, Rogler C, Stanley P. Reduced hepatocyte proliferation is the basis of retarded liver tumor progression and liver regeneration in mice lacking *N*-acetylglucosaminyltransferase III. *Cancer Res* 2003;63:7753-7759.

# Chapter 3.3

## ***“Serum N-glycosylation patterns in diethylnitrosamine-induced hepatocellular carcinoma mice and their evolution after inhibition of the Placental growth Factor”***

**Bram Blomme**<sup>1,3</sup>, Femke Heindryckx<sup>1,3</sup>, Jean-Marie Stassen,<sup>2</sup> Anja Geerts<sup>1</sup>, Isabelle Colle<sup>1</sup>, Hans Van Vlierberghe<sup>1</sup>

<sup>1</sup>Department of Hepatology and Gastroenterology, Ghent University Hospital, Ghent, Belgium

<sup>2</sup>Thrombogenics NV, Leuven, Belgium

<sup>3</sup>These authors contributed equally to this study

**In preparation**

## Abstract

The inhibition of the Placental Growth Factor (PIGF) produced promising results in reducing tumor size and burden in hepatocellular carcinoma (HCC). However, methods to non-invasively assess the progression of HCC in mouse models and their evolution after novel treatments are lacking. HCC was induced in mice by weekly injections with diethylnitrosamine (DEN) for 16w, 20w, 25w and 30w. One group was injected with DEN for 25w and subsequently treated with 25 mg/kg PIGF antibodies (5D11D4) for 5w. Finally, *PIGF*<sup>-/-</sup> mice were injected with DEN and sacrificed after 20w and 30w. Blood was collected at sacrifice and analyzed with DNA sequencer-assisted fluorophore-assisted capillary electrophoresis. Liver slides were immunohistochemically stained for the transcription factor Ets-1. After 16w of DEN, 9 of the 13 peaks were significantly altered in abundance. Maximum altered phenotype on the *N*-glycan level was reached after 20w of DEN i.e. the time point when the first neoplastic lesions started to appear. At this time point, 11 peaks were significantly altered in abundance. Treatment with 5D11D4 improved the glycomic phenotype in DEN-treated mice in which 7 of the 11 altered glycans tended to normalize. Similar results were obtained in *PIGF*<sup>-/-</sup> mice, but not to the same extent. These data correlated with the Ets-1 staining in which a significant reduction of the number of Ets-1 positive cells was observed in both treatment and *PIGF*<sup>-/-</sup> group. Serum *N*-glycomics can non-invasively assess the improvement of tumor burden after PIGF inhibition. Ets-1 might provide a possible link between the glycomic and angiogenesis data.



## Introduction

Annually, more than 560 000 people are diagnosed with primary liver cancer (PLCs) and hepatocellular carcinoma (HCC) accounts for 85-90% of all PLCs [1]. The factors determining the risk for HCC include age, male gender and the etiology of the disease. In particular cirrhosis is associated with a significant risk for HCC [2]. A liver biopsy is currently the gold standard to diagnose the cirrhotic state of the liver, despite the well known limitations and complications [3]. Callewaert *et al* have developed a non-invasive test based on the *N*-glycosylation of serum proteins that can be used to diagnose cirrhotic from non-cirrhotic patients with high sensitivity and specificity [4]. Using the same glycomic technique, Lui *et al* were able to distinct HCC patients from cirrhotic patients [5]. In HCC patients, branched fucosylated tri-antennary glycans (NA3b) were increased, whereas bisecting *N*-acetylglucosamine (GlcNAc) modified biantennary glycans (NA2FB) were decreased compared to cirrhotic patients. However, the latter test was developed in hepatitis B patients. Hepatitis B is considered to be an oncovirus and this can be attributed to one of the four proteins that originate from the HBV genome, the HBx-protein [6]. It was shown that the HBx-protein significantly up-regulates the expressing of *N*-acetylglucosaminyltransferase III (GnT-III), the enzyme responsible for the bisecting GlcNAc modification [7]. During tumor development, expression of GnT-V, responsible for  $\beta$ 1-6 branching to form multi-antennary glycans, is up-regulated in HCC nodules [8]. This is the reason why advanced HCC (more and larger HCC nodules producing more GnT-V) can be more readily differentiated from cirrhosis compared to early HCC stages using this technique. However, these results could not be reproduced in a MALDI-TOF study with a mixed HCC-population of hepatitis B and hepatitis C patients [9]. Surprisingly, in this study, two multi-antennary glycans were significantly decreased and a bisecting GlcNAc modified biantennary glycan was significantly increased in the serum of HCC patients. These glycomic changes also occur in cirrhotic patients [4] and were probably induced by the dominating cirrhotic liver in these HCC patients.

Placental growth factor (PIGF) is a homolog of vascular endothelial growth factor (VEGF), and was originally isolated from the human placenta [10]. VEGF can bind to VEGFR-1 and VEGFR-2, whereas PIGF binds to neuropilines and VEGFR-1 which are up-regulated in disease. It was previously shown that the angiogenic activity of PIGF is restricted to pathologic conditions, without affecting healthy vessels [11]. Furthermore, promising results have been obtained by inhibiting PIGF in several solid tumors [11]. Treatment of HCC in DEN-induced mice with PIGF-antibodies causes a substantial difference in mortality, tumor burden, vascular normalization and arterialization, compared to the control group [12]. In addition, inhibiting PIGF by using transgenic knock out mice, leads to a significant delay in HCC-progression and has a positive influence on mice survival [12].

The transcription factor E26 transformation-specific sequence 1 (Ets-1) is a product of proto-oncogenes related to malignant transformation and metastasis. It plays an important role in the process of angiogenesis and glycosylation. In the context of glycosylation, the GnT-V enzyme is under the oncogenic control of Ets-1 [13, 14]. The expression levels of GnT-V and Ets-1 were quantified by densitometry in 16 human and murine cancer cell lines and a positive correlation was found between these mRNAs [14]. Alternatively, transfection of dominant negative Ets-1 in two of these cell lines with high intrinsic Ets-1 and GnT-V expression, decreased the GnT-V expression significantly [14]. The important role of Ets-1 in

the transcription of GnT-V has also been shown in human gliomas [15] and metastatic macrophage x melanoma fusion hybrids [16]. Increased expression of multi-antennary  $\beta$ 1,6-branching *N*-glycans has been correlated with metastatic potential in rodent tumor models [17, 18] and has also been shown to be a marker of tumor progression in human breast and colon neoplasia [19, 20]. Alternatively, Ets binding motifs are also found in the promoter/enhancer region of numerous genes that are important for angiogenesis. These include VEGFR-1 and -2, Tie-1 and -2 which are involved in the activation of endothelial cells and MMPs and VE-cadherin which are involved in endothelial cell migration and capillary formation [21]. In addition, increased expression of Ets-1 was observed in endothelial cells (EC) during tumor angiogenesis in adults [22-24]. VEGF and bFGF were potent inducers of Ets-1 in ECs and this induction of Ets-1 in ECs was mediated by the activation of a classic MAP kinase, ERK1/2 [25].

Because the sugar chains of glycoproteins are essential for the maintenance of the ordered social behavior of differentiated cells in multicellular organisms, alterations to the sugar chains are the molecular basis of abnormal social behavior in tumors cells, such as invasion into the surrounding tissues and metastasis. Serum *N*-glycosylation patterns could therefore be the ideal tool to non-invasively evaluate to the efficacy of 5D11D4, a murine anti-PIGF monoclonal antibody, on tumor growth in DEN-induced HCC.

## Materials and Methods

### Animals

5-week-old male WT and *PIGF*<sup>-/-</sup> mice (129S2/SvPasCrl) received weekly intraperitoneal (IP) injections with DEN (35 mg/kg) (Sigma-Aldrich, St Louis, MO, USA). Mice were kept under constant temperature and humidity in a 12 hours controlled light/dark cycle and received food and water *ad libitum*. The Ethical committee of experimental animals at the faculty of Medicine and Health Sciences, Ghent University, Belgium, approved the protocols [26].

WT mice injected with DEN and the respective control mice injected with saline solution were sacrificed after 16w (n=5), 20w (n=4), 25w (n=4) and 30w (n=8). *PIGF*<sup>-/-</sup> mice injected with DEN and the respective control *PIGF*<sup>-/-</sup> mice injected with saline solution were sacrificed after 20w (n=6) and 30w (n=8). In the treatment study, WT mice were injected with DEN and control mice were injected with saline solution for 25w and subsequently treated with 5D11D4 (25mg/kg, 2x/week IP), a murine anti-PIGF monoclonal antibody, for 5w (n=9) or IgG for 5w (n=9) [12].

At time of sacrifice, blood was collected from the carotid artery under isoflurane (Forene<sup>®</sup>, Abbott, Brussels, Belgium) anesthesia. These samples were centrifuged at 10 000 rpm for 10 minutes. Serum was taken off the clot and stored at -80°C for glycomic analysis. The right lobe of the liver in control mice and the lobe with HCC nodules in DEN-treated mice were removed and fixed in 4% phosphate buffered formaldehyde solution for 24h (Klinipath, Geel, Belgium).

### N-glycan analysis

The *N*-glycans present in 5 µl of serum were released from the proteins with PNGase F and subsequently fluorescently labeled with APTS and desialylated. Improved DNA sequencer-assisted fluorophore-assisted capillary electrophoresis (DSA-FACE) technology was used to profile and analyze the labeled glycans [27]. Data were analyzed using the Genemapper v3.7 software (Applied Biosystems). 13 peaks were present in the electropherogram of every mouse serum sample. The peak height of every peak was quantified to obtain a numerical description of the profiles. The peak heights were subsequently normalized to the total intensity of the measured peaks (represented as a percentage of the total peak height). Structural analysis of the *N*-glycans was done as previously described [28].

### Ets-1 staining

For Ets-1 staining, paraffin-embedded liver sections were cut at 5 µm thickness and deparaffinized using standard histology protocol. Antigen retrieval was performed by 30 minutes incubation in 95 °C citrate buffer, endogenous peroxidase activity was blocked by 15 minutes incubation in 3% H<sub>2</sub>O<sub>2</sub>. Primary antibody was diluted 1/200 in TBS and applied overnight at 4 °C. DAB-staining was induced using LSAB+ kit (DAKO, ref n° K0690, California, USA), as stated on the product specification sheet; and nuclei were counterstained with Mayer haematoxylin. The number of Ets-1 positive cells were visualized on a Olympus BX41 microscope equipped with a Olympus UC30 camera and electronically quantified using Olympus Cell^D in 10 regions of interest (ROI) inside the HCC lesions, in their active surrounding matrix and in non tumor tissue, leading to 30 ROIs per slide. The number of Ets-1 positive cells are represented per mm<sup>2</sup> and used for subsequent statistical analysis.

### Statistical analysis

Statistical analysis was performed with SPSS 16.0 (SPSS, Chicago, IL, USA). Glycomic data were processed using a Mann-Whitney U test, whereas Ets-1 data were processed using an independent sample *t*-test. A single-factor ANOVA analysis was performed in the control, in the different DEN-injected groups and in the 5D11D4-treated group regarding the value of the developed biomarkers, (log(peak4/peak11) and log(peak2+peak7+peak8)). *Post-hoc* tests were performed using Tukey HSD tests. The degree of linear correlation between the value of the biomarkers and the Ets-1 data was determined by a Spearman rank correlation test. *P*-values < 0.05 were considered significant in all analyses.

## Results

### Histological analysis

These histological data have been published previously [26], but are important for the interpretation of the results, therefore a summary is given. After 16 weeks of weekly DEN-injections, a mild fibrosis occurs and dysplastic lesions start to appear, resulting in a premalignant environment. The following weeks are a progression phase in which the premalignant environment continues to evolve to a malignant state. The tumor burden significantly augments and angiogenic factors persist to increase. After 25w of DEN-injections, the small dysplastic lesions have progressed to vascularized exophytic tumors which are macroscopically visible and give rise to a further increase in angiogenic factors, leading to the formation of new blood vessels. Histologically, tumor burden reached a maximum phenotype after 30w of DEN-injections that was significantly larger compared to 25w. Inhibition of PIGF in this model, leads to a decreased tumor burden, vascular normalization, decreased arterialization and a prolonged survival compared to DEN-induced controls [12].

### N-glycomic analysis

#### *DEN-study*

After 16w of DEN, already 9 of the 13 peaks in the electropherogram were significantly altered in comparison to control mice. Maximum altered phenotype on N-glycomic level (11 of the 13 peaks) was reached after 20w of DEN and this is also the time point that small neoplastic lesions started to appear. After 25w and 30w of DEN, all mice have developed well-vascularized, macroscopic lesions, although the glycomic phenotype did not further aggravate in comparison to 20w of DEN (fig. 1) (for *P* values, see table 1).

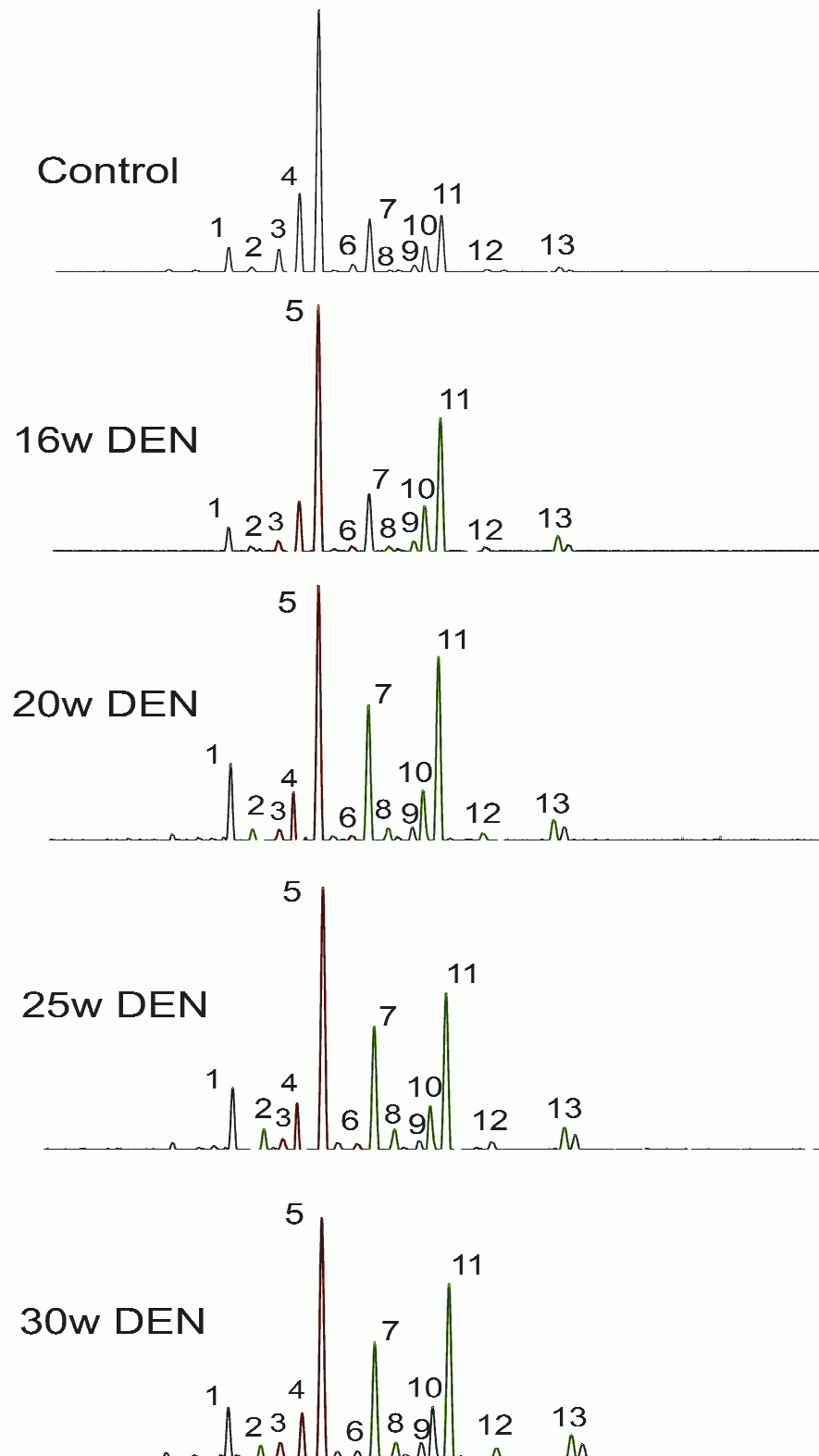


**Figure 1: Representative serum N-glycosylation patterns of control WT mice and WT mice chronically injected with diethylnitrosamine for 16w, 20w, 25w and 30w.** Green: significantly increased in relative peak height compared to control mice; red: significantly decreased in relative peak height compared to control mice.

### Treatment study

We compared the serum *N*-glycosylation patterns of mice injected with DEN for 25w and subsequently treated with 5D11D4 for 5w with the serum *N*-glycosylation patterns of mice injected with DEN for 25w and treated with control IgG for 5w. The latter group shows the same alterations (including a supplementary significant increase of peak 12) compared to 25w DEN alone indicating that IgG treatment did not influence the glycomic phenotype.

7 of the 11 altered peaks, observed after 25w of DEN and 5w of IgG, evolved back into the normal direction after 5w treatment with 5D11D4 i.e. they significantly increased or decreased in peak height into the direction observed in control mice (fig. 2) (for *P* values, see table 1). Interestingly, the biantennary fucosylated glycans (peaks 6 and 7) that were significantly increased after chronic DEN-injections, did not decrease after 5D11D4-treatment indicating that improvement on fucosylation level was not achieved with 5D11D4.

We also compared the serum *N*-glycosylation patterns of WT mice injected with saline solution for 25w and subsequently treated with 5D11D4 with those of the control mice. None of the 13 peaks were significantly altered in peak height compared to control mice indicating that 5D11D4 on itself had no effect on the serum *N*-glycosylation patterns.

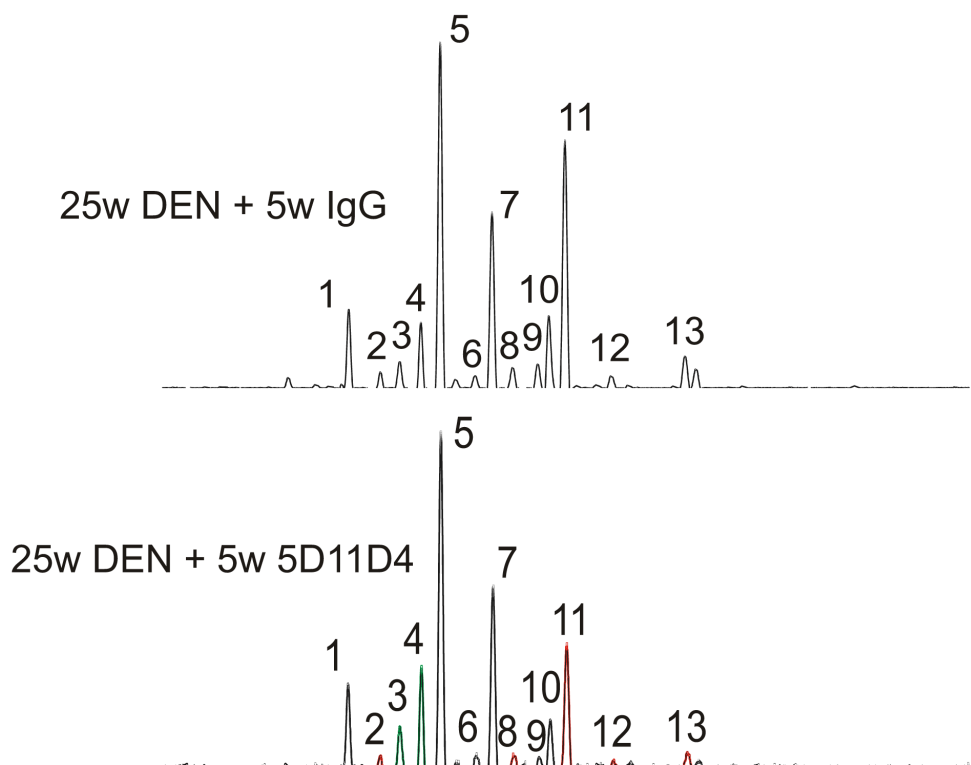


**Figure 2: Representative serum *N*-glycosylation patterns of WT mice chronically injected with DEN for 25w and subsequently treated with IgG for 5w and WT mice chronically injected with DEN for 25w and subsequently treated with 5D11D4 for 5w. Green: significantly increased in relative peak height compared to control IgG; red: significantly decreased in relative peak height compared to control IgG.**

## *PIGF<sup>-/-</sup> study*

First, we compared the serum *N*-glycosylation patterns of *PIGF<sup>-/-</sup>* mice injected with saline solution for 25w with the control WT mice injected with saline solution for 25w. Even at this baseline level, already 6 peaks were significantly altered including a significant increase of two multi-antennary glycans (for *P*-values, see table 1).

Subsequently, we compared the serum *N*-glycosylation patterns of *PIGF<sup>-/-</sup>* mice injected with DEN for 20w and WT mice injected with DEN for 20w. In analogy with the treatment study, a normalization of the altered peaks was observed albeit not as elaborate as in the treatment study. The same conclusion can be drawn when comparing *PIGF<sup>-/-</sup>* mice injected with DEN for 30w with WT mice injected with DEN for 30w. A significant decrease of five peaks (peaks 2, 6, 7, 8 and 12) was observed (for *P* values, see table 1).

Alternatively, we also compared the serum *N*-glycosylation patterns of *PIGF<sup>-/-</sup>* mice injected with saline solution with the *PIGF<sup>-/-</sup>* mice injected with DEN for 20w and 30w. The same pattern of alterations was observed at both time points with a significant increase of peaks 1, 7, 8, 9, 10, 11, 12 and 13, whereas there was a significant decrease of peaks 2, 3, 4 and 5.

**Table 1: *N*-glycomic analysis in the DEN-study, treatment study and *PIGF<sup>-/-</sup>* study**

Study	Time point	Peak 1	Peak 2	Peak 3	Peak 4	Peak 5	Peak 6	Peak 7	Peak 8	Peak 9	Peak 10	Peak 11	Peak 12	Peak 13
DEN†	16w			↓*	↓**	↓**	↓**		↑**	↑*	↑**	↑**		↑**
	20w		↑*	↓**	↓**	↓**	↓**	↑**	↑**		↑*	↑**	↑*	↑**
	25w		↑**	↓**	↓**	↓**	↓**	↑*	↑**		↑*	↑**		↑**
	30w		↑*	↓**	↓**	↓**		↑**	↑**			↑**	↑**	↑**
Treatment‡	5w 5D11D4		↓*	↑**	↑*				↓*			↓**	↓*	↓**
<i>PIGF<sup>-/-</sup></i> ¶	baseline	↓**	↑**					↓**	↓*			↑**		↑**
	20wDEN	↓*			↑*	↑*		↓*	↓*					
	30wDEN		↓*				↓*	↓*	↓*				↓**	

↓: significantly decreased in abundance; ↑: significantly increased in abundance; \**P*<0.05; \*\**P*<0.01; †DEN: diethylnitrosamine, compared to control mice; ‡compared to 25w DEN and 5w IgG; ¶PIGF: Placental Growth Factor, compared to WT counterpart.

### Development of biomarkers for DEN-induced HCC

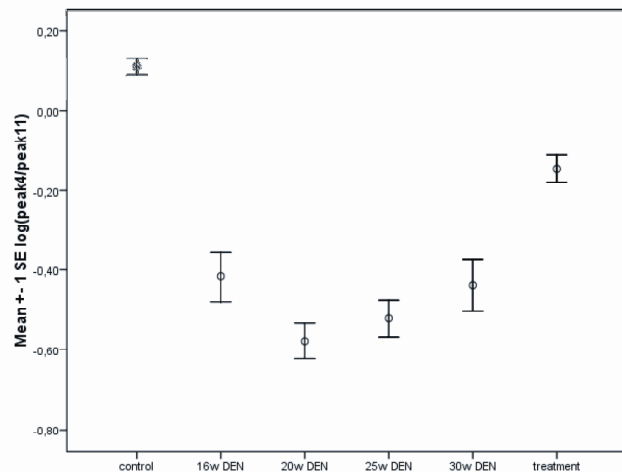
Based on the pattern of significantly altered peaks, we developed two biomarkers,  $\log(\text{peak4}/\text{peak11})$  and  $\log(\text{peak2}+\text{peak7}+\text{peak8})$ . Both biomarkers are expected to have a different mean value in the six groups investigated (single-factor ANOVA, *P*<0.001 for both markers). The first biomarker,  $\log(\text{peak4}/\text{peak11})$ , performed very well in identifying DEN-injected mice. This marker had a mean value of 0.11 ( $\pm 0.06$ ) in control mice and this value significantly decreased in mice injected with DEN for 16w (-0.42 ( $\pm 0.14$ )), 20w (-0.58 ( $\pm 0.09$ )), 25w (-0.52 ( $\pm 0.09$ )) and 30w (-0.44 ( $\pm 0.19$ )) (*P*<0.001 for all analyses, Tukey *post-hoc*). This marker had a perfect Area Under The Curve (100% sensitivity and 100% specificity) for the distinction of control and DEN-injected mice since there is no overlap in

marker score between the control and DEN-injected mice. The optimal cut-off was placed at -0.08. The mean value of the marker significantly increased in mice injected with DEN for 25w and treated with 5D11D4 for 5w compared to mice injected with DEN alone ( $P < 0.001$  for all analyses, Tukey *post-hoc*), but was still significantly decreased compared to control mice ( $P < 0.001$ , Tukey *post-hoc*) (fig. 3A).

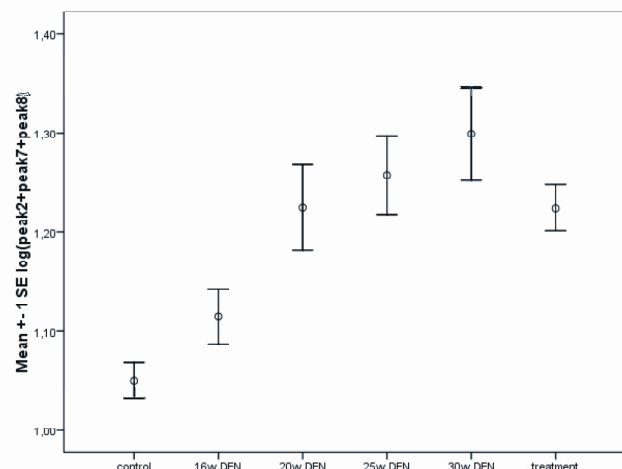
A second biomarker was developed by combining the three peaks that correlated significantly with tumor burden in DEN-injected and 5D11D4-treated mice (peak 2, peak 7 and peak 8). This biomarker had a mean score of 1.05 ( $\pm 0.05$ ) for control mice and 1.11 ( $\pm 0.06$ ) for mice injected with DEN for 16w. This mean value significantly increased in mice injected with DEN for 20w (1.23 ( $\pm 0.09$ )), 25w (1.26 ( $\pm 0.08$ )) and 30w (1.3 ( $\pm 0.13$ )) and mice treated with 5D11D4 for 5w after 25w of DEN (1.22 ( $\pm 0.06$ )) compared to control mice ( $P = 0.033$ ,  $P = 0.008$ ,  $P < 0.001$  and  $P = 0.009$ , respectively, Tukey *post-hoc*). Finally, a significant increase in mean value was observed for mice injected with DEN for 30w compared to mice injected with DEN for 16w ( $P = 0.01$ , Tukey *post-hoc*) (fig. 3B).

**Figure 3: A) Error bars (standard error of mean) represent the evolution of the value of the biomarker ( $\log(\text{peak4}/\text{peak11})$ ) in control, DEN-injected and 5D11D4-treated mice.** There was a significant decrease in biomarker score in DEN-treated mice ( $P < 0.001$ , Tukey *post-hoc*). This score subsequently significantly increased when mice were treated with 5D11D4 for 5w ( $P < 0.001$ , Tukey *post-hoc*), but was still significantly lower than the score in control mice ( $P < 0.001$ , Tukey *post-hoc*). **B) Error bars (standard error of mean) represent the evolution of the biomarker  $\log(\text{peak2}+\text{peak7}+\text{peak8})$  in control, DEN-injected and 5D11D4-treated mice.** There was a significant increase of marker score in mice injected with DEN for 20w, 25w and 30w compared to control mice ( $P = 0.033$ ,  $P = 0.008$  and  $P < 0.001$ , respectively, Tukey *post-hoc*) and also after 16w of DEN compared to 30w of DEN ( $P = 0.01$ , Tukey *post-hoc*).

A



B





### Ets-1 staining

Results are summarized in tables 2 and 3. These tables show the number of Ets-1 positive nuclei per mm<sup>2</sup> in the tumor, around the tumor and in non-HCC tissue. Overall, a significant reduction of the number of Ets-1 positive cells was observed in *PIGF*<sup>-/-</sup> and 5D11D4-treated mice compared to their respective WT and IgG treated counterpart in all three areas investigated (fig. 4).

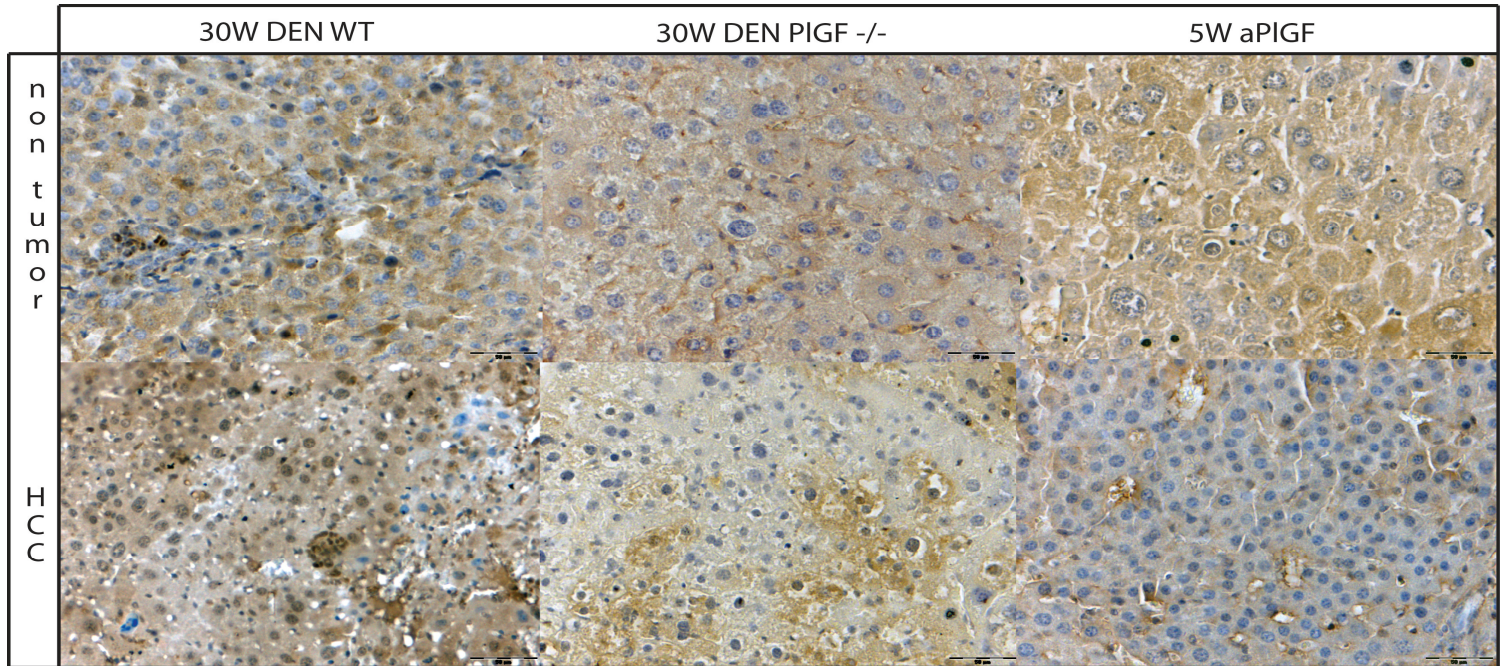


**Figure 4: The number of Ets-1 positive cells significantly decrease in 5D11D4-treated and *PIGF*<sup>-/-</sup> mice.** Representative images (x40) of Ets-1 stained liver sections in non-tumor tissue (*Top*) and in and around the tumor (*Bottom*) after 30w of DEN in WT and *PIGF*<sup>-/-</sup> mice and in mice treated with 5D11D4 (aPIGF) for 5w after 25w of DEN-injections.

**Table 2: summary of the Ets-1 staining in the DEN group and *PIGF*<sup>-/-</sup> group**

	Control			16w DEN <sup>¶</sup>	20w DEN			25w DEN	30w DEN		
	WT	<i>PIGF</i> <sup>†</sup>	<i>P</i> *	WT	WT	<i>PIGF</i> <sup>-/-</sup>	<i>P</i> *	WT	WT	<i>PIGF</i> <sup>-/-</sup>	<i>P</i> *
Inside the tumor	NA	NA		13.2 (±6.2)	114.6 (±56)	33.5 (±10.7)	<0.001	72.3 (±36.5)	102.5 (±21)	70.4 (±12.5)	0.02
Around the tumor	NA	NA		51.5 (±19.4)	133 (±58)	37.2 (±12.2)	<0.001	147.9 (±33.6)	128.2 (±24)	72 (±26.1)	<0.001
Non-HCC <sup>‡</sup> tissue	16.3 (±6.1)	18.5 (±12.1)	0.61	16.4 (±3.9)	48.1 (±21)	17 (±4.7)	<0.001	27.9 (±4.6)	29.9 (±9.1)	19 (±6.1)	<0.001

\*independent samples *t*-test, data are represented mean ± standard deviation, NA: not applicable, †PIGF: Placental Growth Factor, ‡HCC: hepatocellular carcinoma, ¶DEN: diethylnitrosamine

**Table 3: summary of the Ets-1 staining in the treatment study**

	25w DEN <sup>†</sup> + 5w IgG	25w DEN + 5w 5D11D4	<i>P</i> <sup>*</sup>
Inside the tumor	138.1 (±48.4)	42 (±9.2)	<0.001
Around the tumor	161.8 (±42)	57.9 (±13.5)	<0.001
Non-HCC <sup>‡</sup> tissue	37.6 (±14.1)	18 (±6.6)	<0.001

\*independent samples *t*-test, data are represented mean ± standard deviation, †DEN: diethylnitrosamine, ‡HCC: hepatocellular carcinoma

There was a good correlation between the value of our biomarker ( $\log(\text{peak4}/\text{peak11})$ ) and the Ets-1 data. However, the best correlation was found between this biomarker and the number of Ets-1 positive cells in non-HCC tissue ( $P=0.002$ ), whereas a borderline significant correlation was obtained between the biomarker and the number of Ets-1 positive cells around and in the tumor ( $P=0.088$  and  $P=0.085$ , respectively). The opposite situation was observed for the biomarker  $\log(\text{peak2}+\text{peak7}+\text{peak8})$ . A significant correlation was found with the number of Ets-1 positive cells around and in the tumor ( $P=0.028$  and  $P=0.02$ , respectively), whereas the correlation with the number of Ets-1 positive cells in non-HCC tissue was not significant ( $P=0.11$ ).

## Discussion

Mouse models of chronic liver disease produce large quantitative alterations of serum *N*-glycans. We did not only observe this in fibrotic models such as CCl<sub>4</sub> or common bile duct ligation [29], but also in this DEN-induced HCC-model virtually all serum *N*-glycans were significantly altered in abundance. This can be explained by the liver specificity of *N*-glycan alterations in mouse models of chronic liver disease [28]. In human liver disease, IgG is the main glycoprotein on which the glycomic changes occur [30, 31], but in mouse models of chronic liver disease, the impact of IgG *N*-glycosylation on total serum *N*-glycosylation is minimal, and the main alterations can be found on liver-produced proteins [28]. Not only is their a much lower IgG concentration in mice, the number and magnitude of the alterations on IgG are far less significant [28].

This was confirmed by a study similar to ours that also investigated *N*-glycomic changes in a DEN-induced HCC model [32]. They did not found any alteration of IgG glycan profiles in DEN-treated mice compared to controls. The methodology used was different to our study, they used three-week old female C57Bl/6 mice that were injected once a week for 6 weeks and then sacrificed at 23, 30, 36 and 48 weeks. However, HCC mainly occurs in men and this gender disparity can also be seen in mice [33]. DEN-administration causes a greater increase in interleukin-6 concentration in males than in females, probably due to estrogen-mediated inhibition of IL-6 production by Kupffer cells [33]. Moreover, C57Bl/6 mice are less sensitive to the development of HCC [34] and the pure strain is almost never used in HCC research. In our study, using male 129/Sv mice, the first HCC-nodules appeared at 20w and significant amounts of fibrosis were also present after 25 and 30 weeks of DEN-administration [26], whereas Lui *et al* saw the first HCC development only after 30w and no liver fibrosis was observed at any time point studied. Since human HCC mostly develops in a natural background of fibrosis, the model in our study seems to be more representative.

Although the serum *N*-glycosylation patterns can somewhat differ between two mouse strains, the overall pattern and abundances of the different glycans were similar between C57Bl/6 and 129/Sv mice. In the study of Lui *et al*, two peaks were significantly increased (these correspond to peak 4 and 11 in our study) and one peak was significantly decreased (correspond to peak 7 in our study) in DEN-injected mice. Surprisingly, in our study, peak 4 was consistently significantly decreased, whereas peak 7 was consistently significantly increased. Peak 4 is a glycan that is prominently decreased in fibrotic models [29] and this discrepancy between the two studies could therefore be explained by the presence of fibrosis in our HCC-model. Peak 7 is an important core-fucosylated glycan and an increase in core-fucosylation is well documented in HCC [35,36].

Important in the study of Lui *et al* was that they observed a strong up-regulated expression of *Mgat4a* in HCC-mice. This can be linked to the significant increase of peak 11 in our study. *Mgat4a* is the gene that codes for the GnT-IVa enzyme and together with GnT-V, they are mainly responsible for the induction of multi-antennary glycans. As indicated earlier, these enzymes are under the transcriptional control of Ets-1. In GnT-IVb deficient mice, Ets-1 expression is evoked and this considerably induces expression of GnT-IVa and -V to preserve *N*-glycan branch complexity [37].

Treatment with 5D11D4 produced a clear improvement on the *N*-glycomic level in which a trend towards normalization was observed. However, the *N*-glycosylation patterns of the 5D11D4-treated DEN mice were still significantly different from the *N*-glycan profiles of control mice. Of course, anti-angiogenic therapy can prevent tumor growth and cause shrinkage by depriving tumors from their blood supply, yet a complete disappearance of tumor mass will not be accomplished. Nevertheless, there was a strong reduction of Ets-1 positive cells after treatment with 5D11D4, indicating less transcription of enzymes responsible for multi-antennary glycans. The most elaborate changes were therefore observed in the multi-antennary glycan fraction with a strong decrease of all these glycans (peaks 11, 12 and 13). This can be explained by the positive effects of 5D11D4 on tumor size and burden as illustrated in [12]. In this way, Ets-1 might provide a possible link between the improvements on the *N*-glycomic level and the anti-angiogenic properties of 5D11D4 (fig.5).

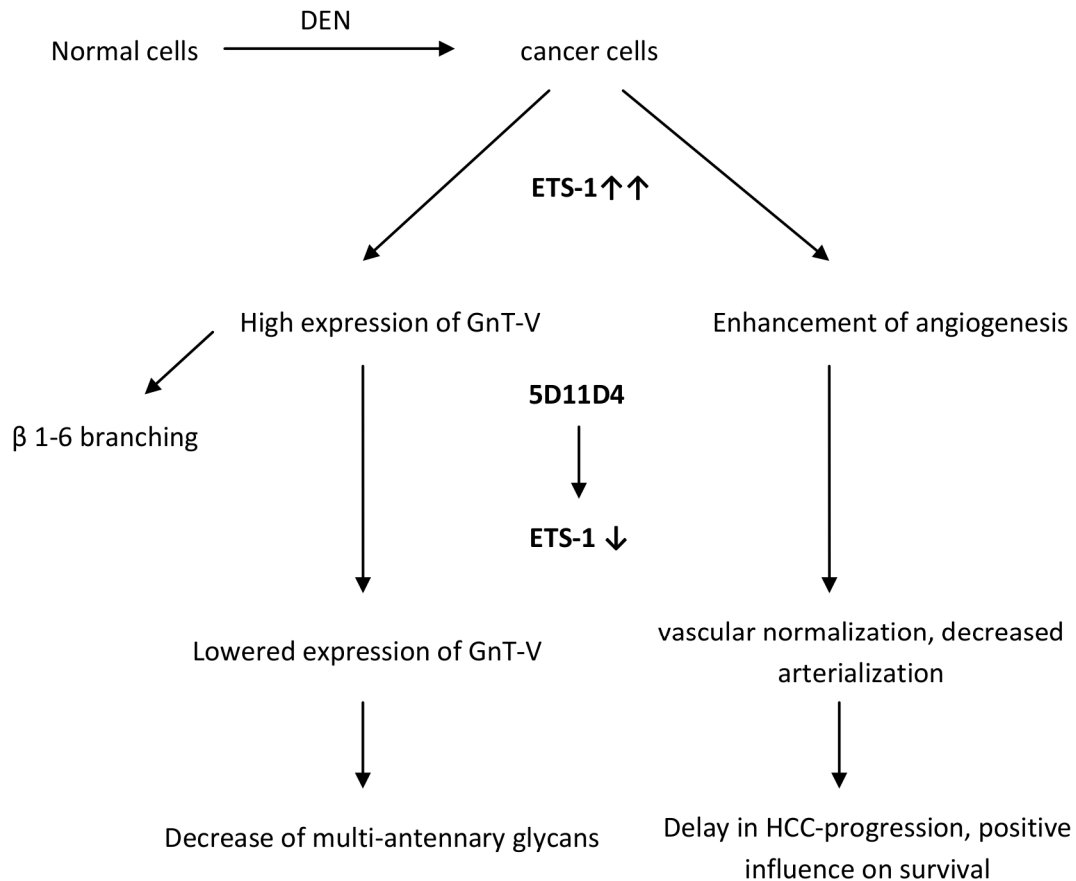


**Figure 5: Proposed model for implication of Ets-1 in the working mechanism of 5D11D4 as anti-angiogenic agent and down-regulator of multi-antennary glycans.** DEN, diethylnitrosamine; Ets-1, E26 transformation-specific sequence 1; GnT-V, *N*-acetylglucosaminyltransferase; HCC, hepatocellular carcinoma.

We have developed a biomarker ( $\log(\text{peak4}/\text{peak11})$ ) that described the abovementioned data very well. A strong decrease of the mean value was observed in DEN-injected mice with a peak after 20w and a significant increase of mean value in 5D11D4-treated mice, however still significantly lower than the control mice. Moreover, a good correlation was found between this marker and the Ets-1 data in all three areas investigated, but the correlation was only significant with the number of Ets-1 positive cells in non-HCC tissue. This suggests that this is a marker of the environment that becomes premalignant. The opposite situation was observed for the second biomarker,  $\log(\text{peak2}+\text{peak7}+\text{peak8})$ , the marker significantly correlated with the Ets-1 data around and in the tumor, but not in HCC-tissue. There was a linear increase in marker score from mice injected with DEN for 16w to mice injected with DEN for 30w and this correlated well with tumor burden. This marker can therefore be used as a tumor marker in DEN-injected and 5D11D4-treated mice.

Although the Ets-1 positive cells were equally strongly declined in *PIGF*<sup>-/-</sup> mice, improvement in the *N*-glycomic data did not follow. There was still a normalization trend, but not as explicit as in the treatment group and this correlated very well with the histological data in which the effects on mortality, tumor size and burden were less profound in the knock out model than in the treatment study [12]. When comparing control *PIGF*<sup>-/-</sup> mice with control WT mice, a

significant increase of multi-antennary glycans (peaks 11 and 13) were observed although Ets-1 levels were comparable. This indicates that, in *PIGF*<sup>-/-</sup> mice, other factors might influence the expression of GnT-IVa and it also can explain why multi-antennary glycans are not decreased in the knock out model injected with DEN, despite the significant lowering of Ets-1 level. Tumors that occur in the knock out model have the chance to adapt to an environment without PIGF. Therefore, these tumors might have a completely different phenotype than those in WT mice.

To our knowledge, this is the first study in which Ets-1 was evaluated in an orthotopic mouse model of HCC. Further study is needed to unambiguously provide evidence for the key role of Ets-1 in the working mechanism of 5D11D4 as a down-regulator of multi-antennary glycans on serum proteins and as an anti-angiogenic agent in HCC, for instance by working with Ets-1 deficient mice.

## References

- [1] Nordenstedt H, White DL, El-Serag HB. The changing pattern of epidemiology in hepatocellular carcinoma. *Dig Liver Dis* 2010;42 Suppl 3:S206-14.
- [2] Sherman M. Hepatocellular carcinoma: epidemiology, risk factors, and screening. *Semin Liver Dis* 2005;25:143-154.
- [3] Piccinino F, Sagnelli E, Pasquale G, Giusti G. Complications following percutaneous liver biopsy. A multicentre retrospective study on 68,276 biopsies. *J Hepatol* 1986;2:165-173.
- [4] Callewaert N, Van Vlierberghe H, Van Hecke A, Laroy W, Delanghe J, Contreras R. Noninvasive diagnosis of liver cirrhosis using DNA sequencer-based total serum protein glycomics. *Nat Med* 2004;10:429-434.
- [5] Liu XE, Desmyter L, Gao CF, et al. N-glycomic changes in hepatocellular carcinoma patients with liver cirrhosis induced by hepatitis B virus. *Hepatology* 2007;46:1426-1435.
- [6] Xu J, Yun X, Jiang J, et al. Hepatitis B virus X protein blunts senescence-like growth arrest of human hepatocellular carcinoma by reducing Notch1 cleavage. *Hepatology* 2010;52:142-154.
- [7] Shim JK, Lee YC, Chung TH, Kim CH. Elevated expression of bisecting N-acetylglucosaminyltransferase-III gene in a human fetal hepatocyte cell line by hepatitis B virus. *J Gastroenterol Hepatol* 2004;19:1374-1387.
- [8] Yanagi M, Aoyagi Y, Suda T, Mita Y, Asakura H. N-Acetylglucosaminyltransferase V as a possible aid for the evaluation of tumor invasiveness in patients with hepatocellular carcinoma. *J Gastroenterol Hepatol* 2001;16:1282-1289.
- [9] Goldman R, Ressom HW, Varghese RS, et al. Detection of hepatocellular carcinoma using glycomic analysis. *Clin Cancer Res* 2009;15:1808-1813.
- [10] Maglione D, Guerriero V, Viglietto G, Dellibovi P, Persico M. Isolation of a human placenta cDNA coding for a protein related to the vascular permeability factor. *Proc Natl Acad Sci USA* 1991;88:9267-71.
- [11] Fischer C, Jonckx B, Mazzone M, et al. Anti-PIGF inhibits growth of VEGF(R)-inhibitor-resistant tumors without affecting healthy vessels. *Cell* 2007;131:463-475.
- [12] Van de Veire S, Stalmans I, Heindryckx F, et al. Further pharmacological and genetic evidence for the efficacy of PIGF inhibition in cancer and eye disease. *Cell* 2010;141:178-190.

- [13] Kang R, Saito H, Ihara Y, et al. Transcriptional regulation of the N-acetylglucosaminyltransferase V gene in human bile duct carcinoma cells (HuCC-T1) is mediated by Ets-1. *J Biol Chem* 1996; 271:26706-12.
- [14] Ko J, Miyoshi E, Noda K, et al. Regulation of the GnT-V Promoter by transcription factor Ets-1 in various cancer cell lines. *J Biol Chem* 1999; 274:22941-48.
- [15] Yamamoto H, Swoger J, Greene S, et al.  $\beta$ 1,6-N-acetylglucosamine-bearing N-glycans in human glioma: implications for a role in regulating invasivity. *Cancer Res* 2000; 60:134-42.
- [16] Chakraborty A, Kolesnikova N, Sousa Jde F, et al. Expression of c-Met-oncogene in metastatic macrophage x melanoma fusion hybrids: implication of its possible role on MSH-induced motility. *Oncol Res* 2003; 14:163-74.
- [17] Asada M, Furukawa K, Segawa K, Endo T, Kobata A. Increased expression of highly branched N-glycans at cell surface is correlated with the malignant phenotypes of mouse tumor cells. *Cancer Res* 1997; 57:1073-1080.
- [18] Dennis J, Laferté S, Waghorne C, Breitmann M, Kerbel R.  $\beta$ 1-6 branching of Asn-linked oligosaccharides is directly associated with metastasis. *Science* 1987; 236:582-85.
- [19] Dennis J, Laferté S. Oncodevelopmental expression of –GlcNAc $\beta$ 1-6Man $\alpha$ 1-6Man $\beta$ 1-branched asparagine-linked oligosaccharides in murine tissues and human breast carcinomas. *Cancer Res* 1989; 49:945-50.
- [20] Fernandes B, Sagman U, Auger M, Demetrio M, Dennis J.  $\beta$ 1-6 branched oligosaccharides as a marker of tumor progression in human breast and colon neoplasia. *Cancer Res* 1991; 51:718-23.
- [21] Sato Y. Role of ETS family transcription factors in vascular development and angiogenesis. *Cell Struct Funct* 2001; 26:19-24.
- [22] Wernert N, Raes MB, Lassalle P, et al. C-ets1 proto-oncogene is a transcription factor expressed in endothelial cells during tumor vascularization and other forms of angiogenesis in humans. *Am J Pathol* 1992;140:119-127.
- [23] Iwasaka C, Tanaka K, Abe M, Sato Y. Ets-1 regulates angiogenesis by inducing the expression of urokinase-type plasminogen activator and matrix metalloproteinase-1 and the migration of vascular endothelial cells. *J Cell Physiol*;169:522-531.
- [24] Tanaka K, Oda N, Iwasaka C, Abe M, Sato Y. Induction of Ets-1 in endothelial cells during reendothelialization after denuding injury. *J Cell Physiol* 1998;176:235-244.
- [25] Sato Y, Kanno S, Oda N, et al. Properties of two VEGF receptors, Flt-1 and KDR, in signal transduction. *Ann N Y Acad Sci* 2000;902:201-205.
- [26] Heindryckx F, Mertens K, Charette N, et al. Kinetics of angiogenic changes in a new mouse model for hepatocellular carcinoma. *Mol Cancer* 2010;9:219.
- [27] Laroy W, Contreras R, Callewaert N. Glycome mapping on DNA sequencing equipment. *Nat Protoc* 2006;1:397-405.
- [28] Blomme B, Van Steenkiste C, Callewaert N, Van Vlierberghe H. Alterations of serum protein N-glycosylation in two models of chronic liver disease are hepatocyte and not B cell driven. Accepted for publication in *Am J Physiol Gastrointest Liver Physiol*.
- [29] Blomme B, Van Steenkiste C, Vanhuyse J, Colle I, Callewaert N, Van Vlierberghe H. Impact of elevation of total bilirubin level and etiology of the liver disease on serum N-glycosylation patterns in mice and humans. *Am J Physiol Gastrointest Liver Physiol* 2010;298:G615-624.
- [30] Klein A, Carre Y, Louvet A, Michalski JC, Morelle W. Immunoglobulins are the major glycoproteins involved in the modifications of total serum N-glycome in cirrhotic patients. *Proteomics Clin Appl* 2010;4:379-93.

- [31] Vanderschaeghe D, Laroy W, Sablon E, et al. GlycoFibroTest is a highly performant liver fibrosis biomarker derived from DNA sequencer-based serum protein glycomics. *Mol Cell Proteomics* 2009;8:986-994.
- [32] Liu XE, Dewaele S, Vanhooren V, et al. Alteration of N-glycome in diethylnitrosamine-induced hepatocellular carcinoma mice: a non-invasive monitoring tool for liver cancer. *Liver Int* 2010;30:1221-8.
- [33] Naugler WE, Sakurai T, Kim S, et al. Gender disparity in liver cancer due to sex differences in MyD88-dependent IL-6 production. *Science* 2007;317:121-124.
- [34] Vesselinovitch SD, Mihailovich N. Kinetics of diethylnitrosamine hepatocarcinogenesis in the infant mouse. *Cancer Res* 1983;43:4253-4259.
- [35] Comunale MA, Lowman M, Long RE, et al. Proteomic analysis of serum associated fucosylated glycoproteins in the development of primary hepatocellular carcinoma. *J Proteome Res* 2006;5:308-315.
- [36] Ang IL, Poon TC, Lai PB, et al. Study of serum haptoglobin and its glycoforms in the diagnosis of hepatocellular carcinoma: a glycoproteomic approach. *J Proteome Res* 2006;5:2691-2700.
- [37] Takamatsu S, Antonopoulos A, Ohtsubo K, et al. Physiological and glycomic characterization of N-acetylglucosaminyltransferase-IVa and -IVb double deficient mice. *Glycobiology* 2010;20:485-497.

# Chapter 3.4

## ***“N-glycosylation based biomarker distinguishing NASH from steatosis independently of fibrosis in non-alcoholic fatty liver disease”***

**Bram Blomme**<sup>1</sup>, Sven Francque<sup>2</sup>, Eric Trépo<sup>3</sup>, Louis Libbrecht<sup>4</sup>, Dieter Vanderschaeghe<sup>5,6</sup>, An Verrijken<sup>7</sup>, Piet Pattyn<sup>8</sup>, Yves Van Nieuwenhove<sup>8</sup>, Dirk Van De Putte<sup>8</sup>, Anja Geerts<sup>1</sup>, Isabelle Colle<sup>1</sup>, Joris Delanghe<sup>6</sup>, Christophe Moreno<sup>3</sup>, Luc Van Gaal<sup>7</sup>, Nico Callewaert<sup>5</sup>, Hans Van Vlierberghe<sup>1</sup>

<sup>1</sup>Department of Hepatology and Gastroenterology, Ghent University Hospital, Ghent, Belgium

<sup>2</sup>Department of Hepatology and Gastroenterology, Antwerp University Hospital, Antwerp, Belgium

<sup>3</sup>Department of Gastroenterology and Hepatopancreatology, Erasmus Hospital, Université Libre de Bruxelles, Brussels, Belgium

<sup>4</sup>Department of Pathology, Ghent University Hospital, Ghent, Belgium

<sup>5</sup>Unit for Molecular Glycobiology, Department for Molecular Biomedical Research, VIB, Ghent University, Ghent, Belgium

<sup>6</sup>Department of Clinical Biology, Microbiology and Immunology, Ghent University Hospital, Ghent, Belgium

<sup>7</sup>Department of Endocrinology, Diabetology and Metabolic Diseases, Antwerp University Hospital, Antwerp, Belgium

<sup>8</sup>Department of Surgery, Ghent University Hospital, Ghent, Belgium

**Submitted to Liver International, in revision**



## Abstract

**Background:** Non-alcoholic fatty liver disease (NAFLD) is a spectrum of disorders ranging from steatosis to non-alcoholic steatohepatitis (NASH). Steatosis of the liver is benign, whereas NASH can progress to cirrhosis or even hepatocellular carcinoma. Currently, a liver biopsy is the only validated method to distinct steatosis from NASH. **Aim:** The objective of this study was to identify a NASH marker based on the *N*-glycosylation of serum proteins. **Methods:** *N*-glycosylation patterns were assessed using DNA-sequencer-assisted fluorophore-assisted capillary electrophoresis and compared with histology. **Results:** Initially, a biomarker ( $\log[\text{NGA2F}]/[\text{NA2}]$ ) was developed based on the results obtained in 51 obese non-alcoholic patients scheduled for bariatric surgery. This biomarker performed the best in a multivariate analysis in distinguishing NASH from steatosis compared to twelve currently used biomarkers. The biomarker was validated in a cohort of 224 NAFLD patients. In both cohorts, a good correlation was observed between our biomarker and the amount of lobular inflammation, whereas no correlation was found with the fibrotic stage. The *N*-glycan profile of immunoglobulin G (IgG) in the NASH population confirmed the important undergalactosylation present in these patients. The mobility of the  $\gamma$ -globulin fraction during serum electrophoresis is largely dependent on this undergalactosylation of IgG and we found a significant slower migration time of  $\gamma$ -globulins in NASH patients on clinical capillary electrophoresis equipment in the pilot study. **Conclusions:** our glycomarker specifically recognizes liver inflammation in obese individuals which is the main trigger for the development of steatohepatitis and can differentiate between simple steatosis and NASH.

**Keywords:** Inflammation; Glycomics; Immunoglobulin G; Electrophoresis, Capillary

## Introduction

The prevalence of obesity is increasing dramatically in Western countries. Overnutrition and physical inactivity has led to an overweight population that reaches epidemic proportions. In the United States alone, one third of the population is obese (Body Mass Index (BMI) > 30) [1]. Obese patients are prone to develop steatosis or steatohepatitis of the liver. Steatosis is a rather benign condition, but non-alcoholic steatohepatitis (NASH) can develop into cirrhosis and hepatocellular carcinoma (HCC) in 10% to 15% of the patients [2].

In this respect, it is of crucial importance to distinguish both liver conditions in the obese population. A liver biopsy is still the golden standard despite the well-known complications such as intraperitoneal hemorrhage, puncture of the gallbladder or pneumothorax. Non-invasive alternatives including ultrasonography or biochemical markers can give an indication of the degree of steatosis, but they can not make the distinction between NASH and simple steatosis [3]. Several biochemical variables have been suggested to make this distinction. These biomarkers can be divided into anthropomorphic variables such as BMI and waist-to-hip ratio (WHR) and biochemical variables including Homeostatic Model Assessment (HOMA) index, serum adiponectin level, alanine aminotransferase (ALT), gamma-glutamyl transferase (GGT), serum cholesterol level, serum high density lipoproteins (HDL) level, serum triglycerides (TG) level and serum uric acid level [4-12]. The current best serological marker for NASH is caspase-cleaved cytokeratin-18 (CK-18). It predicts histological NASH with 70% sensitivity and 83.7% specificity with an area under the curve (AUC) of 0.71 [13]. This is the highest AUC for the diagnosis of NASH patients of all single markers. However, CK-18 is not specific for NASH. Caspase-generated CK-18 fragments are released during hepatocyte apoptosis, a fundamental process in virtually all acute and chronic liver diseases that are characterized by inflammation, steatosis, or fibrosis [14].

Glycomics aims at determining the abundance of the different glycan structures in a quantitative way in a particular biofluid, mostly serum or plasma. It has previously shown its diagnostic value in cirrhotic and HCC patients [15, 16]. The GlycoFibroTest is a similar marker to monitor fibrotic patients in which agalactosylated glycans play an important role. These glycans lack one or both galactoses in the glycan structure, they can only be found on Immunoglobulin G (IgG) and gradually augment with increasing METAVIR-stages [17]. In fact, IgG is the glycoprotein on which the main alterations occur in human chronic liver disease [18].

The mechanism of NASH is poorly understood. It is thought to be immune-mediated and inflammatory stress runs as a second hit in the pathophysiology of NASH [19]. As the distinction between NASH and steatosis is mainly inflammation-related, we investigated whether the agalacto-IgG component could be used to distinguish both patient populations.

## Patients and methods

### Patients

275 NAFLD patients from three Belgian academic centres (Ghent University Hospital, Antwerp University Hospital and Erasmus Hospital Brussels) were included in this study. First, a pilot study (Ghent) was conducted on 51 chronically obese patients that were scheduled for bariatric surgery. Subsequently, the results found in this cohort of patients were validated in two independent cohorts of 50 (Brussels) and 174 (Antwerp) NAFLD patients. The validation study also consisted out of patients that were scheduled for bariatric surgery (n=51; 22.8%), but a large part were patients that were diagnosed with NAFLD through a percutaneous liver biopsy without surgery (n=173; 77.2%). Patients were selected based on clinical data such as BMI (>30 kg/m<sup>2</sup>) and the absence of high amount of alcohol consumption (<200 g per week for men and <100 g for women) and were also tested and found negative for viral hepatitis, auto-immune and cholestatic conditions. All patients signed an informed consent. The Ethical Committee of Ghent University Hospital approved the protocols.

In the pilot study, anthropomorphic data (BMI, WHR) and biochemical markers (serum adiponectin level, ALT, GGT, HDL, TG, serum cholesterol level, serum uric acid level, serum ferritin level, HOMA-index, C-reactive protein (CRP) and CK-18) were determined in every patient. In the validation study, biochemical data was limited to HOMA-index, CRP and CK-18 level of all patients. The HOMA-index was calculated as: [fasting insulin concentration (μU/mL) X fasting glucose concentration (mmol/L)/22.5]. ALT, GGT, HDL, TG, cholesterol, uric acid, glucose and CRP were determined in serum using routine photometric tests on a Modular P800 (Roche Diagnostics GmbH, Mannheim, Germany). Insulin and ferritin were determined in serum on a Modular E170 (Roche Diagnostics GmbH, Mannheim, Germany). Two Enzyme-Linked Immuno Sorbant Assays were used to determine the serum concentration of CK-18 (PEVIVA AB, Bromma, Sweden) and adiponectin (R&D Systems, Minneapolis, MN, USA). An aliquot of serum was also immediately frozen for glycomic analysis and stored at -20 °C until further use.

### Histological analysis

In the pilot study, a wedge liver biopsy was carried out during the planned bariatric procedure (mean diameter 86.2 mm (±50)), whereas a tru-cut liver biopsy was performed on bariatric surgery patients in the validation study. A routine Menghini liver biopsy was carried out in the validation study on the NAFLD patients that were not operated. Mean diameter of the needle biopsies was 18.0 mm (±7). Slides were stained with haematoxylin-eosin and picosirius red. Patients were diagnosed blindly by a pathologist (L.L.) based on classical histopathological features such as inflammation, ballooning, lobular inflammation and the pattern of fibrosis. The NAFLD activity score (NAS) was used to classify the NAFLD patients [20]. Minimal steatosis (under 5% - score 0) was separated from mild steatosis (5%-33% - 1), moderate steatosis (>33%-66% - 2) and severe steatosis (>66% - 3). Lobular inflammation was assessed according to the number of inflammatory foci at a magnification of 200x: no foci (0), <2 foci (1), 2-4 foci (2) and >4 foci (3). Ballooning degeneration was also scored: none (0), few balloon cells (1), prominent ballooning (2). NAS of ≥5 correlates with a

diagnosis of NASH and biopsies with scores less than 3 were diagnosed as simple steatosis. Scores of 3 and 4 correlate with borderline NASH.

### IgG depletion

IgG depletion was performed as previously described with modifications (protein A/G was used in stead of protein A) [21]. This analysis is important for the interpretation of the serum protein electrophoresis in which we specifically study the migration of the  $\gamma$ -globulin fraction.

### Glycomic analysis

Blood was collected at the day the biopsy was performed. The *N*-glycans present in 5  $\mu$ l of serum or pure IgG eluate were released from the proteins with peptide *N*-glycanase F. Subsequently, the glycans are fluorescently labeled and desialylated. DNA sequencer-assisted fluorophore-assisted capillary electrophoresis technology was used to profile the labeled glycans. For an elaborate description of the protocol, we refer to Laroy *et al* [22]. Thirteen peaks were present in the total serum protein electropherogram, whereas only seven peaks were present in the IgG electropherogram (fig. 1). The height of every peak was quantified to obtain a numerical description of the profiles and these were normalized to the total intensity of the measured peaks (represented as a percentage of the total peak height). These data were analyzed with SPSS 16.0 software (SPSS, Chicago, IL, USA). Structural characterization was done as described [15].

### Serum protein electrophoresis

Serum protein electrophoresis was performed using a Capillarys 2<sup>TM</sup> CE system (Sebia, Paris, France) as previously described [23]. Proteins are detected at the cathodic end (deuterium lamp; 200 nm) as 5 fractions ( $\gamma$ -,  $\beta$ -,  $\alpha$ 2-,  $\alpha$ 1-globulines and albumin, which elutes last) that are automatically quantified as percentages of the total signal. The electrophoretic mobility of the  $\gamma$ -fraction was assessed by calculating the difference between the elution times at the points where the  $\gamma$ - and albumin fraction reached their maximum optical density at 200 nm. Albumin is not subject to charge differences or polymorphisms. Therefore, it can be used as an internal standard to correct for migration differences inherent to capillary electrophoresis.

### Statistical analysis

Data are presented as mean  $\pm$  standard deviation. Statistical analysis was performed by a single-factor ANOVA in three groups (steatosis, borderline NASH and NASH) or otherwise indicated (independent samples *t*-test). *Post-hoc* tests were performed using Tukey HSD tests. In the pilot study, a multiple linear regression analysis was performed including all variables that were significant in the univariate analysis. The degree of linear relationship

between two variables was measured with the Pearson correlation test. *P* values < 0.05 were considered significant in all analyses.

## Results

### Pilot study

#### *Clinical and histological findings*

The clinical and histological findings are summarized in Tables 1 and 2.

**Table 1: Anthropomorphic and biochemical data of the pilot study population (n=51)**

Patients scheduled for bariatric surgery					
	Normal liver + steatosis (n=27)	Borderline NASH (n=10)	NASH (n=14)	Univariate <sup>1</sup>	Multivariate <sup>2</sup>
Male/female	3/24	1/9	5/9	NA	
BMI (kg/m <sup>2</sup> )	38.6 (±6.9)	41.6 (±5.4)	43.5 (±9.0)	0.121	
WHR	0.9 (±0.08)	0.97 (±0.1)	0.98 (±0.08)	<b>0.024</b>	0.78
HOMA-index	0.64 (±0.63)	1.3 (±1.5)	2.11 (±2.4)	<b>0.015</b>	0.15
Adiponectin (µg/ml)	4.3 (±7.3)	4.0 (±5.8)	2.4 (±1.96)	0.637	
ALT (IU/l)	24.2 (±10.2)	31.3 (±17.2)	71.4 (±109.9)	0.052	
GGT (U/l)	20.1 (±10.0)	36.6 (±24.8)	61.1 (±45.0)	<b>&lt;0.001</b>	0.71
Cholesterol (mmol/l)	197.1 (±35.3)	194.6 (±34.5)	197.4 (±53.4)	0.984	
HDL (mg/dl)	60.7 (±12.2)	56.0 (±14.5)	41.7 (±12.2)	<b>0.001</b>	0.173
TG (mg/dl)	126.4 (±68.1)	193.3 (±57.3)	203.0 (±122.2)	<b>0.014</b>	0.139
Uric Acid (mg/dl)	5.3 (±1.3)	5.4 (±1.7)	6.3 (±2.1)	0.163	
Ferritin (ng/ml)	108 (±179.2)	151.1 (±132.1)	238.1 (±229.8)	0.144	
CK-18 (U/l)	161.7 (±56.3)	233.8 (±116.5)	635.3 (±1115.8)	0.065	
Glycomarker	-0.89 (±0.16)	-0.79 (±0.22)	-0.65 (±0.25)	<b>0.003</b>	<b>0.069</b>
CRP (mg/dl)	0.53 (±1.21)	0.36 (±0.45)	0.23 (±0.24)	0.6	

Mean (±SD) <sup>1</sup>*P*-value (single-factor ANOVA) <sup>2</sup>*P*-value (multiple linear regression analysis) NA: Not Applicable

**Table 2: Histological findings in the pilot study cohort (n=51)**

Histological feature	Category	Normal (n=12)	Steatosis (n=15)	Borderline NASH (n=10)	NASH (n=14)
		Number of biopsy specimen (%)			
Steatosis	No (<5%)	12 (100%)	1 (6.7%)	0 (0%)	0 (0%)
	Mild (5%-33%)	0 (0%)	10 (66.6%)	3 (30%)	0 (0%)
	Moderate (>33%-66%)	0 (0%)	4 (26.7%)	5 (50%)	5 (35.7%)
	Severe (>66%)	0 (0%)	0 (0%)	2 (20%)	9 (64.3%)
Lobular inflammation	No foci	12 (100%)	15 (100%)	5 (50%)	0 (0%)
	<2 foci	0 (0%)	0 (0%)	5 (50%)	9 (64.3%)
	2-4 foci	0 (0%)	0 (0%)	0 (0%)	4 (28.6%)
	>4 foci	0 (0%)	0 (0%)	0 (0%)	1 (7.1%)
Ballooning	No	12 (100%)	15 (100%)	2 (20%)	0 (0%)
	Few balloon cells	0 (0%)	0 (0%)	8 (80%)	7 (50%)
	Prominent ballooning	0 (0%)	0 (0%)	0 (0%)	7 (50%)
Fibrosis stage	0 = none	12 (100%)	15 (100%)	6 (60%)	2 (14.3%)
	1 = mild, perisinusoidal	0 (0%)	0 (0%)	4 (40%)	10 (71.4%)
	2 = perisinusoidal and portal/periportal	0 (0%)	0 (0%)	0 (0%)	2 (14.3%)
	3 = bridging fibrosis	0 (0%)	0 (0%)	0 (0%)	0 (0%)
	4 = cirrhosis	0 (0%)	0 (0%)	0 (0%)	0 (0%)

### *Glycomic analysis*

#### *Total serum protein*

*N*-glycomic analysis of the glycans present in total serum showed one glycan (peak 1, NGA2F) that was significantly altered in abundance ( $P=0.001$ ). *Post-hoc* tests revealed that peak 1 is significantly increased in NASH patients compared to steatosis patients ( $P<0.001$ ) (fig. 1).

#### *IgG fraction*

*N*-glycomic analysis of the glycans present on IgG revealed three glycans (NGA2F, NGA2FB and NA2F) of which the abundance were significantly altered ( $P<0.001$ ,  $P=0.004$  and  $P<0.001$ , respectively). *Post-hoc* tests revealed that peak 1 (NGA2F) and peak 2 (NGA2FB) were significantly increased in NASH patients in comparison to the borderline NASH and steatosis group ( $P=0.039$  and  $P<0.001$  for NGA2F and  $P=0.031$  and  $P=0.003$  for NGA2FB, respectively). In contrast, *post-hoc* tests revealed that peak 6 (NA2F) is significantly decreased in NASH patients and borderline NASH patients compared to the steatosis group ( $P<0.001$  and  $P=0.043$ , respectively) (fig. 1).

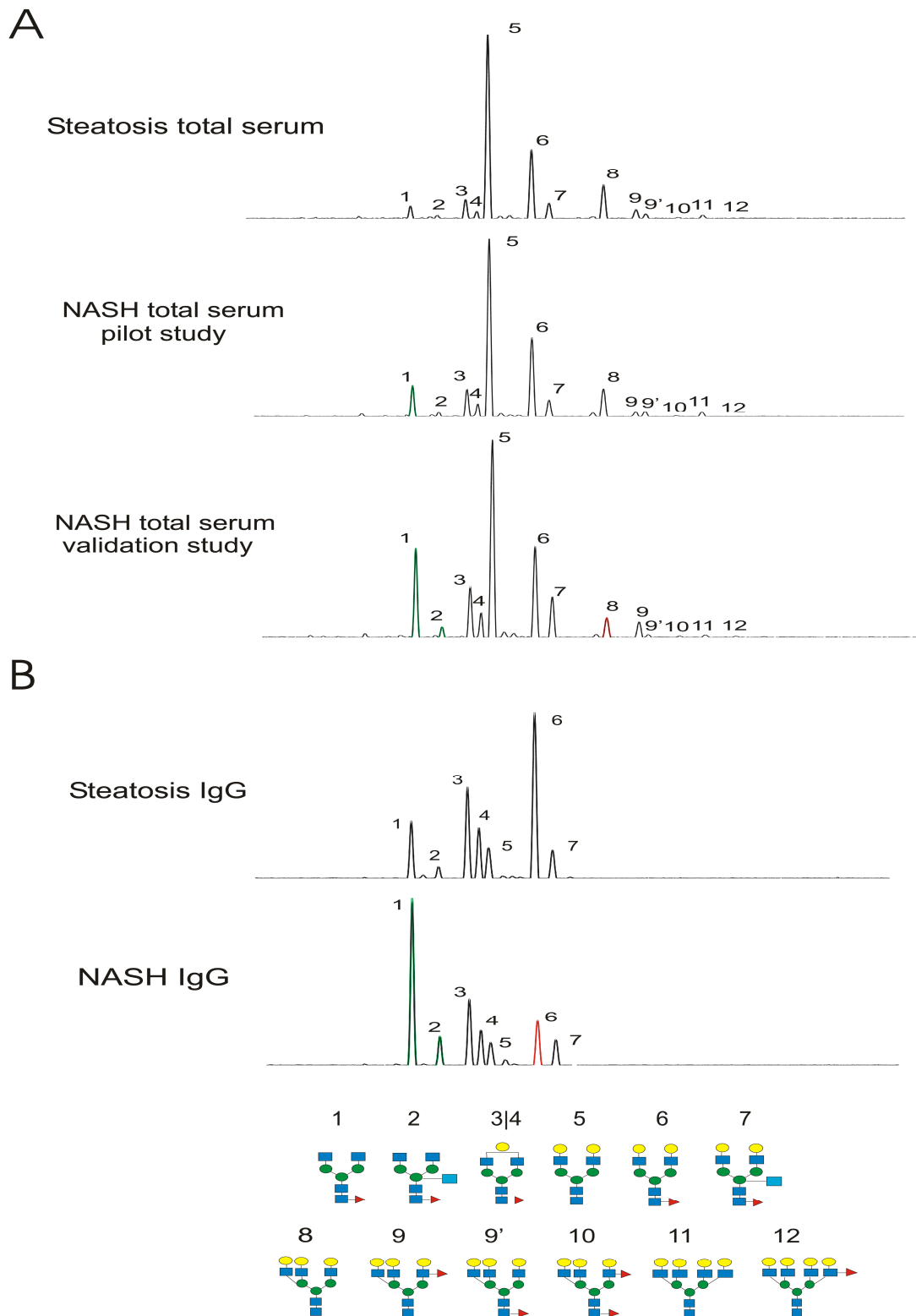


**Figure 1. The structures of the *N*-glycan peaks in the total serum (A) and IgG (B) electropherogram of steatosis and NASH patients.** Peak 1 is an agalacto, core- $\alpha$ -1,6-fucosylated biantennary (NGA2F), peak 2 is an agalacto, core- $\alpha$ 1,6-fucosylated bisecting biantennary (NGA2FB), peak 3 and peak 4 are single agalacto, core- $\alpha$ -1,6-fucosylated biantennaries (NG1A2F), peak 5 is a bigalacto, biantennary (NA2), peak 6 is a bigalacto, core- $\alpha$ -1,6-fucosylated biantennary (NA2F), peak 7 is a bigalacto, core- $\alpha$ -1,6-fucosylated bisecting biantennary (NA2FB), peak 8 is a triantennary (NA3), peak 9 is a branching  $\alpha$ 1,3-fucosylated triantennary (NA3Fb), peak 9' is a core- $\alpha$ -1,6-fucosylated triantennary (NA3Fc), peak 10 is branching  $\alpha$ 1,3-fucosylated and core  $\alpha$ -1,6-fucosylated triantennary (NA3Fbc), peak 11 is a tetra-antennary (NA4) and peak 12 is branching  $\alpha$ 1,3-fucosylated tetra-antennary (NA4Fb). The symbols used in the structural formulas are: square indicates  $\beta$ -linked *N*-acetylglucosamine (GlcNAc); yellow circle indicates  $\beta$ -linked galactose, triangle indicates  $\alpha/\beta$ -1,3/6-linked fucose; green circle indicates  $\alpha/\beta$ -linked mannose.

### *Development and evaluation of glycomarker for NASH*

The biomarker that was put forward was  $\log(\text{peak 1}/\text{peak 5})$ . Peak 5 (NA2) was used in the denominator because this glycan was borderline significantly decreased in total serum of NASH patients ( $P=0.056$ ). We first tested this glycomarker in the three patient groups of our pilot study population. The steatosis group had a mean score of  $-0.89 (\pm 0.16)$ , the borderline NASH group had a mean score of  $-0.78 (\pm 0.22)$  and the NASH group had a mean score of  $-0.65 (\pm 0.25)$  ( $P=0.003$ ). *Post-hoc* tests showed that this score was significantly increased in the NASH group compared to the steatosis group ( $P=0.002$ ). The AUC of this marker to distinguish NASH patients from borderline NASH and steatosis patients was 0.75 ([0.6-0.9]). This was similar to CK-18 that displayed an AUC of 0.67 ([0.49-0.84]) for the same analysis.

We also evaluated our glycomarker in the different categories of lobular inflammation. Patients with no inflammation had a mean score of  $-0.91 (\pm 0.16)$ , patients with a mild inflammation had a mean score of  $-0.75 (\pm 0.14)$  and patients with a moderate amount of inflammation had a mean score of  $-0.42 (\pm 0.05)$ . Only one patient had a severe inflammation and this patient had a score of  $-0.23$  ( $P=0.001$ ) (fig. 2). In contrast, there was no correlation between CRP value and glycomarker score (Pearson correlation test,  $P=0.594$ ).

### *Biomarkers of non-alcoholic steatohepatitis*

Twelve suggested biomarkers for NASH were evaluated in our pilot study population. Most of the markers were significantly or borderline significantly altered in the NASH population (for  $P$ -values, see table 1). Surprisingly, two markers that have been strongly linked with NASH, adiponectin and CK-18, were not significantly altered in our pilot population ( $P=0.637$  and  $P=0.065$ ).

Subsequently, all markers that were significant in the univariate analysis (HOMA, WHR, GGT, HDL, TG and our glycomarker) were evaluated in a multiple linear regression analysis. Our glycomarker showed a borderline significant result and displayed the lowest  $P$ -value of all markers (for  $P$ -values, see Table 1).

### *$\gamma$ -globulin migration in NASH and steatosis patients*

A mean  $\gamma$ -globulin migration of 159.9s ( $\pm 4.3$ ), 162.5 ( $\pm 4.5$ ) and 164.9 ( $\pm 4.8$ ) were obtained for the steatosis, borderline NASH and NASH group, respectively, and a single-factor ANOVA revealed that this difference is significant ( $P=0.006$ ). NASH patients had significantly slower migrating  $\gamma$ -globulins than the steatosis group as revealed by *post-hoc* tests ( $P=0.005$ ). ROC analysis showed that the AUC to distinguish NASH from borderline NASH and steatosis was 0.797 ([0.66-0.93]).

## Validation study

### *Clinical and histological findings*

The clinical and histological findings of the validation study are summarized in Tables 3 and 4, respectively.



**Table 3: Anthropomorphic and biochemical data of the validation study population (n=224)**

Patients scheduled for bariatric surgery (n=51) and diagnosed by liver biopsy (n=173)

	Normal liver + steatosis (n=78)	Borderline NASH (n=84)	NASH (n=62)	Univariate <sup>1</sup>
Male/female	35/43	37/47	28/34	NA
HOMA-index	2.79 (±2)	4.06 (±3.9)	5.38 (±3.8)	<0.001
CK-18 (U/l)	169.5 (±111.6)	170.2 (±99.3)	320.2 (±319.8)	<0.001
Glycomarker	-0.88 (±0.18)	-0.87 (±0.18)	-0.77 (±0.15)	<0.001
CRP (mg/dl)	0.84 (±1.3)	0.73 (±0.65)	0.82 (±0.89)	0.12

Mean (±SD) <sup>1</sup>P-value (single-factor ANOVA) NA: Not Applicable

**Table 4: Histological findings in the validation study cohort (n=224)**

Histological feature	Category	Normal (n=18)	Steatosis (n=60)	Borderline NASH (n=84)	NASH (n=62)
		Number of biopsy specimen (%)			
Steatosis	No (<5%)	18(100%)	7 (7.8%)	0 (0%)	0 (0%)
	Mild (5%-33%)	0 (0%)	73 (81.1%)	39 (46.4%)	2 (3.2%)
	Moderate (>33%-66%)	0 (0%)	10 (11.1%)	40 (47.6%)	30 (48.4%)
	Severe (>66%)	0 (0%)	0 (0%)	5 (6%)	30 (48.4%)
Lobular inflammation	No foci	18 (100%)	80 (88.9%)	18 (21.4%)	0 (0%)
	<2 foci	0 (0%)	10 (11.1%)	62 (73.8%)	40 (64.5%)
	2-4 foci	0 (0%)	0 (0%)	4 (4.8%)	22 (35.5%)
	>4 foci	0 (0%)	0 (0%)	0 (0%)	0 (0%)
Ballooning	No	18 (100%)	62 (68.9%)	6 (7.2%)	0 (0%)
	Few balloon cells	0 (0%)	28 (31.1%)	60 (70.2%)	26 (41.9%)
	Prominent ballooning	0 (0%)	0 (0%)	18 (22.6%)	36 (58.1%)
Fibrosis stage	0 = none	16 (88.9%)	61 (67.8%)	26 (31%)	18 (29%)
	1 = mild, perisinusoidal	2 (11.1%)	12 (13.3%)	22 (26.2%)	18 (29%)
	2 = perisinusoidal and portal/periportal	0 (0%)	9 (10%)	21 (25%)	9 (14.5%)
	3 = bridging fibrosis	0 (0%)	6 (6.7%)	13 (15.5%)	14 (22.6%)
	4= cirrhosis	0 (0%)	2 (2.2%)	2 (2.4%)	3 (4.9%)

### Glycomic analysis

#### Total serum protein

N-glycomic analysis of the glycans present in total serum revealed three glycans (peak 1, NGA2F; peak 2, NGA2FB and peak 8, NA3) that were significantly altered in abundance. The first two peaks were significantly increased in NASH patients ( $P=0.001$  and  $P=0.014$ , respectively). *Post-hoc* analysis revealed that NGA2F and NGA2FB were significantly increased compared to steatosis and borderline NASH patients ( $P=0.002$  and  $P=0.005$  respectively for NGA2F and  $P=0.017$  and  $P=0.046$  respectively for NGA2FB). In contrast, peak 8 (NA3) was significantly decreased in abundance in NASH patients ( $P=0.031$ ) and *post-hoc* analysis revealed that this difference was only significant with steatosis patients ( $P=0.029$ ).

*Validation of the biomarker (log(peak1/peak5))*

The steatosis group had a mean score of  $-0.88 (\pm 0.18)$ , the borderline NASH group had a mean score of  $-0.87 (\pm 0.18)$  and the NASH group had a mean score of  $-0.77 (\pm 0.15)$  ( $P < 0.001$ ). *Post-hoc* analysis revealed that the mean score of NASH patients was significantly increased compared to steatosis and borderline NASH patients ( $P < 0.001$  and  $P = 0.005$ , respectively). The AUC of this marker to distinguish NASH patients from borderline NASH and steatosis patients was 0.66 ([0.59;0.73]).

Similar to the pilot study, we also evaluated our biomarker in the different categories of lobular inflammation. NAFLD patients with no inflammation had a mean score of  $-0.9 (\pm 0.19)$ , NAFLD patients with a mild inflammation had a mean score of  $-0.83 (\pm 0.17)$  and NAFLD patients with a moderate amount of inflammation had a mean score of  $-0.76 (\pm 0.17)$  ( $P < 0.001$ ) (fig. 2). *Post-hoc* analysis revealed that NAFLD patients with a mild and moderate amount of inflammation had a significant higher mean score than patients with no inflammation ( $P = 0.001$  and  $P = 0.007$ , respectively). Again, no correlation was found between CRP level and the score of our glycomarker (Pearson correlation test,  $P = 0.12$ ). In contrast to the pilot study, we were able to perform an analysis of our biomarker in the different fibrotic stages. Mean score of patients staged 0 was  $-0.85 (\pm 0.19)$ , staged 1 was  $-0.82 (\pm 0.15)$ , staged 2 was  $-0.91 (\pm 0.18)$ , staged 3 was  $-0.82 (\pm 0.19)$  and staged 4 was  $-0.73 (\pm 0.18)$  ( $P = 0.098$ ) (fig. 2).

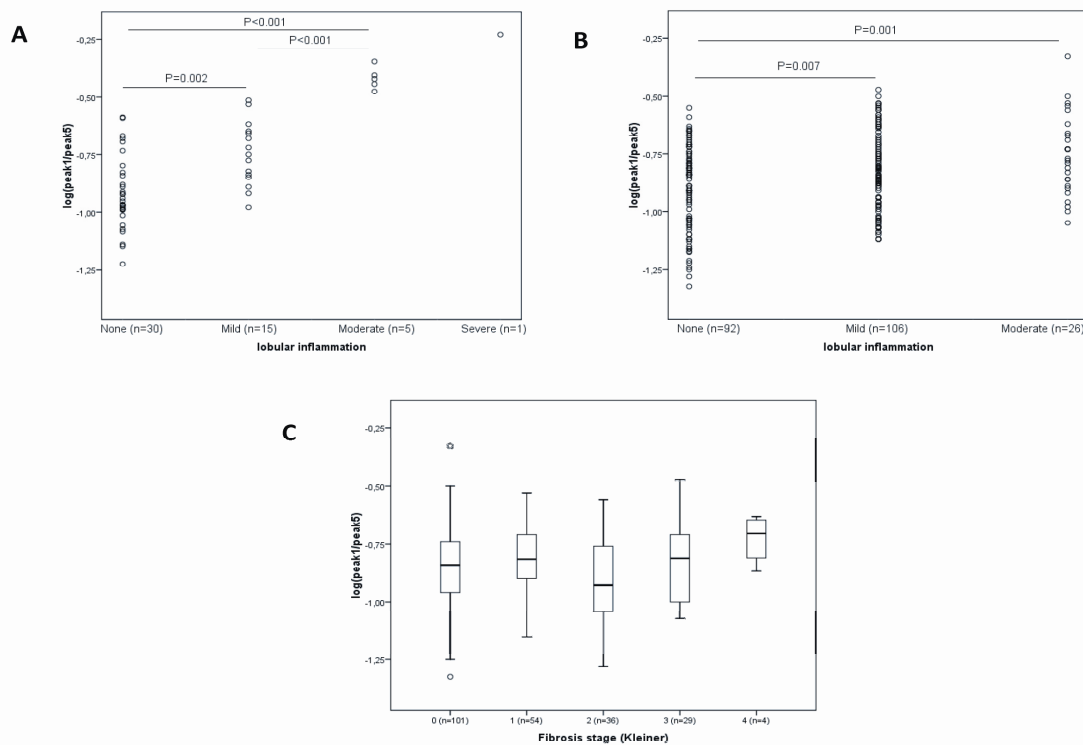


**Figure 2. Glycomarker correlates with stage of lobular inflammation, but not with stage of fibrosis.** Scatter dot of the glycomarker score in the different categories of lobular inflammation in the pilot study (A) and validation study (B). Boxplots of the glycomarker score in the different stages of fibrosis (validation study) (C).

### CK-18 analysis

The CK-18 concentration was determined in steatosis patients and in different fibrotic stages of borderline NASH and NASH patients (fig. 3). In the borderline NASH group, only the cirrhotic patient showed a considerable higher CK-18 value (460 U/l) in comparison to the steatosis group. In the NASH group, CK-18 clearly acted as a fibrosis marker with a stepwise increase in CK-18 concentration from fibrosis stage 0 (169.7 U/l) to fibrosis stage 3 (393.4 U/l). The CK-18 value in the two cirrhotic NASH patients was considerably higher compared to other fibrosis stages (mean level of 1004 U/l).

Mean CK-18 concentration in the steatosis group was 169.5 U/l ( $\pm 111.6$ ), in the borderline NASH group 170.2 U/l ( $\pm 99.3$ ) and in the NASH group 320.2 U/l ( $\pm 319.8$ ) ( $P < 0.001$ ). *Post-hoc* analysis showed that the CK-18 value in the NASH group was significantly increased compared to the steatosis ( $P < 0.001$ ) and the borderline NASH group ( $P < 0.001$ ). The AUC of CK-18 to distinguish NASH from borderline NASH and steatosis was 0.68 ([0.59;0.77]).

We also evaluated the clinically relevant difference between steatosis and NASH patients without fibrosis. As expected, no significant increase in CK-18 level was observed between these two groups (169.7 U/l vs. 201.6 U/l, respectively) ( $P=0.33$ , independent sample  $t$ -test). We did the same analysis for our glycomarker and we found that this marker performed considerably better (-0.87 vs. -0.78, respectively) ( $P=0.073$ , independent sample  $t$ -test).

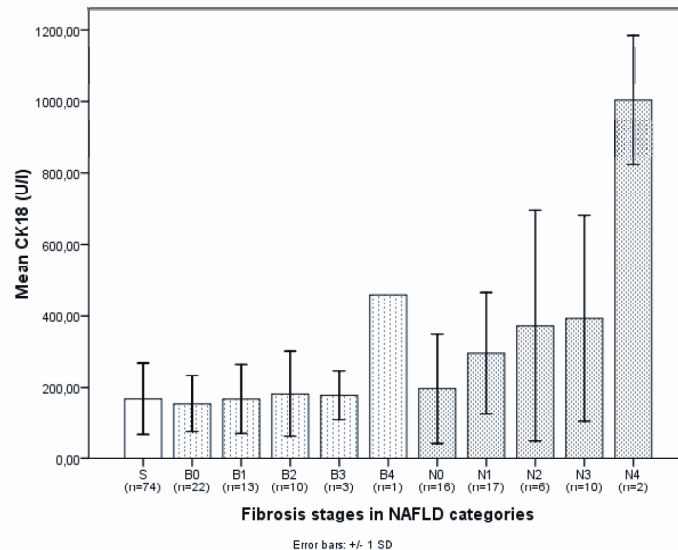


**Figure 3. CK-18 acts as a fibrosis marker in NASH.** Bar graph of the CK-18 concentration in steatosis, borderline NASH and NASH patients. In the borderline NASH and NASH patients, a division into the different stages of fibrosis was made (N0: NASH patients with no fibrosis; N1: NASH patients with fibrosis grade 1; N2: NASH patients with fibrosis grade 2; N3: NASH patients with fibrosis grade 3 and N4: NASH patients with cirrhosis. A similar classification was done for the borderline NASH (B) group. S: steatosis).

#### *γ-globulin migration in NASH and steatosis patients*

A mean  $\gamma$ -globulin migration of 163.1 ( $\pm 4.7$ ), 163.9 ( $\pm 5.4$ ) and 164.5 ( $\pm 4.5$ ) was observed for the steatosis, borderline NASH and NASH group, respectively ( $P=0.262$ ). The AUC of the serum electrophoresis analysis in the validation study was low at 0.55 ([0.47;0.63]).

## Discussion

Most currently used markers to distinguish NASH from steatosis detect the fibrosis present in NASH patients, but they can not measure the essential difference between steatosis and NASH patients which is the onset of a chronic inflammatory reaction. Our results indicate that by quantifying  $N$ -glycans of serum proteins, it is possible to solve this question.

Our glycomarker displayed reasonable AUCs of 0.75 and 0.66 in the pilot and validation study for the distinction of NASH from borderline NASH and simple steatosis, respectively. It is important to keep in mind that we are in fact separating groups of individuals with varying NAS scores and that the numeric score is not meant to replace a pathologist's evaluation of diagnosis.

It was shown that a perfect biomarker would have an expected AUC vs. liver biopsy of 0.76. Moreover, this number was reached with a conservative estimate of biopsy error [24]. This study also showed that needle biopsies (performed in the validation study) are less golden standard than wedge liver biopsies (performed in the pilot study). The surface of biopsies is considerably larger in wedge liver biopsies (five times larger in our study) and the scoring of at least inflammation will therefore be more accurate. This could explain why the glycomarker and the serum protein electrophoresis analysis are less accurate in the validation cohort.

The novelty of our study is that we found a marker that is specific for NASH i.e. a marker that recognizes hepatic inflammation in chronically obese patients. The best illustration that our glycomarker is a marker for hepatic inflammation was the good correlation with the scores of lobular inflammation, both in pilot and validation study. In general, the more inflammation present in the NASH patient, the higher the value of our glycomarker. Even a clinically relevant distinction between NAFLD patients with no inflammation and a mild inflammation was observed.

In the pilot study, we evaluated the performance of our biomarker in comparison to suggested biomarkers for NASH. Six markers displayed a significant result in the single-factor ANOVA analysis. However, in the multiple linear regression analysis, our glycomarker displayed the lowest *P*-value with a borderline significant result. This demonstrates its superiority over the other markers for NASH in this cohort.

The marker that recently has been strongly linked with NASH is CK-18 [25]. CK-18 performed equally well in distinguishing NASH from steatosis in the validation cohort (AUC of 0.68), but this was predominantly due to the CK-18 values of NASH patients with an important amount of fibrosis. Moreover, CK-18 was not able to distinguish steatosis from NASH patients without fibrosis, whereas our glycomarker performed considerably better at this analysis.

The glycans that significantly increase in total serum of NASH patients (NGA2F for both pilot and validation study and NGA2FB for validation study) are fully agalactosylated and inflammation-dependent. NGA2F and NGA2FB are exclusively present on IgG and their significant increase clearly indicates an electropherogram of a patient with an important amount of inflammation [17]. This observation was also made in other chronic necro-inflammatory diseases such as Crohn's disease, ankylosing spondylitis and rheumatoid arthritis and our glycomarker accordingly had a high mean value in these conditions (supplementary data) [17,26]. Yet again, this is a confirmation of the inflammatory character of our glycomarker and other chronic inflammatory diseases have to be excluded when interpreting the glycomarker in chronically obese patients.

This important undergalactosylation was confirmed by the *N*-glycomic composition of the IgG-fraction in NASH patients of the pilot study. This is also the molecular basis for the

slower  $\gamma$ -globulin migration in NASH patients [23]. Sialic acids are the only charged monosaccharides and these are located on top of the galactoses in the glycan structure. Therefore, undergalactosylation of IgG implies that the level of sialylation of antibodies will also be lower and fewer negatively charged sialic acid on IgG will result in a slower migration of the  $\gamma$ -globulin fraction. However, the relative contribution of sialylation heterogeneity to the molecular heterogeneity that affects the  $\gamma$ -globulin mobility, was estimated at only 36%. Nevertheless, a good AUC of 0.8 for the distinction of NASH from the borderline NASH and steatosis was achieved in the pilot study with this extremely simple test. Unfortunately, we could not validate this result in our larger cohort.

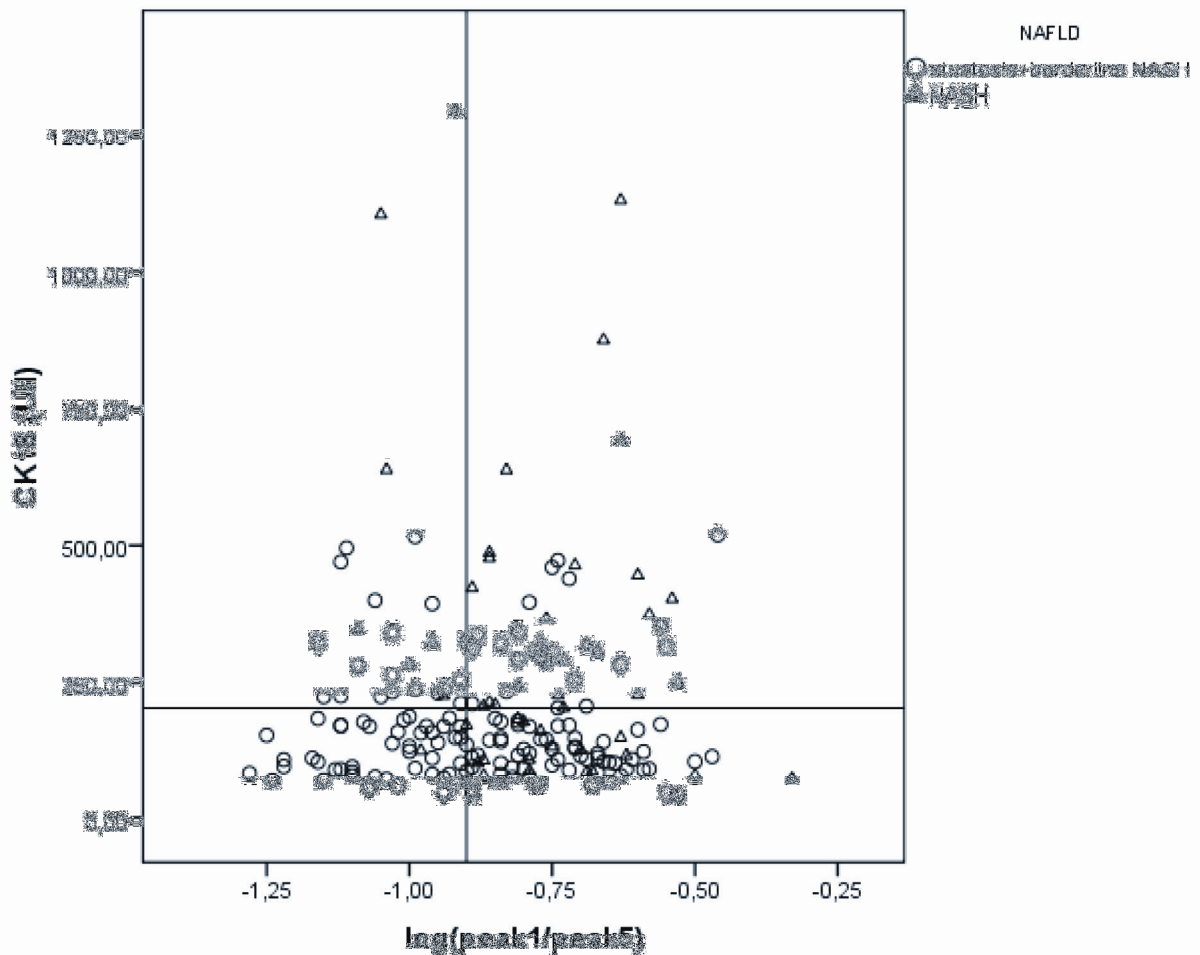
Recently, a similar study on *N*-glycosylation in NAFLD patients has been conducted [27]. Although the same *N*-glycan alterations were observed and therefore the same biomarker was put forward, it was claimed that this marker was associated with fibrosis stage and not with severity of inflammation. However, we could not find a significant correlation between this biomarker and the stage of fibrosis, although a slight increase was observed in the cirrhotic stage. As mentioned earlier, an increase of agalactosylated glycans on IgG have been linked to chronic inflammatory conditions. There are two major fully agalactosylated glycans, NGA2F and NGA2FB. A hallmark of fibrosis/cirrhosis is an increase of bisecting GlcNAc modified glycans, not only the fully galactosylated NA2FB (peak 7) on liver-produced serum proteins that reflects an increased *N*-acetylglucosaminyltransferase III activity in regenerative nodules, but also a slight increase of the agalactosylated NGA2FB (peak 2) on IgGs [15, 17, 18]. However the latter increase is not very large, it is still quantitatively more important than the increase on liver-produced protein, because these bisecting glycans are predominantly present on IgG. In contrast, NGA2F (peak 1) which is not modified with a bisecting GlcNAc, only correlates very well with the amount of inflammation. Moreover, Chen *et al* used an adaptation of the Kleiner and Brunt classification. NAFLD patients with a lobular inflammation and ballooning of hepatocytes or either abnormal (stage 1-4) fibrosis were immediately classified as NASH patients, whereas this study included the borderline NASH patients as a separate group.

In conclusion, our glycomarker specifically recognizes inflammation in chronically obese patients. This test was validated in a large, independent cohort of 224 patients. Our glycomarker is able to distinct simple steatosis from NASH and it is not influenced by the degree of fibrosis present, in contrast to the CK-18 marker which is a clear fibrosis marker in NASH patients. This test has the potential to be transported to the clinic and included as a marker for NASH avoiding liver biopsies in the diagnosis and follow-up of patients.

### **Supporting documents of the Results:**

As our glycomarker has a very good correlation with the amount of lobular inflammation, we correlated our glycomarker with the serum ferritin level. Ferritin is a parameter that is associated with inflammation and it has been suggested to function as a pro-inflammatory cytokine. However, we did not find a significant correlation between the two variables ( $P=0.271$ , Pearson correlation test). Serum ferritin as a marker for inflammation displayed many false positives (high ferritin level, low grade of inflammation) indicating that our glycomarker performed considerably better as NASH marker. Moreover, ferritin was not able to distinguish NASH from steatosis ( $P=0.144$ ) (Table 1).

We combined our glycomarker with the CK-18 marker in the validation cohort (supplementary figure 1). The optimal cut-off for our glycomarker was -0.89 and the optimal cut-off for CK-18 was 203 U/l. The combination glycomarker – CK-18 resulted in a sensitivity of 51% (26/51), a specificity of 85% (125/147), a positive predictive value of 54.2% (26/48) and a negative predictive value of 83.3% (125/150). In other words, if both markers reach their cut-off values, NASH patients can be confirmed with a high degree of certainty, but overall, the combination of these two markers did not result in much extra information.



**Supplementary figure 1. Two-dimensional scatter plots classifying the NASH group (n=51) and steatosis/borderline NASH group (n=147).** Black circles represent steatosis/borderline NASH patients and black triangles represent NASH patients. Optimal results were obtained with a cut-off value for CK-18 of 203 U/l and a cut-off value for the glycomarker of -0.89. This resulted in a sensitivity of 51%, specificity of 85%, positive predictive value of 54.2% and a negative predictive value of 83.3% for the distinction NASH from borderline NASH and steatosis.

#### Evaluation of GlycoFibroTest in pilot and validation study

The glycans that were significantly altered in NASH patients of the validation study (NGA2F, NGA2FB and NA3) suggest that the GlycoFibroTest ( $\log[\text{NGA2FB}]/[\text{NA3}]$ ) [18] could be useful in this population to distinguish NASH patients from steatosis patients. As expected, the mean score of this test was significantly elevated in NASH patients compared to steatosis patients ( $P=0.002$ , Tukey *post-hoc*). Mean score in steatosis patients was -0.77

( $\pm 0.22$ ), in borderline NASH patients  $-0.74 (\pm 0.28)$  and in NASH patients  $-0.64 (\pm 0.23)$  ( $P=0.003$ ). In contrast to the validation study, the difference in mean score between NASH and steatosis patients was not significant in the pilot study ( $P=0.359$ , Tukey *post-hoc*). Mean score was  $-0.73 (\pm 0.3)$  in steatosis patients,  $-0.68 (\pm 0.28)$  in borderline NASH patients and  $-0.59 (\pm 0.31)$  in NASH patients ( $P=0.393$ ). Finally, we evaluated the GlycoFibroTest in the different fibrotic stages of the validation cohort. As expected, we observed a gradually increase of marker score in ascending fibrosis stage. Mean score was  $-0.77 (\pm 0.24)$  for fibrosis stage 0,  $-0.74 (\pm 0.25)$  for fibrosis stage 1,  $-0.72 (\pm 0.29)$  for fibrosis stage 2,  $-0.66 (\pm 0.24)$  for fibrosis stage 3 and  $-0.54 (\pm 0.25)$  for fibrosis stage 4. These data clearly show that the GlycoFibroTest is a fibrosis marker and not a marker for NASH. To strengthen this point, we also analyzed the GlycoFibroTest in steatosis patients versus NASH patients without fibrosis. No significant increase in mean marker score was obtained. The mean score in steatosis patients was  $-0.77 (\pm 0.22)$  and the mean score for NASH patients without fibrosis was  $-0.75 (\pm 0.25)$  ( $P=0.781$ , independent sample *t*-test).

Finally, we evaluated our glycomarker in a group of 24 non-liver auto-immune patients (Crohn's disease ( $n=8$ ), ankylosing spondylitis ( $n=8$ ) and rheumatoid arthritis ( $n=8$ )). Data were taken from [17] and re-analyzed for  $\log(\text{peak1}/\text{peak5})$ . High mean values were observed for patients with ankylosing spondylitis ( $-0.55 (\pm 0.22)$ ) and patients with rheumatoid arthritis ( $-0.66 (\pm 0.19)$ ). Patients with Crohn's disease had a considerable lower mean value ( $-0.92 (\pm 0.14)$ ). Overall, the mean value for the non-liver auto-immune group was  $-0.71 (\pm 0.24)$ . This mean value falls between the mean value of NASH patients in the pilot study ( $-0.65$ ) and the validation study ( $-0.77$ ).

### **Supporting documents of the Discussion:**

A similar story can be told for the GlycoFibroTest. A significant higher mean score was observed in NASH patients of the validation study compared to steatosis patients. We found a gradual increase in mean score in ascending fibrosis stage. We can conclude that, in NASH, GlycoFibroTest accurately performs for what it was designed, to monitor the evolution of fibrosis patients, but it is not a NASH marker i.e. to make the distinction between steatosis and NASH. The significant decrease of NA3 in NASH patients of the validation study also indicates the presence of significant amounts of fibrosis in these patients [15, 17]. As expected, no significant higher mean score for the GlycoFibroTest was found in NASH patients of the pilot study compared to steatosis patients.

### **Acknowledgement**

The authors wish to thank Annelies Van Hecke for her expert technical assistance. BB receives a scholarship GOA BOFF07/GOA/017 of the University Ghent Research Fund (BOF).



## References

- [1] Catenacci VA, Hill JO, Wyatt HR. The obesity epidemic. *Clin Chest Med* 2009;30:415-444.
- [2] Kim CH, Younossi ZM. Nonalcoholic fatty liver disease: a manifestation of the metabolic syndrome. *Cleve Clin J Med* 2008;75:721-728.
- [3] Browning JD. New imaging techniques for non-alcoholic steatohepatitis. *Clin Liver Dis* 2009;13:607-619.
- [4] Promrat K, Kleiner DE, Niemeier HM, Jackvony E, Kearns M, Wands JR, et al. Randomized controlled trial testing the effects of weight loss on nonalcoholic steatohepatitis. *Hepatology* 2010;51:121-9.
- [5] Hossain N, Afendy A, Stepanova M, Nader F, Srishord M, Rafiq M, et al. Independent predictors of fibrosis in patients with nonalcoholic fatty liver disease. *Clin Gastroenterol Hepatol* 2009;7:1224-1229
- [6] Chitturi S, Abeygunasekera S, Farrell GC, Holmes-Walker J, Hui JM, Fung C, et al. NASH and insulin resistance: Insulin hypersecretion and specific association with the insulin resistance syndrome. *Hepatology* 2002;35:373-379.
- [7] Tsochatzis EA, Papatheodoridis GV, Archimandritis AJ. Adipokines in nonalcoholic steatohepatitis: from pathogenesis to implications in diagnosis and therapy. *Mediators Inflamm* 2009;2009:831670.
- [8] Dixon JB, Bhathal PS, O'Brien PE. Weight loss and non-alcoholic fatty liver disease: falls in gamma-glutamyl transferase concentrations are associated with histologic improvement. *Obes Surg* 2006;16:1278-1286.
- [9] Brunt EM, Neuschwander-Tetri BA, Oliver D, Wehmeier KR, Bacon BR. Nonalcoholic steatohepatitis: histologic features and clinical correlations with 30 blinded biopsy specimens. *Hum Pathol* 2004;35:1070-1082.
- [10] Clark JM. The epidemiology of nonalcoholic fatty liver disease in adults. *J Clin Gastroenterol* 2006;40 (Suppl1):S5-10.
- [11] Kashyap SR, Diab DL, Baker AR, Yerian L, Bajaj H, Gray-McGuire C, et al. Triglyceride levels and not adipokine concentrations are closely related to severity of nonalcoholic fatty liver disease in an obesity surgery cohort. *Obesity (Silver Spring)* 2009;17:1696-1701.
- [12] Liew PL, Lee WJ, Lee YC, Wang HH, Wang W, Lin YC. Hepatic histopathology of morbid obesity: concurrence of other forms of chronic liver disease. *Obes Surg* 2006;16:1584-1593.
- [13] Younossi ZM, Jarrar M, Nugent C, Randhawa M, Afendy M, Stepanova M. A novel diagnostic biomarker panel for obesity-related nonalcoholic steatohepatitis (NASH). *Obes Surg* 2008;18:1430-1437.
- [14] Bantel H, Bahr MJ, Schulze-Osthoff K. An apoptosis biomarker for prediction of nonalcoholic steatohepatitis. *Hepatology* 2009;50:991.
- [15] Callewaert N, Van Vlierberghe H, Van Hecke A, Laroy W, Delanghe J, Contreras R. Noninvasive diagnosis of liver cirrhosis using DNA sequencer-based total serum protein glycomics. *Nat Med* 2004;10:429-434.
- [16] Liu XE, Desmyter L, Gao CF, Laroy W, Dewaele S, Vanhooren V. N-glycomic changes in hepatocellular carcinoma patients with liver cirrhosis induced by hepatitis B virus. *Hepatology* 2007;46:1426-1435.
- [17] Vanderschaeghe D, Laroy W, Sablon E, Halfon P, Vanhecke A, Delanghe J, et al. GlycoFibroTest is a highly performant liver fibrosis biomarker derived from DNA sequencer-based serum protein glycomics. *Mol Cell Proteomics* 2009;8:986-994.

- [18] Klein A, Carre Y, Louvet A, Michalski J, Morelle W. Immunoglobulins are the major glycoproteins involved in the modifications of the total serum N-glycome in cirrhotic patients. *Proteomics Clin Appl* 2010;4:379-393.
- [19] Ma KL, Ruan XZ, Powis SH, Chen Y, Moorhead JF, Varghese Z. Inflammatory stress exacerbates lipid accumulation in hepatic cells and fatty livers of apolipoprotein E knockout mice. *Hepatology* 2008;48:770-81.
- [20] Kleiner D, Brunt E, Van Natta M, Behling C, Contos MJ, Cummings OW, et al. Design and validation of a histological scoring system for nonalcoholic fatty liver disease. *Hepatology* 2005;41:1313-1321.
- [21] Debruyne E, Vanderschaeghe D, Van Vlierberghe H, Vanhecke A, Callewaert N, Delanghe J. Diagnostic value of the hemopexin N-glycan profile in hepatocellular carcinoma patients. *Clin Chem* 2010;56:823-831.
- [22] Laroy W, Contreras R, Callewaert N. Glycome mapping on DNA sequencing equipment. *Nat Protoc* 2006;1:397-405.
- [23] Vanderschaeghe D, Debruyne E, Van Vlierberghe, Callewaert N, Delanghe J. Analysis of gamma-globulin mobility on routine clinical CE equipment: exploring its molecular basis and potential clinical utility. *Electrophoresis* 2009;30:2617-23.
- [24] Mehta SH, Lau B, Afdhal NH, Thomas DL. Exceeding the limits of histology markers. *J Hepatol* 2009;50:36-41.
- [25] Feldstein AE, Wieckowska A, Lopez AR, Liu YC, Zein NN, McCullough AJ. Cytokeratin-18 fragment levels as noninvasive biomarkers for nonalcoholic steatohepatitis: a multicenter validation study. *Hepatology* 2009;50:1072-1078.
- [26] Van Beneden K, Coppieters K, Laroy W, De Keyser F, Hoffman IE, Van Den Bosch F, et al. Reversible changes in serum immunoglobulin galactosylation during the immune response and treatment of inflammatory autoimmune arthritis. *Ann Rheum Dis* 2009;68:1360-1365.
- [27] Chen C, Schmilovitz-Weiss H, Liu XE, Pappo O, Halpern M, Sulkes J, et al. Serum protein N-glycans profiling for the discovery of potential biomarkers for nonalcoholic steatohepatitis. *J Proteome Res* 2009;8:463-70.

# Chapter 3.5

## ***“Serum protein N-glycosylation patterns in pediatric NAFLD”***

**Bram Blomme**<sup>1</sup>, Irène T. Tshiamala<sup>1</sup>, Emer Fitzgerald<sup>2</sup>, Ruth De Bruyne<sup>3</sup>, Nico Callewaert<sup>4,5</sup>, Hans Van Vlierberghe<sup>1</sup>

<sup>1</sup>Department of Hepatology and Gastroenterology, Ghent University Hospital, Ghent, Belgium

<sup>2</sup>Paediatric Liver, GI, and Nutrition Centre, King's College London School of Medicine at King's College Hospital, London, UK

<sup>3</sup>Department of Paediatric Gastroenterology, Hepatology, and Nutrition, University Hospital Ghent, Belgium

<sup>4</sup>Unit for Molecular Glycobiology, Department for Molecular Biomedical Research, VIB, Ghent University, Ghent, Belgium

<sup>5</sup>Department of Biochemistry, Physiology and Microbiology, Ghent University, Ghent Belgium

### **Additional Study**

## Abstract

**Background and aim:** We have previously shown the potential of serum protein *N*-glycosylation to distinguish adult patients with simple steatosis from adult patients with non-alcoholic steatohepatitis (NASH). Pediatric NASH patients have distinctive histological liver features compared to an adult population. Therefore, we investigated the *N*-glycosylation patterns of pediatric NAFLD patients to determine if the same alterations were present. **Methods:** Serum protein *N*-glycosylation patterns of 51 pediatric NAFLD patients were assessed with DNA-sequencer assisted fluorophore-assisted capillary electrophoresis and compared with histology. **Results:** In agreement with the adult population, the log(peak1/peak5) marker was the best glycomarker to distinguish NASH from steatosis patients with an area under curve of 0.72 (steatosis and borderline NASH vs. NASH). The biomarker correlated well with the amount of lobular inflammation with a consistent increase of marker score in ascending stage of lobular inflammation, whereas no such association was found with the fibrotic stage. Glyco-analysis of immunoglobulin G (IgG) confirmed the undergalactosylation status with a borderline significant increase of peak 1 (NGA2F;  $P=0.054$ ) and a significant decrease of peak 6 (NA2F;  $P=0.023$ ). Of the ten markers that were evaluated in this population, only four could make a considerable difference between the steatosis and NASH group, however significance was never met. These included GGT ( $P=0.171$ ), INR ( $P=0.174$ ), AST ( $P=0.116$ ) and our glycomarker ( $P=0.058$ ). These markers were evaluated in a multivariate analysis and only our glycomarker displayed a significant result ( $P=0.019$ ). **Conclusion:** The same *N*-glycosylation alterations are observed in pediatric NASH patients when compared to an adult population and therefore the same biomarker can be used. B cells play a dominant role in the *N*-glycan alterations of NASH patients, both in an adult and pediatric population.

## Introduction

In recent years, pediatric NASH has increased in line with the increased prevalence of pediatric obesity and has become a worldwide health problem. In fact, fatty liver is the most common liver abnormality in children aged 2-19 years [1, 2]. However, the true prevalence of pediatric NAFLD and NASH is unknown given that the disease's definition and modalities used for diagnosis are not standardized [3]. Most studies of the prevalence of fatty liver in children have been restricted to the use of indirect measures, such as blood tests or ultrasound, to predict a histological outcome [4]. In most cases, aminotransferase elevation in conjunction with negative markers for other types of liver disease were used as a surrogate markers of fatty liver disease [5, 6]. Other markers, such as insulin resistance index, could have a role in screening [7].

However, the spectrum of fatty liver encompass a wider range of subjects than identified by elevated serum liver chemistries. Franzese *et al* demonstrated that 53% of obese children identified by ultrasound, only 32% had abnormalities in serum aminotransferases [8]. Furthermore, using MR imaging, Burgert *et al* showed that only 48% of obese children with intrahepatic fat accumulation had abnormal ALT levels [9]. Clearly, aminotransferase levels have very limited sensitivity and specificity in the diagnosis of pediatric non-alcoholic fatty liver disease, and more importantly, it can not distinguish between pediatric cases of steatosis and NASH. Therefore, the search for well-performing, non-invasive markers for pediatric NASH continues.

The rationale for this investigation in pediatric cases in addition to our research in adult patients is that there are several differences between both populations, especially at the histological level. Schwimmer *et al* examined the histological appearance of 100 pediatric cases and identified two types of steatohepatitis [10]. Type 1 NASH was consistent with NASH as described in adults and was characterized by steatosis, ballooning degeneration and perisinusoidal fibrosis in the absence of portal changes. Type 2 NASH had a very distinctive histological pattern and was characterized by steatosis, portal inflammation, and/or portal fibrosis in the absence of ballooning degeneration and perisinusoidal fibrosis. Type 1 NASH was reported to be present in only 17% of pediatric NAFLD, whereas type 2 NASH was present in 51%. Children with type 2 NASH were significantly younger and had a greater severity of obesity than children with type 1. Boys were significantly more likely to have type 2 NASH and type 2 was also common in children of Asian, Native American and Hispanic ethnicity. Type 1 and type 2 NASH may have a different pathogenesis, natural history and response to treatment [10].

The abovementioned histological differences between pediatric and adult NAFLD might reflect different etiological factors between them. In particular insulin resistance and sex hormones might play a crucial role in the pathogenesis of pediatric NASH, especially during puberty and adolescence. As a consequence, NAFLD is more prevalent in ages 12-18 than in younger children [11].

## Patients and Methods

### Patients

51 pediatric NAFLD patients from King's College Hospital were included in this study. Patients were all younger than 19 years of age. The decision to biopsy was made by a pediatric hepatologist and the biopsy was usually done in view of abnormal transaminases and/or splenomegaly. The diagnosis of NAFLD was based on the following criteria: liver features of NAFLD as assessed by a liver pathologist, exclusion of other etiologies of liver disease, and exclusion of alcohol intake on history. Blood was taken on the day or within 3 months of diagnostic liver biopsy; serum was stored at -80°C until analysis. Anthropometric and biochemical data were recorded in all of the participants

### Histology

Histological specimens were scored according to NAFLD activity score (NAS), also scoring for stage of fibrosis [12]. This is the nonweighted sum of steatosis (0-3), ballooning (0-2), and lobular inflammation (0-3). NASH is defined as a score  $\geq 5$ , steatosis as a score  $\leq 2$ , and a score of 3 and 4 is classified as "borderline NASH". Fibrosis was scored using a 5-point scale: 0, no fibrosis; 1, mild/moderate perisinusoidal or portal fibrosis; 2, both perisinusoidal and portal fibrosis; 3, bridging fibrosis and 4, cirrhosis. A single histopathologist scored the specimen blinded to other markers.

### IgG depletion

Serum samples were depleted using beads covered with protein A/G (Thermo Scientific, Waltham, MA, USA). 100  $\mu$ l of serum was diluted with 100  $\mu$ l of binding buffer and subsequently incubated with 50  $\mu$ l beads for 1 hour. The mixture was transferred to a 96-well filter plate and centrifuged at 1000g for 15 seconds. The IgG depleted eluate was captured in a microtiter plate. Subsequently, after five wash steps with binding buffer, pure IgG was eluted from the beads after incubation (5 min) with 0.1M glycine pH 2 in the 96-well filter plate. After centrifugation at 1000g for 15 seconds, the eluate is neutralized with 1M Tris pH 8.8. This procedure is repeated three times owing to four elution fractions (E1, E2, E3 and E4). In most analyses, E1 is still a native serum sample and E4 does not contain a sufficient amount of IgG *N*-glycan for analysis. Therefore, only E2 and E3 were analyzed and the elution fraction with the best total peak height is used for statistical analysis. The elution fractions were stored at -80°C for *N*-glycan analysis.

### Glycomic analysis

An elaborate description of the protocol can be found in Laroy *et al* [13]. Briefly, the *N*-glycans present in 5  $\mu$ l of serum or pure IgG elution fraction were released from the proteins with peptide *N*-glycanase F. Subsequently, the *N*-glycans are fluorescently labeled and desialylated. The labeled glycans were profiled and analyzed by DNA sequencer-assisted fluorophore-assisted capillary electrophoresis (DSA-FACE) technology. In analogy with adult

patients, we could observe thirteen peaks in the total serum electropherogram and eight peaks in the IgG electropherogram. The height of every peak was quantified to obtain a numerical description of the profiles and these were normalized to the total intensity of the measured peaks (represented as a percentage of the total peak height). These data were analyzed with SPSS 16.0 software (SPSS, Chicago, IL, USA). Structural characterization of the fluorescently labeled *N*-glycans was done as previously described [14].

### Statistical analysis

Statistical analysis was performed by a single-factor ANOVA in the three NAFLD subcategories (steatosis, borderline NASH and NASH). *Post-hoc* tests were performed using Tukey HSD tests. *P*-values < 0.05 were considered significant.

## Results

### Clinical and histological data

47 pediatric patients had fibrosis (92.2%). 35 of these patients were diagnosed with a type 2 NASH (74.5%), 11 had mixed features (23.4%) and only 1 patient had proper type 1 NASH (2.1%). Clinical and histological data of the patients in the steatosis, borderline NASH and NASH group are summarized in Tables 1 and 2.

**Table 1: anthropomorphic and clinical data of the pediatric NAFLD population**

	NAFLD-classification			Univariate*	Multivariate**
	Steatosis (n=5)	Borderline NASH (n=18)	NASH (n=28)		
Male/female	3/2	11/7	17/9	NA	
Age (y)	10.6 (±5)	12.9 (±1.7)	12.7 (±2.1)	NA	
Weight (kg)	56.3 (±35.1)	74.1 (±26.8)	71.5 (±16.9)	NA	
Length (cm)	145.8 (±37.9)	159.6 (±13.5)	160.3 (±10.1)	NA	
GGT (U/L)	24.2 (±17.1)	46.3 (±31.8)	59.1 (±46.2)	0.171	0.166
ALP (U/L)	279.2 (±29.3)	253.1 (±103.5)	304.3 (±101.3)	0.253	
Albumin (g/L)	45.3 (±4.65)	47.3 (±3.7)	47.6 (±2.5)	0.39	
Cholesterol (mmol/L)	4.76 (±0.82)	4.9 (±1.43)	4.4 (±0.98)	0.401	
Triglycerides (mmol/L)	1.96 (±2)	2.7 (±1.8)	2 (±1.41)	0.391	
Platelets (x10 <sup>9</sup> )	329.8 (±67.9)	318.3 (±62.1)	311.8 (±85.2)	0.876	
INR	0.958 (±0.055)	0.983 (±0.055)	0.999 (±0.04)	0.174	0.061
Tot Bil (µMol/L)	7.2 (±2.28)	9.8 (±4.2)	10.6 (±9.1)	0.627	
AST (lu/L)	46.4 (±24.4)	59.1 (±27.2)	78.4 (±45.9)	0.116	0.328
Glycomarker	-0.9 (±0.1)	-0.83 (±0.25)	-0.73 (±0.12)	<b>0.058</b>	<b>0.019</b>

NA: Not applicable; \**P*-value (single-factor ANOVA); \*\**P*-value (multiple linear regression analysis)

**Table 2: histological findings in the pediatric population**

Histological feature	Category	Normal (n=1)	Steatosis (n=4)	Borderline NASH (n=18)	NASH (n=28)
		Number of biopsy specimen (%)			
Steatosis	No (<5%)	1 (100%)	0 (0%)	1 (5.6%)	0 (0%)
	Mild (5%-33%)	0 (0%)	4 (100%)	11 (61.1%)	0 (0%)
	Moderate (>33%-66%)	0 (0%)	0 (0%)	4 (22.2%)	3 (10.7%)
	Severe (>66%)	0 (0%)	0 (0%)	2 (11.1%)	25 (89.3%)
Lobular inflammation	No foci	1 (100%)	3 (75%)	5 (27.8%)	0 (0%)
	<2 foci	0 (0%)	1 (25%)	12 (66.6%)	17 (60.7%)
	2-4 foci	0 (0%)	0 (0%)	1 (5.6%)	11 (39.3%)
	>4 foci	0 (0%)	0 (0%)	0 (0%)	0 (0%)
Ballooning	No	1 (100%)	2(50%)	2 (11.1%)	0 (0%)
	Few balloon cells	0 (0%)	2 (50%)	7 (38.9%)	11 (39.3%)
	Prominent ballooning	0 (0%)	0 (0%)	9 (50%)	17 (60.7%)
Fibrosis stage	0 = none	0 (0%)	1(25%)	1 (5.6%)	2 (7.2%)
	1 = mild, perisinusoidal	1 (100%)	2 (50%)	8(44.4%)	3 (10.7%)
	2 = perisinusoidal and portal/periportal	0 (0%)	1 (25%)	3 (16.7%)	9 (32.1%)
	3 = bridging fibrosis	0 (0%)	0 (0%)	6 (33.3%)	13 (46.4%)
	4= cirrhosis	0 (0%)	0 (0%)	0 (0%)	1 (3.6%)

### Glycomic analysis

#### *Total serum*

*N*-glycomic analysis of the glycans present in total serum revealed no glycan that was significantly altered in abundance. Only peak 1 (NGA2F) was borderline significantly increased in the serum of NASH-patients ( $P=0.075$ ). Also peak 9' (NA3Fb) showed a trend towards significantly increased in the serum of NASH patients ( $P=0.083$ ) (Table 3).

#### *Immunoglobulin G*

*N*-glycomic analysis of the glycans present on IgG revealed one peak (NA2F) that was significantly altered in abundance in NASH patients ( $P=0.023$ ). *Post-hoc* analysis showed that NASH patients had a significant decreased abundance of peak 6 (NA2F) in comparison to steatosis patients ( $P=0.047$ ). In analogy with the analysis in total serum, peak 1 (NGA2F) on IgG was borderline significantly increased in NASH patients ( $P=0.054$ ) (Table 3).



**Table 3: relative percentages of the different peaks in the electropherogram in the three patients groups**

	Total serum			<i>P-value*</i>	Immunoglobulin G			<i>P-value*</i>
	Steatosis (=5)	Borderline NASH (n=18)	NASH (n=28)		Steatosis (=5)	Borderline NASH (n=18)	NASH (n=28)	
Peak 1 (%) (NGA2F)	5.86 (±1.1)	7.06 (±3)	8.1 (±1.78)	0.075	21.56 (±5.2)	20.32 (±6.1)	23.95 (±3.9)	0.054
Peak 2 (%) (NGA2FB)	1.38 (±0.65)	1.26 (±0.52)	1.18 (±0.26)	0.574	2.88 (±1.44)	3.2 (±1.38)	3.31 (±0.79)	0.724
Peak 3 (%) (NG1A2F)	7.32 (±1.32)	7.69 (±2)	7.8 (±1.45)	0.837	21.03 (±2.73)	21.89 (±3.01)	22.78 (±2.12)	0.263
Peak 4 (%) (NGA1A2F)	2.6 (±0.87)	3 (±0.85)	3.29 (±0.75)	0.169	9.77 (±1.02)	9.59 (±1.53)	10.45 (±1.48)	0.145
Peak 5 (%) (NA2)	45.45 (±2.53)	44.24 (±5.03)	43.09 (±3.73)	0.373	5.05 (±1.32)	7.08 (±3.33)	5.67 (±1.57)	0.088
Peak 6 (%) (NA2F)	21.4 (±2.96)	21.33 (±2.94)	21.0 (±2.22)	0.901	33.25 (±7.93)	31.23 (±6.2)	27.7 (±3.65)	0.023
Peak 7 (%) (NA2FB)	4.73 (±1.09)	4.01 (±0.81)	4.32 (±0.87)	0.22	6.19 (±1.75)	6.15 (±2.98)	5.4 (±1.79)	0.497
Peak 8 (%) (NA3)	6.39 (±1.15)	6.54 (±2.05)	6.37 (±1.57)	0.946	0.26 (±0.18)	0.52 (±0.59)	0.73 (±1.35)	0.601
Peak 9 (%) (NA3Fb)	2.04 (±1.36)	1.99 (±0.69)	1.78 (±0.81)	0.638				
Peak 9' (%) (NA3Fc)	0.98 (±0.2)	1.02 (±0.37)	1.27 (±0.43)	0.083				
Peak 10 (%) (NA3Fbc)	0.46 (±0.14)	0.47 (±0.18)	0.52 (±0.17)	0.556				
Peak 11 (%) (NA4)	0.91 (±0.29)	0.8 (±0.22)	0.85 (±0.2)	0.523				
Peak 12 (%) (NA4F)	0.51 (±0.28)	0.4 (±0.12)	0.4 (±0.12)	0.275				

Mean (±SD); \*single-factor ANOVA

### *Development and evaluation of glycomarker in the pediatric population*

A glycomarker for NASH is developed by taking the ratio of the *N*-glycan that is most increased in the serum of NASH patients and the *N*-glycan that is most decreased in the serum of NASH patients. In agreement with our results in adult NAFLD patients, this was also (peak1/peak5) in this pediatric population. We used the logarithmically transformed ratio to obtain a normally distributed population. The biomarker was evaluated in the three patient groups of the NAFLD-classification. The steatosis group had a mean score of -0.9 (±0.1), the borderline NASH group had a mean score of -0.83 (±0.25) and the NASH group had a mean score of -0.73 (±0.12) ( $P=0.058$ ). The Area under the Curve (AUC) to distinguish patients with steatosis and borderline NASH from NASH patients was 0.72 ([0.57;0.86]). The AUC to distinguish patients with simple steatosis from borderline NASH and NASH patients was 0.79 ([0.64;0.94]).

The glycomarker had a good correlation with the amount of inflammation with a consistent increase in ascending stages of lobular inflammation: a mean score of -0.89 (±0.23) in patients with no lobular inflammation, -0.76 (±0.18) in patients with a mild amount of lobular inflammation and -0.74 (±0.08) in patients with a moderate amount of inflammation ( $P=0.101$ ) (Figure 1). In contrast, no consistent increase in marker score could be observed

in the different fibrotic stages: a mean score of  $-0.82 (\pm 0.1)$  in patients without fibrosis,  $-0.88 (\pm 0.27)$  in patients with fibrosis score 1,  $-0.74 (\pm 0.16)$  in patients with fibrosis score 2,  $-0.76$  in patients with fibrosis score 3 and the only cirrhotic patient had a high score of  $-0.52$ .

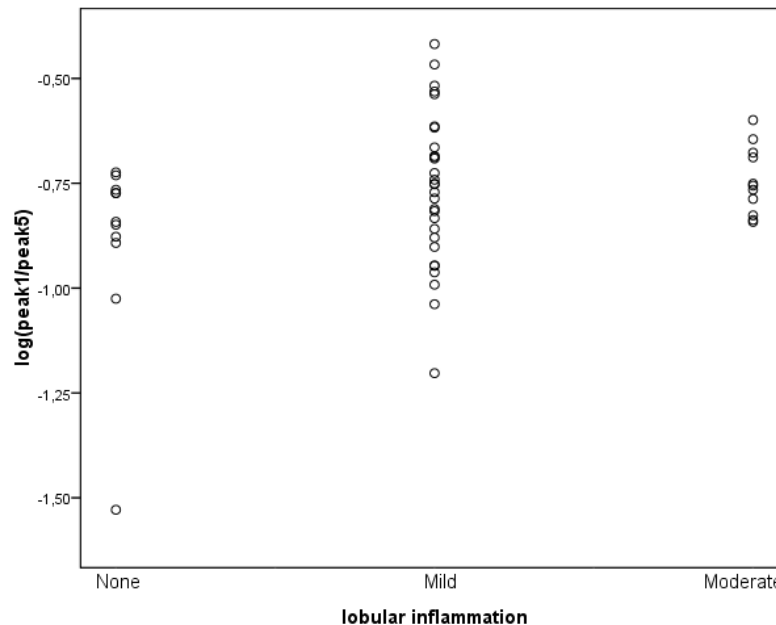


**Figure 1. The evolution of the glycomarker (log (peak1/peak5)) score in ascending amount of lobular inflammation.** Mean score of patients with no inflammation was  $-0.89 (\pm 0.23)$ ,  $-0.76 (\pm 0.18)$  for patients with borderline NASH and  $-0.74 (\pm 0.08)$  for patients with NASH ( $P=0.101$ ).

#### *Evaluation of the GlycoFibroTest in the pediatric population*

This population included a lot of pediatric patients with an important amount of fibrosis in which we could evaluate the GlycoFibroTest ( $\log([NGA2FB]/[NA3])$ ) [15]. However, the mean score of the GlycoFibroTest did not differ significantly in the different categories of the NAFLD-classification and even displayed very similar scores ( $P=0.917$ ). Mean score of the steatosis patients was  $-0.7 (\pm 0.13)$ , mean score of the borderline NASH patients was  $-0.72 (\pm 0.18)$  and the mean score of the NASH patients was  $-0.73 (\pm 0.14)$ . We also evaluated the GlycoFibroTest for what it was developed, to monitor fibrosis progression. Mean score of patients without fibrosis was high at  $-0.6 (\pm 0.25)$ ,  $-0.73 (\pm 0.12)$  for patients with fibrosis score 1,  $-0.78 (\pm 0.14)$  for patients with fibrosis score 2,  $-0.71 (\pm 0.14)$  for patients with fibrosis score 3 and  $-0.51$  for the cirrhotic patient ( $P=0.149$ ).

#### Comparison of Glycomarker with other NASH markers

Most of the markers evaluated performed poorly in differentiating between steatosis and NASH patients (Table 1). Only four markers showed a considerable difference between the NASH and steatosis group, although this difference was never significant. These markers were gamma-glutamyl transferase ( $P=0.171$ ), International Normalized Ratio ( $P=0.174$ ),

aspartate aminotransferase ( $P=0.116$ ) and our Glycomarker ( $P=0.058$ ). These four markers were evaluated in a multiple linear regression analysis (multivariate analysis). In this analysis, our glycomarker was the only marker that displayed a significant result ( $P=0.019$ ) indicating its supremacy over the other markers in this population.

## Discussion

Non-invasive methods to screen an obese, pediatric population are not readily available. Most research efforts have focused on adult NAFLD, however the pediatric population is not far behind in terms of prevalence with up to 10% of the children affected [2, 16]. Moreover, the problems of adult NAFLD patients generally originate in childhood, mostly during adolescence, and a correction in lifestyle or even clinical treatment in this early phase would be beneficial for the management of the disease.

Our data indicate that pediatric NAFLD patients show very similar results in a glycomic analysis compared to adult NAFLD patients. Most of the results were borderline significant owing to the relatively small number of patients included with especially a small proportion of steatosis patients. This is not surprising as the children studied were those who presented to a tertiary-level pediatric hepatology unit and therefore the more severe cases (borderline NASH and NASH) could be included in this study. Nevertheless, a trend towards undergalactosylation was observed in NASH patients. This undergalactosylation occurs on IgG and its glycomic profile confirmed the (borderline significant) increase of NGA2F in favor of the (significant) decrease of NA2F. This is also characteristic for other chronic necro-inflammatory conditions such as rheumatoid arthritis or Crohn's disease [17]. In conclusion, the glycomic alterations in pediatric NASH patients are determined by an altered B cell physiology instead of a change of liver homeostasis.

In agreement with the results in adult NAFLD patients, the  $\log(\text{peak1/peak5})$  biomarker displayed the best result in distinguishing steatosis from NASH. The AUC to differentiate steatosis from borderline NASH and NASH was high at 0.79. However, the analysis to distinguish steatosis and borderline NASH patients from NASH patients will provide a better representation of real-life practice because of the small number of steatosis patients included. This analysis still had a reasonable AUC of 0.72. Recently, very high AUCs of 0.93 and 0.85 have been reported to distinguish NASH from simple steatosis in a pediatric population using CK-18 fragments [18, 19]. The golden standard used in this study were percutaneous needle liver biopsies. It was previously shown that results based on such liver biopsies would have a maximum AUC of 0.76 and therefore validation of these results in large cohorts is necessary [20]. Moreover, CK-18 levels were predictive of fibrosis and are thereby not specific for NASH [19].

Our glycomarker showed a good correlation with the amount of inflammation with a consistent, gradual increase of mean marker in ascending amount of lobular inflammation. This observation is important because the appearance of an inflammatory reaction in chronically obese patients defines the onset of NASH [21]. Importantly in this context, the most elaborate difference was observed between patients with no inflammation and patients with a mild inflammation, mean marker score does not augment further when patients progressed to a moderate amount of lobular inflammation. Although many patients displayed

a significant amount of fibrosis ( $\geq F2$ ), we could not validate the use of the GlycoFibroTest in this population. Even in patients with no fibrosis, mean marker score was high and there was no consistent increase in ascending fibrosis stage. This might be linked with the different pattern of fibrosis in pediatric patients and we found a particularly high incidence of type 2 NASH (75%) in the present study. In fact, only one patient showed a proper adult-like (type 1) liver histology.

Finally, we compared our glycomarker with other markers for chronic liver disease and markers that have been specifically associated with NASH. Only four markers were able to present a considerable difference in the three patients groups, although significance was never met. These were GGT, INR, AST and our glycomarker. In a multiple linear regression analysis, our glycomarker was the only marker that displayed a significant result. This indicates that the glycomarker will be more informative than basic biochemical variables in distinguishing NASH from simple steatosis. Moreover, the technology used has recently been brought to a clinical platform. It will therefore be equally easy to perform a glycomic analysis than to determine the classical biochemical variables in the near future [22].

## References

- [1] Feldstein A, Charatcharoenwithaya P, Treeprasertsuk S, Benson J, Enders F, Angulo P. The natural history of non-alcoholic fatty liver disease in children: a follow-up study for up to 20 years. *Gut* 2009;58:1538-1544.
- [2] Patton H, Sirlin C, Behling C, Middleton M, Schwimmer J, Lavine J. Pediatric nonalcoholic fatty liver disease: a critical appraisal of current data and implications for future research. *J Pediatr Gastroenterol Nutr* 2006;43:413-427.
- [3] Oh M, Winn J, Poordad F. Review article: diagnosis and treatment of non-alcoholic fatty liver disease. *Aliment Pharmacol Ther* 2008;28:503-522.
- [4] Schwimmer J. Definitive diagnosis and assessment of risk for nonalcoholic fatty liver disease in children and adolescents. *Semin Liver Dis* 2007;27:312-318.
- [5] Schwimmer J, McGreal N, Deutsch R, Finigold M, Lavine J. Influence of gender, race, and ethnicity on suspected fatty liver in obese adolescents. *Pediatrics* 2005;115:e561-e565.
- [6] Nobili V, Reale A, Alisi A, Morino G, Trenta I, Pisani M, et al. Elevated serum ALT in children presenting to the emergency unit: relationship with NAFLD. *Dig Liver Dis* 2009;41:749-752.
- [7] Reinehr T, Toschke A. Onset of puberty and cardiovascular risk factors in untreated obese children and adolescents: a 1-year follow-up study. *Arch Pediatr Adolesc Med* 2009;163:709-715.
- [8] Franzese A, Vajro P, Argenziano A, Puzziello A, Iannucci M, Saviano M, et al. Liver involvement in obese children. Ultrasonography and liver enzyme levels at diagnosis and during follow-up in an Italian population. *Dig Dis Sci* 1997;42:1428-1432.
- [9] Burgert T, Taksaki S, Dziura J, Goodman T, Yeckel C, Papademetris X, et al. Alanine aminotransferase levels and fatty liver in childhood obesity: associations with insulin resistance, adiponectin, and visceral fat. *J Clin Endocrinol Metab* 2006;91:4287-4294.
- [10] Schwimmer J, Behling C, Newburg R, Deutsch R, Nievergelt C, Schork M, et al. Histopathology of pediatric nonalcoholic fatty liver disease. *Hepatology* 2005;42:641-649.
- [11] Takahashi Y. Pediatric nonalcoholic fatty liver disease: overview with emphasis on histology. *World J Gastroenterol* 2010;16:5280-5285.

- [12] Kleiner D, Brunt E, Van Natta M, Behling C, Contos M, Cummings O, et al. Design and validation of a histological scoring system of nonalcoholic fatty liver disease. *Hepatology* 2005;41:1313-1321.
- [13] Laroy W, Contreras R, Callewaert N. Glycome mapping on DNA sequencing equipment. *Nat Protoc* 2006;1:397-405.
- [14] Callewaert N, Van Vlierberghe H, Van Hecke A, Laroy W, Delanghe J, Contreras R. Noninvasive diagnosis of liver cirrhosis using DNA sequencer-based total serum protein glycomics. *Nat Med* 2004;10:429-434.
- [15] Vanderschaeghe D, Laroy W, Sablon E, Halfon P, Van Hecke A, Delanghe J, et al. GlycoFibroTest is a highly performant liver fibrosis biomarker derived from DNA sequencer-based serum protein glycomics. *Mol Cell Proteomics* 2009;8:986-994.
- [16] Schwimmer J, Deutsch R, Kahen T, Lavien J, Stanley C, Behling C. Prevalence of fatty liver in children and adolescents. *Pediatrics* 2006;118:1388-1393.
- [17] Van Beneden K, Coppieters K, Laroy W, de Keyser F, Hoffman I, Van den Bosch F, et al. Reversible changes in serum immunoglobulin galactosylation during the immune response and treatment of inflammatory autoimmune arthritis. *Ann Rheum Dis* 2008;68:1360-1365.
- [18] Wieckowska A, Zein N, Yerian L, Lopez A, McCullough A, Feldstein A. In vivo assessment of liver cell apoptosis as a novel biomarker of disease severity in nonalcoholic fatty liver disease. *Hepatology* 2006;44:27-33.
- [19] Fitzpatrick E, Mitry R, Quaglia A, Hussain M, deBruyne R, Dhawan A. Serum levels of CK18 M30 and leptin are useful predictors of steatohepatitis and fibrosis in pediatric NAFLD. *J Pediatr Gastroenterol Nutr* 2010;51:500-506.
- [20] Mehta S, Lau B, Afdhal M, Thomas D. Exceeding the limits of histology markers. *J Hepatol* 2009;50:36-41.
- [21] Tilg H, Moscher A. Evolution of inflammation in nonalcoholic fatty liver disease: the multiple parallel hits hypothesis. *Hepatology* 2010;52:1836-1846.
- [22] Vanderschaeghe D, Szekrényes A, Wenz C, Gassman M, Naik N, Bynum M, et al. High-throughput profiling of the serum N-glycome on capillary electrophoresis microfluids systems: towards clinical implementation of GlycoHepatoTest. *Anal Chem* 2010;82:7408-7415.

# Chapter 3.6

***“The unfolded protein response in plasma cells of patients with non-alcoholic fatty liver disease”***

**Bram Blomme<sup>1</sup>, Kim Olievier<sup>1</sup>, Debby Laukens<sup>1</sup>, Hans Van Vlierberghe<sup>1</sup>**

<sup>1</sup>Department of Hepatology and Gastroenterology, Ghent University Hospital, Ghent, Belgium

**Pilot Study**

## Abstract

**Background and aims:** A mechanism for the undergalactosylation of immunoglobulin G that is a hallmark of several chronic inflammatory diseases, remains to be elucidated. Several lines of evidence indicate that endoplasmic reticulum (ER) stress could play an important role in this. Our research focused on plasma cells, the activated B cell type that produce and secrete the immunoglobulins. Plasma cells already have a limited unfolded protein response (UPR) with an activation of the IRE1/XBP1 and ATF6 branch, but not of the PERK branch. The aim of this study was to evaluate the expression of important ER stress genes in plasma cells of the obese population. **Methods:** Total RNA was extracted from plasma cells isolated from whole blood collected from patients with non-alcoholic fatty liver disease (NAFLD). Quantitative real-time polymerase chain reaction analysis was used to quantify the transcription of genes located in the three branches of the UPR. **Results:** There was a significantly increased transcription of almost all ER stress genes in plasma cells of obese patients with liver inflammation compared to obese patients without liver inflammation. Importantly, an activation of the PERK branch was observed in plasma cells of obese patients, although the expression of downstream genes was significantly larger in obese patients with liver inflammation. **Conclusion:** Obese patients with liver inflammation have a significantly increased transcription of ER stress genes in plasma cells compared to obese patients without liver inflammation. Hypothetically, we suggest that an increased UPR would lead to an increased influx of secreted proteins in the Golgi apparatus. This would result in a premature saturation of the  $\beta$ -1,4-galactosyltransferase necessary for the attachment of galactose moieties during biosynthesis.

## Introduction

It has been postulated that the most important function of *N*-glycosylation is associated with protein folding in the endoplasmic reticulum (ER) [1, 2]. Although it has not been proven that *N*-glycosylation is a prerequisite for protein folding, it increases folding efficiency, prevents premature glycoprotein oligomerization and degradation, and suppresses formation of non-native disulfide bonds by hindering aggregation and thus allowing interaction of protein moieties of folding glycoproteins with classical chaperones and other proteins that assist in folding. In various pathological conditions, there is an accumulation of unfolded proteins in the ER. To cope with accumulated unfolded ER proteins, mammalian cells trigger a specific response called the unfolded protein response (UPR) [3, 4]. As a consequence, inhibitors of *N*-glycosylation (eg tunicamycin) will result in more unfolded protein and the induction of the UPR [5].

There are three distinct pathways that are induced by ER stress mediated by three ER-resident stress sensors, i.e. the activating transcription factor 6 (ATF-6), the inositol requiring enzyme 1 (IRE1), and the double-stranded RNA-activated protein kinase-like ER kinase (PERK) [6]. ATF-6 is synthesized as a precursor protein and anchored to the ER membrane, where it is retained by a ER chaperone, BiP (also known as glucose-related protein (GRP) 78). In response to ER stress, ATF-6 is released from BiP and transported to the Golgi complex, where ATF-6 undergoes regulated intramembrane proteolysis. This is carried out by two proteases that sequentially cleave the protein, S1P and S2P. The processed form of ATF-6, which may target genes since it is a transcription factor (belonging to the basic-region leucine zipper (bZIP) family), translocates to the nucleus. The second UPR branch involves IRE1 and X-box-binding protein 1 (XBP-1). IRE1 contains both serine/threonine kinase and ribonuclease domains. Under normal conditions, XBP1 mRNA is translated, but its product is a weak transcriptional activator with a short protein half-life. During ER stress, activated IRE1 cuts 26 nucleotides from XBP1 mRNA to generate spliced XBP1 mRNA, which encodes the more stable and transcriptionally active XBP-1S protein (which belongs to the family of bZIP transcription factors). The third UPR branch is mediated by PERK, which is a serine/threonine protein kinase that phosphorylates the alpha subunit of eukaryotic translation initiation factor 2 (eIF2-alpha). Phosphorylation of eIF2-alpha subsequently inhibits global protein synthesis. Remarkably, eIF2-alpha phosphorylation induces translation of activating transcription factor 4 (ATF-4) mRNA into the bZIP transcription factor ATF-4.

The UPR is not only initiated in pathological conditions. Particular cells burdened with a high secretory or metabolic capacity induce a UPR to be able to adapt their protein-folding capacity to meet the fluctuations in demand for protein synthesis and secretion [7]. The antibody-secreting plasma cell under study is here an example of [8, 9]. Importantly, it has been shown that activation of the IRE1/XBP-1 pathway is a requirement for expansion of the ER and antibody formation in order to complete the transformation from resting B cell to plasma cell. Furthermore, the UPR transcriptional activator ATF-6 is also induced in plasma cells. In contrast, the third ER stress sensor, PERK, is not fully activated in plasma cells in normal conditions. It was shown that PERK is partially activated to the intermediate mobility form, but there was no evidence of the hyperphosphorylated form that is able to phosphorylate and activate its downstream target, eIF2A [10]. Moreover, it was recently



demonstrated in mice that *Perk*<sup>-/-</sup> B cells develop and are fully component for induction of Ig synthesis and antibody secretion when stimulated with LPS [9].

The quantitatively most important glycomic alteration in liver diseases is the increase of agalactosylated glycans (undergalactosylation) [11]. This undergalactosylation of immunoglobulin G (IgG) is strongly linked with chronic inflammatory conditions as exemplified by our research in patients with non-alcoholic steatohepatitis [12]. The mechanism that lies at the basis of this undergalactosylation has not been unraveled. Several lines of evidence suggest that the UPR might play an important part in this. A close examination of UPR pathways has demonstrated major inflammatory and stress signaling networks, including the activation of JNK-AP1 and NF-kappaB pathways as well as production of ROS and nitric oxide [13-16]. Interestingly, these are also the pathways that play a critical role in obesity-induced inflammation and metabolic abnormalities, particularly abnormal insulin action [17]. Moreover, the relationship between ER stress and inflammation is not likely to be one-sided. Recent studies in the brain, for instance, provide evidence supporting the model that both ER stress and inflammation are able to activate each other and to inhibit normal cellular metabolism [18]. Finally, as the lipotoxicity of immune cells such as macrophages is a common feature of obesity, the action of lipid chaperones in controlling lipid-induced ER stress has critical implications for obese patients and its complications, including NASH [19, 20].

## **Patients and methods**

### Patients

In this pilot study, we included eight NAFLD patients. Six NAFLD patients were chronically obese patients that were scheduled for a gastric bypass and two patients were diagnosed with NAFLD through a percutaneous liver biopsy without surgery. 80 ml blood was collected before the bariatric procedure or within three months of the percutaneous liver biopsy. Patients were selected based on clinical data such as BMI (>25 kg/m<sup>2</sup>) and the absence of high amount of alcohol consumption (<200g per week for men and <100 g for women) and were also tested and found negative for viral hepatitis, auto-immune and cholestatic conditions. All patients signed an informed consent. The Ethical Committee of Ghent University Hospital approved the protocols.

### Histology

A wedge liver biopsy was performed during the planned bariatric procedure and a routine Menghini liver biopsy was carried on the two NAFLD patients that were not operated. Slides were stained with haematoxylin-eosin and picosirius red. Patients were diagnosed blindly by a pathologist based on classical histological features such as inflammation, ballooning, lobular inflammation and the pattern of fibrosis. The NAFLD activity score (NAS) was used to classify the NAFLD patients [21]. This is the nonweighted sum of steatosis (0-3), ballooning (0-2) and lobular inflammation (0-3). NAFLD and NASH were respectively defined as a score <5 and ≥5 .

### Plasma cell isolation

The collected blood was centrifuged at 400g for 7 min. The buffy coat was removed and diluted four times with buffer (PBS pH 7.2 and 2mM EDTA). 35 ml of diluted cell suspension was carefully layered over 15 ml of Ficoll-Paque (Amersham Pharmacia, Piscataway, NJ) and centrifuged for 30 min in a swinging-bucket rotor without break. The mononuclear layer was transferred to a new 50 ml conical tube, mixed with buffer and centrifuged for 10 min at 300g. This was repeated twice after which the mononuclear cell number was determined with trypan blue dye (Invitrogen, Carlsbad, CA).

Purification of the plasma cells out of this mononuclear leukocyte population was performed with the Plasma Cell Isolation Kit II (Miltenyi Biotec Inc., Auburn, CA). Briefly, the first phase consists of a depletion of non-plasma cells through an indirect magnetic labeling of non-target cells with a non-plasma cell biotin-antibody cocktail, CD56 microbeads and a non-plasma cell microbead cocktail. The non-plasma cell biotin antibody cocktail consists of biotin-conjugated monoclonal antibodies against CD2, CD3, CD10, CD13, CD15, CD22, CD34, CD123 and CD235a whereas the non-plasma cell microbead cocktail is made up of CD14 microbeads and anti-biotin microbeads. This is followed by a magnetic separation using an LD column that results in pre-enriched CD38<sup>+</sup> plasma cells (flow-through fraction). The next phase is the positive selection of the CD38<sup>+</sup> plasma cells by direct magnetic labeling with CD38 microbeads followed by a magnetic separation using an MS column. This magnetic separation was performed twice to obtain a pure plasma cell fraction. Plasma cell number is determined by trypan blue dye

### RNA extraction and quantitative real-time PCR

Total RNA was extracted from plasma cells using an RNeasy Mini Kit (Qiagen, Westburg BV, The Netherlands) with on-column DNase treatment and converted to cDNA for real-time quantification. All reactions were run in duplicate and normalized to stably expressed reference genes. Primer sequences are given in Table 1. Patients characteristics are given in Table 2.

**Table 1: Sequence of used qRT-PCR primers**

Gene symbol	Forward primer (5'-3')	Reverse primer (5'-3')
hGAPDH	TGC ACC ACC ACC TGC TTA GC	GGC ATG GAC TGT GGT CAT GAG
hSDHA	TGG GAA CAA GAG GG ATC TG	CCA CCA CTG CAT CAA ATT CAT G
hEIF2A	CTG CAC TCC TTC GAT CTT CTG	AGT TGT AGG TTG GGT ATC CCA G
hHSPA5	GGG AAC GTC TGA TTG GCG AT	CGT CAA AGA CCG TGT TCT CG
hATF6	TCA GAC AGT ACC AAC GCT TAT GC	GTT GTA CCA CAG TAG GCT GAG A
hATF4	GAC CAC GTT GGA TGA CAC TTG	GGG AAG AGG TTG TAA GAA GGT G
hEIF2AK3	TGC CTG GCT CGA AGC ACC AC	TGG TGC ATC CAT TGG GCT AGG A
hXBP1 U	U/S: AGA CAG CGC TTG GGG ATG GAT	CCT GCT GCA GAG CTG CAC GTA G
hXBP1 S		CCT GCA CCT GCT GCG GAC TC
hDDIT3	AAG GCA CTG AGC GTA TCA TGT	TGA AGA TAC ACT TCC TTC TTG AAC A
hGADD34	TCC TCT GGC AAT CCC CCA TA	GGA ACT GCT GGT TTT CAG CC

hGAPDH, human glyceraldehyde-3 phosphate dehydrogenase; hSDHA, human succinate dehydrogenase complex subunit A; hEIF2A, human eukaryotic translation initiation factor 2A; hHSPA5, human heat shock 70kDA protein 5; hATF6, human activating transcription factor 6; hATF4, human activating transcription factor 4; hEIF2AK3, human eukaryotic translation initiation factor 2A kinase 3; hXBP1 U/S, human X-box binding protein 1 unspliced/spliced; hDDIT3, human DNA-damage-inducible transcript 3; hGADD34, human growth arrest and DNA damage inducible protein.

### Statistical analysis

Data analysis was performed with SPSS version 16.0 (SPSS Inc, Chicago, IL). A Mann-Whitney *U* test was performed for all analyses. Data are presented as median  $\pm$  range. *P* values less than .05 (2-tailed probability) were considered as significant.

## Results

### Anthropomorphic and histological characteristics

These results are summarized in Table 2.

**Table 2: anthropomorphic and histological characteristics**

	NAFL (n=6)	NASH (n=2)
Male/Female	1/5	1/1
Age (y)	42 ( $\pm$ 11.7)	27.5 ( $\pm$ 9.2)
Weight (kg)	109.3 kg ( $\pm$ 9.5)	93 ( $\pm$ 11.3)
BMI	38.4 ( $\pm$ 3.9)	29.6 ( $\pm$ 3.7)
	Fibrosis stage (%)	
0	6 (100%)	0 (0%)
1	0 (0%)	1 (50%)
2	0 (0%)	1 (50%)
3	0 (0%)	0 (0%)
4	0 (0%)	0 (0%)
	Steatosis severity (%)	
0	3 (50%)	0 (0%)
1	2 (33.3%)	0 (0%)
2	1 (16.7%)	0 (0%)
3	0 (0%)	2 (100%)
	Inflammation severity (%)	
0	3 (50%)	0 (0%)
1	3 (50%)	1 (50%)
2	0 (0%)	0 (0%)
3	0 (0%)	1 (50%)
	Ballooning severity (%)	
0	6 (100%)	0 (0%)
1	0 (0%)	1 (50%)
2	0 (0%)	1 (50%)

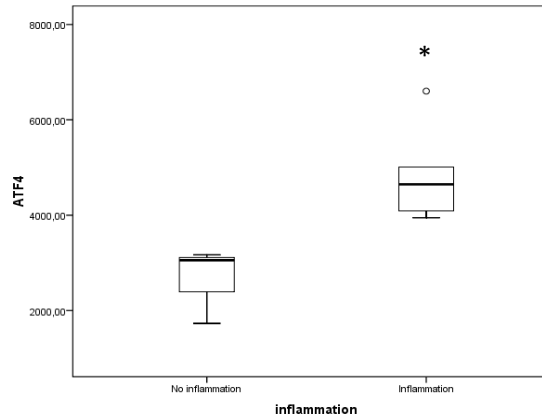
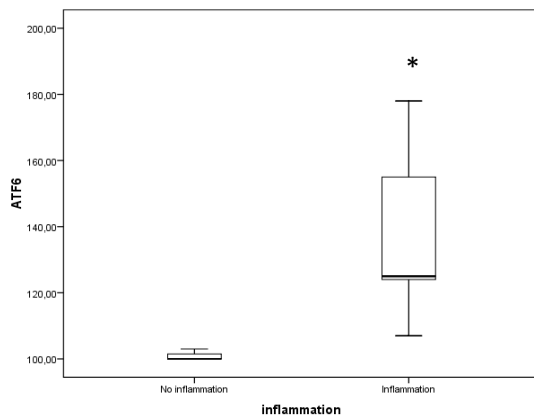
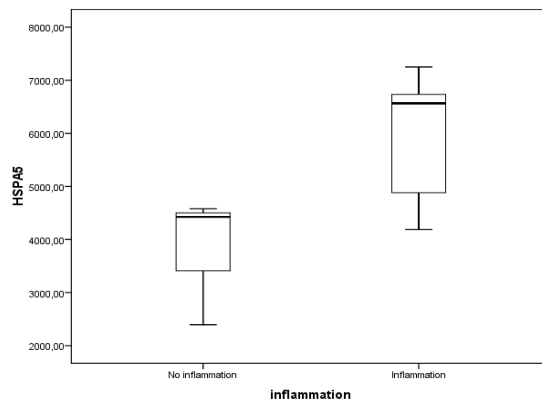
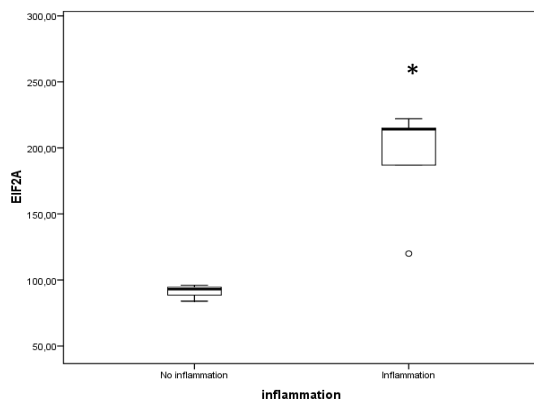
### Quantitative real-time polymerase chain reaction (qRT-PCR) analysis

A significantly increased expression of *hEIF2A*, *hATF6*, *hATF4*, *hDDIT3* and *hGADD34* was observed in obese patients with liver inflammation compared to obese patients without liver inflammation (all analyses  $P=0.025$ ). Additionally, the ratio of the expression of spliced (S) and unspliced (U) *hXBP1* was also significantly increased in obese patients with liver inflammation ( $P=0.025$ ) (Table 3 and figure 1). The latter result indicates an increased activation of the IRE1 branch in which more (unspliced) XBP1 mRNA will be transformed into (spliced) XBP1s mRNA.

**Table 3: Comparison of the expression levels of ER stress genes in plasma cells of obese patients with and without liver inflammation**

Gene Symbol	Number of transcripts		P-value*
	No inflammation (n=3)	Inflammation (n=5)	
hEIF2A	91 (±12)	191.6 (±102)	0.025
hHSPA5	3800 (±2182)	6566 (±3063)	0.101
hATF6	100 (±3)	125 (±71)	0.025
hATF4	3055 (±1440)	4647 (±2655)	0.025
hEIF2AK3	362 (±221)	641 (±575)	0.101
hXBP1 S/U	0.23 (±0.03)	0.33 (±0.06)	0.025
hDDIT3	17.5 (±2.2)	43.2 (±45.5)	0.025
hGADD34	213 (±103)	616 (±424)	0.025

Median (±range); \*Mann-Whitney *U* Test, see Table 1 for full name of gene symbols



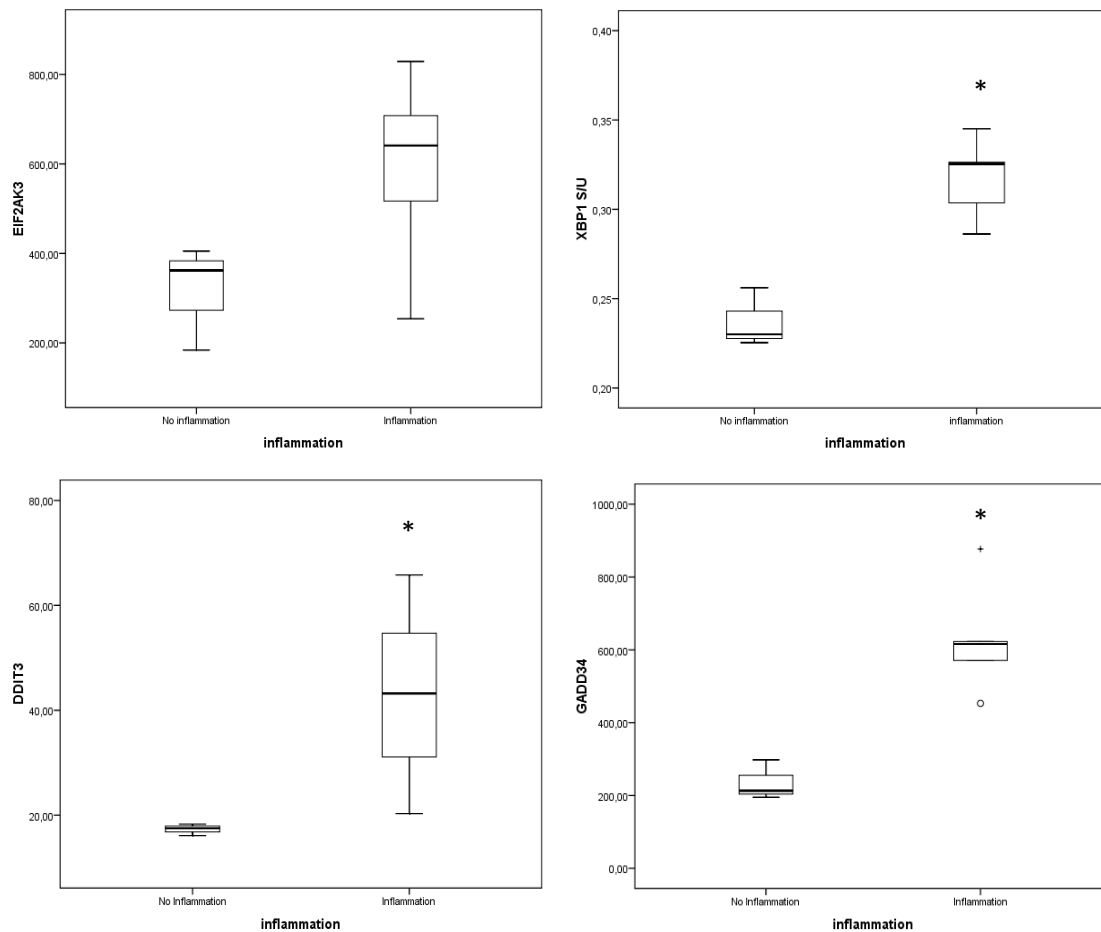


**Figure 1. Boxplots of the expression level of ER stress genes in plasma cells of NAFLD-patients.** The left boxplot represent the expression level of NAFLD patients without inflammation (n=3) and the right boxplot represents th expression level of NAFLD patients with liver inflammation (n=5). \* $P < 0.05$

## Discussion

The biosynthesis of the final glycan structure (complex type *N*-glycans) occurs in the Golgi-apparatus [22]. Therefore, the undergalactosylation status of immunoglobulins will be determined in the Golgi-apparatus, but it is conceivable that the mechanism originates in the endoplasmic reticulum. The ER stress response can be regarded as an autoregulatory system adjusting ER capacity to cellular demand. A concept that is rapidly emerging is that other cell organelles (mitochondrion, peroxisome and Golgi apparatus) will also regulate their capacity in response to the changed cellular homeostasis inflicted by the UPR. If the ER stress response enhances the capacity of ER functions, large amounts of secretory proteins are transported to the Golgi apparatus, causing insufficiency of Golgi function (Golgi stress) [23]. This phenomenon will especially be prominent in plasma cells with its very large ER and high-secreting capacity.

We have shown in this study that there is an increased ER stress reponse in the plasma cells of obese patients with liver inflammation in addition to the existing ER stress response

necessary for the maturation of resting B cells to antibody-secreting plasma cells. Beta-1,4-galactosyltransferase (beta-1,4-GalT) is the enzyme that will determine the undergalactosylation status of the secreted immunoglobulin. It catalyzes the transfer of a galactose monosaccharide from an activated sugar donor (UDP-Gal) in a beta-1,4-linkage to *N*-acetylglucosamine residues that appear on various antennas of the *N*-glycan structure. The enzyme is located in *trans*-Golgi and the addition of a galactose moiety is one of the last modification steps that is carried out before the protein with the mature complex oligosaccharide is transferred to the plasma membrane [24]. Therefore, when the Golgi apparatus is overwhelmed with secretory proteins as a result of an increased ER stress response (Golgi stress), it is very plausible that the maximum capacity of the beta-1,4-GalT enzyme to modify the glycan chain will be reached at an earlier stage. Moreover, several papers have shown that there is no increased activity of beta-1,4-GalT in patients with rheumatoid arthritis (RA) compared to normal control individuals, nor is there an altered gene expression of the transferase, further supporting this hypothesis [25-27]. RA is a similar chronic inflammatory condition in which IgG undergalactosylation is also a well known hallmark. As a result, an increased proportion of antibodies without galactose moieties in their glycan structure will be transported to the plasma membrane for secretion. Further research is necessary to confirm this hypothesis.

An interesting observation was the activation of the PERK pathway in the plasma cells of obese patients. This activation was significantly larger in obese patients with liver inflammation, although also present in obese patients without liver inflammation. As outlined in the introduction, PERK is not fully activated in plasma cells of healthy controls, but our results show transcription of downstream genes of the PERK pathway such as GADD34 and DDIT3 (CHOP) in chronically obese patients. ER stress has been shown in various cell types of obese patients including adipocytes, hepatocytes and pancreatic exocrine cells [28-30], but how ER stress in immune cells relates to chronic metabolic disease remains to be elucidated. However, these results suggest that obesity is a systemic disease. Despite the clear and significant difference in ER stress response between patients with and without liver inflammation, this research was conducted in a very limited number of obese patients and it needs validation in a larger cohort including NASH patients with high amount of lobular inflammation and obese steatotic patients without inflammation.

## References

- [1] Shental-Bechor D, Levy Y. Folding of glycoproteins: toward understanding the biophysics of the glycosylation code. *Curr Opin Struct Biol* 2009;19:524-533.
- [2] Paodi A. Protein glycosylation and its role in protein folding. *Ann Rev Biochem* 2000;69:63-93.
- [3] Mori K. Signalling pathways in the unfolded protein response: development from yeast to mammals. *J Biochem* 2009;146:743-750.
- [4] Kapoor A, Sanyal A. Endoplasmic stress and the unfolded protein response. *Clin Liver Dis* 2009;13:581-590.
- [5] Han C, Nam M, Park H, Seong Y, Kang S, Rhim H. Tunicamycin-induced ER stress upregulates the expression of mitochondrial HtrA2 and promotes apoptosis through the cytosolic release of HtrA2. *J Microbiol Biotechnol* 2008;18:1197-1202.

- [6] Hotamisligil G, Erbay E. Nutrient sensing and inflammation in metabolic diseases. *Nat Rev Immunol* 2008;8:923-934.
- [7] Ron D, Walter P. Signal integration in the endoplasmic reticulum unfolded protein response. *Nat Rev Moll Cell Biol* 2007;8:519-529.
- [8] Gass J, Gunn K, Sriburi R, Brewer J. Stressed-out B-cells? Plasma cell differentiation and the unfolded protein response. *Trends in Immunol* 2004;25:17-24.
- [9] Gass J, Jiang H, Wek R, Brewer J. The unfolded protein response of B-lymphocytes: PERK-independent development of antibody-secreting cells. *Mol Immunol* 2008;45:1035-1043.
- [10] Ma Y, Shimizu Y, Mann M, Jin Y, Hendershot L. Plasma cell differentiation initiates a limited ER stress response by specifically suppressing the PERK-dependent branch of the unfolded protein response. *Cell Stress Chaperones* 2010;15:281-293.
- [11] Blomme B, Van Steenkiste C, Vanhuysse J, Colle I, Callewaert N, Van Vlierberghe H. Impact of elevation of total bilirubin level and etiology of the liver disease on serum N-glycosylation patterns in mice and humans. *Am J Physiol Gastrointest Liver Physiol* 2010;298:G615-G624.
- [12] Blomme B, Francque S, Trépo E, Libbrecht L, Vanderschaeghe D, Verrijken A, et al. N-glycosylation-based biomarker distinguishing steatosis from NASH independently of fibrosis in non-alcoholic steatohepatitis. Submitted to *Liver Int*.
- [13] Deng J, Lu P, Zhang Y, Scheuner D, Kaufman R, Sonenberg N, et al. Translational repression mediates activation of nuclear kappaB by phosphorylated translation initiation factor 2. *Moll Cell Biol* 2004;24:10161-10168.
- [14] Hu P, Han Z, Couvillon A, Kaufman R, Exton J. Autocrine tumor necrosis factor alpha links endoplasmic reticulum stress to the membrane death receptor pathway through IRE1alpha-mediated NF-kappaB activation and down-regulation of TRAF2 expression. *Moll Cell Biol* 2006;26:3071-3084.
- [15] Cullinan S, Diehl J. Coordination of ER and oxidative stress signaling: the PERK/Nrf2 signaling pathway. *Int J Biochem Cell Biol* 2006;38:317-332.
- [16] Gotoh T, Mori M. Nitric oxide and endoplasmic reticulum stress. *Arterioscler Thromb Vasc Biol* 2006;26:1439-1446.
- [17] Hotamisligil G. Inflammation and metabolic disorders. *Nature* 2006;444:860-867.
- [18] Zhang X, Zhang G, Zhang H, Karin M, Bui H, Cui D. Hypothalamic IKKbeta/NF-kappaB and ER stress link overnutrition to energy imbalance and obesity. *Cell* 2008;135:61-73.
- [19] Erbay E, Babaev V, Mayers J, Makowski L, Charles K, Snitow M, et al. Reducing endoplasmic reticulum stress through a macrophage lipid chaperone alleviates arteriosclerosis. *Nat Med* 2009;15:1383-1391.
- [20] Makowski L, Boord J, Maeda K, Babaev V, Uysal K, Morgan M, et al. Lack of macrophage fatty-acid-binding protein aP2 protects mice deficient in apolipoprotein E against arteriosclerosis. *Nat Med* 2001;7:699-705.
- [21] Kleiner D, Brunt E, Van Natta M, Behling C, Contos MJ, Cummings OW, et al. Design and validation of a histological scoring system for nonalcoholic fatty liver disease. *Hepatology* 2005;41:1313-1321.

- [22] Roth J. Protein N-glycosylation along the secretory pathway: relationship to organelle topography and function quality control, and cell interactions. *Chem Rev* 2002;102:285-303.
- [23] Yoshida H. ER stress response, peroxisome proliferation, mitochondrial unfolded protein response and Golgi stress response. *IUBMB Life* 2009;61:871-879.
- [24] Qasba P, Ramakrishnan B, Boeggeman E. Structure and function of  $\beta$ -1,4-galactosyltransferase. *Curr Drug Targets* 2008;9:292-309.
- [25] Keusch J, Lydyard P, Isenberg D, Delves P. Beta-1,4-galactosyltransferase activity in B-cells detected using a simple ELISA-based assay. *Glycobiology* 1995;5:365-370.
- [26] Jeddi P, Bodman-Smith K, Lund T, Lydyard P, Mengle-Gaw L, Isenberg D, et al. Agalactosyl IgG and beta-1,4-galactosyltransferase gene expression in rheumatoid arthritis patients and in arthritis-prone MRL lpr/lpr mouse. *Immunology* 1996;87:654-659.
- [27] Keusch J, Lydyard P, Berger E, Delves P. B lymphocyte galactosyltransferase protein levels in normal individuals and in patients with rheumatoid arthritis. *Glycoconj J* 1998;15:1093-1097.
- [28] Puri P, Mirshahi F, Cheung O, Natarajan R, Maher J, Kellum J, et al. Activation and dysregulation of the unfolded protein response in nonalcoholic fatty liver disease. *Gastroenterology* 2008;134:568-576.
- [29] Attie A, Scherer P. Adipocyte metabolism and obesity. *J Lipid Res* 2009;50 Suppl S395-S399.
- [30] Lammert E. The vascular trigger of type II diabetes mellitus. *Exp Clin Endocrinol Diabetes* 2008;116 Suppl 1:S21-S25.



# **Chapter 4: General Discussion**

---

---

## **Hoofdstuk 4: Algemene Discussie**

---

This thesis is a continuation of the work published by Callewaert *et al* in 2004 [1]. In this study, it was shown that by quantifying *N*-glycans in serum, it is possible to distinct cirrhotic from non-cirrhotic patients with very high sensitivity and specificity. Concomitant with this study, a new technology to profile *N*-glycans was developed [2]. This technology makes use of DNA sequencing equipment to map the glycome of a particular biofluid. Important advantages of this capillary electrophoretic technique are the extreme high sensitivity (low femtomolar range) and the reliable quantification due to the laser-induced fluorescence of the APTS-labeled sugar. Following development, important challenges were bringing this technology to a clinical platform and exploring its potential in various clinical fields, including the field of hepatology in which it already had shown its great value. However, still a few questions remained unanswered.

The work performed in this thesis can be divided in two main parts. In the first part, various mouse models of chronic liver disease were used to further explore the mechanisms underlying the alteration of serum protein glycosylation in liver diseases. Initially, three mouse models were used for this purpose, common bile duct ligation (CBDL), chronic injections with the hepatotoxin CCl<sub>4</sub> and partial portal vein ligation (PPVL). In the two fibrotic models, CBDL and CCl<sub>4</sub>, a similar and consistent increase of the tetra-antennary glycan (NA4) was observed. Remarkably, this occurs very early in the fibrotic development of both models and is in contrast to human liver disease in which a decrease of multi-antennary glycans in advanced fibrosis is observed. Despite this similarity, CBDL mice displayed a characteristic increase of core-fucosylated glycans. We were able to extrapolate this finding to human liver patients with hyperbilirubinemia irrespective of etiology. Core-fucosylation on proteins produced in hepatocytes has been shown to be a signal for secretion in the bile ducts [3]. During cholestatic conditions, the basolateral path to the bile ducts becomes blocked off and an accumulation of proteins with core-fucosylated glycans in the hepatocyte develops. The only way out for these glycoproteins is apically to the space of Disse and eventually to the systemic circulation. The precise regulation of this mechanism is yet to be revealed, because in normal conditions, most of the liver-produced protein in serum (eg haptoglobin,  $\alpha$ 1-antitrypsin and transferrin) carry core-fucosylated glycans with NA2F being quantitatively the most important. However, it was shown that the core-fucosylation on these liver-produced proteins is not very abundant [4, 5]. A similar mechanism may apply to patients with hepatocellular carcinoma. Although not identical to cholestasis, a depolarization of the hepatocyte linked with apoptosis has been described in HCC and this may also explain the increase of core-fucosylated glycans in these patients [6]. The third model, PPVL, was used to study if portal hypertension contributed to the alteration of protein glycosylation. Few alterations were observed and they did not show consistency as in the fibrotic models indicating that this factor has no influence on protein *N*-glycosylation.

In human liver patients, five major liver etiologies (alcoholic, cholestatic, viral hepatitis B, viral hepatitis C and non-alcoholic steatohepatitis) were investigated and compared according serum protein glycomic alterations. In human liver disease, three important *N*-glycan alterations can be observed: increase of agalactosylated glycans on IgGs, increase of bisecting GlcNAc modified glycans and decrease of multi-antennary glycans on liver-produced proteins. No significant quantitative difference in each of these alterations were observed between the different etiologies in cirrhotic patients, although some important sub-significant distinctions were apparent. Cirrhotic alcoholic patients had the highest score when evaluated by the GlycoCirrhoTest which can be explained by the micronodular nature

of the cirrhotic liver. In these regenerative nodules, there is an upregulation of *N*-acetylglucosaminyltransferase III (GnT-III), the enzyme responsible for the bisecting GlcNAc modification [1]. More nodules correspond to a more elevated GnT-III expression and an increase of NA2FB on liver-produced protein. However, it has been recently shown that there is also a slight increase of bisecting GlcNAc modified glycans on IgG during liver fibrosis and this increase is quantitatively much more important [4]. Finally, undergalactosylation of IgG was observed to be quantitatively most important in patients with non-alcoholic steatohepatitis and this observation led to the development of a marker to distinguish steatosis from NASH patients (see further).

The differences in the alteration of protein glycosylation described between the mouse models of chronic liver disease and human liver disease were further explored by inducing the CBDL and CCl<sub>4</sub> model in B cell deficient mice. It was shown that hepatocytes are the dominant factor responsible for the observed glycomic alterations in mouse models of chronic liver disease. This is in sharp contrast to human liver diseases in which the total serum alterations were predominantly attributed to IgG glycosylation. As a direct consequence, this partially explained the increase of multi-antennary glycans in the fibrotic models because IgGs contain very little amounts of multi-antennary glycans and the lack of undergalactosylation. However, rheumatoid arthritis (RA) is also a chronic inflammatory disease with an important IgG undergalactosylation and this feature could be extrapolated to a mouse model for RA [7]. The increase of core-fucosylation in the CBDL model was also shown to be liver-dependent thereby confirming the hypothesis outlined in the first study. Finally, the large amount of alterations seen in these fibrotic models can be ascribed to the hepatocyte-specific nature of the glycomic alterations. Almost all *N*-glycans identified in the electropherogram are significantly altered in these mouse models. In human liver diseases, IgG acts as a buffer because it does not contain all the *N*-glycans present in total serum and an altered B cell physiology will only correlate indirectly with liver injury. Therefore, it can be postulated that the glycomic profile in mouse models of chronic liver disease is a better representation of the pathological state of the liver compared to the glycomic profile in human liver diseases.

In addition to the fibrotic models used in the first two studies, a glycomic investigation was performed in a mouse model for hepatocellular carcinoma (HCC). This mouse model was induced by weekly chronic injections with diethylnitrosamine (DEN). Two similarities can be drawn with the fibrotic models. First, maximum phenotype was observed at an early level of carcinogenesis, when the first dysplastic nodules started to appear. Second, the *N*-glycosylation of IgG does not play a role in these alterations. In contrast to the fibrotic models, the observed alterations are quite similar to the human situation in which it was shown that branch-fucosylated glycans are increased in HCC patients [8]. However, this was only shown in HBV patients and our data could not reproduce these results in HBV or other liver etiologies. The relatively small HCC nodules mostly develop in a cirrhotic background and cirrhotic specific alterations (increase of bisecting glycans) will therefore dominate in the glycomic profile of HCC patients. Approximately 10% of HCC develops in non-cirrhotic liver and it would be interesting to study the glycomic profile of these patients [9].

Angiogenesis is one of the hallmarks of malignant transformation. The growing tumor will induce new blood vessels from the existing vasculature to meet its increasing demand for oxygen and nutrients. The placental growth factor (PlGF) is an analog of vascular endothelial growth factor (VEGF) and it has recently gained a lot of interest as therapeutic target.

Inhibition of PIGF only targets the pathological vessels induced by the tumor leaving the normal vasculature untouched [10]. A mouse monoclonal antibody against PIGF was investigated in the DEN mouse model and this treatment had a significant positive impact on survival and tumor burden [11]. The *N*-glycosylation patterns of the DEN mice treated with anti-PIGF for 5w were evaluated and a significant improvement of most of the altered peaks was observed. Especially a decrease of all multi-antennary glycans was seen. This drew our attention to the Ets-1 transcription factor. Ets-1 not only plays a major role in various stages of new blood formation [12, 13], but is also a prerequisite for the induction of the genes of which the corresponding enzymes are responsible for the formation of multi-antennary glycans, i.e. GnT-IV and GnT-V [14]. Importantly, we showed a significant reduction of the number of Ets-1 positive cells upon anti-PIGF treatment, thereby providing evidence that Ets-1 is a possible link between angiogenesis and the increase of multi-antennary glycans in cancer.

The second part of this thesis dealt with the development of a biomarker based on the *N*-glycosylation of serum proteins to distinguish patients with simple steatosis and NASH. First, a pilot study was conducted including patients that were scheduled for bariatric surgery. This population was suitable to develop an 'inflammation marker' for NASH because none of the patients had a significant amount of fibrosis that could interfere in the analysis. The biomarker developed in this population correlated very well with the amount of lobular inflammation and had a reasonable Area Under the Curve (AUC) of 0.75 to distinguish steatosis and borderline NASH patients from NASH patients. Importantly, the biomarker was evaluated in a multivariate analysis together with other markers that were significant in the univariate analysis. It displayed the lowest *P*-value with a borderline significant result demonstrating its supremacy over other markers in this population. The glycomarker ( $\log[\text{NGA2F}]/[\text{NA2}]$ ) was subsequently validated in a large population of which the majority of the patients were diagnosed through a percutaneous needle liver biopsy without surgery and in a pediatric population. Both validation populations had a lot of patients with significant fibrosis ( $\geq\text{F2}$ ) in which we could evaluate the biomarker. We observed that mean marker score was stable until fibrosis stage 3 (bridging fibrosis) and it showed a slight increase in the cirrhotic stage. In agreement with the pilot study, a good correlation with the amount of inflammation was obtained with a consistent increase in ascending stages of lobular inflammation. An important reason for the lower AUC of the glycomarker in these populations is the use of needle biopsies to diagnose the severity of the disease. The surface of these biopsies was considerably smaller in comparison with the surface of the wedge liver biopsies that were collected during the bariatric procedure. Scoring of the histological features will be more accurate with the larger wedge liver biopsies.

The pediatric population showed very similar results in distinguishing simple steatosis from NASH in comparison with the adult population, despite a different histological liver pattern. This again confirmed that the alterations on the glycomic level in NASH patients are determined by B cells and not the liver. The mechanism that lies at the basis of this undergalactosylation is yet to be unraveled. Previously, research groups have shown in RA patients a decrease in beta1,4-galactosyltransferase (beta1,4-GalT) expression and activity, but another group could not confirm this result on the protein level [15-17]. In contrast, inflammatory conditions will result in an increased beta1,4-GalT mRNA and protein expression in microglia and in synovial tissue of arthritic patients, rather than a decrease [18, 19].

Because of these contradicting results, we investigated whether endoplasmic reticulum (ER) stress could provide an explanation for the undergalactosylation of IgG in NASH patients. The ER is the organelle responsible for protein folding, maturation, quality control and trafficking. *N*-glycans play an important part in all these processes. When the ER becomes stressed due to the accumulation of newly synthesized unfolded proteins, the unfolded protein response (UPR) is initiated. Importantly, the three branches of the UPR intersect with a variety of inflammatory and stress signaling systems including the NF- $\kappa$ B I $\kappa$ B kinase (IKK) and JNK-AP1 [20]. The plasma cell, the B cell type responsible for production and secretion of immunoglobulins, already has a limited UPR with an activation of the ATF6 and IRE1/XBP branch. This enables a resting B cell to transform into a high-rate secretory plasma cell. The PERK pathway is not activated in normal conditions [21, 22]. We showed that there is a significantly increased expression of all ER stress genes in all three branches of the UPR, including the PERK branch, in obese patients with liver inflammation compared to obese patients without liver inflammation. As a consequence, we hypothesize that more secretory proteins will be directed to the Golgi apparatus and the beta-1,4-GalT enzyme, that transfers a galactose monosaccharide to the glycan structure during biosynthesis, will be saturated prematurely. Therefore, a larger proportion of agalactosylated immunoglobulins will be secreted in the extracellular environment of obese patients with liver inflammation.

The results that we obtained in this thesis are very promising and they provide an explanation for some of the questions that were originally put forward, but they also raise a lot of new questions. Especially the link between ER stress and undergalactosylation of IgG in chronic inflammatory conditions needs to be explored further in depth. Crucial for this purpose will be the confirmation of the strong increased UPR in plasma cells of obese patients with liver inflammation in a large NAFLD population. Another important aspect will be to determine the influence of ER stress on Golgi function and especially on the beta-1,4-GalT enzyme as it is the final determinant of the undergalactosylation status. Important challenges are also present in the field of endocrinology. It has been shown that visceral adiposity is a critical determinant for the association between low testosterone (T) levels and insulin resistance and low T levels in the presence of a disturbed glucose metabolism are linked with high estradiol (E2) levels [23]. The low free T/E2 ratio associates with increased pro-inflammatory adipokines and decreased levels of regulators of insulin sensitivity, both contributing to diabetes type 2. As a continuation of our research in NASH patients, it would be interesting to investigate the association of our 'inflammation-dependent' glycomarker with pro-inflammatory adipokines and hormones secreted by visceral adipocytes that regulate insulin sensitivity. Exploring these associations will provide insight in the link between visceral adiposity and the development of liver inflammation in obese patients. Finally, two important hallmarks of cancer are neo-angiogenesis and an increase of multi-antennary glycans. Our results indicate that both phenomena might be linked by the Ets-1 transcription factor. An important future challenge is the validation of the lowered Ets-1 expression in anti-PIGF treated HCC mice by other quantitative methods including real-time PCR and western blotting. Furthermore, most Ets family proteins are nuclear targets for activation of Ras-MAP signaling pathway [24] and detailed investigation of this pathway would provide insight into the molecular mechanisms by which Ets-1 expression was down-regulated by 5D11D4 treatment. Importantly, This is also the pathway that regulates *Mgat5* gene transcription [25, 26] and *Mgat5*-modified glycans (multi-antennary glycans) correlate with progression [27] and reduced patient survival time [28] in several cancers. Alternatively, this mechanism can also be further explored by working with Ets-1 deficient mice [29].

Deze thesis is een voortzetting van het werk dat gepubliceerd werd door Callewaert *et al* in 2004 [1]. Er werd in deze studie aangetoond dat het mogelijk is om door kwantificatie van serum *N*-glycanen cirrotische patiënten te onderscheiden van niet-cirrotische patiënten met hoge sensitiviteit en specificiteit. Samengaan met deze studie werd een nieuwe technologie ontwikkeld om *N*-glycanen te profileren [2]. Deze technologie maakt gebruik van DNA sequencing apparatuur om het glycoom van een bepaalde bio-vloeistof te bepalen. Belangrijke voordelen van deze capillaire electroforetische techniek zijn de zeer hoge gevoeligheid (femtomolaire range) en de betrouwbare kwantificatie door de laser geïnduceerde fluorescentie van de APTS-gelabelde suikers. Na ontwikkeling van de technologie, waren er enkele belangrijke uitdagingen. Eén doel was om deze technologie naar een klinisch platform te brengen. Simultaan wou men het potentieel van deze technologie verkennen in verschillende klinische specialisaties waaronder de hepatologie waarin het al zijn grote waarde had bewezen. Een aantal belangrijke vragen bleven echter onbeantwoord.

Het werk uitgevoerd in deze thesis kan in twee delen opgesplitst worden. In het eerste deel werden verschillende muismodellen van chronisch leverlijden aangewend om de mechanismen die aan de basis liggen van veranderingen in serum eiwit glycosylatie verder te verkennen. Initieel werden hiervoor drie muismodellen geïnduceerd: het common bile duct ligation (CBDL) model, chronische injecties met het hepatotoxine CCl<sub>4</sub> en het partial portal vein ligation (PPVL) model. In de twee fibrotische modellen, CBDL en CCl<sub>4</sub>, werd een consistente toename van het tetra-antennaire glycaan (NA4) geobserveerd. Opvallend was dat dit zeer vroeg gebeurt in de fibrotische ontwikkeling van beide modellen en staat in contrast tot humaan leverlijden waarin een afname van multi-antennaire glycanen in gevorderde fibrose werd vastgesteld. Ondanks deze overeenkomst vertoonden de CBDL muizen een karakteristieke toename van core-gefucosyleerde glycanen. We waren in staat om deze vondst te extrapoleren naar lever patiënten met een verhoogde serum bilirubine concentratie ongeacht etiologie. Er werd eerder aangetoond dat core-fucosylatie op eiwitten geproduceerd in hepatocyten een signaal is voor secretie in de galkanalen. Het basolaterale pad naar de galwegen wordt afgeblokt tijdens cholestase en er ontwikkelt zich een accumulatie van eiwitten gemodificeerd met core-gefucosyleerde glycanen in de hepatocyten. De enige uitweg is apicaal naar de ruimte van Disse en uiteindelijk naar de systemische circulatie. De precise regulatie van dit mechanisme moet nog worden opgehelderd; want in normale omstandigheden dragen de meeste lever-geproduceerde eiwitten (haptoglobine,  $\alpha$ 1-antitrypsine en transferrine) core-gefucosyleerde glycanen. Er werd echter aangetoond dat core-fucosylatie op deze lever-geproduceerde glycanen niet erg veel voorkomend is [4, 5]. Een gelijkaardig mechanisme kan ook betrekking hebben op patiënten met hepatocellulaire carcinoma (HCC). Het mechanisme is waarschijnlijk niet volledig identiek aan cholestatische patiënten, maar een depolarisatie van de hepatocyte gelinkt aan apoptose is ook beschreven bij HCC en dit kan een verklaring bieden voor de toename van core-gefucosyleerde glycanen bij deze patiënten [6]. Het derde model, PPVL, werd gebruikt om te bestuderen of portale hypertensie bijdraagt tot de veranderingen in eiwit *N*-glycosylatie. Weinig veranderingen werden vastgesteld in dit muismodel en deze vertoonden geen overeenkomsten in de bestudeerde tijdstippen zoals in de fibrotische modellen wat aangeeft dat portale hypertensie geen invloed heeft op eiwit *N*-glycosylatie.

Vijf etiologieën van leverlijden (alcoholisch, cholestatisch, viraal hepatitis B, viraal hepatitis C en niet-alcoholisch steatohepatitis) werden onderzocht en vergeleken naargelang de

glycomisch veranderingen. Er kunnen zich drie belangrijke *N*-glycaan veranderingen voordoen bij humaan leverlijden: een toename van agalactosyleerde glycanen op IgGs en een toename van bisecting GlcNAc gemodificeerde glycanen en afname van multi-antennaire glycanen op lever-geproduceerde eiwitten. Er werd geen significant verschil in elk van deze veranderingen vastgesteld bij de verschillende etiologieën in cirrotische patiënten, alhoewel sommige sub-significante veranderingen werden vastgesteld. Cirrotische alcoholische patiënten hadden de hoogste score voor de GlycoCirrhoTest. Dit kan verklaard worden door het micronodulaire patroon van de cirrotische lever. In de regeneratieve nodules is er een opregulatie van *N*-acetylglucosaminyltransferase III (GnT-III), het enzyme verantwoordelijk voor de bisecting GlcNAc modificatie [1]. Meer nodules komen overeen met een meer toegenomen GnT-III expressie en de productie van NA2FB op lever-geproduceerde eiwitten. Er werd echter aangetoond dat er ook een lichte toename is van bisecting GlcNAc gemodificeerde glycanen op IgG tijdens lever fibrose en deze toename is kwantitatief veel belangrijker [4]. Ondergalactosylatie van IgG was het meest prominent aanwezig in patiënten met niet-alcoholisch steatohepatitis en deze vaststelling leidde tot de ontwikkeling van een merker die patiënten met steatose van NASH patiënten kan onderscheiden (zie verder).

De verschillen in veranderingen van eiwit glycosylatie tussen muismodellen van chronisch leverlijden en humaan leverlijden werden onderzocht door het CBDL en CCl<sub>4</sub> model te induceren in B cel deficiënte muizen. Er werd aangetoond dat hepatocyten de meest bepalende factor zijn verantwoordelijk voor de geobserveerde glycomische veranderingen in muismodellen voor leverlijden. Dit staat in sterk contrast tot humaan leverlijden waarin de totaal serum veranderingen hoofdzakelijk toe te schrijven zijn aan IgG glycosylatie. Dit verklaart gedeeltelijk de toename van multi-antennaire glycanen in de fibrotische modellen omdat IgGs zeer weinig dergelijke glycanen bevatten en het gebrek aan IgG ondergalactosylatie. Echter, reumatoid arthritis (RA) is ook een chronisch inflammatoire aandoening met een belangrijke ondergalactosylatie en dit kenmerk kon wel geëxtrapoleerd worden naar een muismodel voor RA [7]. De toename van core-fucosylatie in het CBDL model was ook lever-afhankelijk en dit bevestigde de hypothese vooropgesteld in de eerste studie. Nagenoeg alle *N*-glycanen die geïdentificeerd konden worden in het electroferogram waren significant gewijzigd in de fibrotische muismodellen en dit kan toegeschreven worden aan de hepatocyte-specifieke aard van deze veranderingen. IgG gedraagt zich als een buffer bij humaan leverlijden, omdat het niet alle *N*-glycanen bevat die in totaal serum aanwezig zijn en een gewijzigd B cel fysiologie zal enkel indirect correleren met leverschade. Hierdoor kan gesteld worden dat het glycomische profiel van de muismodellen van chronisch leverlijden een betere weergave is van de pathologische staat waarin de lever zich bevindt in het vergelijking tot het glycomische profiel bij humaan leverlijden.

In aanvulling op de fibrotische modellen werd ook een glycomisch onderzoek uitgevoerd in een muismodel voor hepatocellulair carcinoma (HCC). Dit muismodel werd geïnduceerd door wekelijkse injecties met diethylnitrosamine (DEN). Er kunnen twee parallellen getrokken worden met de fibrotische modellen. Ten eerste, het maximale fenotype werd geobserveerd in een vroeg stadium van carcinogenese wanneer de eerste dysplastische nodules begonnen te verschijnen. Ten tweede, de glycosylatie van IgG had geen rol in deze veranderingen. Echter, in tegenstelling tot de fibrotische modellen waren de geobserveerde veranderingen vrij gelijkaardig aan de humane situatie waarbij werd aangetoond dat branch-gefucosyleerde glycanen toegenomen zijn in HCC patiënten [8]. Dit werd echter enkel

aangetoond bij HBV patiënten en onze data konden deze resultaten niet reproduceren in HBV of andere lever etiologieën. De relatief kleine HCC nodules ontwikkelen zich meestal in een cirrotische achtergrond en veranderingen specifiek voor cirrose (toename van bisecting glycanen) zal daardoor domineren in het glycomische profiel van HCC patiënten. Ongeveer 10% van HCC ontwikkelt zich in een niet-cirrotische lever en het zou interessant zijn om een glycomische analyse te maken bij deze patiënten [9].

Angiogenese is één van de karakteristieken van maligne transformatie. De groeiende tumor zal nieuwe bloedvaten induceren uit de bestaande vasculatuur om zijn toenemende vraag naar zuurstof en nutriënten te beantwoorden. De placentale groeifactor (PIGF) is een analoog van de vasculaire endotheliale groeifactor (VEGF) en het heeft recent aandacht getrokken als therapeutische target. Inhibitie van PIGF zal enkel de nieuwe bloedvaten, geïnduceerd door de tumor, aantasten en de normale vasculatuur zal niet verstoord worden [10]. Een muis monoclonaal antilichaam tegen PIGF werd onderzocht in de DEN-muis en deze behandeling had een positief effect op overleving en op de grootte van de tumoren [11]. *N*-glycosylatie patronen van DEN-muizen die behandeld werden met anti-PIGF vertoonden een significante verbetering bij de meerderheid van de gewijzigde pieken. Er werd vooral een afname van alle multi-antennaire glycanen geobserveerd. Dit trok de aandacht naar de Ets-1 transcriptie factor. Ets-1 speelt niet alleen een belangrijke rol in verschillende stadia van nieuw-bloedvatvorming [12, 13], maar het is ook noodzakelijk voor de inductie van genen waarvan de overeenkomstige enzymen verantwoordelijk zijn voor de vorming van multi-antennaire glycanen, zoals GnT-IV en GnT-V [14]. We konden een significante afname van de hoeveelheid Ets-1 positieve cellen aantonen waardoor we bewijs leverden voor een mogelijke link tussen angiogenese en de toename van multi-antennaire glycanen bij kanker.

Het tweede gedeelte van deze thesis is gewijd aan de ontwikkeling van een biomarker gebaseerd op de *N*-glycosylatie van serum eiwitten om patiënten met steatose te onderscheiden van NASH patiënten. Eerst werd een piloot studie uitgevoerd met patiënten die gepland stonden voor een bariatrische ingreep. Deze populatie was geschikt om een 'inflammatie merker' voor NASH te ontwikkelen, omdat geen enkele patiënt een belangrijke hoeveelheid fibrose had dat kon interfereren in deze analyse. De biomarker correleerde zeer goed met de hoeveelheid lobulaire inflammatie in deze populatie en had een aanvaardbare Area Under The Curve (AUC) van 0.75 om steatose en borderline NASH patiënten te onderscheiden van NASH patiënten. De biomarker werd geëvalueerd in een multivariate analyse met andere merkers die significant scoorden in de univariate analyse. Het vertoonde de laagste *P*-waarde met een borderline significant resultaat waardoor zijn suprematie over de andere merkers werd aangetoond in deze populatie. De glycomerker ([NGA2F]/[NA2]) werd vervolgens gevalideerd in een grote populatie waarvan de diagnose bij de meeste patiënten werd gesteld door een percutane naaldbiopsie zonder operatie en in een pediatrie populatie. Beide validatie-populaties hadden veel patiënten met een belangrijke hoeveelheid fibrose ( $\geq$ F2) waarin we onze biomarker konden evalueren. We stelden vast dat gemiddelde merker score stabiel bleef tot fibrose stadium 3 (bridging fibrose) en het vertoonde een kleine toename in het cirrotische stadium. In overeenstemming met de piloot studie werd een goede correlatie gevonden met de hoeveelheid lobulaire inflammatie met een consistente stijging bij toenemende graad lobulaire inflammatie. Een belangrijke reden voor de lagere AUC van de glycomerker in deze populaties is het gebruik van naaldbiopsieën om de ernst van de leveraandoening vast te



stellen. De oppervlakte van deze biopsieën was veel kleiner in vergelijking met de oppervlakte van de wedge lever biopsieën die afgenomen werden tijdens de bariatrische ingreep. Scoring van de histologische kenmerken zal accurater zijn met de grotere wedge lever biopsieën.

De pediatrie populatie vertoonde zeer gelijkaardige resultaten in vergelijking met de volwassen populatie ondanks een verschillend histologisch lever patroon. Dit was opnieuw een bevestiging dat de veranderingen op het glycomische niveau bij NASH patiënten bepaald worden door B cellen en niet door de lever. Het mechanisme dat aan de basis ligt van deze ondergalactosylatie is nog niet opgehelderd. In het verleden hebben onderzoeksgroepen aangetoond dat er een afname is in expressie en activiteit van het beta-1,4-galactosyltransferase (beta-1,4-GalT) enzyme in patiënten met RA, maar een andere groep kon deze resultaten niet bevestigen op het eiwit niveau [15-17]. In tegenstelling hiermee werd aangetoond dat inflammatie leidt tot een toegenomen beta-1,4-GalT mRNA en eiwit expressie in microglia en synoviaal weefsel van arthritische patiënten [18, 19].

Door deze tegenstrijdige resultaten onderzochten we of endoplasmatisch reticulum (ER) stress een uitleg kan geven voor de IgG ondergalactosylatie in NASH patiënten. Het ER is het organel verantwoordelijk voor eiwitopvouwing, maturatie, kwaliteitscontrole en vervoer. *N*-glycosylatie speelt een belangrijke rol in al deze processen. Wanneer het ER onder druk komt te staan door een accumulatie van nieuw gesynthetiseerde eiwitten, wordt een 'unfolded protein response' (UPR) geïnitieerd. De 3 takken van de UPR zijn verbonden met inflammatoire en stress signalisatie systemen zoals NFκB IκB kinase (IKK) en JNK-AP1. De plasma cel, het B celttype dat verantwoordelijk is voor de productie en secretie van immunoglobulines, heeft al een beperkte UPR met activatie van de ATF6 en IRE1/XBP1 tak. Hierdoor kan een rustende B cel zich transformeren in een antilichaam-secreterende plasma cel. De PERK pathway is niet geactiveerd in normale omstandigheden. We konden aantonen dat er een significant toegenomen expressie is van alle ER stress genen in obese patiënten met lever inflammatie in vergelijking met obese patiënten zonder leverinflammatie. Als hypothese stellen we voorop dat hierdoor meer eiwit naar het Golgi apparaat zal gestuurd worden. Het beta-1,4-GalT enzyme, dat de transfer van een galactose eenheid naar de glycaan structuur tijdens biosynthese katalyseert, zal voortijdig gesatureerd zijn en een grotere proportie agalactosyleerde immunoglobulines zal hierdoor gesecreteerd worden in het extracellulaire milieu bij obese patiënten met lever inflammatie.

De resultaten die behaald werden in deze thesis zijn veelbelovend en ze leveren een uitleg voor sommige vragen die bij aanvang naar voor zijn geschoven, maar ze roepen ook een aantal nieuwe vragen op. Vooral de link tussen ER stress en IgG ondergalactosylatie in chronisch inflammatoire aandoeningen moet verder onderzocht worden. Cruciaal voor dit doel zal de bevestiging zijn van de sterk toegenomen UPR in plasma cellen van obese patiënten met lever inflammatie in een grote NAFLD populatie. Een ander belangrijke uitdaging zal het onderzoek zijn naar de invloed die ER stress heeft op het functioneren van het Golgi apparaat en vooral op het beta-1,4-GalT enzyme als finale determinant van de ondergalactosylatie status van IgG. Er zijn ook belangrijke uitdagingen te vinden in de endocrinologie. Er werd aangetoond dat viscerale adipositas een belangrijke determinant is voor de associatie tussen een lage testosteron (T) spiegel en insuline resistentie en lage T levels in de aanwezigheid van een verstoord glucose metabolisme zijn gelinkt aan hoge estradiol (E2) concentraties [23]. De lage T/E2 ratio is geassocieerd met een toegenomen concentratie van pro-inflammatoire adipokines en verlaagde concentraties van insuline

resistentie regulatoren, beide dragen bij tot diabetes type 2. Als aanvulling op ons onderzoek in NASH patiënten zou het interessant zijn om de associatie te onderzoeken tussen onze 'inflammatie-afhankelijke' glycomerker en pro-inflammatoire adipokines en hormonen gesecreteerd door viscerale adipocyten die insuline sensitiviteit reguleren. Het verkennen van deze associaties zal een inzicht geven in de link tussen viscerale adipositas en de ontwikkeling van leverinflammatie bij obese patiënten. Ten slotte, twee belangrijke karakteristieken van kanker zijn neo-angiogenese en een toename van multi-antennaire glycanen. Onze resultaten geven aan dat beide fenomenen gelinkt zijn door de Ets-1 transcriptie factor. Een belangrijke toekomstig doel is de validatie van de verlaagde Ets-1 expressie in anti-PIGF behandelde HCC muizen door andere kwantitatieve methodes zoals real-time PCR en western blotting. De meeste eiwitten van de Ets familie zijn de nucleaire targets voor de activatie van de Ras-MAP signalisatie pathway [24] en een gedetailleerd onderzoek van deze pathway zou inzicht verschaffen in de moleculaire mechanismen waardoor de Ets-1 expressie is neergereguleerd door anti-PIGF behandeling. Dit is ook de pathway dat de *Mgat5* gen transcriptie reguleert [25, 26] en *Mgat5*-gemodificeerde glycanen (multi-antennaire glycanen) correleren met progressie [27] en een verlaagde patiënt overlevingstijd [28] in verschillende kankers. Als alternatief kan dit mechanisme ook verder verkend worden door te werken met Ets-1 deficiënte muizen [29].

## References

- [1] Callewaert N, Van Vlierberghe H, Van Hecke A, Laroy W, Delanghe J, Contreras R. Noninvasive diagnosis of liver cirrhosis using DNA sequencer-based totalserum protein glycomics. *Nat Med* 2004;10:429-434.
- [2] Laroy W, Contreras R, Callewaert N; Glycome mapping on DNA sequencing equipment. *Nat Protoc* 2006;1:397-405.
- [3] Nakagawa T, Uozumi N, Nakano M, Mizuno-Horikawa Y, Okuyama N, Tagachi T, et al. Fucosylation of N-glycans regulates the secretion of hepatic glycoproteins into bile ducts. *J Biol Chem* 2006;281:29797-29806.
- [4] Klein A, Carre Y, Louvet A, Michalski J, Morelle W. Immunoglobulins are the major glycoproteins involved in the modifications of total serum N-glycome in cirrhotic patients. *Proteomics Clin Appl* 2010;4:379-393.
- [5] Kolarich D, Weber A, Turecek P, Schwarz H, Altmann F. Comprehensive glyco-proteomic analysis of human alpha 1-antitrypsin and its charge isoforms. *Proteomics* 2006;6:3369-3380.
- [6] Gonda K, Tsuchiya H, Sahabe T, Akechi Y, Ikeda R, Nishio R, et al. Synthetic retinoid CD437 induces mitochondria-mediated apoptosis in hepatocellular carcinoma cells. *Biochem Biophys Res Commun* 2008;370:629-633.
- [7] Van Beneden K, Coppieters F, Laroy W, De Keyser F, Hoffman I, Van den Bosch F, et al. Reversible changes in serum immunoglobulin galactosylation during the immune response and treatment of inflammatory autoimmune arthritis. *Ann Rheum Dis* 2009;68:1360-1365.
- [8] Liu X, Desmyter L, Gao C, Laroy W, Dewaele S, Vanhooren V, et al. N-glycomic changes in hepatocellular carcinoma patients with liver cirrhosis induced by hepatitis B virus. *Hepatology* 2007;46:1426-1435.
- [9] De Mitri M, Pisi E, Poussin K, Paterlini P, Bréchet C, Baccarini P, et al. HCV-associated liver cancer without cirrhosis. *Lancet* 1995;345:413-415.
- [10] Fischer C, Jonckx B, Mazzone M, Zacchigna S, Loges S, Pattarini L, et al. Anti-PIGF inhibits growth of VEGF(R)-inhibitor-resistant tumors without affecting healthy vessels. *Cell* 2007;131:463-475.
- [11] Van de Veire S, Stalmans I, Heindryckx F, Oura H, Tijerbas-Raballand A, Scmidt T, et al. Further pharmacological and genetic evidence for the efficacy of PIGF inhibition in cancer and eye disease. *Cell* 2010;141:178-190.
- [12] Oettgen P. The role of ets factors in tumor angiogenesis. *J Oncol* 2010;2010:767384.
- [13] Sato Y. Role of ETS family transcription factors in vascular development and angiogenesis. *Cell Struct Funct* 2001;26:19-24.
- [14] Taniguchi Y, Miyoshi E, Ko J, Ikeda Y, Ihara Y. Implication of N-acetylglucosaminyltransferases III and V in cancer: gene regulation and signaling mechanism. *Biochem Biophys Acta* 1999;1455:287-300.
- [15] Jeddli PA, Lund T, Bodman K, Sumar N, Lydyard P, Pouncey L, et al. Reduced galactosyltransferase mRNA levels are associated with the agalactosyl IgG found in arthritis-prone MRL-lpr/lpr strain mice. *Immunology* 1994;83:484-488.
- [16] Furukawa K, Matsuta K, Takeuchi F, Kosuge E, Miyamoto T, Kobata A. Kinetic study of a galactosyltransferase in the B cells of patients with rheumatoid arthritis. *Int J Immunol* 1990;2:105-112.

- [17] Keusch J, Lydyard P, Berger E, Delves P. B lymphocyte galactosyltransferase protein levels in normal individuals and in patients with rheumatoid arthritis. *Glycoconj J* 1998;15:1093-1097.
- [18] Shen A, Chen J, Qian J, Zhu J, Hu L, Yan M, et al. Elevated beta-1,4-galactosyltransferase-I induced by the intraspinal injection of lipopolysaccharide. *Glycoconj J* 2009;26:19-31.
- [19] Wang H, Xu D, Tao R, Ni X, Shen A, Wang Y, et al. Beta 1,4-galactosyltransferase-I in synovial tissue of collagen-induced rat model of rheumatoid arthritis. *Clin Exp Med* 2010 Dec 16 [Epub ahead of print].
- [20] Hotamisligil G. Endoplasmic reticulum stress and the inflammatory basis of metabolic disease. *Cell* 2010;140:900-917.
- [21] Gass J, Gifford N, Brewer J. Activation of an Unfolded protein response during differentiation of antibody-secreting B cells. *J Biol Chem* 2002;277:49047-49054.
- [22] Gass J, Jiang H, Wek R, Brewer J. The unfolded protein response of B-lymphocytes: PERK-independent development of antibody-secreting cells. *Mol Immunol* 2008;45:1035-43.
- [23] Ruige J. Does low testosterone affect adaptive properties of adipose tissue in obese men? *Arch Physiol Biochem* 2011;117:18-22.
- [24] Oikawa T, Yamada T. Molecular biology of the Ets family of transcription factors. *Gene* 2003;303:11-34.
- [25] Chen L, Zhang W, Fregein N, Pierce M. The her-2/neu oncogene stimulates the transcription of N-acetylglucosaminyltransferase V and expression of its cell surface oligosaccharide products. *Oncogene* 1998;17:2087-2093.
- [26] Ko J, Miyoshi E, Noda K, Ekuni A, Kang R, Ikeda Y, et al. Regulation of the GnT-V promoter by transcription factor Ets-1 in various cancer cell lines. *J Biol Chem* 1999;274:22941-22948.
- [27] Dennis J, Laferté S, Waghorne C, Breitman M, Kerbel R.  $\beta$ 1-6 branching of Asn-linked oligosaccharides is directly associated with metastasis. *Science* 1987;236:582-585.
- [28] Dennis J, Laferté S. Oncodevelopment expression of  $-\text{GlcNAc}\beta 1-6\text{Man}\alpha 1-6\text{Man}\beta 1$ -branched asparagines-linked oligosaccharides in murine tissues and human breast carcinomas. *Cancer Res* 1989;49:945-950.
- [29] Eyquem S, Chemin K, Fasseu M, Chopin M, Sigaux F, Cumano A, et al. The development of early and mature B cells is impaired in mice deficient for the Ets-1 deficient factor. *Eur J Immunol* 2004;34:3187-3196.

# CURRICULUM VITAE

---

## Personal details:

**First name:** Bram  
**Last name:** Blomme  
**Date of birth:** 13-06-1983  
**Birthplace:** Roeselare  
**Nationality:** Belgian  
**Address:** Beversesteenweg 127 8800 Roeselare  
**Mobile:** +32 (0)474 97 03 92  
**E-mail:** [bram.blomme@ugent.be](mailto:bram.blomme@ugent.be)

## Education:

**1995-2001:** Modern languages-Sciences, Onze Lieve Vrouw van Vreugde Institute, Roeselare, Belgium

**2001-2005:** Biomedical Sciences (Major: Nutrition and Metabolism), Ghent University, Ghent, Belgium  
Thesis: "determination of the essential fatty acid status in patients with chronic fatigue syndrome"  
Graduated with great distinction

**2005-2006:** Medical Molecular Biotechnology, Ghent University, Ghent, Belgium  
Thesis: "study of the molecular mechanism of the anti-tumor effect of dexamethasone in several tumor models in mice"  
Graduated with distinction

**2007-2011:** PhD candidate in the Biomedical Sciences at the department of Gastroenterology and Hepatology, Ghent University Hospital, Ghent, Belgium.  
Thesis: "*N*-glycosylation of serum protein in mouse models of chronic liver disease and in human conditions with liver disease"

## Additional training:

- Basic course in laboratory animal science partim 1: general topics (2008)
- Basic course in laboratory animal science partim 2: specific topics (2008)
- SPSS statistics, institute for continuing education in science (ICES) (2007)

- Introductory statistics: basic of statistical inference, ICES (2008)
- Analysis of variation, ICES (2009)
- Applied linear regression, ICES (2010)
- Quality Research skills, Doctoral schools (2009)
- Project management, Doctoral schools (2010)
- Advanced Academic English: Writing Skills, doctoral schools (2009)

## **A1-Publications**

B. Blomme, C. Van Steenkiste, N. Callewaert, H. Van Vlierberghe. Alteration of protein glycosylation in liver diseases. *J Hepatol* 2009 Mar;50(3):592-603.

B. Blomme, C. Van Steenkiste, J. Van Huysse, I. Colle, N. Callewaert, H. Van Vlierberghe. The impact of elevation of total bilirubin level and etiology of the liver disease on serum N-glycosylation patterns in mice and men. *Am J Physiol Gastrointest Liver Physiol*. 2010;298:G615-G624.

B. Blomme, C. Van Steenkiste, Paola Grassi, Stuart M Haslam, Anne Dell, Nico Callewaert, Hans Van Vlierberghe. Alterations of serum protein N-glycosylation in two models of chronic liver disease are hepatocyte and not B cell driven. Accepted for publication in *Am J Physiol Gastrointest Liver Physiol*.

B. Blomme, F. Heindryckx, J. Stassen, A. Geerts, I. Colle, H. Vlierberghe. Serum N-glycosylation patterns in diethylnitrosamine-induced hepatocellular carcinoma and their evolution after inhibition of the Placental growth Factor. Submitted to *Mol Carcinog*.

B. Blomme, S. Francque, E. Trépo, L. Libbrecht, D. Vanderschaeghe, A. Verrijken, P. Pattyn, Y. Van Nieuwenhove, D. Van De Putte, A. Geerts, I. Colle, J. Delanghe, C. Moreno, L. Van Gaal, N. Callewaert, H. Van Vlierberghe. N-glycosylation based biomarker distinguishing NASH from steatosis independently of fibrosis in non-alcoholic fatty liver disease. Submitted to *Liver Int*.

C. Van Steenkiste, J. Ribera, A. Geerts, M. Pauta, S. Tugues, C. Casteleyn, L. Libbrecht, K. Olievier, B. Schroyden, H. Reynaert, L. Van Grunsven, B. Blomme, S. Coulon, F. Heindryckx, M. De Vos, J. Stassen, S. Vinckier, J. Altamirano, R. Bataller, P. Carmeliet, H. Van Vlierberghe, I. Colle, M. Morales-Riuz. Inhibition of PIGF activity reduces the severity of fibrosis, inflammation and portal hypertension in cirrhotic mice. Accepted for publication in *Hepatology*.

### **Oral presentation:**

B. Blomme, F. Heindryckx, I. Colle, JM. Stassen, N. Callewaert, H. Van Vlierberghe. *N*-glycosylation patterns in HCC-mice chronically injected with DEN and their evolution after treatment with anti-PIGF. Belgian Week of Gastroenterology, 4<sup>th</sup> March 2010, Antwerp, Belgium.

B. Blomme, S. Francque, L. Van Gaal, J. Delanghe, N. Callewaert, H. Van Vlierberghe. A Biomarker based on the *N*-glycosylation of serum proteins is a marker for inflammation but not fibrosis in patients with non-alcoholic fatty liver disease. AASLD 2010, October 29- November 2, Boston, MA, USA.

### **Poster presentation**

B. Blomme, C. Van Steenkiste, J. Van Huysse, I. Colle, N. Callewaert, H. Van Vlierberghe. Different glycosylation patterns in mice models of cirrhosis and portal hypertension. UEGW 2008, 18-22 October, Vienna, Austria.

B. Blomme, I. Colle, N. Callewaert, H. Van Vlierberghe. *N*-glycosylation of immunoglobulin G and its role in the alteration of total serum *N*-glycome in two mouse models of chronic liver diseases. Belgian Week of Gastroenterology 2010, March 4, Antwerp, Belgium.

B. Blomme, C. Van Steenkiste, J. Van Huysse, I. Colle, N. Callewaert, H. Van Vlierberghe. The impact of elevation of total bilirubin level on serum *N*-glycosylation patterns in mice and men. EASL 2010, April 14-18, Vienna, Austria.

B. Blomme, L. Libbrecht, P. Pattyn, Y. Van Nieuwenhove, D. Van De Putte, A. Geerts, I. Colle, N. Callewaert, H. Van Vlierberghe. *N*-glycosylation patterns of serum proteins to make the distinction between steatosis of the liver and non-alcoholic steatohepatitis in obese patients scheduled for bariatric surgery. EASL 2010, April 14-18, Vienna, Austria.

B. Blomme, F. Heindryckx, A. Geerts, I. Colle, N. Callewaert, H. Van Vlierberghe. *N*-glycosylation patterns in mice chronically injected with DEN and their evolution after inhibition of the Placental Growth Factor. Knowlegde for growth 2010, May 20, Ghent, Belgium.

B. Blomme, S. Francque, L. Van Gaal, J. Delanghe, N. Callewaert, H. Van Vlierberghe. *N*-glycosylation based biomarker distinguishing NASH from steatosis independently from fibrosis in non-alcoholic steatohepatitis. Joint Glycobiology meeting 2010, November 7-9, Ghent, Belgium.

## DANKWOORD

---

Uit ervaring weet ik dat het dankwoord het enige is dat ‘men’ leest van een doctoraat. Ik zou het nochtans appreciëren moest U de tijd nemen om de vorige 200 bladzijden ten minste eens te doorbladeren.

Maar het ging over mensen bedanken. Op de eerste plaats zijn dit natuurlijk mijn ouders. Jullie hebben mij altijd gesteund in alle keuzes die ik gemaakt heb en alleen ik weet wat jullie allemaal voor mij gedaan hebben. Zonder jullie was dit werk nooit tot stand gekomen of was er nu iemand anders aan het schrijven over ‘glycosyatie en leverlijden’. Ik wil dit werk dan ook opdragen aan mijn ouders. Heel echt super bedankt voor alles!

Met stip op de tweede plaats volgt mijn promotor, Prof Hans Van Vlierberghe. Vier jaar geleden zag het er naar uit dat ik aan een saaie kantoorjob zou moeten beginnen, maar U gaf mij de kans om aan wetenschappelijk onderzoek te doen, volgens mij de mooiste job ter wereld. Ondanks uw drukke agenda vond U altijd de tijd voor een snelle feedback of een motiverend gesprek. Bedankt voor de goede onderzoeksideeën en de vlotte samenwerking!

De mensen die ik ook zeker niet mag vergeten zijn mijn hepato-collega's: Christophe, Kin Jip Stéphanie en Femke. Jullie moet ik bedanken voor de aangename tijd die ik de voorbije vier jaar mocht beleven, zowel in het labo als daarbuiten. Counting Cows, de snowboardtrips of de walvissen in Boston; allemaal heel toffe herinneringen. Wie daar zeker ook aan meegeholpen heeft, is Julien. Prettig gestoord, maar met een hart van goud. Bedankt voor de vele Knoppers (mét gentse r), de befaamde winegums en de vele flessen water dat je voor ons meebracht, al kan ik je “zen” radio nog altijd niet appreciëren. Ik ben er van overtuigd dat ik jullie in de toekomst nog veel zal tegenkomen.

Daarnaast moet ik de mensen van de K12 bedanken. Isabelle en Anja voor het opvolgen van ons onderzoek en voor de nuttige raad en advies. Annette voor het afhandelen van de bestellingen en Maud voor de betalingen. Natuurlijk ook de mensen van het labo op 3K12 (Debby, Nancy, Eline, Pieter, Hugo, Lindsay, Kim, Christel, Ellen, Sarah en Evi). Ik heb het labo zien evolueren van ‘streng’ naar een toffe plek waar je op een aangename manier kan aan onderzoek doen. Nadrukkelijk wil ik Debby bedanken voor het nuttige wetenschappelijke advies en Kim voor het afhandelen van de qPCRs de laatste maanden.

Tenslotte moet ik Prof Nico Calllewaert bedanken voor de gastvrijheid waarmee ik in zijn labo mocht werken. Speciale aandacht verdient Annelies Van Hecke voor het aanleren van het ‘suiker’ protocol, de vele goede adviezen en het laden van mijn stalen op de capillairen. Heel erg bedankt voor de voorbije jaren!

Ziezo, het zit erop. Misschien krijgt het nog een vervolg in het UZ Gent, maar desondanks zal ik altijd met een goed gevoel terugkijken op de vier jaar van mijn doctoraat. Nogmaals heel erg bedankt!

Bram Blomme  
Februari 2011